LBL-33532
UC-000

Lawrence Berkeley Laboratory
UNIVERSITY OF CALIFORNIA

EARTH SCIENCES DIVISION

Hydrological and Geochemical Investigations of Selenium Behavior at Kesterson Reservoir

S.M. Benson, T. Tokunaga, P. Zawislanski, C. Wahl, P. Johannis,
M. Zavarin, A. Yee, L. Tsao, D. Phillips, and S. Ita

December 1992

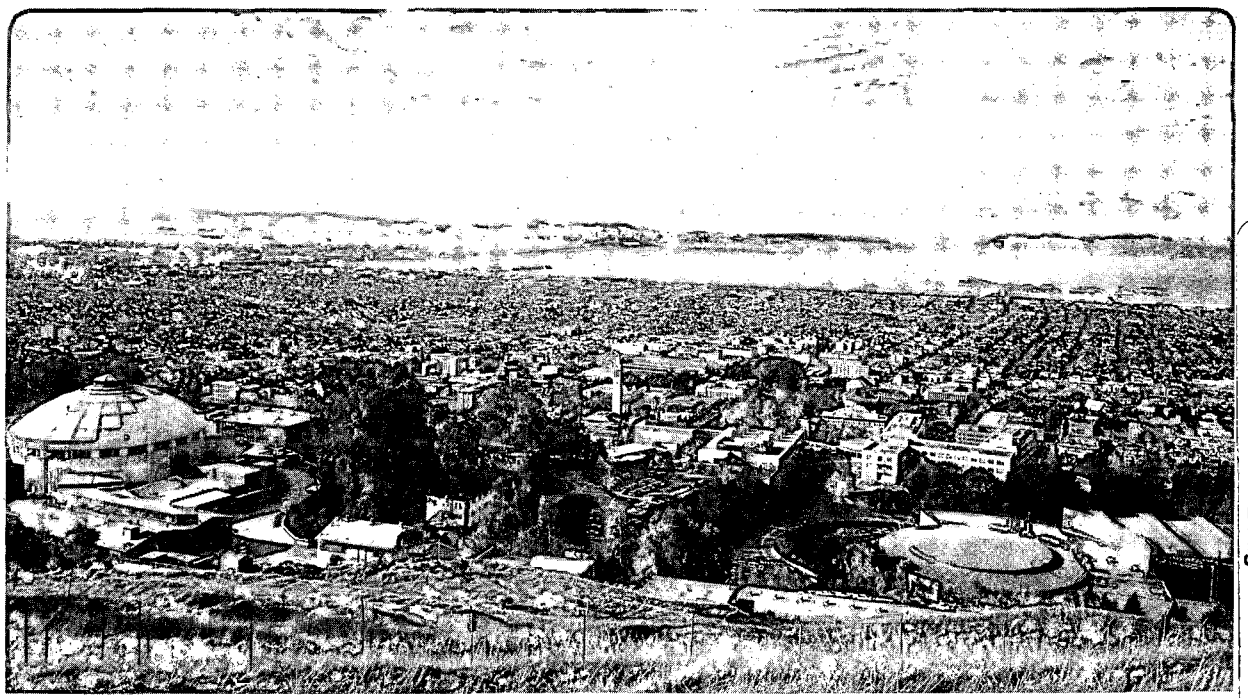

REFERENCE COPY
Does Not
Circulate
Bldg. 50 Library.
LBL-33532
Copy 1

Prepared for the U.S. Department of Energy under Contract Number DE-AC03-76SF00098

DISCLAIMER

This document was prepared as an account of work sponsored by the United States Government. While this document is believed to contain correct information, neither the United States Government nor any agency thereof, nor the Regents of the University of California, nor any of their employees, makes any warranty, express or implied, or assumes any legal responsibility for the accuracy, completeness, or usefulness of any information, apparatus, product, or process disclosed, or represents that its use would not infringe privately owned rights. Reference herein to any specific commercial product, process, or service by its trade name, trademark, manufacturer, or otherwise, does not necessarily constitute or imply its endorsement, recommendation, or favoring by the United States Government or any agency thereof, or the Regents of the University of California. The views and opinions of authors expressed herein do not necessarily state or reflect those of the United States Government or any agency thereof or the Regents of the University of California.

LBL-33532

Hydrological and Geochemical Investigations of Selenium Behavior at Kesterson Reservoir

Sally M. Benson, Tetsu Tokunaga, Peter Zawislanski, Caroline Wahl, Paul Johannis, Mavrik Zavarin, Andy Yee, Leon Tsao, Dan Phillips and Stacey Ita

Earth Sciences Division
Lawrence Berkeley Laboratory
University of California
Berkeley, CA 94720

Annual Report
October 1, 1990 through September 30, 1992

December 1992

This work was supported by the U. S. Bureau of Reclamation, under U. S. Department of Interior Interagency Agreement 9-AA-20-20, through U. S. Department of Energy Contract No. DE-AC03-76SF00098.

recycled paper

Table of Contents

Table of Contents iii

List of Figures vii

List of Tables xvii

Acknowledgment xix

1.0. Introduction 1

2.0. Vadose Zone Monitoring 3

2.1. Soil Water Monitoring in the Northern Portion of Pond 9 5

2.1.1. Site Description 5
2.1.2. Soluble Selenium Concentrations in Northern Pond 9 Soil Waters 9
2.1.3. Summary 12

2.2. Soil Selenium and Salinity Monitoring in Soil Profiles of Plots 8EP and 9BE 15

2.2.1. In-Situ Soil Water Monitoring 15
2.2.2. Soil Selenium and Salinity Monitoring 24
2.2.2.1. Plot 8EP 24
2.2.2.2. Plot 9BE 28
2.2.3. Quantitative Assessment of Chloride and Selenium Concentration Changes 30

2.3. Measurement of Chemical Changes in Near-Surface Soils of Plots 8EP and 9BE 33

2.4. Field Investigation of the Effects of Rainfall Infiltration on Soil Selenium and Salinity 37

2.4.1. Site Characterization and Monitoring 37
2.4.2. Hydrogeologic Conditions 38
2.4.3. Solute Data 38
2.4.3. Data Analysis 43
2.4.3.1. Solute Mass Inventories 43
2.4.3.2. Species Ratios 43
2.4.4. Selenium Transformations 45
2.4.5. Summary 46

2.5. Reservoir-Wide Monitoring of Soil Selenium 47

2.5.1. Results and Interpretation 50
2.5.2. Spatial Trends 50
2.5.3. Temporal Trends due to the Oxidation of the Selenium Inventory 52
2.54. Temporal Trend due to Seasonal Cycles 54
2.5.5. Discussion and Summary 56
2.5.6. Conclusion 59

3.0. Anticipated Soil Selenium Concentrations at Kesterson Reservoir 61

3.1. Introduction 61

3.2. Objectives 62

3.3. Soil Selenium Data Base from Kesterson Reservoir 63

3.3.1. Soil Selenium Fractionation and Speciation Studies 63
3.3.2. Long Term Soil and Soil-Water Selenium Monitoring 68
3.3.3. Pond 11 69
3.3.4. Pond 8EP 72
3.3.5. Annual Synoptic Sampling of Soil Selenium at Kesterson Reservoir 72
3.3.6. Field-Measured Selenium Volatilization Rates at Kesterson Reservoir 75

3.4. Expected Trends in Soil Selenium At Kesterson Reservoir 78

3.5. Predicted Changes in the Selenium Inventory and Distribution 79

3.5.1. Approach and Model Description 80
3.5.2. Computational Procedure 84
3.5.3. Model Calibration Procedure 87
3.5.4. Plot 8EP 87
3.5.5. Plot 11C 90
3.5.6. Prediction of Soil Selenium Concentrations for a Twenty-five Year Period 94

3.6. Use of Model Predictions for Biological Risk Assessment 97

4.0. Offsite Migration of Selenium 103

4.1. Off-Site Soil Sampling (former Freitas Property) 105

4.1.1. Introduction 105
4.1.2. Location, and Sampling Methods 107
4.1.2.1. Location 107
4.1.2.2. Field Methods 108
4.1.2.3. Lab Methods 108
4.1.3. Trace Elements and Conductivity Evaluations 110
4.1.3.1. Electrical Conductivity Values 110
4.1.3.2. Selenium 113
4.1.3.3. Boron 117
4.1.3.4. Molybdenum and Arsenic 117
4.1.4. EC Comparison to 1988,1989–EM Survey 132
4.1.5. Conclusion 132

4.2. Groundwater Quality on the Freitas Ranch 133

4.2.1. Groundwater Sampling and Chemical Analyses Program 133
4.2.2. Spatial and Temporal Trends in Groundwater Quality 135
4.2.3. Speciation of Selenium 142
4.2.4. Recommended Monitoring Plan 142
4.2.5. Summary 145

5.0. Pond 2 Pilot Scale Microbial Volatilization Study: Soil Monitoring 147

5.1. Irrigation, Rototilling, and Rainfall 149

5.2. Soil Monitoring 149

5.2.1. Soil Moisture Conditions 150
5.2.2. Groundwater Level Fluctuations 153

5.3. Soil and Soil Water Selenium and Salt Distribution: Time Trends 156

5.3.1. Soil-Se Along N-S Transects: Spatial and (Early) Temporal Distribution 157

5.3.2. Plot-wide Soil-Se Distribution Based on Subplot Data 162
5.3.3. Temporal and Spatial Trends in Soil-Water Selenium and Salts 162
5.4. Conclusions 171

6.0. Laboratory Accelerations of Soil Selenium Transformations 175
6.1. Field-Sample Collection and Preparation 175
6.2. Experiment Design 177
6.3. Environmental Control 178
6.4. Sampling, Extraction, and Analysis 178
6.5. Initial Selenium Speciation 180
6.6. Results of Quarterly Sampling - Part I 180
6.7. Results of Quarterly Sampling - Part II 185
6.8. Summary 185

7.0. Water Quality in Winter 1992 Ephemeral Pools 193
7.1. Water Quality in Ephemeral Pools Shortly After the Feb. 12, 1992 Rain 193
7.1.1. Data 195
7.1.2. Discussion 195
7.2. Time Trends in Ephemeral Pool Water Quality 201
7.2.1. Data 201
7.2.2. Discussion 201

8.0. Analytical Quality Control - June 1992 215
8.1. Introduction 215
8.2. Measurement Statistics 215
8.3. Operations 215
8.4. Blanks 216
8.5. Selenium Standards 216
8.6. Spike Recoveries 217
8.7. Duplicates 218
8.8. Personnel Change 218

9.0. References 221

List of Figures

Figure 2.1. Location map of the northern Pond 9 soil monitoring sites and surrounding shallow groundwater monitoring wells. 6

Figure 2.2. Particle-size analysis profiles (a) for sites P9C, and (b) for P9R. (The USDA size classes have been used in these delineations.) 8

Figure 2.3. Site P9C soil water sampler selenium data. (a) Soil water selenium concentrations in representative samplings from 1987 to 1991. (b) and (c) Soil water selenium concentrations during 1992. The major storm event which resulted in ponding at this site was on Feb. 12, 1992. 10

Figure 2.4. Site P9R soil water sampler selenium data. (a) Soil water selenium concentrations in representative samplings from 1987 to 1991. (b) and (c) Soil water selenium concentrations during 1992. The major storm event which resulted in ponding at this site was on Feb. 12, 1992. 11

Figure 2.5a. Hydraulic head profiles as measured using tensiometers in plot 8EP. 16

Figure 2.5b. Hydraulic head profiles as measured using tensiometers in plot 9BE. 16

Figure 2.6. Changes in chloride concentrations in soil water of plot 9BE, collected with soil water samplers over a three year period. 17

Figure 2.7. Changes in selenium concentrations in soil water of plot 9BE, collected with soil water samplers over a three year period. 17

Figure 2.8a. Changes in chloride concentrations in soil water in plot 9BE 19

Figure 2.8b. Changes in selenium concentration in soil water of plot 9BE 19

Figure 2.9a. Changes in chloride concentration in soil water of plot 9BE 20

Figure 2.9b. Changes in selenium concentration in soil water of plot 9BE 20

Figure 2.10a. Changes in chloride concentration in soil water of plot 9BE 21

Figure 2.10b. Changes in selenium concentration in soil water of plot 9BE; daily rainfall in upper graph. 21

Figure 2.11. Changes in chloride concentration in soil water of plot 8EP, nest C, collected with soil water samplers over a three year period. 22

Figure 2.12. Changes in selenium concentration in soil water of plot 8EP, nest C, collected with soil water samplers over a three year period. 22

Figure 2.13. Changes in chloride concentration in soil water of plot 8EP, nest ML, collected with soil water samplers from 1/90 through 6/91. 23

Figure 2.14. Changes in selenium concentration in soil water of plot 8EP, nest ML, collected with soil water samplers from 1/90 through 6/91. 23

Figure 2.15. Changes in gravimetric moisture content in the soil profile of plot 8EP, over a three year period. 25

Figure 2.16a. Changes in chloride concentration in plot 8EP, normalized to the mass of soil. 26

Figure 2.16b. Changes in cumulative chloride mass distribution, plot 8EP, normalized to projected soil area. 26

Figure 2.17a. Changes in water-extractable selenium concentration in plot 8EP, normalized to the mass of soil. 27

Figure 2.17b. Changes in cumulative water-extractable selenium mass distribution, plot 8EP, normalized to projected soil area. 27

Figure 2.18. Changes in gravimetric moisture content in the soil profile of plot 9BE, over a three year period. 28

Figure 2.19a. Changes in chloride concentration in plot 9BE, normalized to the mass of soil. 29

Figure 2.19b. Changes in cumulative chloride mass distribution, plot 9BE, normalized to projected area. 29

Figure 2.20a. Changes in water-extractable selenium concentration, plot 9BE, normalized to projected area. 31

Figure 2.20b. Changes in cumulative water-extractable mass distribution, plot 9BE, normalized to projected area. 31

Figure 2.21. Changes in chloride concentration in the top 9 cm of soil in plot 8EP: July 1988 - October 1991. 34

Figure 2.22 Changes in water-extractable selenium in the top 9 cm of soil in plot 8EP: July 1988 - October 1991. 34

Figure 2.23. Changes in chloride concentration in the top 9 cm of soil in plot 9BE: July 1988 - October 1991. 36

Figure 2.24. Changes in water-extractable selenium in the top 9 cm of soil in plot 9BE: July 1988 - October 1991. 36

Figure 2.25. Water content profiles for P3RI at location B. Selected dates were chosen to represent the seasonal trends. 39

Figure 2.26. Chloride concentrations in the top 5 cm of soil at site P3RI. Arrows indicate the main rainy season. 41

Figure 2.27. Water-extractable selenium concentrations in the top 5 cm of soil at site P3RI. Arrows indicate the main rainy season. 41

Figure 2.28. Chloride concentrations in three selected depth intervals at site P3RI location #4. Arrows indicate the main rainy season. 42

Figure 2.29. Water-extractable selenium concentrations in three selected depth intervals at site P3RI location #4. Arrows indicate the main rainy season. 42

Figure 2.30. Mass of chloride in the complete 60 cm soil samples collected at site P3RI over the study period. Arrows indicate the main rainy season. 44

Figure 2.31. Mass of water-extractable selenium in the complete 60 cm soil samples collected at site P3RI over the study period. Arrows indicate the main rainy season. 44

Figure 2.32. Ratio of water-extractable selenium (mg) to chloride (gm) for selected depth intervals at site P3RI location #4. Arrows indicate the main rainy season. 45

Figure 2.33. Map of habitat and trisection delineations at Kesterson Reservoir (CH2M-Hill, 1991). 48

Figure 2.34. Geometric mean value for the ratio of water-extractable to total selenium concentrations in the top 15 cm of the soil profile. The ratio in 1991 is significantly higher than the ratio in either 1989 or 1990, representing a 43% increase over the three-year monitoring period. 52

Figure 2.35. Geometric mean value for the ratio of selenite to water-extractable selenium concentrations in the top 15 cm of the soil profile. The ratio shows a significant decrease of 42% between 1989 and 1991, and a significant decrease of 58% between 1990 and 1991. 53

Figure 2.36 Geometric mean chloride concentrations in the top 15 cm of the soil profile. Chloride concentrations show a significant decrease of 60% between 1989 and 1990, and a significant increase of 56% between 1990 and 1991. 54

Figure 2.37. Mean sulfate concentrations in the top 15 cm of the soil profile. The sulfate inventory is significantly decreasing over the three-year monitoring period. 55

Figure 2.38. Distribution and range of selenium concentrations in the top 15 cm of the soil profile (1991) by habitat delineations. 56

Figure 2.39. Range and geometric mean values of total selenium concentrations in the top 15 cm of the soil profile. 57

Figure 2.40. Range and geometric mean values of total water-extractable selenium concentrations in the top 15 cm of the soil profile. 58

Figure 2.41. Range and geometric mean values of the ratio of water-extractable selenium to total selenium concentrations in the top 15 cm of the soil profile. 59

Figure 3.1a. Illustrative example showing the dominant forms of selenium in two Kesterson soils. These data were collected from former cattail habitat in Pond 2 (now open habitat) in November, 1990. Data illustrated in the top panel are from the surface soil (0 -0.10 m) and the lower panel from a sub-soil (0.45 - 0.5 m). 66

Figure 3.1b. Illustrative example showing the dominant forms of selenium in two Kesterson soils. These data were collected from re-vegetated playa habitat in Pond 9 (now grassland habitat) in November, 1990. Data illustrated in the top panel are from the surface soil (0 -0.10 m) and the lower panel from a sub-soil (0.45 - 0.5 m). 67

Figure 3.1c. Illustrative example showing the dominant forms of selenium in two Kesterson soils. These data were collected from grassland habitat in Pond 11 in November, 1990. Data illustrated in the top panel are from the surface soil (0 -0.10 m) and the lower panel from a sub-soil (0.45 - 0.5 m). 68

Figure 3.2a. Time trends in electrical conductivity (EC) of the soil solution at experimental plot 11C in the southwest corner of former Pond 11. 70

Figure 3.2b. Time trends in soil solution selenium concentrations at experimental plot 11C in the southwest corner of former Pond 11. 70

Figure 3.3a and 3.3b. Time trends in water-extractable selenium concentrations at experimental plot 11C in the southwest corner of former Pond 11. (a) water-extracted selenium [mg/(kg-dry soil)] and (b) depth integrated water-extractable selenium (mg/m2) 71

Figure 3.4a. Time trends in water-extractable chloride concentrations in the top 9 cm at experimental plot 8EP in the north east corner of former Pond 8. 73

Figure 3.4b. Time trends in water-extractable selenium concentrations in the top 9 cm at experimental plot 8EP in the north east corner of former Pond 8. 73

Figure 3.5. Time trends in water-extractable selenium concentrations at experimental plot 8EP in the north east corner of former Pond 8. Error bars represent cumulative error from three replicates to a depth of 1 m. No replicates are available below this depth. 74

Figure 3.6. Geometric mean total selenium concentrations in the top 0.15 m of soil from 54 samples collected as part of the synoptic sampling for 1989, 1990 and 1991. Note that no significant changes in the inventory of total selenium in the top 0.15 m have been observed over this period. 76

Figure 3.7. Geometric mean water-extractable selenium concentrations in the top 0.15 m of soil from 54 samples collected as part of the synoptic sampling for 1989, 1990 and 1991. Note that no significant changes in the reservoir-wide water-extractable selenium has been observed over this period. 77

Figure 3.8. Geometric mean value for the ratio of water-extractable to total selenium concentrations in the top 0.15 m of soil from 54 samples collected as part of the synoptic sampling for 1989, 1990 and 1991. Note that a significant increase in this ratio was observed from 1989 to 1991 and from 1990 to 1991. 78

Figure 3.9 Schematic illustrating the distribution of water-extractable selenium concentrations in 1987, 1991 and under predicted future conditions. 80

Figure 3.10. Illustration of the three subunits that the top 2 m of Kesterson soils have been divided into for model calibration and prediction. 81

Figure 3.11 Illustration indicating the dominant processes affecting the selenium inventory within each of the three subunits of the model. 83

Figure 3.12. Flow chart for the mass balance model used to calibrate and predict the future behavior of selenium in Kesterson soils: data input and program initialization. 85

Figure 3.13. Flow chart for the mass balance model used to calibrate and predict the future behavior of selenium in Kesterson soils: calculation algorithm. 86

Figure 3.14. Comparison between measured and calculated water-extractable selenium concentrations in the top 0.15 m of soil at Plot 8EP. 89

Figure 3.15. Comparison between measured and calculated water-extractable selenium concentrations in the depth interval of 0.15 to 1 m of soil at Plot 8EP. 90

Figure 3.16. Comparison between measured and calculated water-extractable selenium concentrations in the depth interval of 1 to 2 m of soil at Plot 8EP. 91

Figure 3.17. Comparison between measured and calculated water-extractable selenium concentrations in the top 0.15 m of soil at Plot 11C. 92

Figure 3.18. Comparison between measured and calculated water-extractable selenium concentrations in the depth interval of 0.15 to 1 m of soil at Plot 11C. 92

Figure 3.19. Comparison between measured and calculated water-extractable selenium concentrations in the depth interval of 1 to 2 m of soil at Plot 11C. 93

Figure 3.20. Comparison between measured and calculated inventories of water-extractable selenium in the top 2 m of soil in Plot 11C (note that inventories are expressed as grams of selenium per m2). 93

Figure 3.21. Predicted concentrations of water-extractable selenium in the top 0.15 m of soil at Kesterson Reservoir for the cases listed in Table 3.5. 97

Figure 3.22. Predicted concentrations of water-extractable selenium in the depth interval from 0.15 to 1 m at Kesterson Reservoir for the cases listed in Table 3.5. 98

Figure 3.23. Predicted inventories of water-extractable selenium in the top 2 m of soil at Kesterson Reservoir for the cases listed in Table 3.5. 99

Figure 3.24. Predicted concentrations of total selenium in the top 0.15 m of soil at Kesterson Reservoir for the initial conditions and cases listed in Tables 3.6 and Table 3.7, respectively. 100

Figure 3.25. Predicted concentrations of total selenium in the 0.15 to 1 m depth interval at Kesterson Reservoir for the initial conditions and cases listed in Tables 3.6 and Table 3.7, respectively. 101
Figure 4.1a. Off-site soil sampling points. 106
Figure 4.1b. Freitas Property water table levels (meters above mean sea level). 107
Figure 4.2a. Depth of soil sample and local water table (southern transect). 109
Figure 4.2b. Depth of soil sample and local water table (central transect). 109
Figure 4.2c. Depth of soil sample and local water table (northern transect). 110
Figure 4.3a. Average electrical conductivities by transect from San Luis Drain outward along transects. 113
Figure 4.3b. Electrical conductivities for soil samples 1-4 (southern transect). 114
Figure 4.3c. Electrical conductivities for soil samples 5–8(southern transect). 114
Figure 4.3d. Electrical conductivities for soil sample 9 (southern transect). 115
Figure 4.3e. Electrical conductivities for soil samples 1–4 central transect). 115
Figure 4.3f. Electrical conductivities for soil samples 5–8(central transect). 116
Figure 4.3g. Electrical conductivities for soil samples 1–4 (northern transect). 116
Figure 4.3h. Electrical conductivities for soil samples 5–10 (northern transect). 117
Figure 4.4a. Average water extractable selenite concentrations (ppb) by transect from San Luis Drain outward along transect. 118
Figure 4.4b. Average water extractable selenium concentrations (ppb) by transect from San Luis Drain outward along transect. 118
Figure 4.4c. Water-extractable selenite concentrations (ppb) soil samples 1–4 (southern transect). 119
Figure 4.4d. Water-extractable selenite concentrations (ppb) soil sample 7 (southern transect). 119
Figure 4.4e. Water-extractable selenite concentrations (ppb) soil samples 5–9 (southern transect). 120
Figure 4.4f. Water-extractable selenium concentrations (ppb) soil samples 1–4 (southern transect). 120
Figure 4.4g. Water-extractable selenium concentrations (ppb) soil samples 5–8 (southern transect). 121
Figure 4.4h. Water-extractable selenium concentrations (ppb) soil samples 7 and 9 (southern transect). 121
Figure 4.4i. Water-extractable selenite concentrations (ppb) soil samples 1–4 (central transect). 122
Figure 4.4j. Water-extractable selenite concentrations (ppb) soil samples 5–7 (central transect). 122
Figure 4.4k. Water-extractable selenium concentrations (ppb) soil samples 1–4 (central transect). 123
Figure 4.4l. Water-extractable selenium concentrations (ppb) soil samples 5–7 (central transect). 123
Figure 4.4m. Water-extractable selenite concentrations (ppb) soil samples 1–4 (northern transect). 124

Figure 4.4n. Water-extractable selenite concentrations (ppb) soil samples 5–10 (northern transect). 124

Figure 4.4o. Water-extractable selenium concentrations (ppb) soil samples 1–4 (northern transect). 125

Figure 4.4p. Water-extractable selenium concentrations (ppb) soil samples 5–8 (northern transect). 125

Figure 4.4q. Water-extractable selenium concentrations (ppb) soil samples 9 and 10 (northern transect). 126

Figure 4.5a. Average boron water-extractable concentrations (ppm) by transect from San Luis Drain outward along transect. 126

Figure 4.5b. Water-extractable boron concentrations (ppm) cores 1–4 (southern transect). 127

Figure 4.5c. Water-extractable boron concentrations (ppm) cores 1–4 (southern transect). 127

Figure 4.5d. Water-extractable boron concentrations (ppm) core 9 (southern transect). 128

Figure 4.5e. Water-extractable boron concentrations (ppm) cores 1–4 (central transect). 128

Figure 4.5f. Water-extractable boron concentrations (ppm) cores 5–7 (southern transect). 129

Figure 4.5g. Water-extractable boron concentrations (ppm) cores 1–4 (northern transect). 129

Figure 4.5h. Water-extractable boron concentrations (ppm) cores 5–10 (northern transect). 130

Figure 4.6a. Water-extractable arsenic concentrations (ppb) cores 1, 2, 3, 4, 5, 8, and 9 (southern transect). 130

Figure 4.6b. Water-extractable arsenic concentrations (ppb) cores 6 and 7 (southern transect). 131

Figure 4.7. Location of soil sample points, (southern and central transects), and EM survey transects. 131

Figure 4.8. Map showing the location of monitoring ells on the Freitas Ranch. 134

Figure 4.9. Electrical conductivity of groundwater along transects perpendicular to the San Luis Drain for December 1990. 137

Figure 4.10. Electrical conductivity of groundwater along transects perpendicular to the San Luis Drain for May 1990. 138

Figure 4.11. Boron concentrations in groundwater along transects perpendicular to the San Luis Drain for December 1990. 139

Figure 4.12. Boron concentrations in groundwater along transects perpendicular to the San Luis Drain for May 1990. 140

Figure 4.13. The ratio of the boron concentration in 1992 to the boron concentration in 1990 along transects perpendicular to the San Luis Drain. 141

Figure 4.14. Concentrations of selenite in groundwater for both 1990 and 1992., plotted as a function of distance from the San Luis Drain. 143

Figure 4.15. Concentrations of total selenite in groundwater for both 1990 and 1992., plotted as a function of distance from the San Luis Drain. 144

Figure 5.1. Pond 2 (Pilot Scale) Volatilization Site (P2VS). 148

Figure 5.2. Irrigation and rainfall in plot P2VS between 10/90 and 12/91. 149

Figure 5.3. Cumulative irrigation and rainfall in plot P2VS between 10/90 and 12/91. 150

Figure 5.4. Hydraulic head distribution in the irrigated treatment as measured by tensiometers in nest I2. Hydraulic head was beyond the measurable range for the remainder of 1991. 151

Figure 5.5. Hydraulic head distribution in the irrigated/disked treatment as measured by tensiometers in nest ID1. 151

Figure 5.6. Hydraulic head distribution in the disked treatment as measured by tensiometers in nest D2. 152

Figure 5.7. Hydraulic head distribution in the control treatment as measured by tensiometers in nest C2. Hydraulic head was beyond the measurable range for the remainder of 1991. 152

Figure 5.8. Volumetric moisture content as estimated via neutron probe measurements, as a function of depth in well W-i, irrigated treatment. 154

Figure 5.9. Volumetric moisture content as estimated via neutron probe measurements, as a function of depth in well W-id, irrigated/disked treatment. 154

Figure 5.10. Volumetric moisture content as estimated via neutron probe measurements, as a function of depth in well W-d, disked treatment. 155

Figure 5.11. Volumetric moisture content as estimated via neutron probe measurements, as a function of depth in well W-i, irrigated treatment. 155

Figure 5.12. Depths to the water table relative to the soil surface in wells W-i, W-id, W-d, and W-c. 156

Figure 5.13. Water table elevation relative to mean sea level in wells W-i, W-id, W-d, and W-c. 157

Figure 5.14. Total soil selenium in the irrigated treatment along a roughly N-S transect, 7/90 and 7/91. 158

Figure 5.15. Total soil selenium in the irrigated/disked treatment along a roughly N-S transect, 7/90 and 7/91. 159

Figure 5.16. Total soil selenium in the disked treatment along a roughly N-S transect, 7/90 and 7/91. 160

Figure 5.17. Total soil selenium in the control treatment along a roughly N-S transect, 7/90 and 7/91. 161

Figure 5.18. Water-extractable selenium (from 1:5 soil:water extracts), normalized to soil mass, in the irrigated treatment along a roughly N-S transect, 7/90 and 7/91. 163

Figure 5.19. Water-extractable selenium (from 1:5 soil:water extracts), normalized to soil mass, in the irrigated/disked treatment along a roughly N-S transect, 7/90 and 7/91. 164

Figure 5.20. Water-extractable selenium (from 1:5 soil:water extracts), normalized to soil mass, in the controlled treatment along a roughly N-S transect, 7/90 and 7/91. 165

Figure 5.21. Results of survey of soil surface of plot P2VS. 166

Figure 5.22. Contour maps of total selenium in the 0-15 cm and 15-30 cm depth intervals, based on subplot data from 9/90. 167

Figure 5.23. Contour maps of total selenium in the 30-45 cm and 45-60 cm depth intervals, based on subplot data from 9/90. 168

Figure 5.24. Soil-water selenium, as sampled via soil-water samplers in nest i2, irrigated treatment. 169

Figure 5.25. Soil-water EC, as sampled via soil-water samplers in nest i2, irrigated treatment. 169

Figure 5.26. Soil-water selenium, as sampled via soil-water samplers in nest id1, irrigated/disked treatment. 170

Figure 5.27. Soil-water EC, as sampled via soil-water samplers in nest id1, irrigated/disked treatment. 170

Figure 5.28. Soil-water selenium, as sampled via soil-water samplers in nest d2, disked treatment. 172

Figure 5.29. Soil-water EC, as sampled via soil-water samplers in nest d2, disked treatment. 172

Figure 5.30. Soil-water selenium, as sampled via soil-water samplers in nest c2, control treatment. 173

Figure 5.31. Soil-water EC, as sampled via soil-water samplers in nest c2, control treatment. 173

Figure 6.1. Relative growth rates of psychrophiles, mesophiles, and thermophiles as a function of temperature (from Brock, 1970). 176

Figure 6.2. Incubator and room temperature over the first 144 days of the experiment. 179

Figure 6.3. Initial fractionation of selenium in soils from plot P2VS: P2A - 0.00-0.10 m and P2B - 0.45-0.55 m. 181

Figure 6.4. Initial fractionation of selenium in soils from plot P9TM: P9A - 0.00-0.10 m and P9B - 0.45-0.55 m. 182

Figure 6.5. Initial fractionation of selenium in soils from plot P11TM: P11A - 0.00-0.10 m and P11B - 0.45-0.55 m. 183

Figure 6.6a. Changes in selenium speciation in soil P2A, at 0.3 bar, initial extracts vs. extracts after 3 months of incubation. Error bars denote one standard deviation. 186

Figure 6.6b. Changes in selenium speciation in soil P2A, at 5 bar, initial extracts vs. extracts after 3 months of incubation. Error bars denote one standard deviation. 186

Figure 6.7a. Changes in selenium speciation in soil P2B, at 0.3 bar, initial extracts vs. extracts after 3 months of incubation. Error bars denote one standard deviation. 187

Figure 6.7b. Changes in selenium speciation in soil P2B, at 5 bar, initial extracts vs. extracts after 3 months of incubation. Error bars denote one standard deviation. 187

Figure 6.8a. Changes in selenium speciation in soil P9A, at 0.3 bar, initial extracts vs. extracts after 3 months of incubation. Error bars denote one standard deviation. 188

Figure 6.8b. Changes in selenium speciation in soil P9A, at 5 bar, initial extracts vs. extracts after 3 months of incubation. Error bars denote one standard deviation. 188

Figure 6.9a. Changes in selenium speciation in soil P9B, at 0.3 bar, initial extracts vs. extracts after 3 months of incubation. Error bars denote one standard deviation. 189

Figure 6.9b. Changes in selenium speciation in soil P9B, at 5 bar, initial extracts vs. extracts after 3 months of incubation. Error bars denote one standard deviation. 189

Figure 6.10a. Changes in selenium speciation in soil P11A, at 0.3 bar, initial extracts vs. extracts after 3 months of incubation. Error bars denote one standard deviation. 190

Figure 6.10b. Changes in selenium speciation in soil P11A, at 5 bar, initial extracts vs. extracts after 3 months of incubation. Error bars denote one standard deviation. 190

Figure 6.11a. Changes in selenium speciation in soil P11B, at 0.3 bar, initial extracts vs. extracts after 3 months of incubation. Error bars denote one standard deviation. 191

Figure 6.11b. Changes in selenium speciation in soil P11B, at 5 bar, initial extracts vs. extracts after 3 months of incubation. Error bars denote one standard deviation. 191

Figure 6.12. Changes in selenium speciation in Part II, initial extracts vs. extracts after 1 "modeled" year, or 20 real weeks. 192

Figure 7.1. (a) Yearly cumulative rainfall at Kesterson Reservoir. The data are primarily from the USBR weather station, supplemented with CIMIS records. (b) Monthly total rainfall at Kesterson Reservoir. 194

Figure 7.2. Selenium concentrations in various surface waters sampled within the first 10 days after the 2-12-92 rain storm. The data are ordered according to general locations within Kesterson Reservoir. 199

Figure 7.3. Estimated probability of exceeding particular selenium concentrations in the initially sampled February 1992 surface waters. 199

Figure 7.4. (a) Histogram of selenium concentrations in February 1992 surface water samples. (b) Close-up of data from (a) with [Se] ≤ 50 μg L-1. 200

Figure 7.5. Correlations between selenium and EC in Kesterson Reservoir, February 1992 surface waters. The diagonal line represents the case where the original (pre-closure) seleniferous drainwaters are diluted with rain water or evaporatively concentrated. 202

Figure 7.6. Locations of pools sampled for water quality time trends. 204

Figure 7.7. Pond 1 ephemeral pool time trends in (a) salinity (as indicated by EC), and (b) total selenium. Pools at P 1 UZ3 and P1 UZ5 formed over the original Kesterson Reservoir soils. Pools P1 fp 5 and P1 fp H formed over fill soil. 205

Figure 7.8. Pond 3 ephemeral pool time trends in (a) salinity (as indicated by EC), and (b) total selenium. With the possible exception of site P3 NNW, these pools formed over fill soil. 206

Figure 7.9. Pond 4 ephemeral pool time trends in (a) salinity (as indicated by EC), and (b) total selenium. The P4 N pool formed over original Kesterson Reservoir soils in cattail litter. The P4 W pool formed over fill soil. 207

Figure 7.10. Pond 5 ephemeral pool time trends in (a) salinity (as indicated by EC), and (b) total selenium. Both the P5 S and P5 W pools formed over original Kesterson Reservoir soils in a mix of cattail litter and Bassia. 208

Figure 7.11. Pond 6 ephemeral pool time trends in (a) salinity (as indicated by EC), and (b) total selenium. All P6S12 data are from the 1 ft excavation test plot. This site was previously vegetated with cattails, but has been maintained as a bare soil since 1987. The 6 PB site is filled. The 6 PC site is on original Kesterson Reservoir soil, sparsely vegetated with annual grasses and Bassia. 209

Figure 7.12. Pond 9 ephemeral pool time trends in (a) salinity (as indicated by EC), and (b) total selenium. Site P9BE is on original Kesterson Reservoir soil. Sites P9 H, P9 E, and P9 S are on fill soil. 210

Figure 7.13. Pond 10 ephemeral pool time trends in (a) salinity (as indicated by EC), and (b) total selenium. The data shown here are all from filled areas. 211

Figure 7.14. Pond 10 GC and GS ephemeral pool time trends in salinity (as indicated by EC). (a) Salinity data in ephemeral pools sampled since 1987. (b) Salinity in the sites during 1992. The time interval during which surface waters connected the two sites are indicated in (b). 212

Figure 7.15. Pond 10 GC and GS ephemeral pool time trends in selenium. (a) Selenium data in ephemeral pools sampled since 1987. (b) Selenium concentrations in the site surface waters during 1992. The time interval during which surface waters connected the two sites are indicated in (b). 213

Figure 7.16. Pond 11 ephemeral pool time trends in (a) salinity (as indicated by EC), and (b) total selenium. Sites P11S6 and P11S12 are on excavated Kesterson Reservoir soils. The P11,UCR site is the former Pond 11 selenium volatilization test area operated by Dr. Frankenberger of U.C. Riverside. 214

Figure 8.1. Control chart for selenite. 219

Figure 8.2. Control chart for total selenium. 220

List of Tables

Table 2.1. Mean values of profile-averaged gravimetric moisture content, chloride and water-extractable selenium concentrations, and changes relative to the previous year. 32

Table 2.2. Summary of soil selenium concentrations in the top 15 cm of the soil profile over the three-year sampling period. 51

Table 3.1. Geometric mean concentrations of total selenium, water-extractable selenium, sulfate and chloride in the top 0.15 m of soil from 54 samples collected annually as part of the biological monitoring program. Within a column, values sharing the same letters are not significantly different at the 95% confidence level. 75

Table 3.2. Summary of field-measured selenium volatilization rates from untreated soils at Kesterson Reservoir. 79

Table 3.3 Summary of soil selenium concentrations in Plot 8EP from 1988 to 1991. 88

Table 3.4. Summary of leaching and remobilization rate constants determined from Plot 8EP and 11C. 88

Table 3.5. Summary of soil selenium concentrations in Plot 11C from 1988 to 1991. 91

Table 3.6. Initial conditions used to compute future trends in soil-selenium concentrations at Kesterson Reservoir. 95

Table 3.7. Initial conditions and rate constants used to compute changes in soil-selenium concentrations. 95

Table 4.1. Transect, point naming, and location. 108

Table 4.2a. Southern transect. Plant identification and approximate cover (rough estimate). 111

Table 4.2b. Central transect. Plant identification and approximate cover. 112

Table 4.2c. Northern transect. Plant identification and approximate cover. 112

Table 4.3. Tabulated values of electrical conductivity, selenite (SE(IV)), total selenium, and boron concentrations for wells on the Freitas Ranch. 136

Table 6.1. Gravimetric moisture content and moisture release curve of P2A,B, P9A,B, and P11A,B soils 176

Table 6.2 Schedule for soil treatment in Part II. 178

Table 6.3. Sampling and extraction frequency for incubated soils 179

Table 6.4. Initial selenium fractionation in soils (all values in ppm) 184

Table 7.1. Summary of surface water samples collected between February 15 and February 21, 1992 196

Table 7.2. Summary of the soil type (habitat) and dominant vegetation at the surface water sampling sites illustrated in Figure 7.6 203

Table 8.1. Selenium standard statistics 6/6/90 - 10/30/91 217

Table 8.2. Selenium standard statistics 3/12/91 - 6/10/92 217

Acknowledgment

We thank Mike Delamore and Art Tuma of the U. S. Bureau of Reclamation for their continued support. In addition, we thank Robert Giauque at LBL for the many XRF analyses he has performed over the last seven years. Thanks are also due to Rich McClimans, Steve Stehman and Gil Pontius of SUNY College of Environmental Sciences and Forestry for overseeing and guiding the Masters Thesis work of Carolyn Wahl.

Most importantly we thank Ellen Klahn for outstanding work in preparing this report and others like it published over the last five years. Thanks are also due to Nigel Quinn and Harold Wollenberg at LBL for the review and comments on this report.

This work as supported by the U. S. Bureau of Reclamation, under U. S. Department of Interior Interagency Agreement No. 9-AA-20-07250, through U. S. Department of Energy Contract No. DE-AC03-76SF00098.

1.0. Introduction

This report describes work carried out at Kesterson Reservoir by scientists and engineers from Lawrence Berkeley Laboratory over the two-year period from October 1990 to September 1992. Efforts described in this report include the following:

- Results from vadose zone monitoring of selenium and salt transport at numerous locations throughout Kesterson Reservoir (Chapter 2);
- Quantitative analysis of the biogeochemical evolution of selenium in surfaces soils at Kesterson, including discussion of implications for biological exposure to selenium (Chapter 3);
- Measurement and analysis of the first two comprehensive data sets on soil and groundwater quality on the former Freitas Ranch (Chapter 4);
- Preliminary results from the pilot-scale selenium volatilization experiment in Pond 2 (Chapter 5);
- Evaluation of the rates of selenium transformation from one species to another based on laboratory experiments (Chapter 6);
- Data on water quality in surface water pools that formed from ponded rainwater during the winters of 1990-1991 and 1991-1992 (Chapter 7); and
- Quality control and assurance statistics on our analytical laboratory (Chapter 8).

In addition to the information provided here, we have published the following articles in a variety of journals over the past two years.

- Benson, S. M., A. F. White, S. F. Halfman, S. Flexser, and M. Alavi, 1991. Groundwater contamination at Kesterson Reservoir, California, Part 1. Hydrogeologic setting and conservative solute transport, *Water Resources Research, 27,* (6) 1071-1084.
- Benson, S. M., M. Delamore, and S. Hoffman, 1990. Kesterson Crisis: Sorting out the facts. In S. C. Harris (ed.) Irrigation and Drainage Proceedings of the 1990 National Conference. American Society of Civil Engineers, New York.

  Ita, S. P., and S. M. Benson, 1992. Field investigation of the effect of rainfall infiltration on soil selenium and salinity at Kesterson Reservoir, in Earth Sciences Division Annual Report, Lawrence Berkeley Laboratory Report, LBL -31500, Berkeley, CA.
- Lawrence Berkeley Laboratory, 1990b. Hydrological and Geochemical Investigations of Selenium Behavior at Kesterson Reservoir, Lawrence Berkeley Laboratory Report, LBL-29689, Berkeley, CA.
- Long, R. H., S. M. Benson, T. K. Tokunaga, and T. N. Narasimhan, 1990. Selenium immobilization in a pond bottom sediment at Kesterson Reservoir, *Journal of Environmental Quality, 19,* (2) 302-311.

- Poister, D, and T. K. Tokunaga, 1992. Selenium in Kesterson Reservoir ephemeral pools formed by groundwater rise: II. Laboratory experiments, *Journal of Environmental Quality, 21,* 252-258.

- Tokunaga, T. K., and S. M. Benson, 1992. Selenium in ephemeral pools formed by groundwater rise at Kesterson Reservoir: I. Field study, *Journal of Environmental Quality, 21,* 246-251.

- Tokunaga, T. K., D. S. Lipton, S. M. Benson, A. W. Yee, J. M. Oldfather, E. C. Duckart, P. W. Johannis, and K. Halvorsen, 1991. Soil selenium fractionation , depth profiles and time trends in a vegetated site at Kesterson Reservoir, *Water, Air and Soil Pollution, 57-58,* 31-41.

- Wahl, C., 1992. Analysis of Temporal and Spatial Trends in Soil Selenium Concentrations at Kesterson Reservoir, Merced County, California, M. S. Thesis, State University of New York, Syracuse, New York.

- White, A. F., S. M. Benson, A. W. Yee, H. A. Wollenberg, and S. Flexser, 1991. Groundwater contamination at Kesterson Reservoir, California, Part 2. Geochemical parameters influencing selenium mobility, *Water Resources Research, 27,* (6) 1085-1098.

- Zawislanski, P., T. Tokunaga, S. Benson, J. Oldfather and T. N. Narasimhan, 1992. Bare Soil evaporation and solute movement of selenium in contaminated soils at Kesterson Reservoir, California, *Journal of Environmental Quality, 21,* 447-457

2.0. Vadose Zone Monitoring

Since 1987, soil water selenium concentrations in the vadose zone have been monitored in a variety of habitats at Kesterson. These data provide the single-most valuable information on the rate of transformation of insoluble to soluble forms of selenium and on the physical transport of soluble selenium in the soil profile. Specific activities carried out over the past two years and described here include the following:

- Soil water monitoring in the north portion of Pond 9 which demonstrates transport of selenium below the water table (Section 2.1);
- Soil selenium and salinity monitoring which demonstrate the role of rainfall and evaporation on solute transport in the soil profile (Section 2.2);
- Surface soil monitoring data which demonstrate gradual declines in salt and soluble selenium concentrations due to rainfall infiltration (Section 2.3);
- Soil water selenium data demonstrate the role of rainfall infiltration on transport of selenium deep in the vadose zone (Section 2.4); and
- Reservoir-wide soil selenium monitoring that provides an overall status of the selenium inventory at Kesterson (Section 2.5).

2.1. Soil Water Monitoring in the Northern Portion of Pond 9

Tetsu Tokunaga and Paul Johannis
Earth Sciences Division
Lawrence Berkeley Laboratory

Observations of elevated selenium concentrations in shallow groundwater monitoring wells in the northern corner of Pond 9 (USBR, Oct. 15, 1992) indicate the importance of soil and groundwater interactions. In shallow groundwaters sampled from the four wells surrounding the northern Pond 9 soil monitoring sites, and screened in the 3.0 to 4.6 m (10 to 15 ft) depths, selenium concentrations have ranged from 2 to 10 $\mu g\ L^{-1}$ (ppb) prior to the February 1992 rain storms. Following the storms, selenium concentrations in these wells ranged from 6 to 175 $\mu g\ L^{-1}$. Such observations of elevated selenium concentrations in groundwaters at Kesterson Reservoir have been limited to this portion of Pond 9 and to the area along the western edge of Pond 2. Groundwater samples collected from deeper monitoring wells (9.1 to 10.6 m, or 30 to 35 ft screened intervals) at the northern Pond 9 area do not exhibit elevated selenium concentrations. In these deeper wells, selenium concentrations are generally $\leq 1.0\ \mu g\ L^{-1}$.

Although elevated selenium concentrations have not been detected in the numerous other monitoring wells, information from the northern Pond 9 area wells and soil water samplers provide valuable information for understanding conditions under which significant selenium transport into groundwater is possible. Soil water quality data from the monitoring sites in the northern area of Pond 9 have been collected since February 1987. Thus, a unique data set is available with which to begin evaluation of post-closure selenium transport from Kesterson Reservoir soils into groundwaters. In this chapter, selenium data collected between 1987 and 1992 from two northern Pond 9 monitoring sites are reviewed. These are sites P9C and P9R. (Data from a third site, P9D, will not be included since it is relatively incomplete.) Locations of these sites are indicated in Figure 2.1. It will be shown that the soil water data and soil properties do in fact indicate that the area is relatively susceptible to leaching of selenium into shallow groundwaters. This is because of both high concentrations of soluble selenium in deeper portion of the soil profiles, and because of shallow depths to highly permeable sands. It will be shown that these factors are consistent with both the long-term observation of moderately high selenium concentrations in these groundwaters, and the more recently observed pulse of higher selenium concentrations appearing in the monitoring wells.

2.1.1. Site Description

The northern Pond 9 region was an extensive playa environment during active use of Kesterson Reservoir for disposal of seleniferous drain waters (1981-1986). Beginning in 1987, the area quickly revegetated with invading annual shrubs (probably with Kochia scoparia in 1987, followed by Bassia hyssopifolia in 1988). Site P9C is a monitoring site in which invading vegetation was permitted to grow

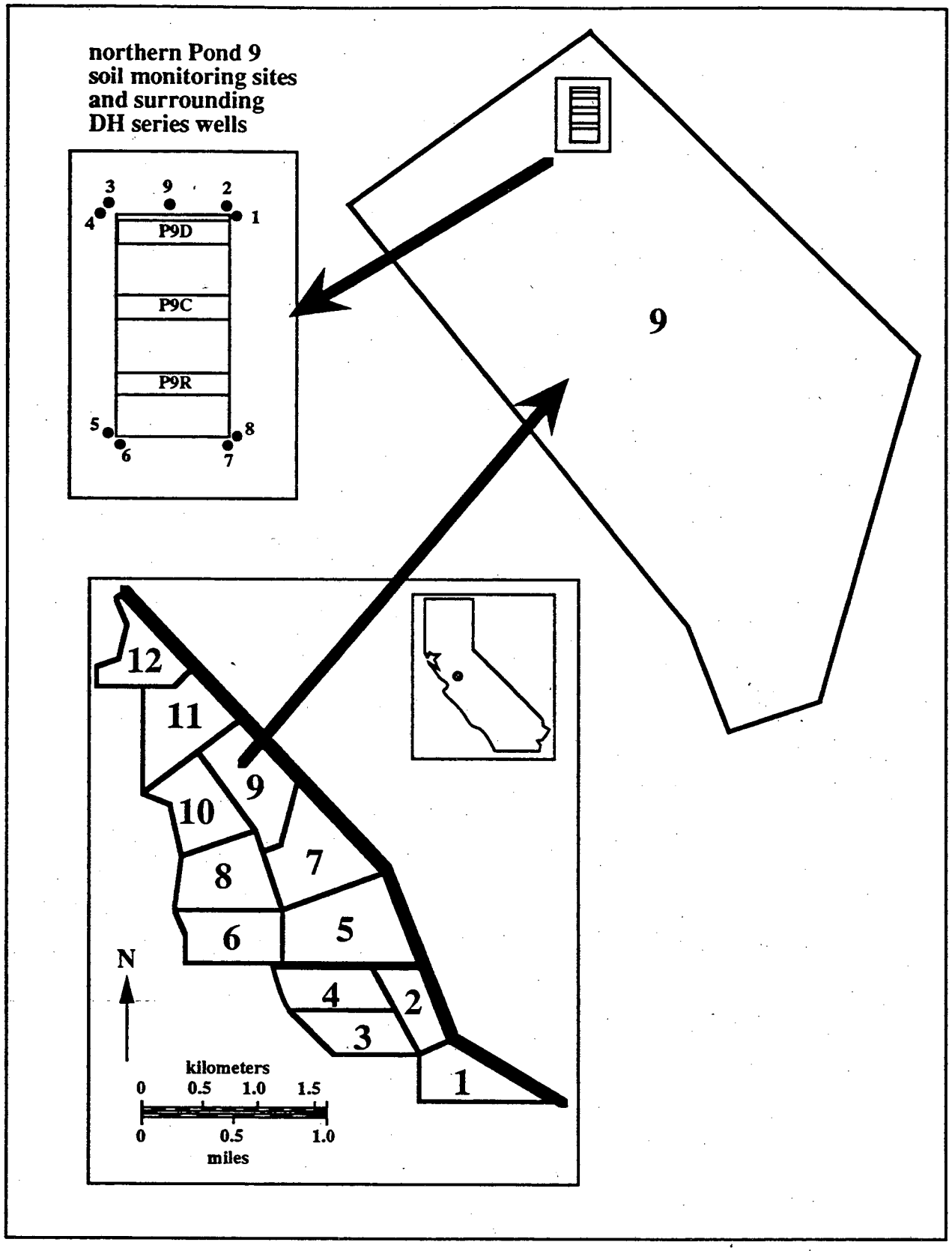

Figure 2.1. Location map of the northern Pond 9 soil monitoring sites and surrounding shallow groundwater monitoring wells.

without significant disturbance. Site P9R is a monitoring site which has been maintained under devegetated conditions. While some distinctions may be observed between the two sites, the similarities are more relevant for the purpose of addressing the occurrence of selenium, in shallow groundwaters of the area.

Although site characteristics of the northern Pond 9 soils have been described in previous reports (e.g., LBL, 1987; LBL, 1988), the more pertinent physical features with respect to selenium transport will be reviewed in this section. While much of this area was filled during the summer of 1988, some of the more important information concerning soil properties are associated with the underlying Kesterson Reservoir soils. Field observations prior to filling strongly suggest that about 0.3 m (1 ft) of the surface soil in much of this area was previously removed, perhaps for use in berms bordering Pond 9. In addition, the depth of remaining sandy loam surface soil in this area appears to be relatively shallow in some locations. Particle-size profiles for sites P9C and P9R are shown in Figures 2.2 a and b respectively. Note that at site P9R, the soil is 80% to 90% sand below depths of 1.1 m. Although the two profiles shown are the only set of particle-size data for this portion of Pond 9, it is reasonable to expect that some profiles in this region would have even shallower depths to sands. Since highly permeable sands occur immediately below the surface soil, shallow thicknesses of the latter are conducive to rapid leaching of soil water during the wet season. The present data set on particle-size profiles is insufficient for inferring the distribution of soil thicknesses and permeabilities. Nevertheless, it is of interest to note that the P9R soil monitoring site, which has the shallowest depth to sands, is closest to the two wells which exhibited the highest shallow groundwater selenium concentrations. Wells DH9-5 and DH9-8 have yielded shallow groundwater selenium concentrations as high as 175 and 103 $\mu g\ L^{-1}$ respectively. (Refer to Figure 2.1 for locations.)

A secondary feature of the surface soil in this, and many other areas of Kesterson Reservoir, is the presence of macropores resulting from shrinkage during drying cycles, root channels, and boundaries between stable soil aggregates. Macropore networks provide more rapid downwards transport of waters ponding at the soil surface during rainstorms. While downwards leaching of salts and selenium does occur through these channels as well as through bulk soil aggregates, the efficiency of solute displacement may be limited. This is because only a small fraction of the solute inventory is quickly displaced when water flow is largely restricted to a network of macropores which have limited interactions with solutes within aggregate interiors. Because of the very high soluble selenium concentrations in the soil pore waters, even a small fraction of such pore waters displaced deeper without reduction can result in significant increases in selenium concentrations in shallow groundwaters.

A topographic effect associated with fill soils surrounding native Kesterson Reservoir soils may have also contributed to the observed increases in selenium in shallow monitoring wells following the February 1992 rains. The monitoring sites and the DH series shallow wells shown in Figure 2.1 are all located in unfilled soils. However, the areas immediately surrounding these monitoring sites and wells have been filled with at least 0.15 m (0.5 ft) of imported soil. This configuration may enhance leaching of

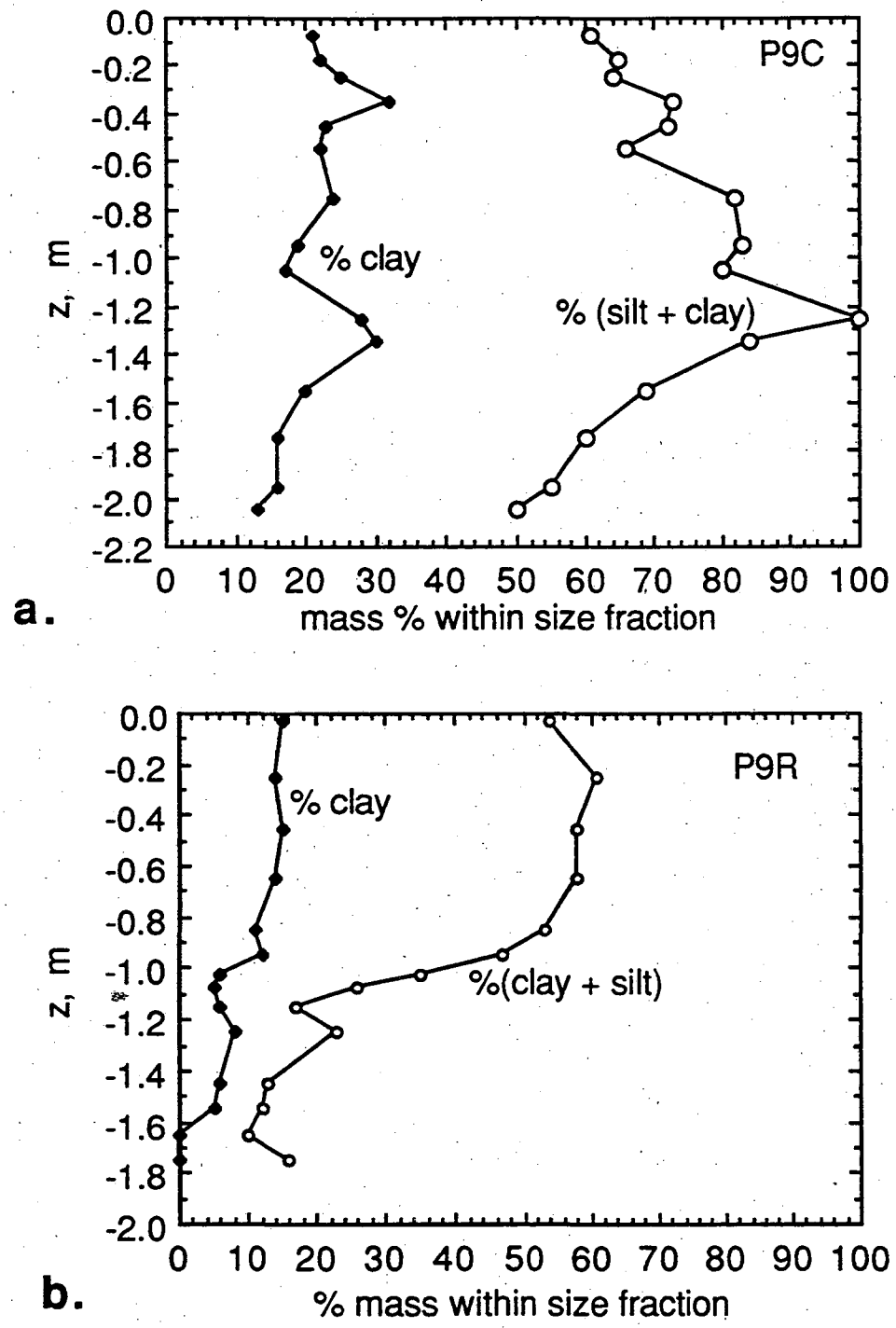

Figure 2.2. Particle-size analysis profiles (a) for sites P9C, and (b) for P9R. (The USDA size classes have been used in these delineations.)

soil waters in the unfilled areas during and shortly after periods of intense rainfall since runoff from the filled areas tends to pond over lower, adjacent unfilled soils. The February 1992 rain storms were the first time such ponding has been observed since emplacement of fill soils.

2.1.2. Soluble Selenium Concentrations in Northern Pond 9 Soil Waters

Soluble selenium data in soil waters at sites P9C and P9R have been collected since February 1987. The initial sampling depths were at 0.15, 0.30, 0.46, 0.61, 0.91, and 1.22 m. In the winter of 1988-89, additional soil water samplers were installed at intermediate depths as well as to deeper positions in each profile. At site P9C, the deeper soil water samplers were located at 1.38, 1.65, 1.87, and 2.12 m below the soil surface. At site P9R, the deeper samplers were installed at 1.42 and 1.70 m below the soil surface. (The presence of a rising water table prevented deeper installations at both sites.)

Selenium concentrations in some of the soil water samples at sites P9C and P9R are shown in Figures 2.3 and 2.4, respectively. Figures 2.3a and 2.4a consist of depth profiles of soluble selenium concentrations in soil waters sampled under conditions which are believed to provide close correspondence between sampled waters and bulk soil waters, prior to the February 1992 rain storms. The samples included in Figures 2.3a and 2.4a were collected at times significantly removed from major rainfall events, and with at least one set of samples collected between the rainfall events and the plotted sample sets. Thus, the selected data shown in these figures are less influenced by macropore flow, and are believed to provide reliable measures of selenium concentrations in the bulk soil waters.

An important feature of the profiles shown in both Figures 2.3a and 2.4a is the very high concentration of soluble selenium found at substantial depths below the soil surface. At site P9C, soluble selenium concentrations in the range of 200 to 1,000 $\mu g\ L^{-1}$ are typically found between the 1.0 m and 2.1 m depths. At site P9R, soluble selenium concentrations in the range of 200 to 500 $\mu g\ L^{-1}$ are found in soil waters between the 1.0 and 1.7 m depths. Recall that the original drain waters contained about 300 $\mu g\ L^{-1}$ selenium. Thus, the concentrations of soluble selenium at depths below 1 m at each site are similar to or substantially higher than those found in the originally ponded waters. The higher concentrations at site P9C may result from evapotranspirative concentration of soil waters by the invading plants or leaching of high concentrations of selenium from surface soils. Additional data from water-extracts of soil cores indicate similarly high concentrations of water-soluble selenium in these soils to depths greater than 2.0 m. Given such high soil water selenium concentrations at these depths, it becomes clear that movement of even a small fraction of such waters to greater depths will result in elevated groundwater selenium concentrations. The high concentrations of soluble selenium in the deeper portions of the Pond 9 soils have not been observed at similar depths at many other locations within Kesterson Reservoir. It should also be noted that the total soil selenium inventory at this site is not exceptionally high. Data from both USBR surface soil analyses and LBL indicate that about 80% of the total soil selenium occurs within the upper 0.15 m of these soils. The total selenium concentrations within the upper 0.15 m in these soils is in the range of 3 to 5 $mg\ kg^{-1}$ (ppm).

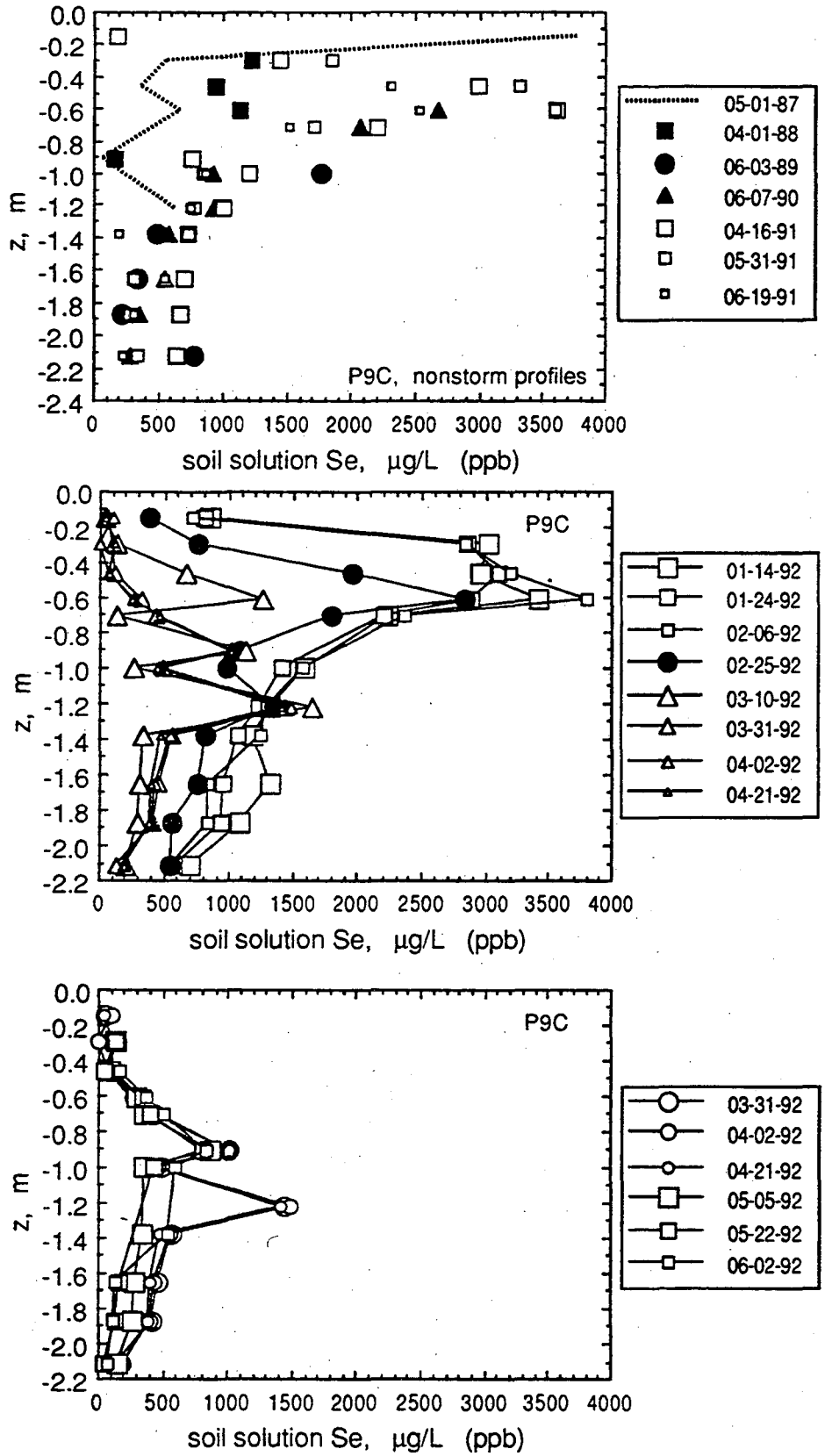

Figure 2.3. Site P9C soil water sampler selenium data. (a) Soil water selenium concentrations in representative samplings from 1987 to 1991. (b) and (c) Soil water selenium concentrations during 1992. The major storm event which resulted in ponding at this site was on Feb. 12, 1992.

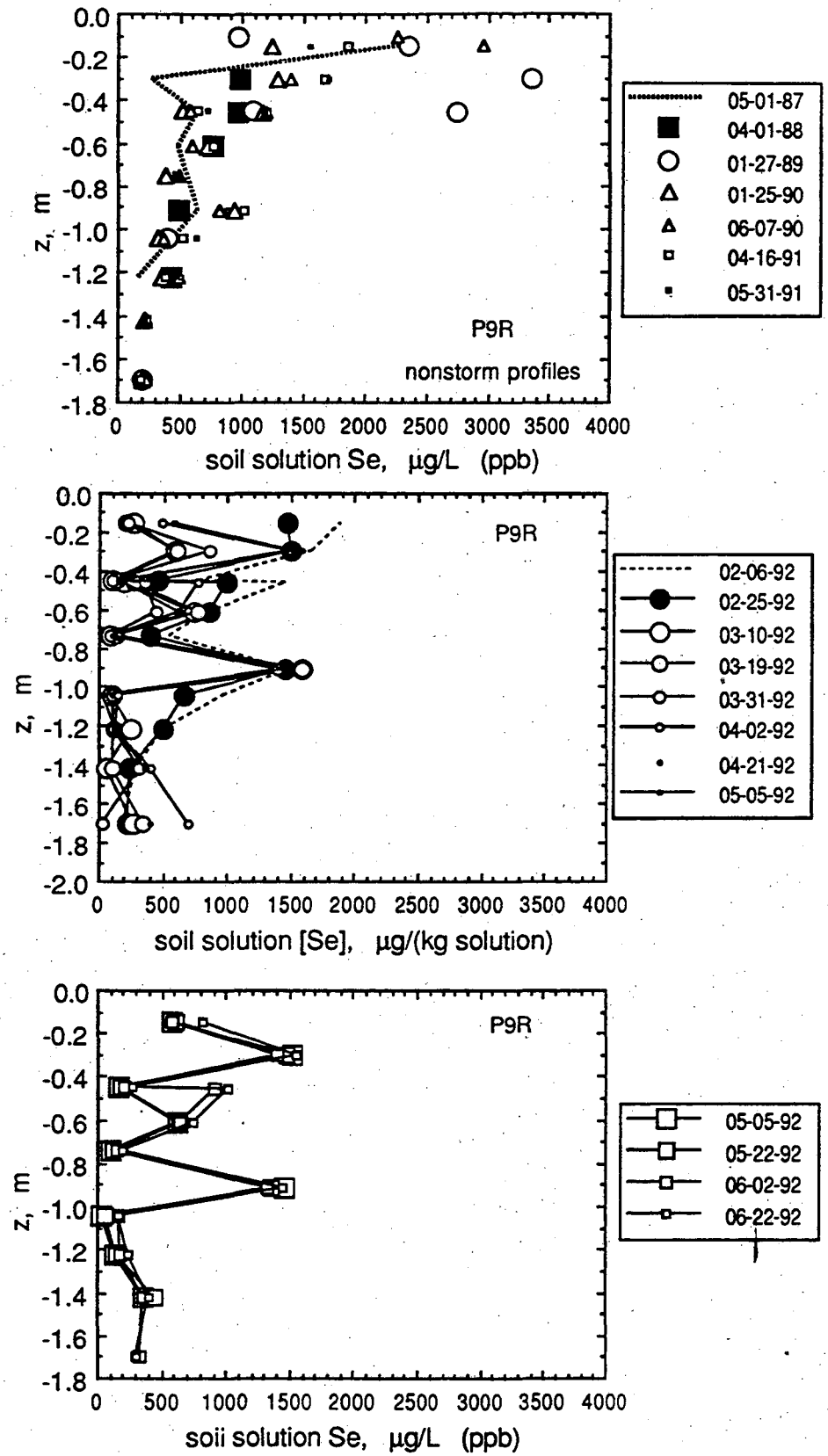

Figure 2.4. Site P9R soil water sampler selenium data. (a) Soil water selenium concentrations in representative samplings from 1987 to 1991. (b) and (c) Soil water selenium concentrations during 1992. The major storm event which resulted in ponding at this site was on Feb. 12, 1992.

The occurrence of high concentrations of soluble selenium at depth in the northern Pond 9 sites indicates that reduction of selenium in the surface sediments during ponding of drain waters was less efficient than at other sites throughout Kesterson Reservoir. Probable explanations for the less efficient selenium reduction in these soils are associated with removal of the original surface soil and the close proximity to a sandy subsoil (Benson et al., 1991 and White et al., 1991). Removal of the original surface soil probably resulted in a residual surface soil with lower organic matter content. A lower organic matter content may in turn limit microbial activity, hence limit oxygen consumption within the soils. With lower rates of oxygen consumption, selenium infiltrating into the soils may remain in the Se(VI) oxidation state without reduction to the more readily adsorbed Se(IV). As Se(VI) is leached deeper into the profile, the probably even less biologically active sandy strata are encountered where the likelihood of reduction diminishes. In addition, the relatively thin layer of sandy loam soil (≈ 1.0 m) found in portions of the Pond 9 sites provides lower hydraulic resistance to percolation of ponded drain waters than found in other sites with higher clay contents and/or greater thicknesses of fine-texture soils.

Thus, in the northern portion of Pond 9, we have an area where generation of reducing conditions probably occurs more slowly, and leaching probably occurs more rapidly than in most other parts of Kesterson Reservoir. Both effects will lead to more efficient leaching of soil water and a higher probability of finding selenium in the shallow groundwater as described in Benson et al. (1991) and White et al. (1991).

Profiles of soil water selenium concentrations shortly before, and for over 4 months after the February 1992 rain storms are shown in Figure 2.3b,c, and 2.4b,c, for sites P9C and P9R respectively. Decreases in soluble selenium concentrations throughout most of both profiles are evident. Comparisons of soluble selenium concentrations at sites P9C and P9R at depths approaching 2.0 m before and after the storms are not consistent. In P9C, decreases in water-soluble selenium concentrations are observed in the soil water sampler data. However, in site P9R, a slight increase in soluble selenium concentrations was observed in the data from the 1.42 m and 1.70 m soil water samplers. The extent to which preferential flow from the soil surface to the subsurface sampling tips occurred is difficult to evaluate, but salinity data indicate that it was significant in some cases. A more complete evaluation of changes in the soil water selenium profiles will soon become available when recently collected soil core samples are analyzed.

2.1.3. Summary

Certain characteristics of soils and soil pore waters from two monitoring sites in the northern area of Pond 9 are conducive to transport of selenium into shallow groundwaters. Important physical aspects of the area include the probable past excavation of the original surface soil, and a relatively shallow depth to high permeability sands. Excavation of the original soil surface probably removed a substantial portion of the soil organic matter inventory, thereby diminishing microbial activity associated with generation of reducing conditions needed to immobilize selenium. Excavation also decreased the thickness of the lower permeability sandy loam to clay loam surface soils which overlie high permeability sands. Depths to

sandy soil horizons are probably as little as about 1 m. These features of the soil profiles enhance leaching of waters ponded at the soil surface, and also diminish the effectiveness of selenium immobilization.

A past history of inefficient selenium immobilization in the northern Pond 9 soils is suggested in the observed high concentrations of soluble selenium to depths of about 2.1 m. Such high concentrations have been observed several years prior to the 1992 rain storms. The high concentrations of soluble selenium distributed throughout the soil profile provides a large inventory of readily leachable selenium.

The February 1992 rain storms provided the first major ponding event in this area since termination of drain water disposal, resulting in leaching of soil waters into the shallow groundwater system. While the rainfall ponding was in some ways similar to the previous ponding of drain waters, there are some significant differences. The obvious difference is the fact that rainfall does not bring in additional selenium, and introduces insignificant amounts of salts. A second important difference relates to the fact that about 6 years have elapsed since the last ponding at the site. During this span of time, the previously immobilized soil selenium inventory has been gradually diminished, resulting in significant increases in the water soluble selenium inventory (Benson et al., 1992). Thus, unlike ponding episodes of the past (1981-1986), the rainfall ponding in February 1992 may have resulted in leaching of a larger amount of selenium into the shallow groundwaters.

2.2. Soil Selenium and Salinity Monitoring in Soil Profiles of Plots 8EP and 9BE

Peter Zawislanski and Mavrik Zavarin
Earth Sciences Division
Lawrence Berkeley Laboratory

Changes in selenium and salt concentrations in a soil profile may be followed using both in-situ soil water samplers, which provide information on actual solute concentrations in soil water, and soil cores, extracts of which contain both soil water solutes, and soluble selenium and salts which may have been precipitated or adsorbed in the soil profile. Information gleaned from soil water sampling gives a notion of the magnitude of solute concentrations moving through the soil, while soil cores predominantly provide data on accumulation rates of selenium and salts in the profile. Concentrations of solutes in soil water are less ambiguous, the major uncertainty being due to the small soil volume being sampled and the result of macropore flow described in Section 2.1. Soil cores are more reliable a source of information when they are taken in replicates, especially near the soil surface, where spatial variability is greatest. Both approaches have been taken at plots 8EP and 9BE. Data from three years of monitoring in sites 8EP and 9BE are described below.

2.2.1. In-Situ Soil Water Monitoring

Tensiometers and soil water samplers are being used to monitor the soil water regime in plots 8EP and 9BE. Short-term perturbations in this regime are caused by seasonal infiltration and evapotranspirative removal of water. In order to surmise long-term changes, comparisons of hydraulic head and solute concentrations in profile are best made at the same time of year, preferably toward the end of the summer, when the distributions of the above variables are most stable. Hydraulic head, as measured using tensiometers, is presented in Figure 2.5. Both in plot 8EP (Figure 2.5a) and plot 9BE (Figure 2.5b), soil moisture content decreased throughout the profile between 8/88 and 8/90. This is in large part due to the invasion of both plots by *Kochia scoparia or Bassia hyssopifolia*, as discussed in Section 2.1. Despite a rainy spring (1991), the plant density and height were lower than in 1990. This effect, combined with significant infiltration of rainwater, resulted in an increase in moisture content in the summer of 1991.

Changes in chloride and selenium concentrations in plot 9BE confirm a wetting trend during the last year (Figures 2.6 and 2.7). Chloride concentrations increased by three- to four-fold between 5/89 and 6/90. The changes between 6/90 and 6/91 suggest dilution of soil water in the top 60cm by infiltrating rainwater with a corresponding increase at 90 cm, possibly due in part to further root extraction of soil water and also due to the displacement of solutes by downward movement of soil water.

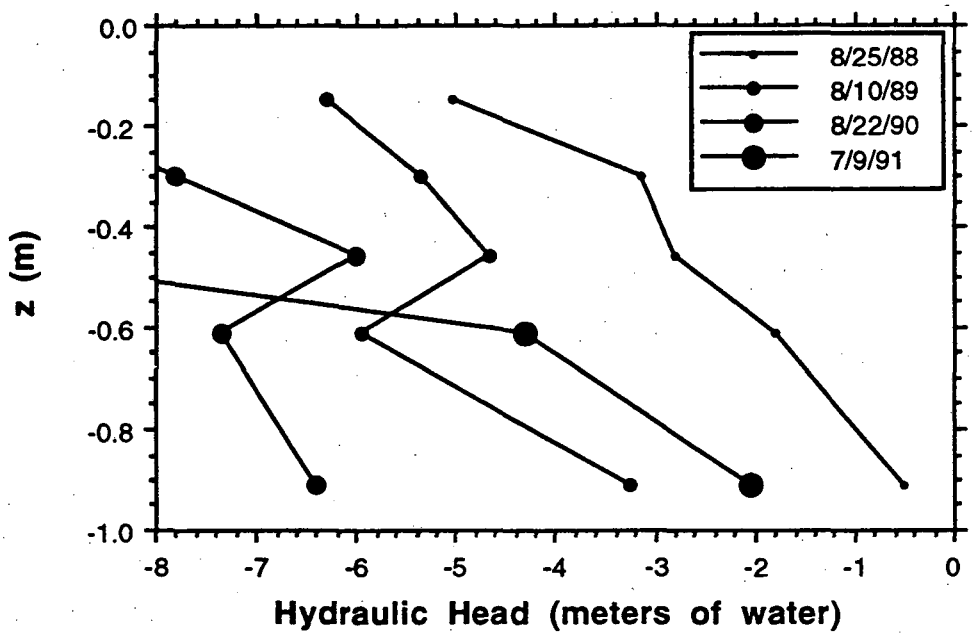

Figure 2.5a. Hydraulic head profiles as measured using tensiometers in plot 8EP.

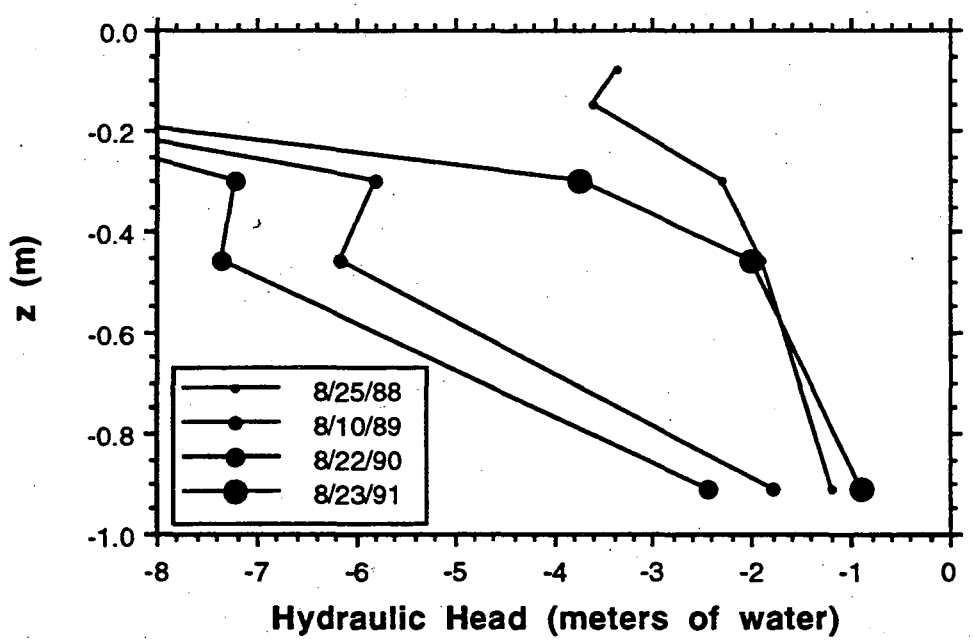

Figure 2.5b. Hydraulic head profiles as measured using tensiometers in plot 9BE.

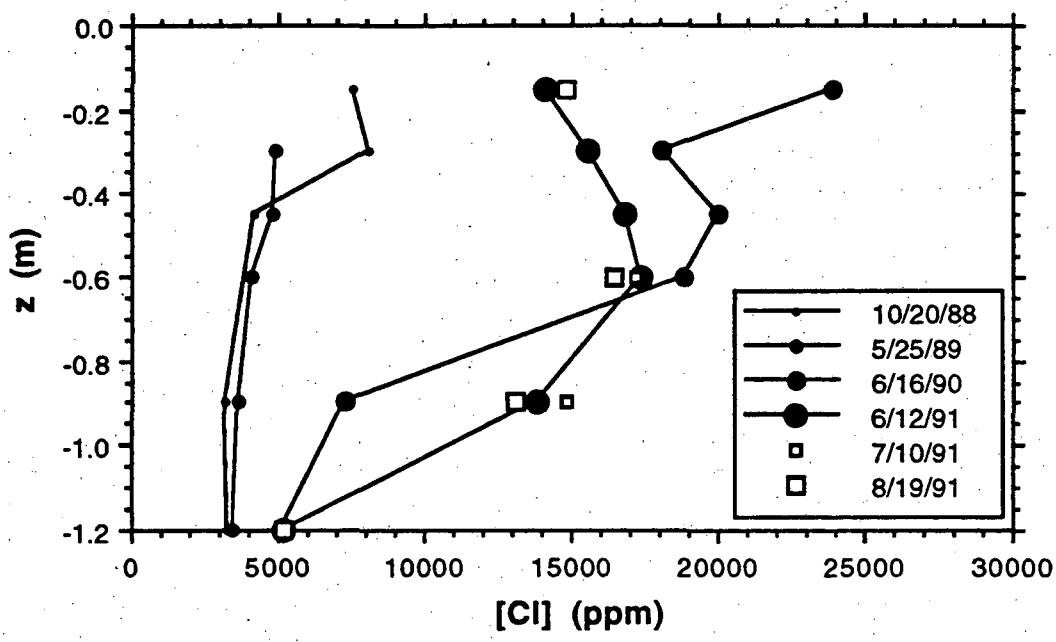

Figure 2.6. Changes in chloride concentrations in soil water of plot 9BE, collected with soil water samplers over a three year period.

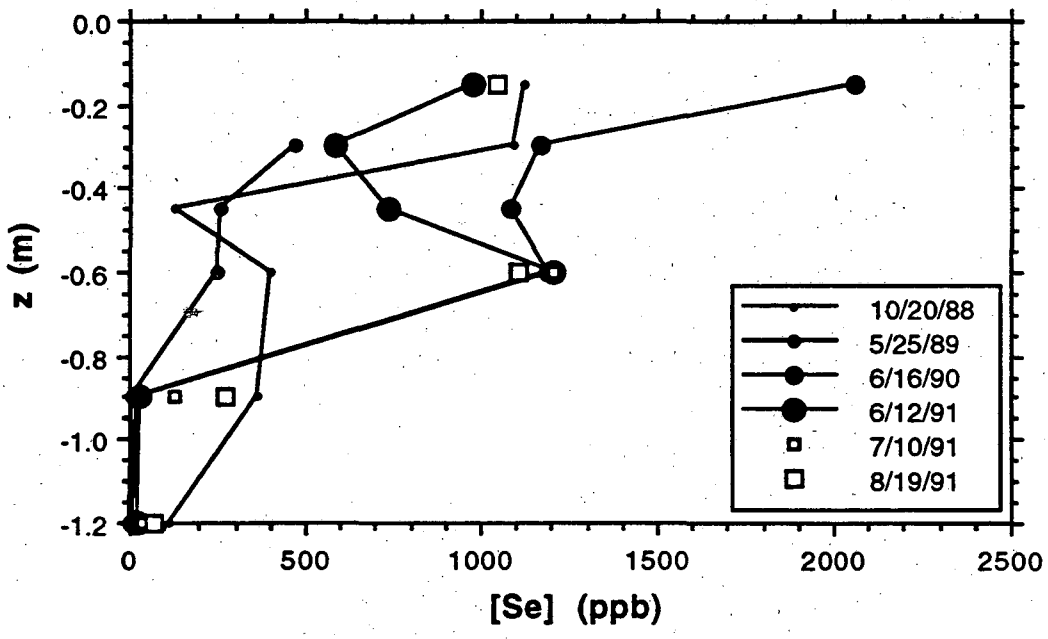

Figure 2.7. Changes in selenium concentrations in soil water of plot 9BE, collected with soil water samplers over a three year period.

Selenium concentration profiles exhibit similar, but less pronounced trends. An increase occurred during the spring of 1990. An apparent decrease in the top 45 cm between 6/90 and 6/91 may be attributed to dilution by infiltrating water and possibly the associated chemical reduction of selenium under wetter conditions. Unfortunately, samples from the late summer are not available for any year, except 1988. Therefore, these comparisons are somewhat tenuous, especially since the groundwater table in plot 9BE remains above the depth of 120 cm until June.

The relationship between seasonal weather patterns and movement of solutes in the vadose zone of plot 9BE may be observed in greater detail by plotting chloride and selenium concentrations at each depth against time (Figures 2.8 through 2.10). As seen in these figures, the greatest perturbations are observed during the rainy seasons. These data show that while changes on an annual basis are not always substantial, there are very significant increases and decreases in concentrations, especially selenium concentrations, due to the rise of the groundwater table and infiltration of rainwater.

Due to the much finer texture of sediments in plot 8EP (predominantly clay loam vs. sandy loam), and a deeper groundwater table (shallowest at a depth of 140 cm vs. 30 cm), the chloride and selenium distributions in 8EP are less disturbed by seasonal rainfall infiltration and the regional rise in groundwater table. This is seen in Figures 2.11 through 2.14. As in plot 9BE, chloride concentrations rose most significantly between 4/89 and 6/90. Due to the rainfall events during the spring of 1991, concentrations declined in the top 30 cm (nest C). However, the last complete sample set was taken in early May (5/9/91). Subsequent incomplete profiles (6/12/91; 6/27/91) show increases in chloride concentrations at 45 cm and 60 cm. Presumably, similar changes took place in the upper part of the profile. Apparently, selenium distribution was not affected as strongly as chloride distribution by spring 1991 rains. As seen in Figure 2.12, soil water selenium has steadily increased over the last three years (nest C). Data from nest ML in the same plot, while somewhat less complete, suggest similar increases (Figure 2.14). Relatively greater increases in selenium than chloride in 8EP (compare for example Figures 2.11 and 2.12) are suggestive of selenium oxidation in the soil profile.

The difficulty in making firm conclusions on the changes in salt and selenium concentrations based on soil water sampler data, stems from the fact that soil water samples are usually unavailable during the late summer, when a comparison is most valid. Analysis of soil cores taken at those times provides more quantitative results.

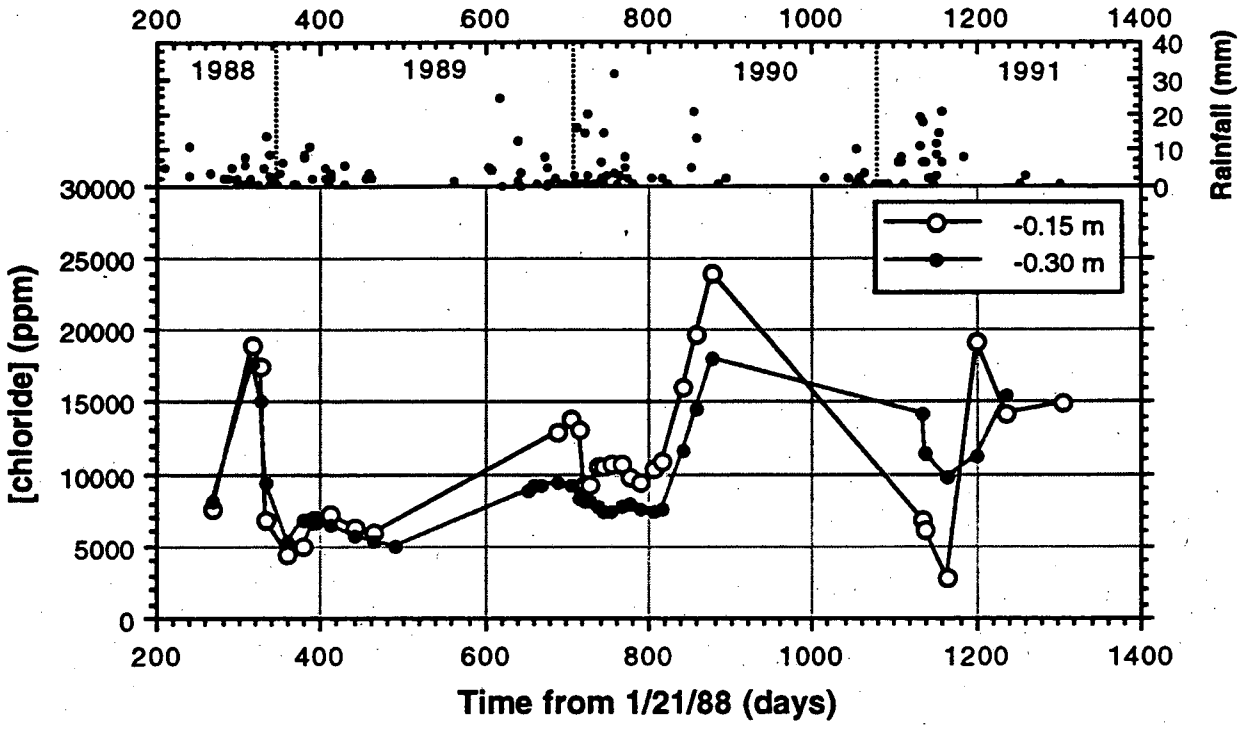

Figure 2.8a. Changes in chloride concentrations in soil water in plot 9BE; daily rainfall in upper graph.

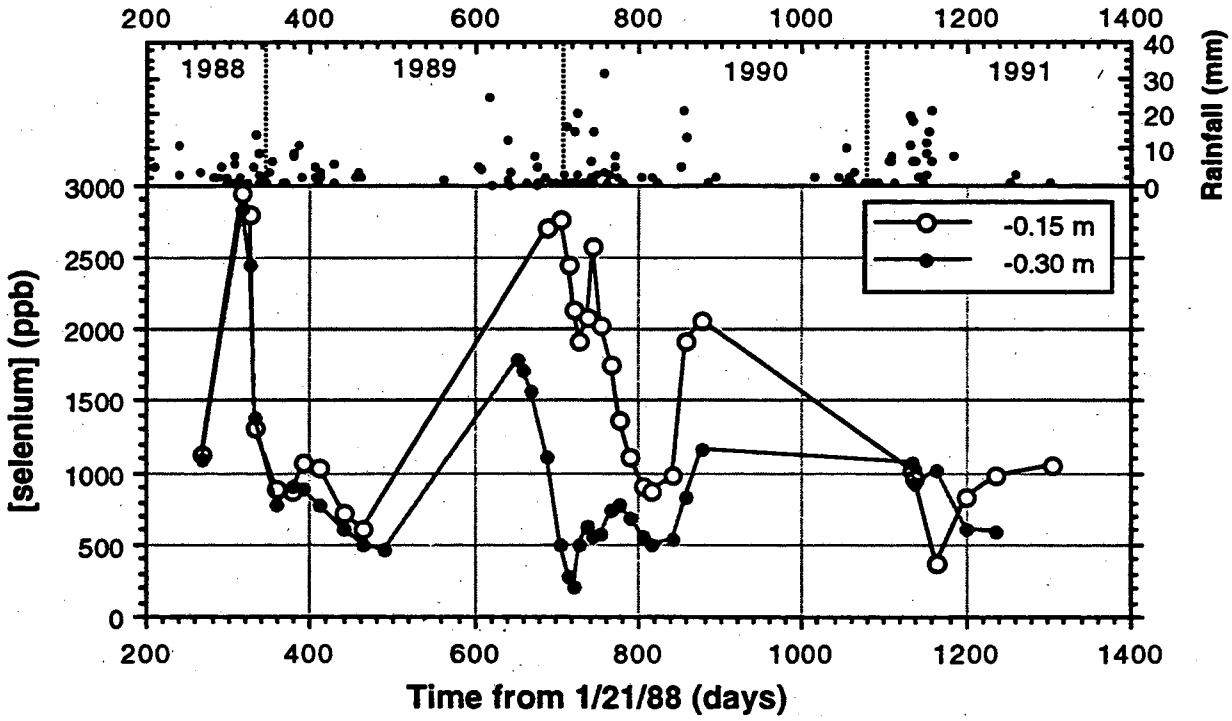

Figure 2.8b. Changes in selenium concentration in soil water of plot 9BE; daily rainfall in upper graph.

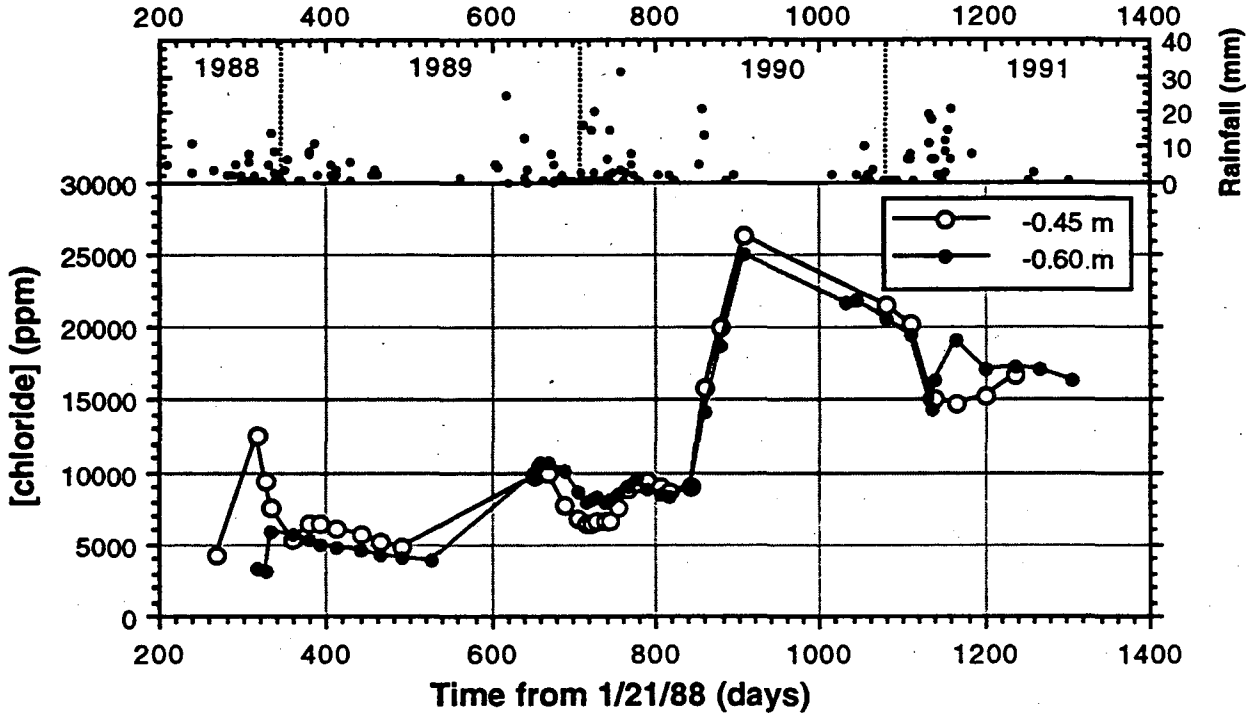

Figure 2.9a. Changes in chloride concentration in soil water of plot 9BE; daily rainfall in upper graph.

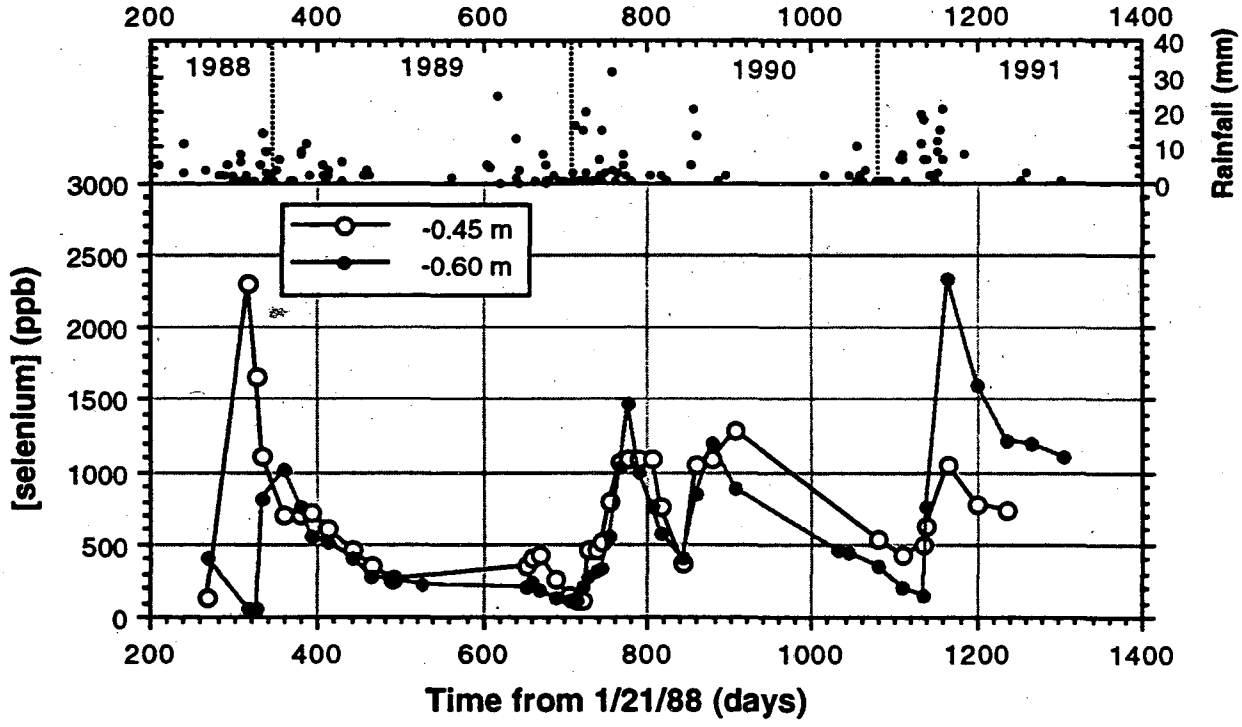

Figure 2.9b. Changes in selenium concentration in soil water of plot 9BE; daily rainfall in upper graph.

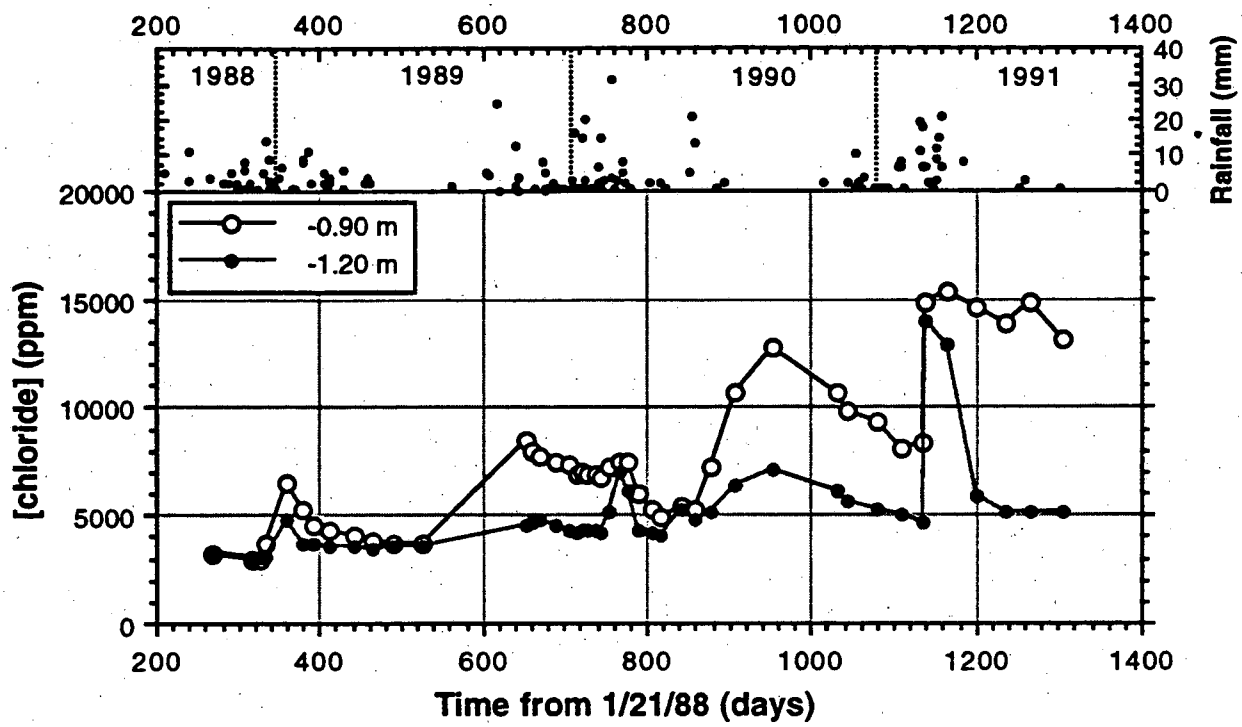

Figure 2.10a. Changes in chloride concentration in soil water of plot 9BE; daily rainfall in upper graph.

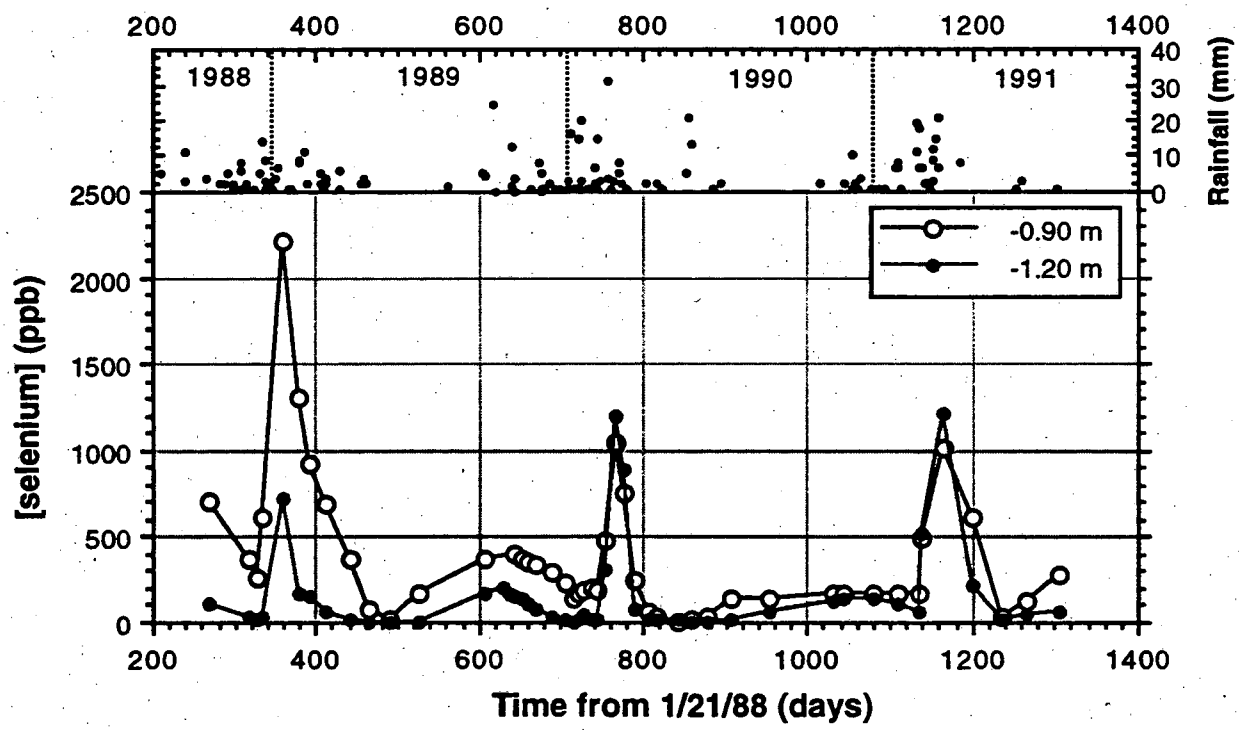

Figure 2.10b. Changes in selenium concentration in soil water of plot 9BE; daily rainfall in upper graph.

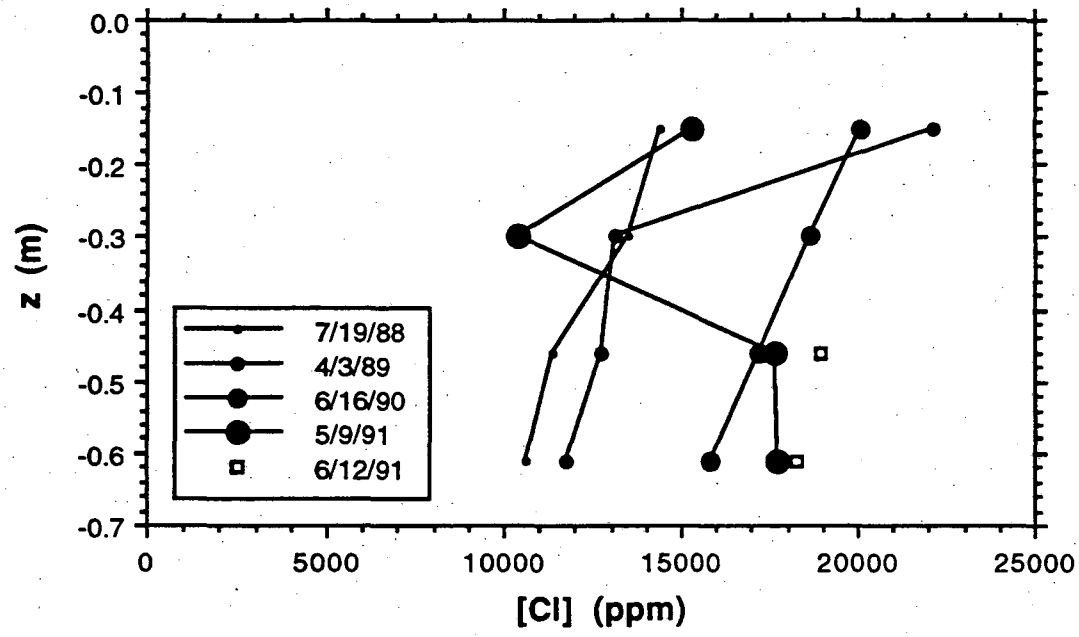

Figure 2.11. Changes in chloride concentration in soil water of plot 8EP, nest C, collected with soil water samplers over a three year period.

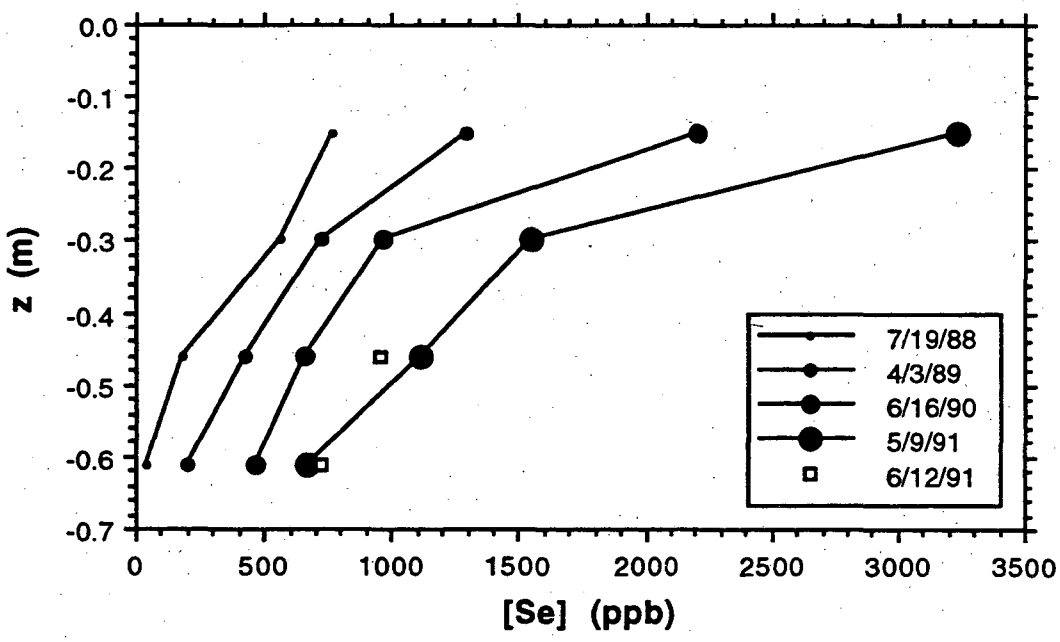

Figure 2.12. Changes in selenium concentration in soil water of plot 8EP, nest C, collected with soil water samplers over a three year period.

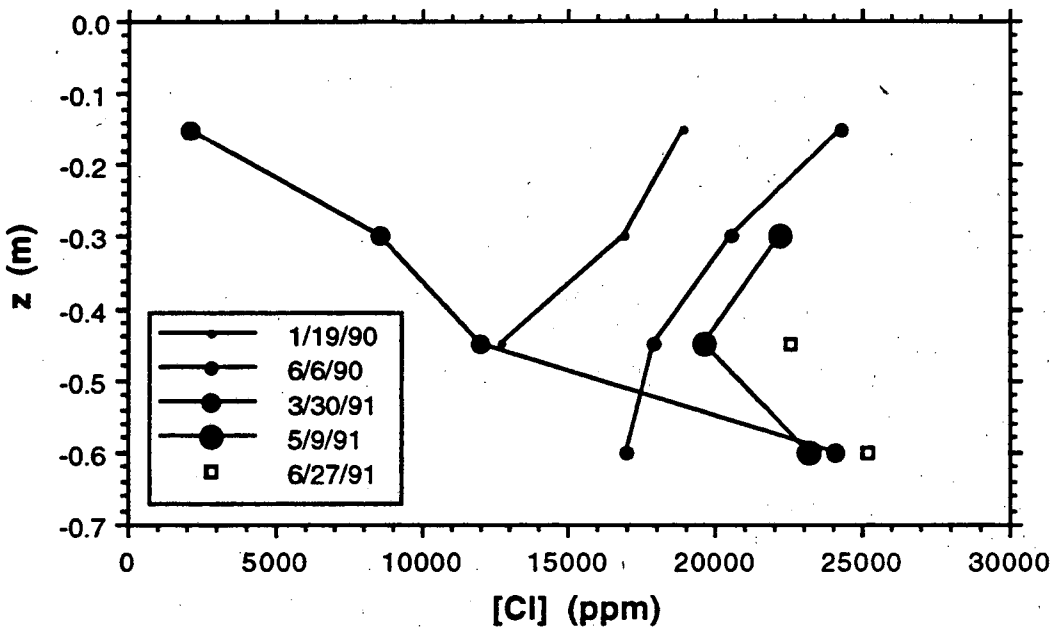

Figure 2.13. Changes in chloride concentration in soil water of plot 8EP, nest ML, collected with soil water samplers from 1/90 through 6/91.

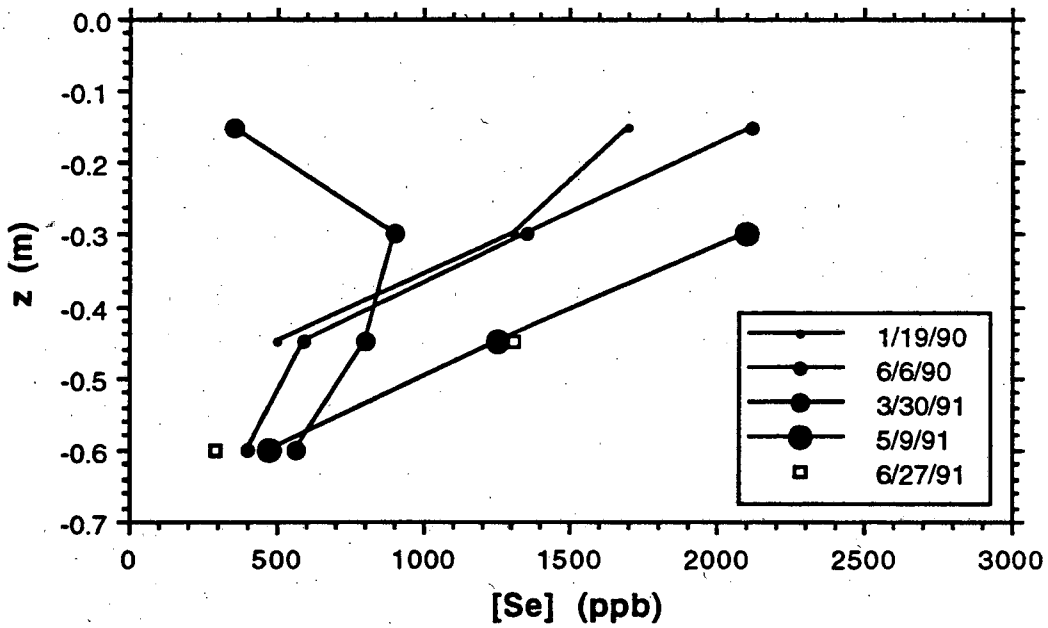

Figure 2.14. Changes in selenium concentration in soil water of plot 8EP, nest ML, collected with soil water samplers from 1/90 through 6/91.

2.2.2. Soil Selenium and Salinity Monitoring

Changes in soil selenium and salt distribution are commonly affected by evapotranspiration and rainfall infiltration, as shown in Section 2.2.1. Therefore, when long-term, and not seasonal changes are sought to be observed, it is important to collect samples at roughly the same time of year, and preferably long after the rainy season. Soil cores have been collected in plots 8EP and 9BE on the following dates: 7/21/88, 7/25/88, 11/16/89, 11/21/89, 8/15/90, 8/22/90, and 9/24/91. Additional cores have been taken during the rainy season and will not be discussed here in detail.

The following is a brief description of the soil sampling, preparation and analysis procedures. Cores were taken using a hand-auger with a 2-inch barrel, except on 11/89 when a Giddings hydraulic sampling rig was used. Cores were divided in the field into 10-cm intervals, except the top 20 cm which was divided into 0.5-cm to 5-cm intervals, the top 10 cm being sampled using a 10-cm long, 2-inch diameter pipe, the sample from which was split in the lab. Samples were stored in heavy-duty freezer bags. After each sample was homogenized, a subsample of known mass (on the order of 10 to 20 g) was used to prepare a 1:10 soil:water extract which was stirred or shaken for 2 hours. Subsequently, the suspension was centrifuged at between 3000 and 6000 revolutions per minute for 5 to 20 minutes, depending on the texture of the soil. The supernatant liquid was then poured off and filtered through a 0.45 μm filter in preparation for chemical analysis. Selenite and selenium were analyzed for using atomic absorption spectroscopy (AAS) coupled with a hydride generator. Chloride was analyzed for using Mohr titration, as described by Flaschka and others (1969). Boron and major ions other than chloride were analyzed for using inductively coupled plasma spectrophotometry (ICP). All concentrations presented herein are normalized to the mass of dry soil, thereby providing a reference to a constant mass.

2.2.2.1. Plot 8EP

Changes in gravimetric moisture content of the cores taken are shown in Figure 2.15. The most apparent change took place between 11/89 and 8/90 in the top 1 m of the soil profile. There the mean moisture content declined by roughly 25% to 30%, while moisture content below 1 m did not change significantly. This is not surprising as it coincides with an increased density of plants in this plot in the spring and early summer of 1990 (LBL, 1990b). Likely most of this moisture loss took place between 3/90 and 8/90, suggesting a lower boundary on an evapotranspiration rate of approximately 0.5 mm/day. The actual rate was of course higher, since water also enters the root zone from the water table. Moisture content decreased slightly in the top 0.5 m between 8/90 and 9/91, and increased between 0.5 and 1.0 m, suggesting either a lesser effect of plant-root extraction and/or significant infiltration of rainwater to this depth.

Root extraction of soil water leads not only to loss of moisture but also to an increase in solutes and the possible precipitation of salts. Chloride was chosen to study this effect because of its high solubility and lack of reactivity in the soil system. Changes in chloride in the soil profile of

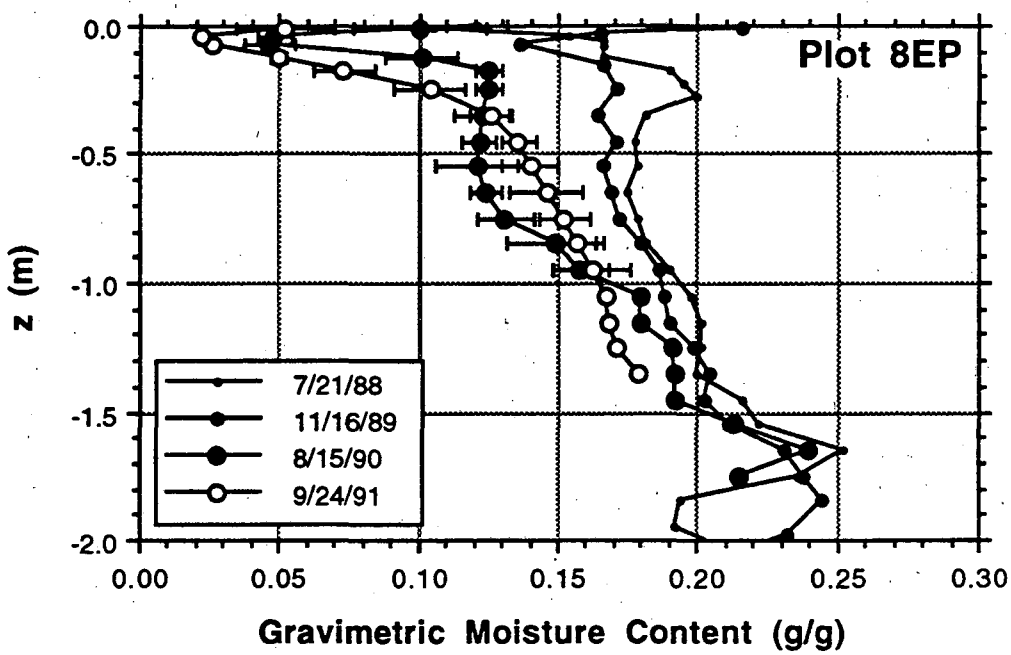

Figure 2.15. Changes in gravimetric moisture content in the soil profile of plot 8EP, over a three year period.

plot 8EP are shown in Figure 2.16 As expected, chloride concentrations at depth increased significantly between 11/89 and 8/90. There was also a significant increase in chloride between the depths of 1.0 m and 1.5 m, while a significant decrease in soil moisture was not observed in this interval. This may be due to a more rapid re-wetting of soil in that region due to its proximity to the water table in the spring (depth to water was 1.4 m to 1.8 m). As an apparent result of downward displacement of soil water, chloride concentrations declined in the top 0.25 m and increased below 0.30 m between 8/90 and 9/91. As seen in Figure 2.16b, the cumulative chloride concentration, normalized to the projected soil area, has gradually increased from year to year, with the most pronounced change taking place between 11/89 and 8/90. There is also a marked overall displacement of chloride deeper into the profile.

The mass of water-soluble selenium relative to the mass of soil also increased in the top 1 m of the soil, though a significant fraction of that increase occurred between 7/88 and 11/89 (Figure 2.17a,b). Mechanisms for accumulation in the vadose zone are different for chloride and selenium. Chloride accumulates due to its transport in water coming up from the water table: concentrations of chloride in groundwater are roughly the same as those in the vadose zone. This, however, is not the case with water-soluble selenium. Its concentration in groundwater is very low (usually < 5 ppb) and therefore water coming up from the water table cannot contribute significant amounts of selenium. An increase in water soluble selenium (mostly selenate, and to a lesser extent selenite), is predominantly a result of oxidation of more reduced forms, such as Se(IV), Se_0 and $Se_{organic}$. It has been shown in previous and ongoing

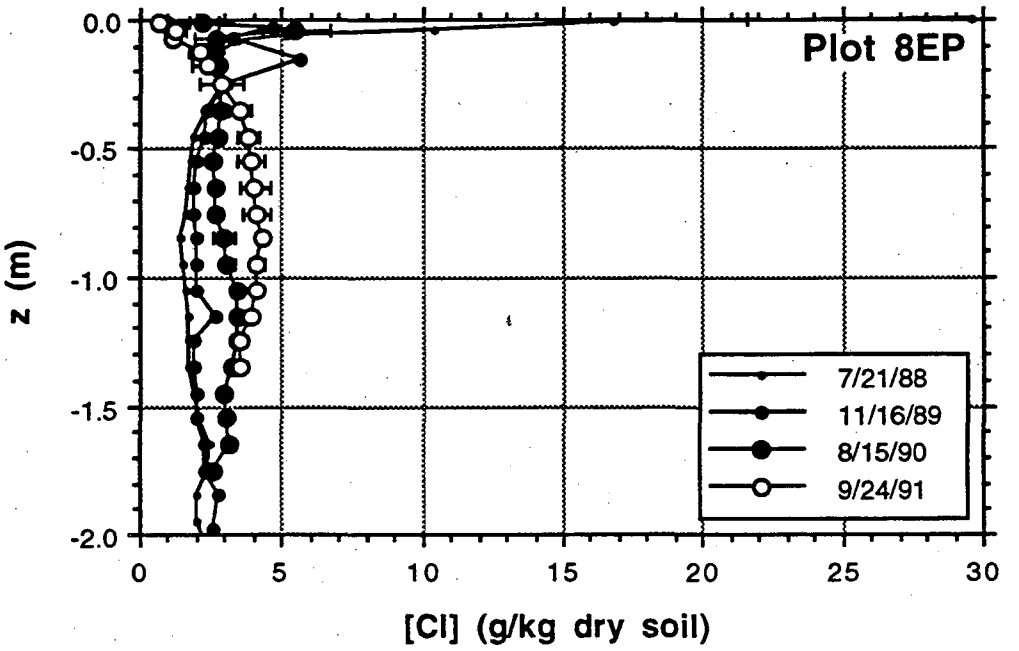

Figure 2.16a. Changes in chloride concentration in plot 8EP, normalized to the mass of soil.

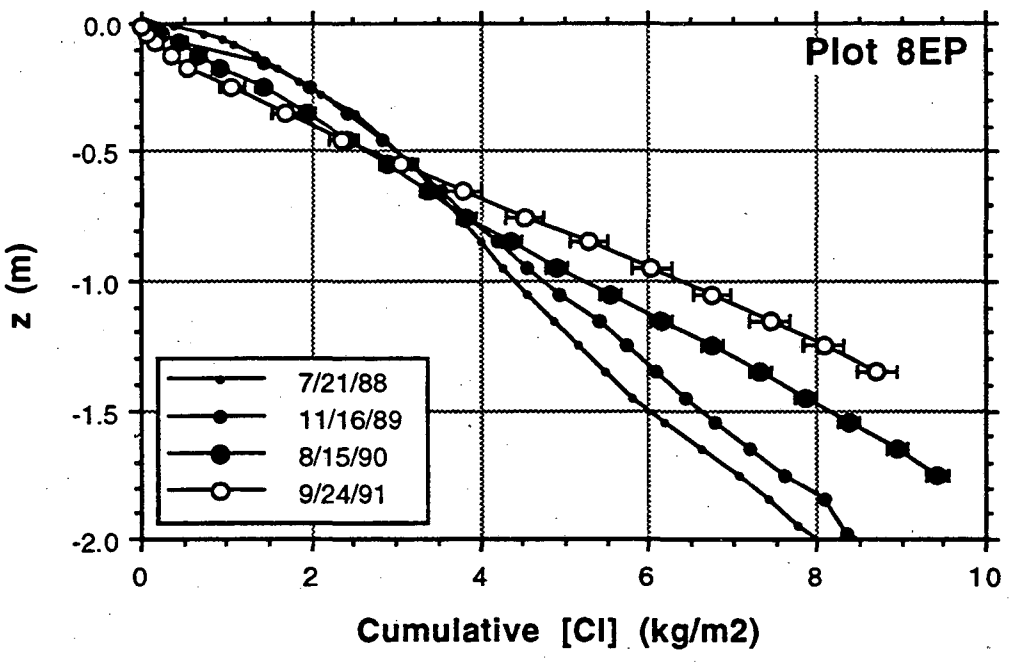

Figure 2.16b. Changes in cumulative chloride mass distribution, plot 8EP, normalized to projected soil area.

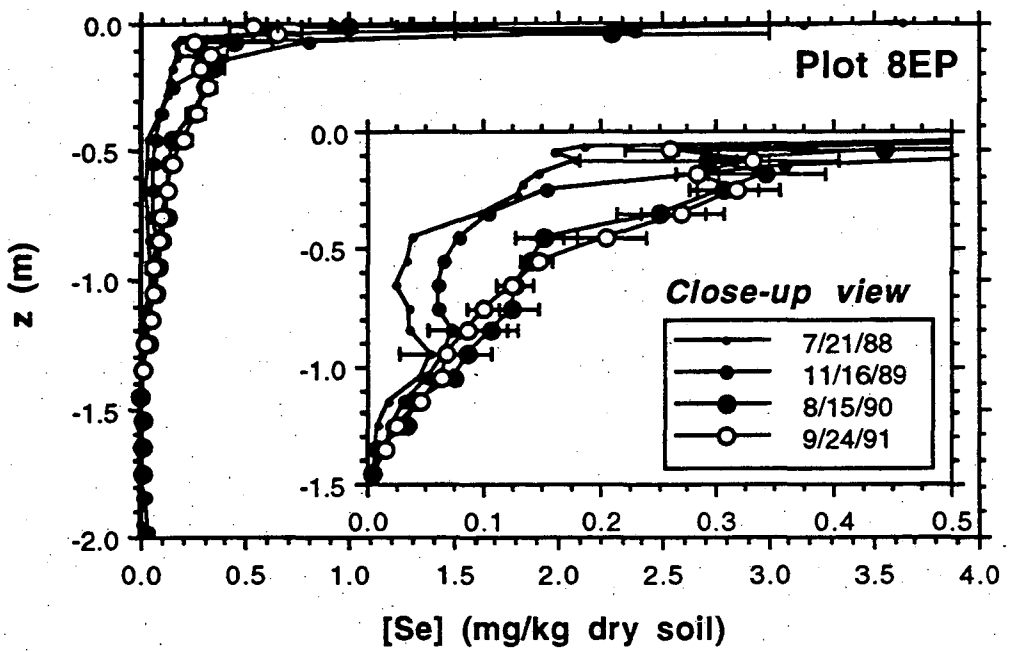

Figure 2.17a. Changes in water-extractable selenium concentration in plot 8EP, normalized to the mass of soil.

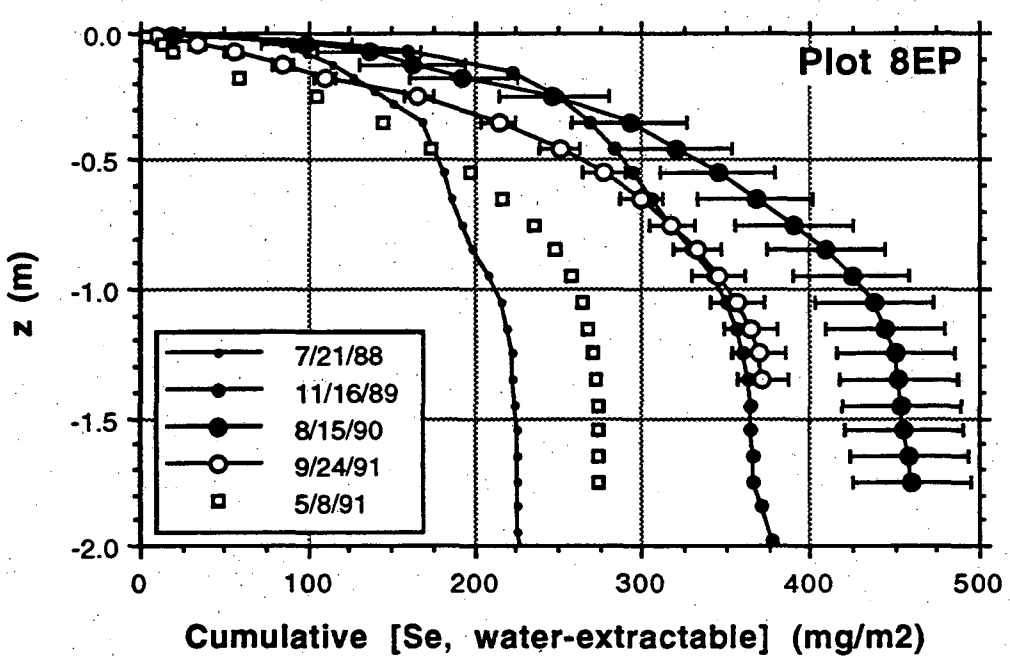

Figure 2.17b. Changes in cumulative water-extractable selenium mass distribution, plot 8EP, normalized to projected soil area.

studies, that most of the selenium inventory is not in its most oxidized forms and is thus subject to oxidation over the long term (LBL, 1990b, Section 2.5; Benson et al., 1992). Between 8/90 and 9/91, water-extractable selenium concentrations declined in the top 0.20 m, likely due to leaching of soluble selenium to greater depths and reduction to less soluble forms deeper in the soil profiles. As a result, the cumulative water-extractable selenium mass in the profile declined to 11/89 levels. This pattern is clearly visible in Figure 2.17b. In addition, the cumulative water-extractable Se concentrations from 5/31/91 are shown in this figure and stress the magnitude of chemical reduction of selenium shortly after early spring storms. Such a pattern emphasizes the relatively faster reduction process over the slower oxidation of selenium.

2.2.2.2. Plot 9BE

With minor exceptions, similar patterns of change have been observed in plot 9BE. The complicating factor is that the water table in 9BE rises to within 0.3 m of the soil surface during the winter months, thereby saturating all but 0.3 m of the summertime vadose zone. Nonetheless, the marked decrease in moisture content (Figure 2.18) between 11/89 and 8/90 is seen (below 0.6 m, the gravimetric moisture content is higher in 11/89 than 7/88 due to a higher groundwater level). Similarly to plot 8EP, moisture content increased in the 0.5 to 1.0 m depth interval between 8/90 and 9/91, and also increased, though not significantly in the top 0.5 m. Again, this is indicative of the effects of rainwater infiltration during the winter/spring of 1991, as well as the diminished density of vegetation in the plot.

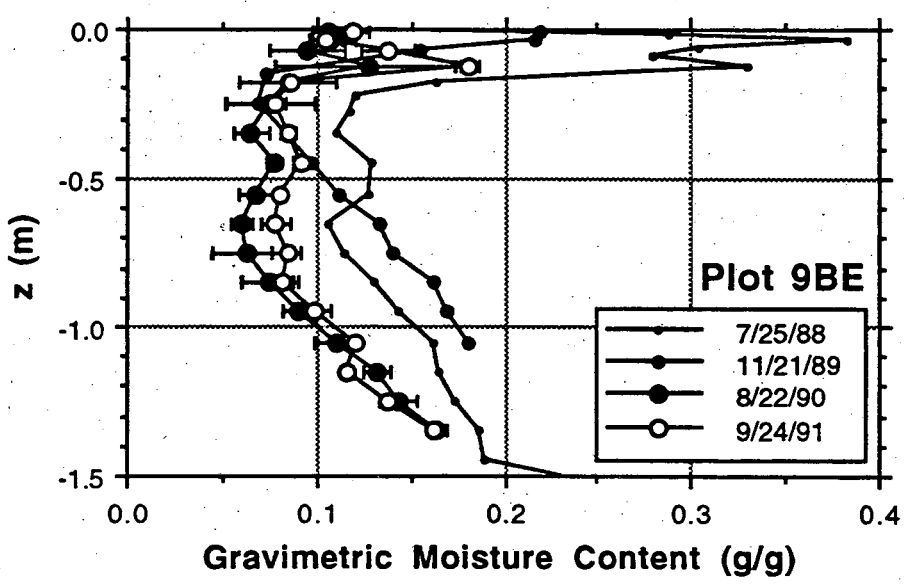

Figure 2.18. Changes in gravimetric moisture content in the soil profile of plot 9BE, over a three year period.

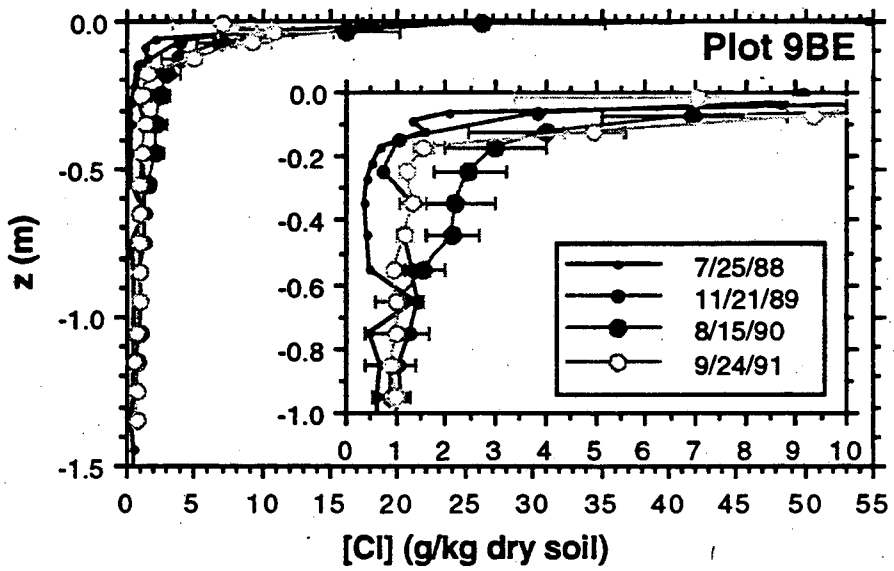

Figure 2.19a. Changes in chloride concentration in plot 9BE, normalized to the mass of soil.

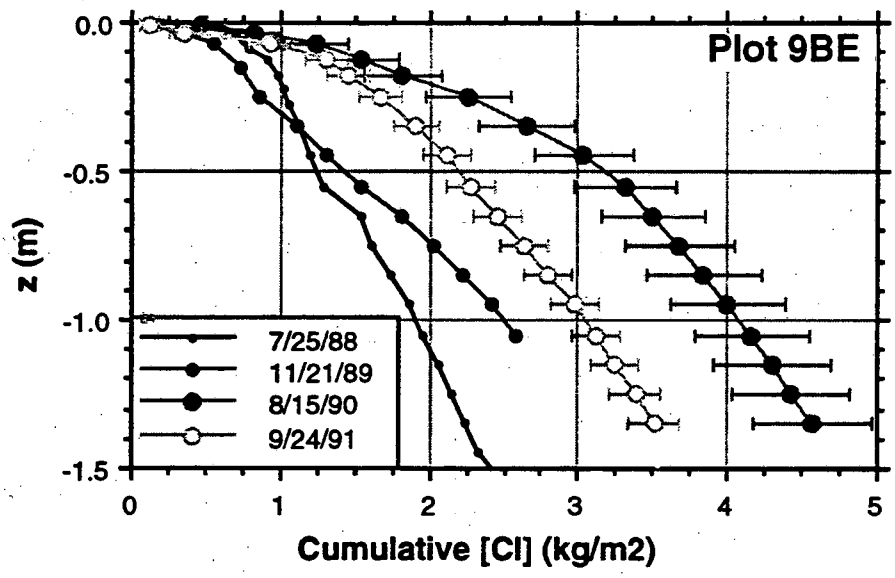

Figure 2.19b. Changes in cumulative chloride mass distribution, plot 9BE, normalized to projected area.

Major changes in chloride concentrations are observed in the top 0.6 m of the profile (Figure 2.19). There are marked increases from 7/88 to 11/89 and especially from 11/89 to 8/90, corresponding to the invasion of the plot by *Kochia* or *Bassia*. However, a large decrease between 8/90 and 9/91 is observed in the 0.1 to 0.6 m depth interval, due to the flushing of chloride deeper into the soil profile during the rainy period and the reduced presence of *Bassia* during the summer of 1991. As opposed to chloride, water-extractable selenium concentrations increased throughout the profile between 7/88 and 11/89 and 11/89 and 8/90 (Figure 2.20). However, roughly one-half of that increase took place between 7/88 and 11/89, suggesting selenium oxidation. Water-extractable selenium declined between 8/90 and 9/91, presumably chiefly due to reduction and leaching. Data from 5/8/91 are also presented in Figure 2.20b and show the degree to which the water extractable selenium inventory declined.

2.2.3. Quantitative Assessment of Chloride and Selenium Concentration Changes

Even though groundwater levels fluctuate seasonally, a nominal vadose zone may be assumed for the purpose of the following analysis. The criteria were: the interval to be unsaturated during part of the year, water-soluble selenium concentrations to be non-zero (or more precisely, concentrations to exceed analytical detection limit), and soil sample was available. In plot 8EP, this interval extends down to 1.4 m, in plot 9BE, to 1.1 m. Table 2.1 contains the results of calculations of mean profile values for: gravimetric moisture content (θ), chloride concentrations normalized to projected soil area ($[Cl]/m^2$), water-soluble selenium concentrations normalized to projected soil area ($[Se]/m^2$), chloride concentrations relative to water volume (*[Cl]/water*), and water-soluble selenium concentrations relative to water volume (*[Se]/water*) (assuming all selenium and chloride were dissolved.) Also, percentage of change relative to the previous year is shown.

As expected, major increases in chloride concentrations occurred between 11/89 and 8/90, due to evapotranspiratively driven soil water movement into the vadose zone. On the other hand, major soluble selenium concentration increases occurred between 7/88 and 11/89 as well, likely the result of oxidation of reduced selenium forms. Between 8/90 and 9/91, there was a decrease in water-extractable selenium in both plots, roughly by 18% (plot 8EP) and 32% (plot 9BE), which further supports the scenario of selenium reduction. During the same period of time, chloride concentrations increased in plot 8EP (by 19%) and decreased in plot 9BE (by 25%). It should be pointed out that even though most values in the table have three significant digits, the precision of this approach is far less, and relative changes should not be trusted to better than 5%. Values for "dissolved" chloride and selenium should be considered for relative comparison, since not all of the selenium and chloride in the system will be dissolved. Qualitatively, these concentration changes correspond well to those found in in-situ soil water in plot 8EP (see Figure 2.12) but are much higher than those found in plot 9BE (Figure 2.7).

Data from wintertime soil cores was not presented herein, but it should be noted that a core taken at the conclusion of the rainy season in 1991 (5/9/91) in plot 8EP, contained a mean profile chloride concentration of 7.82 kg/m^2, and a mean profile water-soluble selenium concentration of 272 mg/m^2. This

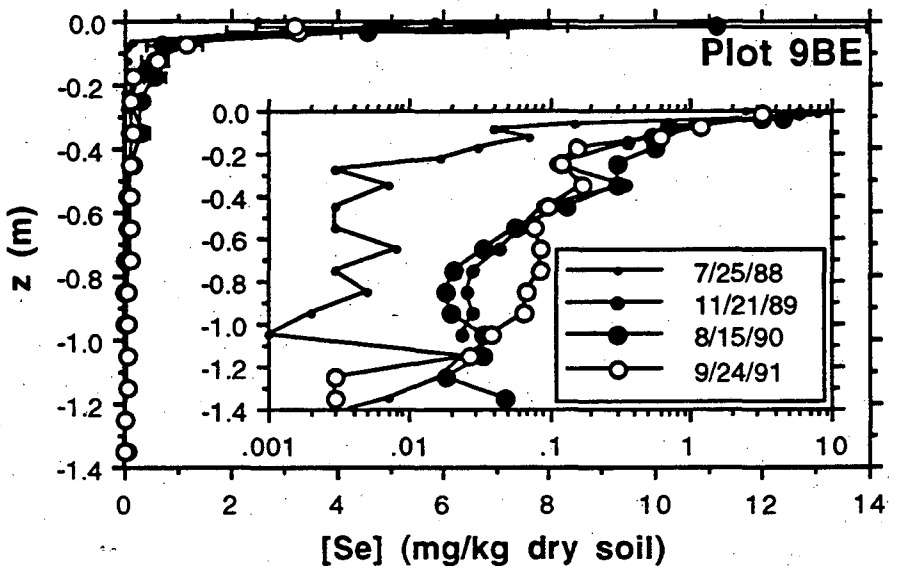

Figure 2.20a. Changes in water-extractable selenium concentration, plot 9BE, normalized to projected area.

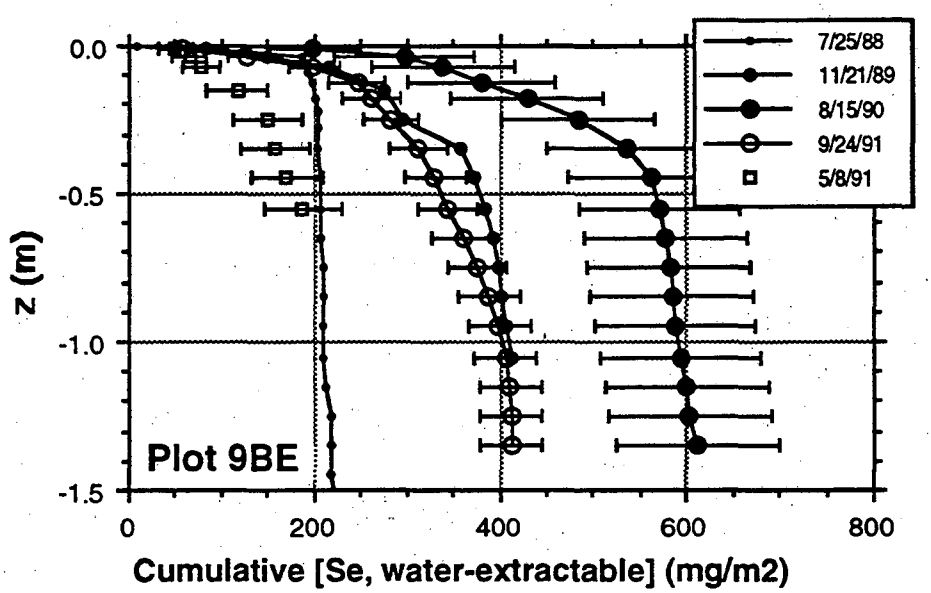

Figure 2.20b. Changes in cumulative water-extractable mass distribution, plot 9BE, normalized to projected area.

Table 2.1. Mean values of profile-averaged gravimetric moisture content, chloride and water-extractable selenium concentrations, and changes relative to the previous year.

Sample Date	θ (g/g)	[Cl]/soil (kg/m^2)	Change [Cl] %	[Se]/soil (mg/m^2)	Change [Se] %	[Cl]/water (g/L)	[Se]/water (μg/L)
Plot 8EP							
7/21/88	0.186	5.47	—	223	—	12.0	490
11/16/89	0.178	6.07	+11.0%	363	+62.8%	13.9	832
8/15/90	0.142	7.33	+20.8%	453	+24.8%	21.1	1302
9/24/91	0.137	8.70	+18.7%	372	-17.9%	25.9	1108
Plot 9BE							
7/25/88	0.146	1.96	—	209	—	6.97	744
11/21/89	0.125	2.58	+31.6%	412	+97.1%	10.7	1712
8/22/90	0.080	4.17	+61.6%	594	+44.2%	27.1	3856
9/24/91	0.094	3.12	-25.2%	406	-31.6%	17.3	2246

corresponds to a +7% change in chloride (marginally significant) and a -40% change in selenium relative to soil collected on 8/15/90. Such a change in selenium indicates very significant reduction of selenium due to infiltrating rainwater and a rising water table. Therefore, while most annual changes in selenium speciation indicate oxidation, reduction appears to be occurring on a seasonal basis. Given the possibility of a non-drought winter, soil selenium may become reduced to a degree similar to that found shortly after the draining of Kesterson ponds in soil profiles that become nearly fully water saturated.

2.3. Measurement of Chemical Changes in Near-Surface Soils of Plots 8EP and 9BE

Peter Zawislanski
Earth Sciences Division
Lawrence Berkeley Laboratory

Beginning in July 1988 and ending in July 1989, samples of the top 9 cm of soil were taken from plots 8EP and 9BE for analysis on a monthly basis. The impetus for this sampling strategy was to track changes in chemical species concentrations in these surface soils as affected by bare soil evaporation and rainfall infiltration. The 1988/89 series of samples yielded data which suggested that while seasonal fluctuations in this interval were significant (species flushed down deeper into the soil profile during the wet season, and evaporatively concentrated during the dry season), the net differences over a twelve month period were very small; these changes were recognized to be strongly dependent on atmospheric conditions, especially rainfall amount and intensity. In summary, salt concentrations over that twelve month period dropped slightly, while water-extractable selenium concentrations did not change significantly (for a full discussion see LBL, 1990a). Since then, five more sets of samples have been taken from those plots (9/89; 4/90; 10/90; 5/91; 10/91).

The following is a description of the soil preparation and analysis procedures. After each sample was homogenized, a subsample of known mass (on the order of 10 to 20 g) was used to prepare a 1:10 soil:water extract which was stirred or shaken for 2 hours. Subsequently, the suspension was centrifuged at between 3000 and 6000 revolutions per minute for 5 to 20 minutes, depending on the texture of the soil. The supernatant liquid was then poured off and filtered through a 0.45 μm filter in preparation for chemical analysis. Selenite and selenium were analyzed for using atomic absorption spectroscopy (AAS) coupled with a hydride generator. Chloride was analyzed for using Mohr titration, as described by Flaschka and others (1969). All concentrations presented herein are normalized to the mass of dry soil, thereby providing a reference to a constant mass and avoiding the apparent dilution effects of higher moisture contents during the rainy season.

Figure 2.21 shows changes in chloride concentrations in the top 9 cm of soil in plot 8EP. A pattern of higher concentrations at the end of the summer and lower concentrations at the end of the winter corresponds to the evaporative accumulation of salts at the surface during dry months and the flushing down of solutes deeper into the profile during the rainy season, respectively. Overall, chloride concentrations appear to be declining over the last three years, suggesting a solute gradient toward the root zone of *Bassia* plants which have become

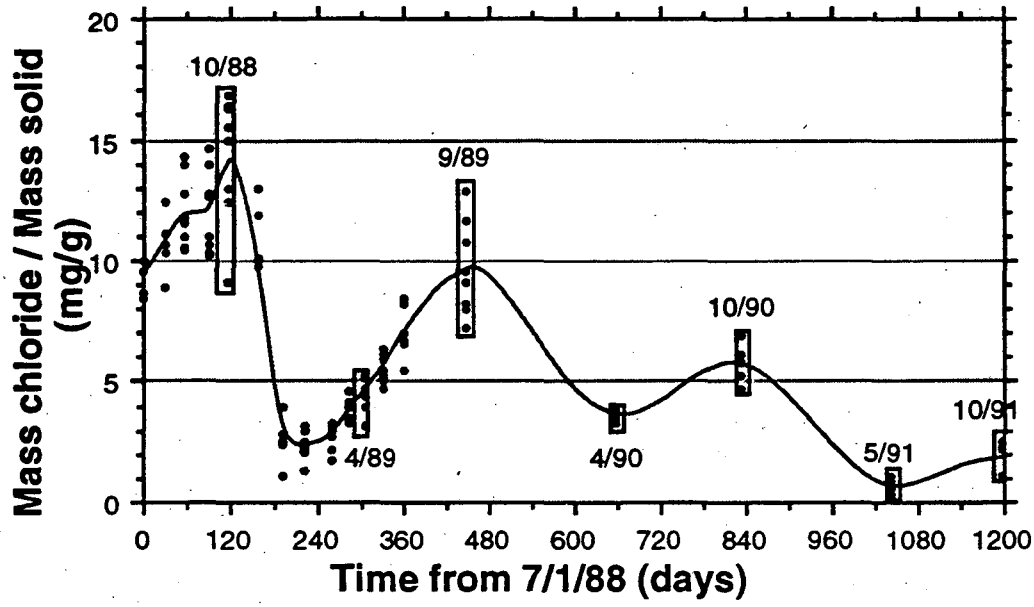

Figure 2.21. Changes in chloride concentration in the top 9 cm of soil in plot 8EP: July 1988 - October 1991.

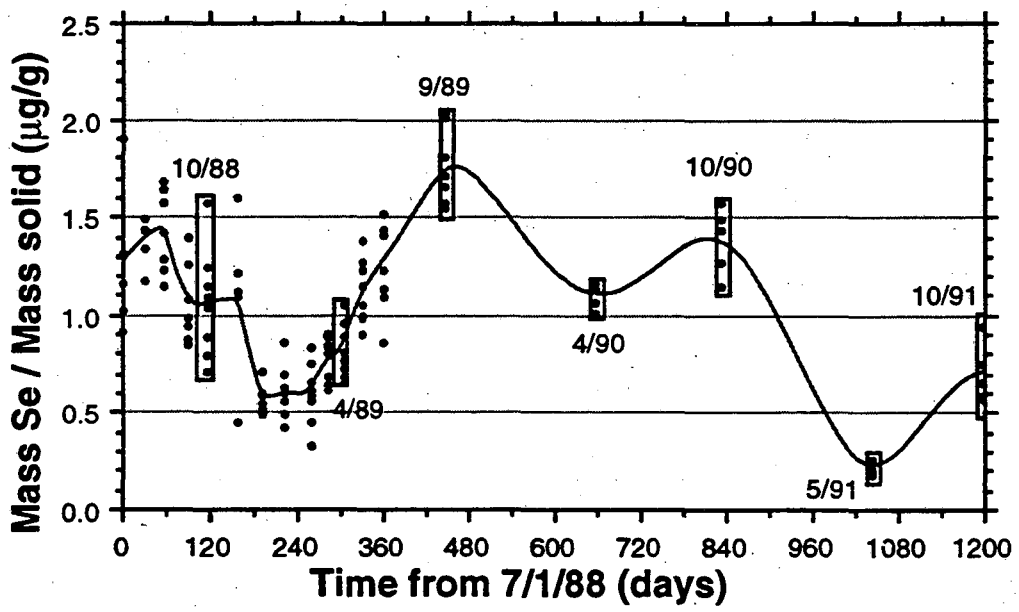

Figure 2.22. Changes in water-extractable selenium in the top 9 cm of soil in plot 8EP: July 1988 - October 1991.

more dominant over the last two years. Salt distribution is never in equilibrium from year to year due to varying rainfall patterns. For example, chloride concentrations in this interval were lowest in May of 1991, likely due to rather intense rainfall of the preceding two months. A comparison of water-soluble selenium concentrations (Figure 2.22) reveals a similar overall pattern, although summertime concentrations of selenium (9/89, 10/90) did not decline markedly, as chloride concentrations did. This may be in large part due to the oxidation of selenium in soil, which leads to increased concentrations of soluble selenium (selenate). Very low selenium concentrations in May 1991 are likely due to soluble selenium being flushed deeper into the soil profile with infiltrating rainwater. Further discussion of selenium oxidation in the soil profile may be found in Section 2.2 and Chapter 3.

Surface salt and selenium concentration changes in plot 9BE are more difficult to discern given their large spatial variability. Changes in chloride concentrations in the top 9 cm of this plot are shown in Figure 2.23. The pattern here differs from plot 8EP in that in April 1990 concentrations did not decline significantly. This may be due to the fact that ≈75% of the rainfall of that season occurred by the end of February, while in 1989 and 1991, much of the rainfall occurred in March and April. In contrast to plot 8EP, where the groundwater table is usually no shallower than 140 cm below the soil surface, the groundwater table in plot 9BE is within 50 cm of the soil surface during the late winter and early spring, wetting up the soil profile, and allowing for more rapid accumulation of solutes near the soil surface when the rain ceases. Unfortunately, the spatial variability of soluble selenium within this plot (Figure 2.24) obscures seasonal changes, with the exception of the decline of selenium concentrations during the winter of 1988/89 and especially the spring of 1991.

Overall, soluble selenium concentrations in the surface soils of this plot have not changed significantly over the last three years.

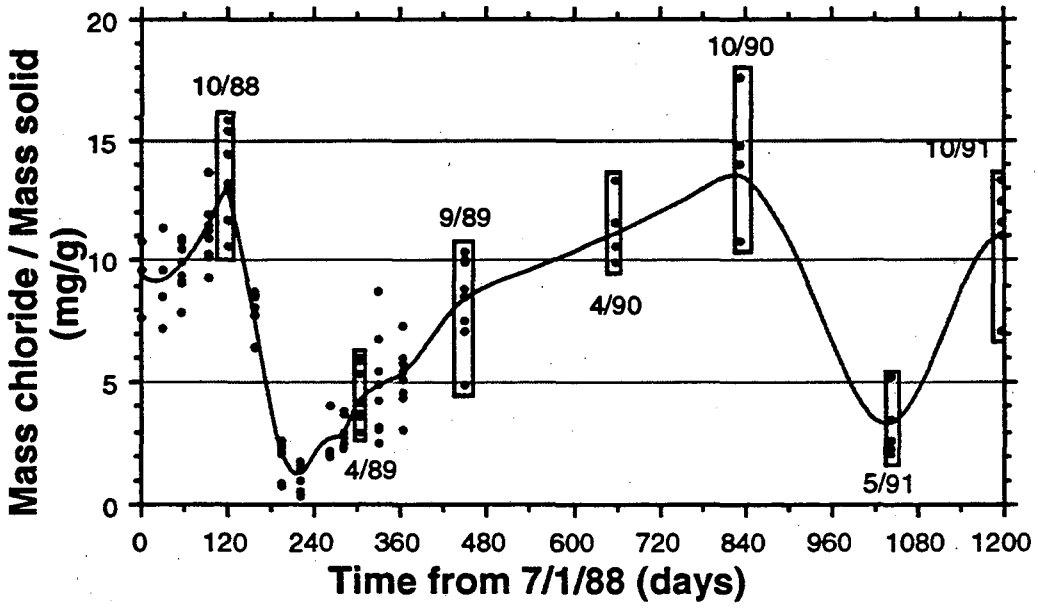

Figure 2.23. Changes in chloride concentration in the top 9 cm of soil in plot 9BE: July 1988 - October 1991.

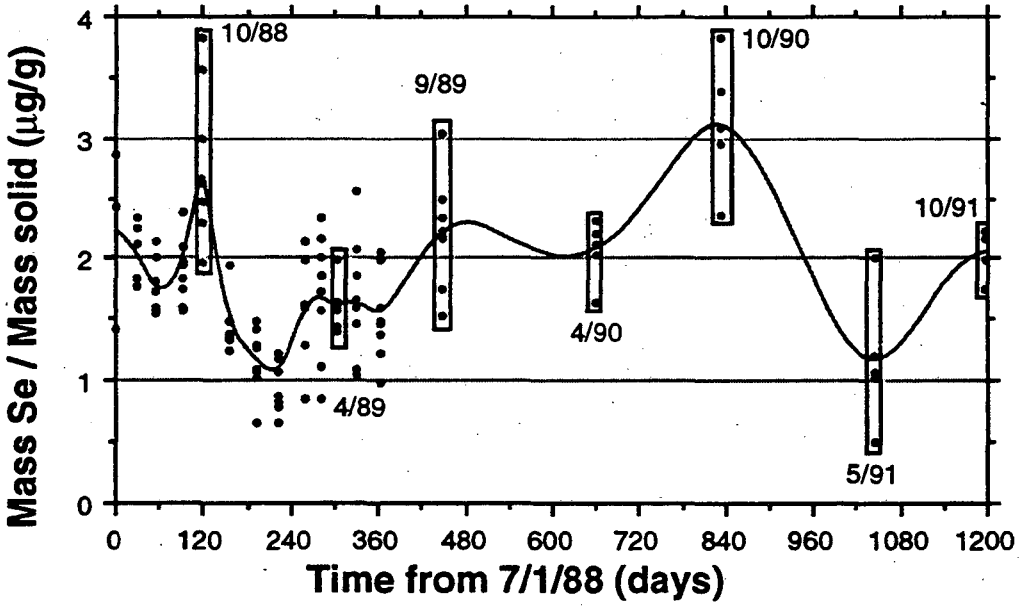

Figure 2.24. Changes in water-extractable selenium in the top 9 cm of soil in plot 9BE: July 1988 - October 1991.

2.4. Field Investigation of the Effects of Rainfall Infiltration on Soil Selenium and Salinity

S. L. Ita and S. M. Benson
Earth Sciences Division
Lawrence Berkeley Laboratory

This study was designed to determine the effects of rainfall infiltration on the seasonal distributions of selenium and chloride in the top 60 cm of soil. It was designed to be a counterpart to an investigation done from July 1988 to 1989 that focused on the evaporative concentration of the same solutes in the top 9 cm of soil and is described in Section 2.3. Together these detailed seasonal investigations should form the basis for identifying the mechanisms for long-term redistribution of solutes in the vadose zone and enable a quantification of the annual transport rates.

2.4.1. Site Characterization and Monitoring

Two sites were chosen for this investigation, named P3RI and P6RI. The soils at site P3RI were of sandy loam texture. The soils at site P6RI were of silty loam texture. At the time of the study site P3RI was sparsely vegetated with *Bassia*, then the most prevalent invading plant species in the former Reservoir. P6RI was more heavily vegetated with saltgrass, typical of the more stably vegetated areas of the former Reservoir.

Monitoring devices were installed at the sites beginning in August 1989. Two dry boreholes were pushed at each site to allow the neutron probe access to the subsurface in order to measure the moisture content of the surrounding soils. During measurement, the tool was lowered in 15-cm intervals down to a maximum depth of 150 cm. Two sets of soil water samplers were emplaced at each site to collect pore water samples at 15-cm intervals to 90 cm and then 30-cm intervals to 150 cm. One set of tensiometers per site was installed to measure the fluid pressure in the unsaturated soil, again at 15-cm intervals to 90 cm and then at 30-cm intervals to 150 cm. A shallow groundwater well was augered at each site to monitor both the elevation of the local water table and the chemical conditions in the local groundwater.

Monitoring began on October 19, 1989, and continued to October 19, 1990. In addition to making readings or collecting samples from the various instruments, 60-cm soil cores were taken from the four corners of each site to monitor the conditions in the overall soil system. The soils were analyzed for chloride and water extractable selenium by making a 5:1 water-to-dry-soil-weight extraction. The water-extracted amount is nearly equal to the readily soluble pools of these constituents in the soils. The results from the water extractions are the focus of this report, since they were the most illustrative of the solute changes occurring at the sites.

2.4.2. Hydrogeologic Conditions

At Kesterson, water enters the soil system by either rainfall infiltration or water table rise and leaves the system by evaporation or transpiration. Little if any net deep percolation occurs except in areas with relatively coarse sediments at the soil surface and during some major storms. Infiltration and evaporation will mainly affect the near-surface soil concentrations, whereas the water table fluctuations will mainly affect the soils lower in the vadose zone.

The amount of infiltration depends on the amount of precipitation. A record of rainfall events was obtained from on-site weather stations operated by the U.S. Bureau of Reclamation. This record shows that isolated rainfall events occurred throughout the fall, winter, and spring. The main rainy season began in mid-October and lasted through mid-March. However, sustained events did not start until early January. Redistribution of solutes was expected to be most notable during the sustained events, since the transport of solutes requires both sufficient water influx and sufficient moisture content in the soils.
Water table rise was also expected to affect the distribution of soluble selenium in the vadose zone. Monitoring over the study period showed that elevation of the water table was nearly cyclic. At both sites the deepest values, ~ 250 cm, were measured in late summer and early fall; the highest values, ~ 100 cm, were measured in early spring.

Water content monitoring by the neutron probe reflects the seasonal effects of rainfall infiltration and water table rise. Representative seasonal trends from neutron probe access tube B at site P3RI are presented in Figure 2.25 Readings began in early December 1989, when the moisture contents in the soil profiles were near their lowest extremes. By January, the deepest moisture content readings had increased in response to the rising water table. Readings in the upper profile increased during January and February in response to the end of the rainy season. In late April, all portions of the profile, aside from the very top 15 cm, were at their highest moisture content values. The decrease in the top 15 cm from the end of March was due to the cessation of sustained rainfall and an increase in the evaporation rate. The moisture content at all depths decreased throughout the remainder of the study. By October 1990, evaporation and transpiration throughout the summer had reduced the entire moisture content profile to its lowest extreme.

The nature of the neutron probe and tensiometer data suggests that moisture changes in the lower and upper parts of the profile are separately attributable to water table rise and rainfall infiltration, respectively. The transition between the two zones appears to be located at ~ 75 cm depth. Moreover, it can be seen that the measurements always show a trend of increasing water content with depth. In areas with fine-grained soils and a shallow groundwater table, such as these sites have, this profile trend is typical of an evaporation-dominated soil moisture system.

2.4.3. Solute Data

Seasonal variations in the solute concentrations attributable to the physical processes of infiltration and evaporation are the result of a few simple mechanisms. Soluble inventories of both selenium and

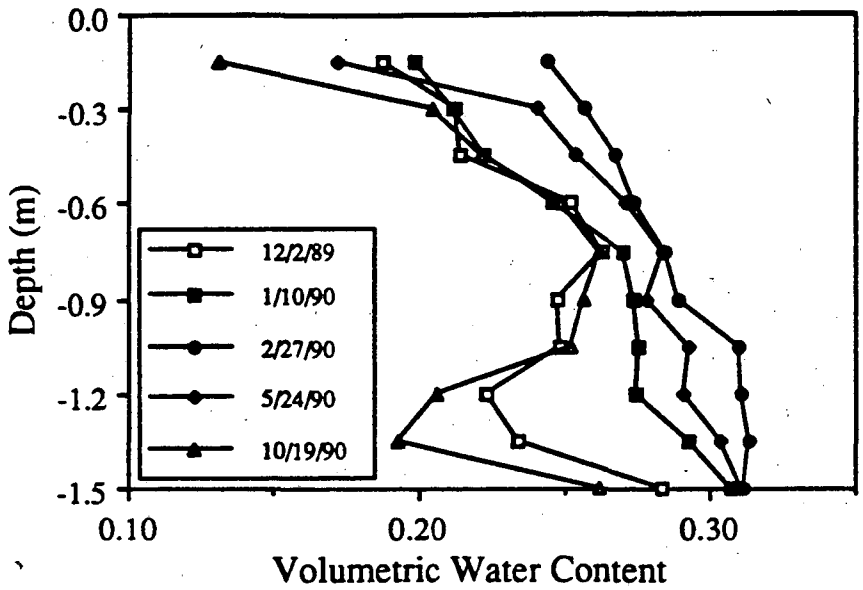

XBL 924-660

Figure 2.25. Water content profiles for P3RI at location B. Selected dates were chosen to represent the seasonal trends.

chloride will decrease as a result of displacement and/or mixing with fresher water. They will increase as a result of displacement and/or mixing with more concentrated water and also accumulation due to evaporative loss of water. In addition, the inventory of soluble selenium will be affected by changes in the redox potential. When the redox potential is high, such as in oxygen-rich unsaturated soils, a large fraction of the selenium will eventually be in oxidized, and thus soluble, forms. When the redox potential is low, such as in oxygen-poor saturated soils, the selenium will be in reduced, and thus insoluble, forms (Geering et al., 1968; Masscheleyn et al., 1990).

A mechanism based on this redox sensitivity of selenium mobility has been proposed that may lead to long-term decreases in the surface selenium inventory. As rainfall moves into the surface layer, it acquires solutes by dissolving the precipitated salts and mixing with the highly concentrated pore water. The rainwater then carries these solutes lower in the soil profile as it continues to infiltrate. When it reaches oxygen-poor zones lower in the profile, the selenium species may be reduced and immobilized while chloride remains with the migrating soil water. After the rainy season, the soils begin to dry as a result of evaporation, and the mobile solutes are carried up toward the soil surface. Reduced selenium species will not be transported out of these zones until they oxidize. Oxidation of selenium is believed to be a relatively slow process at Kesterson. Moreover, as the water content drops in late spring and summer, solute transportation will decrease significantly as the water content, and thus hydraulic conductivity decreases. Therefore, selenium may be trapped in these lower soil zones. Over time this process could lead to substantial decreases in the surface selenium inventory.

Inspection of the solute data provides the basis for determining the effects of these various mechanisms. Only the data from site P3RI will be presented here, since they were illustrative of the changes that occurred. The chloride and water-extractable selenium concentrations in the 0–5 cm soil interval at both soil sampling sites are shown in Figures 2.26 and 2.27 respectively. Figures 2.28 and 2.29 present the chloride and water-extractable selenium concentrations, respectively, at representative depth intervals over the study period.

A notable fluctuation is seen in the water-extractable selenium concentrations for the 0–5 cm soil interval in late January. Both solute concentrations decreased in mid-January with the onset of infiltration. Immediately following this decrease, the concentrations of selenium species increased while the chloride concentrations remained constant. This increase took place within a week and appears to be associated with increased moisture content in the surface soils. It will be discussed in greater detail later in this report. Other changes that can be related specifically to rainfall infiltration and evaporation are discussed below. Infiltration causes decreases in solute concentrations in the near-surface soils by providing the fresher water that displaces and mixes with the highly concentrated surface pore water. This type of change is evident in the concentration data for 0–5 cm shown in Figures 2.26 and 2.27. In mid-January, the solute concentrations at both sampling areas decreased. These decreases correspond to the beginning of sustained rainfall events and follow the saturation of the surface soils, as shown in the soil moisture content data in Figure 2.25. The chloride concentration levels remained low through the remainder of the rainy season. After increasing immediately with the onset of sustained rains, the selenium concentrations dropped and remained low through the rest of the rainy season.

Infiltration also causes increases in solute concentrations deeper in the profile as the surface inventories are flushed to this zone by the migrating rainwater. This type of change is evident in Figures 2.28 and 2.29, where solute concentrations increase at the 15–20 cm depth in mid-January at the same time as the surface concentrations decrease. Following these increases, the chloride concentrations fall as the infiltrating rainwater displaces the resident pore water. This was not the case for the water-extractable selenium. Following the mid- to late-January increases, the selenium concentrations slowly returned to previous levels.

Evaporation causes increases in the near-surface soil concentrations by establishing the gradient that causes deeper water to migrate upward. These types of changes are evident in Figures 2.26, 2.27, and 2.28. After the rainy season ends in mid-March, the chloride and water-extractable selenium concentrations within the 0–5-cm interval immediately increase. Evaporation was expected to cause increases throughout the summer months in this surface interval, resulting from accumulation of solutes. However, the chloride concentrations remained nearly constant at P3RI#4 and decreased at P3RI#1 (Figure 2.26). The surface-water-extractable selenium concentrations at both sampling areas reached a seasonal maximum in late June, then decreased until late September (Figure 2.27).

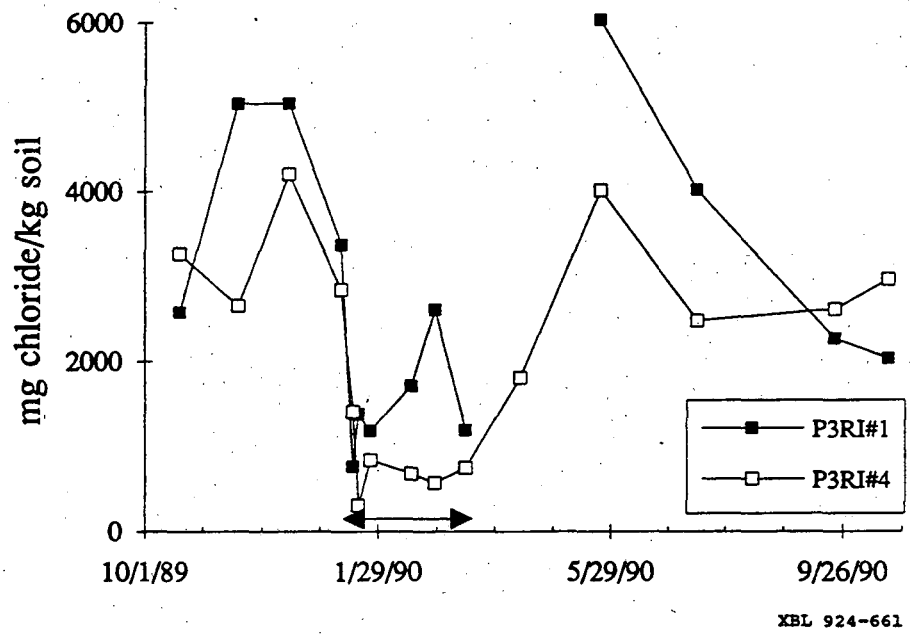

Figure 2.26. Chloride concentrations in the top 5 cm of soil at site P3RI. Arrows indicate the main rainy season.

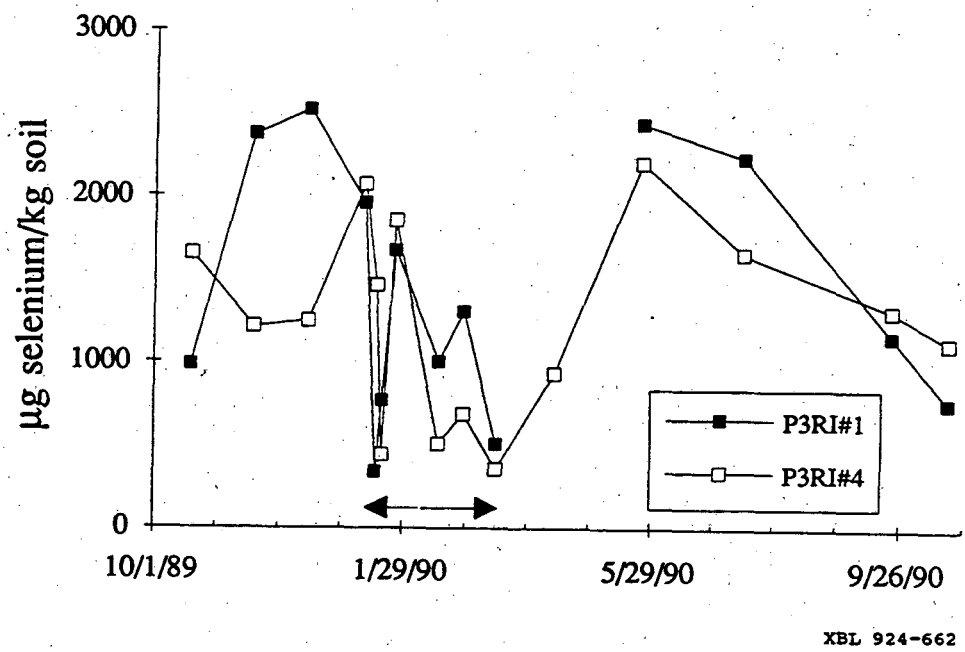

Figure 2.27. Water-extractable selenium concentrations in the top 5 cm of soil at site P3RI. Arrows indicate the main rainy season.

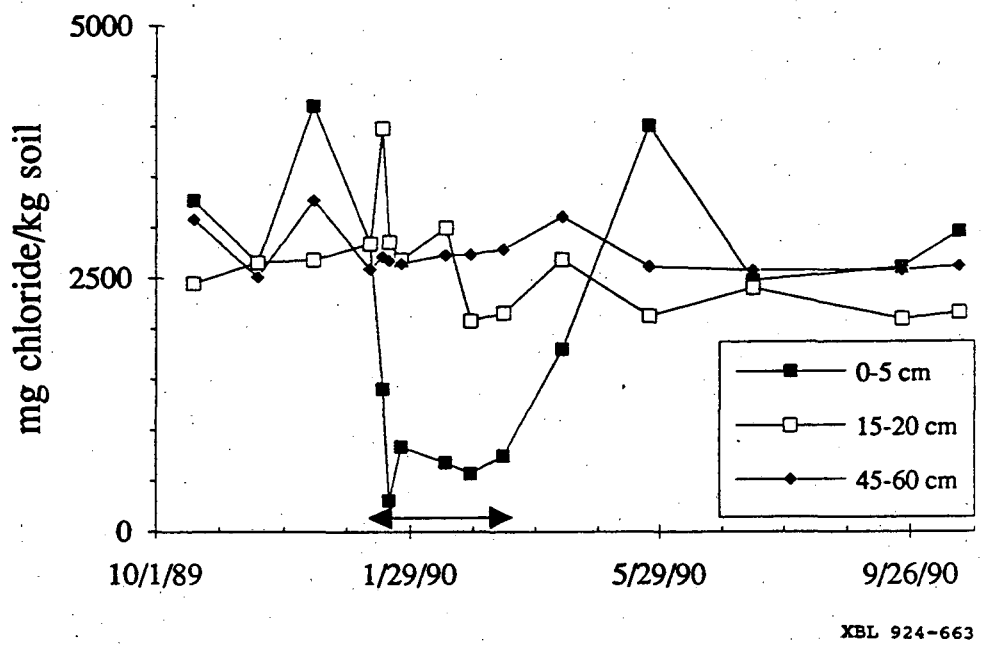

Figure 2.28. Chloride concentrations in three selected depth intervals at site P3RI location #4. Arrows indicate the main rainy season.

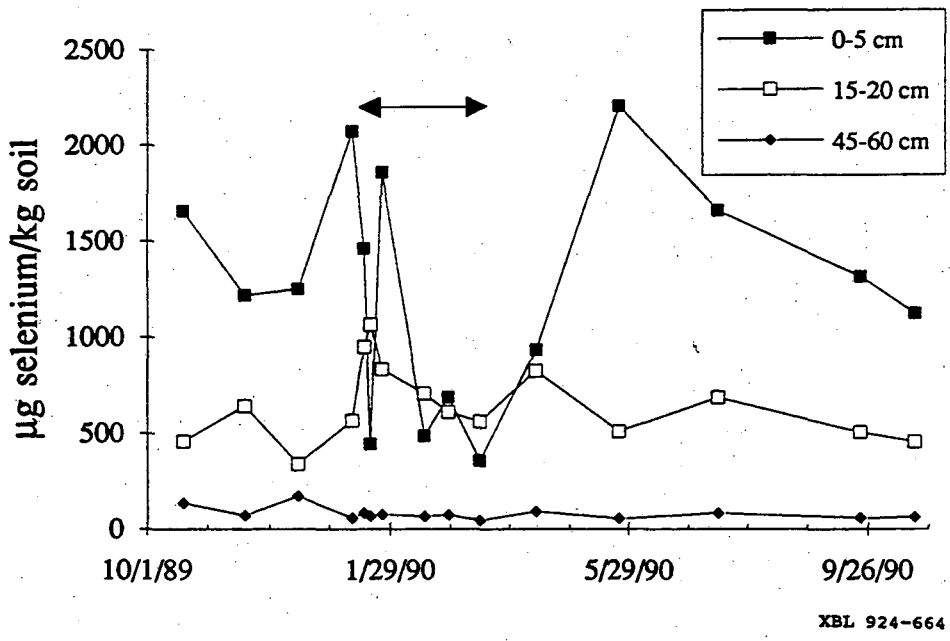

Figure 2.29. Water-extractable selenium concentrations in three selected depth intervals at site P3RI location #4. Arrows indicate the main rainy season.

2.4.3. Data Analysis

In an attempt to obtain a more detailed and quantitative understanding of the processes affecting the solute inventories, two simple calculations were performed on the data. The first involved summing the mass of the particular solute in each interval over the entire profile. The second calculation involved taking the ratio of selenium to chloride.

2.4.3.1. Solute Mass Inventories

The purpose of this calculation was to determine any changes in the annual or seasonal inventories within the top 60 cm of the soil profile. The total inventories of chloride over the study period at P3RI are shown in Figure 2.30 Annual inventories appear to increase slightly over the study period. Two interesting points can be made about seasonal changes. First, there are no notable decreases in the inventory during the main rainy season. This suggests that solute transport by infiltration does not extend beyond 60 cm depth for years with similar or lower rainfall. Second, the total inventory does not increase during spring and summer; this suggests that evaporation is not transporting chloride, and thus water, up from depths below 60 cm. Both observations indicate that the seasonal redistribution of water and solutes may be confined to the upper 60 cm of the soil system at these two sites when weather patterns are similar to that of 1989-1990.

The inventories of total water-extractable selenium from the two sampling areas at P3RI over the study period are shown in Figure 2.31. At the end of monitoring, the annual inventories at both sites appear to have increased slightly. The seasonal inventories decrease significantly over the rainy season and then increase in spring. This indicates that selenium is being reduced because of the increasing soil moisture over the rainy season. Moreover, the inventories of water-extractable selenium do not appear to increase significantly over the summer months, suggesting that oxidation of selenium may not significantly add to the soluble inventory over a single season at this location as suggested from data at site 9B5 described in Section 2.3. However, two-fold increases in the water-extractable selenium inventory have been observed annually at other locations (Tokunaga et al., 1991) indicating that a range of conditions which exist within the former Reservoir.

2.4.3.2. Species Ratios

The purpose of taking the ratio between various solutes is to investigate the differences in transport between chloride and selenium. Since chloride is a conservative, nonreactive tracer, it can be used to indicate water movement. The transport of selenium, however, should also depend on its oxidation state.

Figure 2.32 shows the ratios of extractable selenium to chloride in the soil extract samples from sample area P3RI#4. The most notable feature is the dramatic increase in the ratios for the 0–5-cm interval at the beginning of the rainy season. Similar but much smaller increases are seen at 15–20 cm. Comparison with the concentration data shows that these increases are primarily the result of an increase in the water-extractable selenium concentration along with a slight decrease in the chloride concentration.

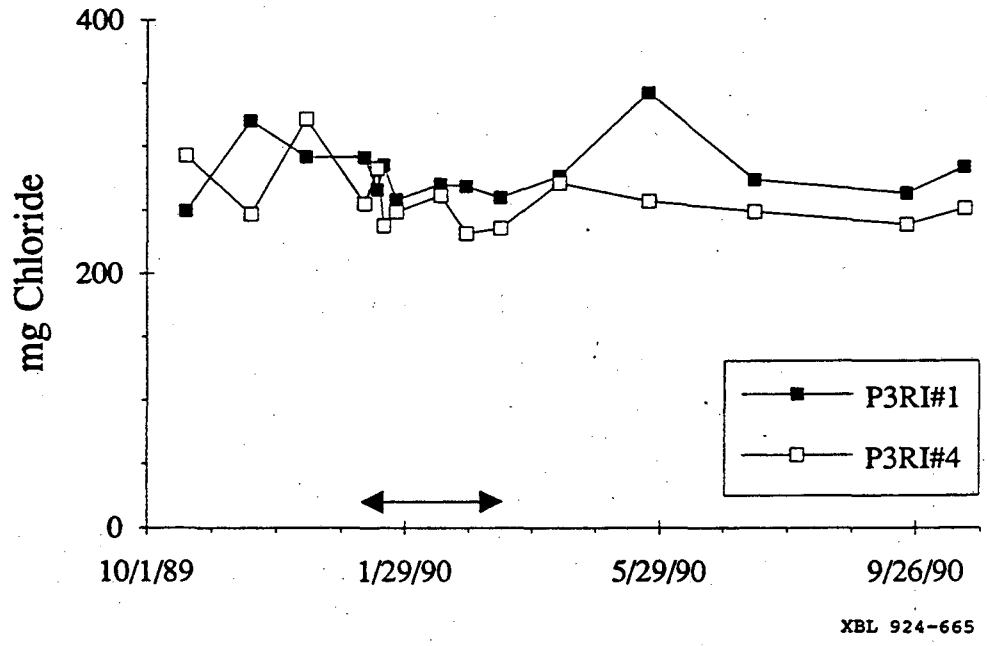

Figure 2.30. Mass of chloride in the complete 60 cm soil samples collected at site P3RI over the study period. Arrows indicate the main rainy season.

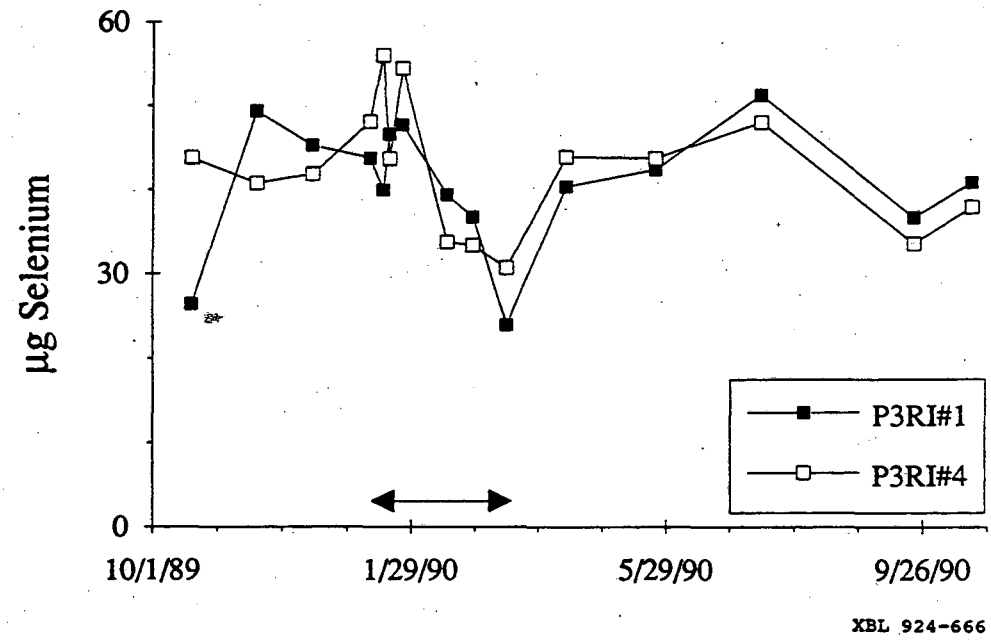

Figure 2.31. Mass of water-extractable selenium in the complete 60 cm soil samples collected at site P3RI over the study period. Arrows indicate the main rainy season.

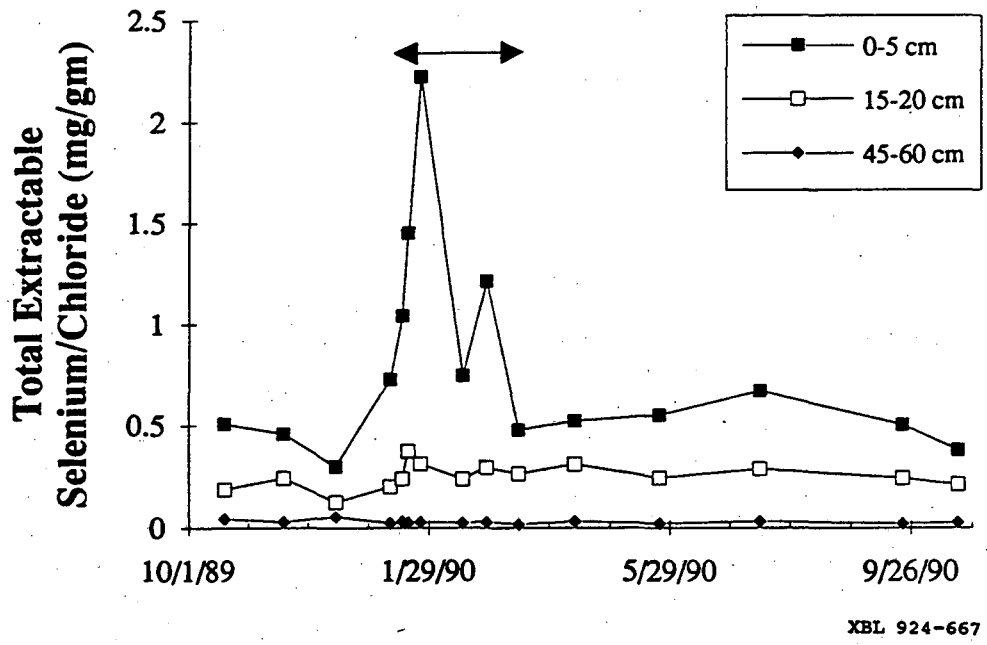

Figure 2.32. Ratio of water-extractable selenium (mg) to chloride (gm) for selected depth intervals at site P3RI location #4. Arrows indicate the main rainy season.

This suggests that undetermined processes are remobilizing selenium at the soil surface early in the rainy season. With time this remobilized selenium is transported deeper in the profile, where some fraction of it is reduced to less mobile forms.

2.4.4. Selenium Transformations

Two unexpected changes were seen in both the concentration and ratio data for water-extractable selenium in the surface interval (0–5 cm) of the soil samples. First, one week after sustained rainfall events began, the amount of water-extractable selenium increased, as seen in the concentration data and ratio calculations. Since the rainwater contained negligible selenium, these increases in water-extractable selenium concentration can only have come from the insoluble inventory already in the soil system. Second, after recovering to pre-rainfall values in early spring, the concentrations of water-extractable selenium decreased over the summer months instead of increasing as expected. The steady chloride concentrations may indicate that solute transport had ceased because of the low hydraulic conductivity in the extremely dry soils. However, this does not account for the large decreases in the water-extractable selenium concentrations.

Neither of these phenomena were observed in previous studies. They may be due to a mechanism involving the high organic content in the surface interval, root activity affecting water movement, and

changes in soil conditions such as pH. Detailed laboratory work under controlled conditions may be required to fully identify the processes.

2.4.5. Summary

This and other studies have clearly demonstrated that solutes in the soils at Kesterson Reservoir undergo significant seasonal transport. Therefore, different solute inventories will be measured at different periods depending on the seasonal soil conditions. It also demonstrated that seasonal transport, and thus redistribution, appears to be confined to the top 60 to 75 cm of this soil profile for similar soils and similar weather patterns. The combination of the cyclical redistribution processes of infiltration and evaporation is expected to gradually transport selenium from the soil surface, where it is presently concentrated, downward in the profile.

A notable and potentially important phenomenon observed here indicated that previously immobile selenium in the depth interval 0–5 cm was remobilized shortly after heavy rainfall events began. Moreover, a fraction of the mobile selenium was removed from this interval over the dry summer months. These changes had not been observed in previous investigations. A detailed laboratory investigation, under more controlled conditions, may clarify the existence and significance of these changes.

2.5. Reservoir-Wide Monitoring of Soil Selenium

Carolyn Wahl and Sally Benson
Earth Sciences Division
Lawrence Berkeley Laboratory

Since 1989, LBL and CH2M Hill researchers have cooperated to provide a data set on the overall status of the selenium inventory at Kesterson Reservoir. Kesterson Reservoir is divided into three distinct habitat types: fill (F), grassland (G) and open (O) and three trisections (T1, T2, T3) (Figure 2.33). Fill areas represent areas where the soil surface was previously below the maximum height of annual groundwater rise. The fill areas were frequently flooded with drain waters. An organic-rich ooze was deposited in the pond bottoms. Fill habitat is presently vegetated with annual vegetation dominated by *Bassia hyssopifolia* and annual grasses. Fill habitat covers about 56 percent of the Reservoir.

Grassland areas, although present in patches throughout the Reservoir, dominate the relatively dry, upland northern ponds and contain large areas covered by saltgrass *(Distichlis spicata).* This habitat normally remained above water most of the year, and a loose deposit of organic detritus accumulated under the canopy of the living vegetation. Grassland sites are dominated by saltgrass and cover 31 percent of the Reservoir.

Open habitats represent areas above high groundwater levels which were flooded during the winter and remained damp during the summer and fall. These areas were dominated by cattails (*Typha* sp.) which accumulated large amounts of selenium. As flow ceased, and the Reservoir dried, loose thick organic deposits of selenium-rich material accumulated and presently remain in these areas. Open areas are former cattail areas that were dewatered and disced in 1988 to eliminate nesting for tri-colored blackbirds. Open sites are sparsely vegetated with *Bassia,* prickly lettuce *(Lactuca serriola)*, and clover (*Medicago, Melilotus, Trifolium spp.).* Open habitat covers about 13 percent of the Reservoir (CH2M Hill, 1991).

Trisection 1 (T1) consists of the southern Ponds 1, 2, 3, and 4; Trisection 2 (T2) consists of the central Ponds (5, 6, 7, and 9); and Trisection 3 (T3) consists of the northern ponds 8, 10, 11, and 12. Ponds 1 and 2 of T1 received the largest amounts of agricultural drainage water from the San Luis Drain during 1978-1986, as water flowed by gravity from south to north, with Ponds 1 through 5 being used most extensively. The ponds in this trisection have the highest reported soil selenium levels (LBL, 1990b; CH2M Hill, 1991), and contained mostly open water and cattail areas in the past, and presently contain mostly open and fill habitats.

The ponds in T2 also received substantial amounts of drainwater in the past (LBL, 1990b; CH2M Hill, 1991). However, these ponds generally have lower soil selenium levels than those in

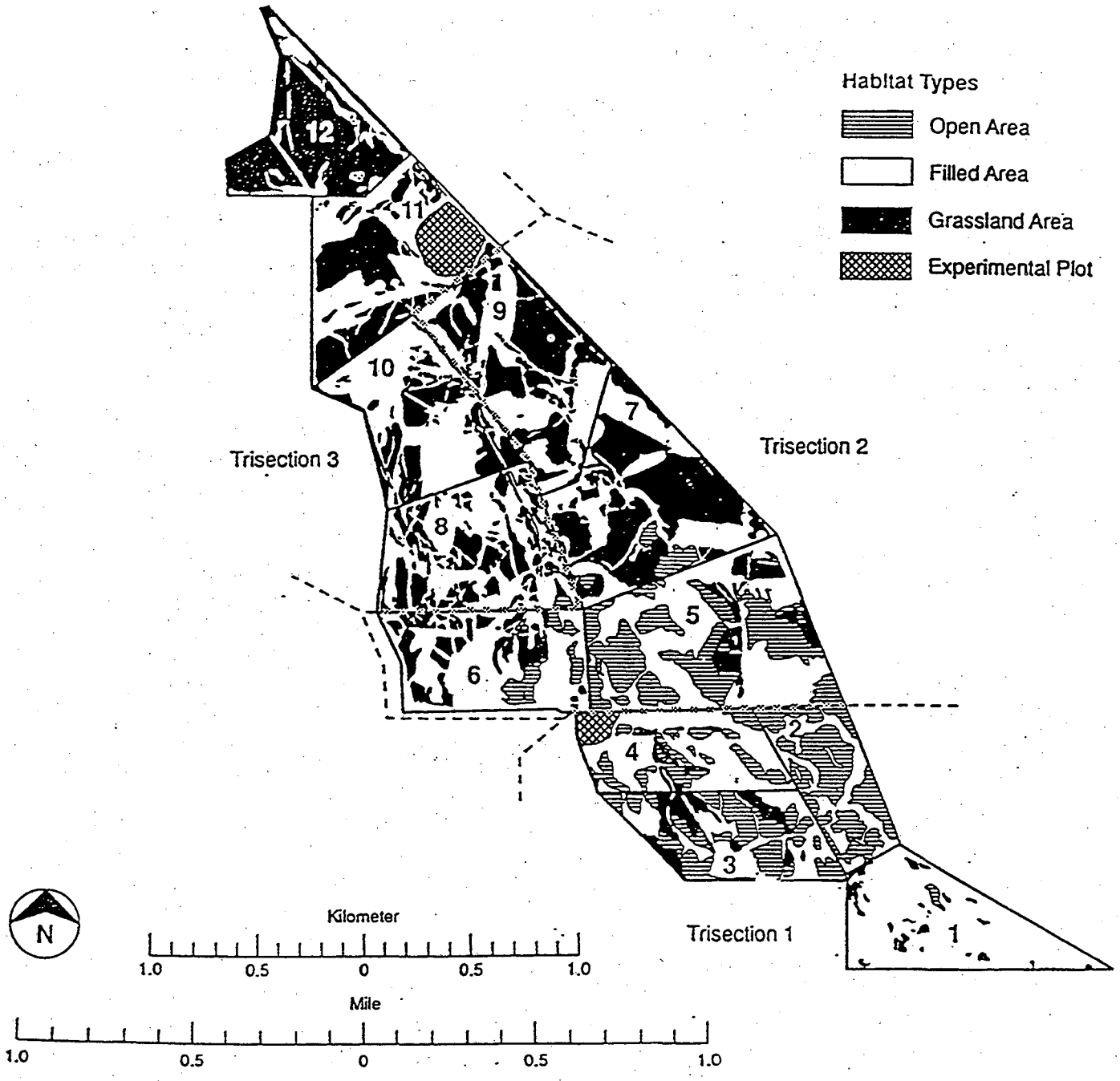

Figure 2.33. Map of habitat and trisection delineations at Kesterson Reservoir (CH2M-Hill, 1991).

T1. Open water, and cattail areas were characteristic of T2 in the past, and presently open grassland and fill habitats are all found in the trisection. Trisection 3 received the least amount of drainwater and ponds in this trisection have the lowest reported soil selenium levels (LBL, 1990b; CH2M Hill, 1991). Trisection 3 is dominated by large areas of grassland and fill habitats.

Within each trisection, six sites of each habitat type were chosen for long-term monitoring of soils for a total of 54 sampling sites. Soil samples were collected by inserting a 2.54 cm diameter push-tube sampler to a depth of 15 cm from six stations in each habitat type of each trisection, for a total of 18 stations per trisection. Three samples (A,B,C) were collected at each site within a radius of about 8 m of the stations center. The sampling dates for the soils over the three-year period were as follows: 1989 (May 8,9); 1990 (March 7); 1991 (Feb. 20, 26, 27).

Soil samples were homogenized at field-moist conditions by hand chopping and passed through a 4.75-mm sieve. A known mass (between 20 and 30 g) of the homogenized subsample was then placed into an open stainless steel can and oven dried at 105°C for 24 hours. The common practice of air drying samples prior to extraction was not employed in order to minimize possible accelerated oxidation of Se during sample processing (Tokunaga and Benson, 1992). At the end of the 24-hour period, the subsample was weighed and the gravimetric moisture content of the soil (mass of water per mass of dry soil) calculated. Approximately two grams of the subsample was pulverized in a ball mill and pressed into a pellet for energy dispersive X-ray fluorescence (XRF) analysis which measures the total selenium concentrations of the sample (Giauque et al., 1976).

For the water-soluble selenium determination, another subsample of the homogenized soil (20 to 25 g) was used to prepare a 5:1 water to soil extract (distilled water:dry soil). After being placed on a reciprocating shaker table and agitated for 60 minutes the mixtures were centrifuged at 7800 revolutions per minute for 15 minutes and the supernatant solution was filtered through a 0.45 micron membrane filter prior to analysis.

Soil water extracts were analyzed for water-extractable selenium, water-extractable selenite; and the two major anions: sulfate and chloride. Sulfate was analyzed using an Inductively Coupled Plasma Spectrophometer (ICP). Chloride was analyzed using a Mohr titration, as described by Flaschka et al. (1969). Water-extractable selenium and water-extractable selenite were analyzed using atomic absorption spectroscopy (AAS) coupled with a hydride generator (LBL, 1990b). Samples were fed untreated into the instrument to determine selenite concentrations. Water-extractable selenium was analyzed by treating 5.0 ml of the sample with 0.2 ml of 2% ammonium persulfate and 5.0 ml of concentrated HCL before it was fed into the instrument. Water-extractable selenium includes water-extractable selenite, water-extractable selenate, and minor amounts of organically associated selenium (Weres et al., 1989; Long et al., 1990).

2.5.1. Results and Interpretation

Analysis of Variance (ANOVA) was performed to determine if there were significant differences in soil selenium concentrations between year (1989, 1990, and 1991), trisection (T1,T2,T3) and habitat (F,G,O) delineations. Total selenium, water-extractable selenium, water-extractable selenite, and chloride data were determined to be log-normally distributed using the fractile method described in Warrick and Nielsen (1980). Sulfate concentrations were similarly shown to be normally distributed. The Fisher's PLSD method was used to determine significant differences in concentrations within year, trisection, and habitat ($P<.05$) (Mead, 1988). Mean values and confidence intervals are summarized in Table 2.2 and Figures 2.34 through 2.37. All concentrations reported are in units of mg/kg on a dry weight basis.

Within each habitat (F, G, O), selenium concentrations range over an order of magnitude as illustrated in Figure 2.38, where total water-extractable selenium has been plotted versus total selenium. Figure 2.38 illustrates that soil selenium concentrations may be broadly grouped by habitat, yet a large overlapping range between habitats is observed. This large spatial variability observed within the Reservoir soil system is due to the different depositional environments that existed while drainwater was entering the Reservoir. Additional factors contributing to the soil variability observed within the Reservoir include: the displacement of material by earth moving equipment, sampling sites located at boundaries between different soil types, the multiple sources of the fill material applied to the Reservoir and the uncertainty of the depth of the fill material, and the redistribution of selenium from deep in the soil profile to the upper soil surface.

The distribution and temporal changes therein provided in Table 2.2 can be categorized in terms of three main factors or trends which include: 1) spatial trends based on habitat and trisection delineations; 2) temporal trends due to the oxidation of the selenium inventory and the decomposition of organic matter; and 3) temporal trends due to the seasonal cycling of the surface solute selenium inventory. These are described in detail in the following sections.

2.5.2. Spatial Trends

When 1989, 1990 and 1991 samples are combined and grouped by habitat, selenium concentrations are greatest in the open habitat and least in the fill habitat as shown in Table 2.2. This is consistent with the historical use of the Reservoir and the filling operations. As previously noted, selenium concentrations in the sediments of Kesterson Reservoir are reflective of past depositional environments and the corresponding amount of soil organic matter associated with these sediments. Fill habitats represent former wetland areas which were covered with imported soil. Grassland areas include areas dominated by saltgrass which remained above water most of the year. Open habitats include areas which were flooded during the winter and remained damp during the summer and fall. These previously cattail vegetated soils accumulated large amounts of selenium. The higher selenium values observed for the open habitat are associated with the

Table 2.2. Summary of soil selenium concentrations in the top 15 cm of the soil profile over the three-year sampling period. Values represent geometric mean concentrations * expressed in mg/kg-soil. Confidence intervals within the ninety-five percentile are indicated below geometric mean concentrations.

	Total Selenium	Tot Wat-Ext. Se	Ratio Wat-Ext./Tot Se	Selenite	Ratio Selenite/ Wat-Et. Se	Sulfate (*Mean)	Chloride
Year							
1989	3.9 A	.17 A	.05 A	.02 A	.12 A	2120 A	545 A
	(2.8 - 5.5)	(.11 - .25)	(.04 - .06)	(.01 - .03)	(.08 - .17)	(1650-2600)	(380 - 775)
1990	2.7 A	.12 A	.04 A	.02 A	.16	1800 A,B	220
	(1.9 - 3.8)	(.08 - .17)	(.03 - .06)	(.01 - .03)	(.12 - .22)	(1430-2170)	(140 - 350)
1991	2.9 A	.19 A	.07	.02 A	.07 A	1380 B	500 A
	(2.1 - 4.1)	(.12 - .30)	(.05 - .10)	(.01 - .03)	(.05 - .10)	(1030-1730)	(370 - 670)
Habitat							
Fill	1.3	.06	.06 A	.01	.11 A,B	1160	240 A
	(.96 - 1.7)	(.04 - .10)	(.04 - .07)	(.01 - .02)	(.07 - .18)	(640-1690)	(280 - 810)
Grassland	2.9	.17	.05 A	.03 A	.16 A	1300	480 A
	(2.1 - 4.1)	(.12 - .32)	(.05 - .07)	(.02 - .04)	(.12 - .20)	(970-1620)	(170 - 340)
Open	7.9	.35	.04 A	.03 A	.07 B	2640	650
	(6.2 - 10)	(.27 - .47)	(.03 - .06)	(.02 - .04)	(.05 - .10)	(2300-2970)	(500 - 850)
Trisection							
T1	4.5	.29	.06	.02 A	.07 A	2120 A	630
	(3.2 - 6.2)	(.19 - .44)	(.05 - .08)	(.01 - .03)	(.05 - .11)	(1700-2540)	(450 - 890)
T2	2.9 A	.13 A	.05 A	.02 A	.12 A,B	1620 A,B	300 A
	(1.9 - 3.7)	(.09 - .19)	(.04 - .07)	(.01 - .03)	(.08 - .17)	(1250-1990)	(215 - 425)
T3	2.5 A	.10 A	.04 A	.01 A	.14 B	1560 B	350 A
	(1.8 - 3.6)	(.07 - .15)	(.03 - .05)	(.01 - .02)	(.10 - .19)	(1095-2020)	(230 - 530)

*Within year, habitat, or trisection, geometric means not sharing the same letter are significantly different at a 95% confidence level.

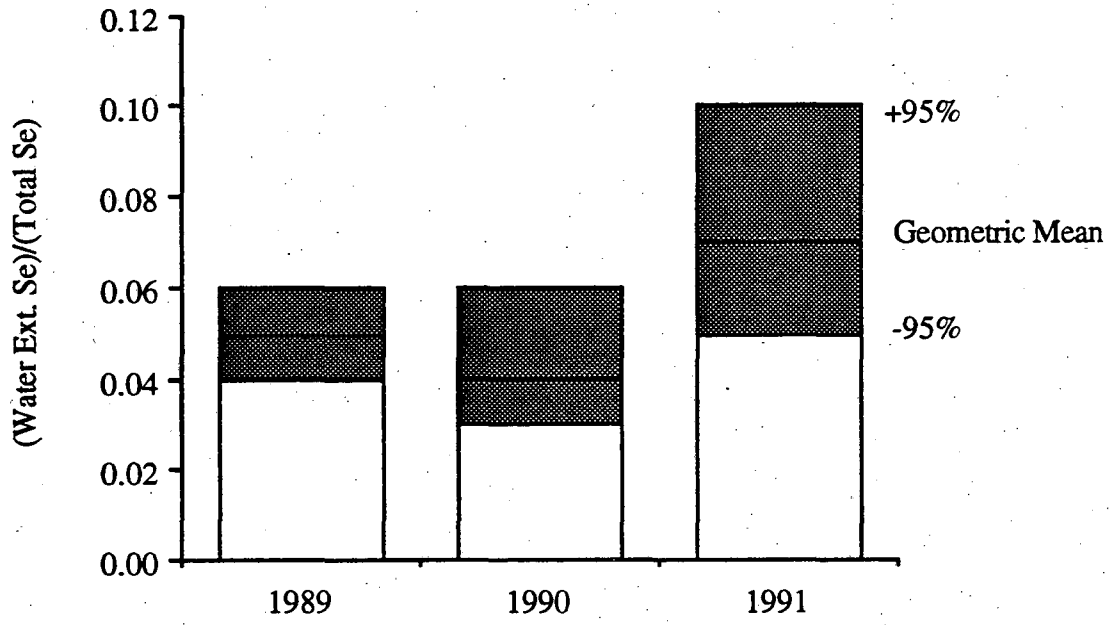

Figure 2.34. Geometric mean value for the ratio of water-extractable to total selenium concentrations in the top 15 cm of the soil profile. The ratio in 1991 is significantly higher than the ratio in either 1989 or 1990, representing a 43% increase over the three-year monitoring period.

high soil organic matter content of this habitat, its exposure to larger volumes of contaminated drainage water, and lower bulk density.

When 1989, 1990 and 1991 samples are combined and grouped by trisection, selenium concentrations are significantly greater in T1 than in either T2 or T3 as shown in Table 2.2. As previously indicated, this is due to the historical use of the Reservoir, as Ponds 1 and 2 of T1 were first to receive agricultural drainage water from the San Luis Drain, as water flowed by gravity from south to north, with Ponds 1 through 5 being used most extensively.

2.5.3. Temporal Trends due to the Oxidation of the Selenium Inventory

Since discontinuing water deliveries to the Reservoir, soil profiles have dried out and conditions in the vadose zone have become increasingly more oxidized. This change in redox conditions should result in the progressive oxidation and solubilization of the selenium inventory (Geering et al., 1968; Elrashidi et al., 1987). These trends have been observed in a few profiles at determine the extent to which this trend or others can be detected.

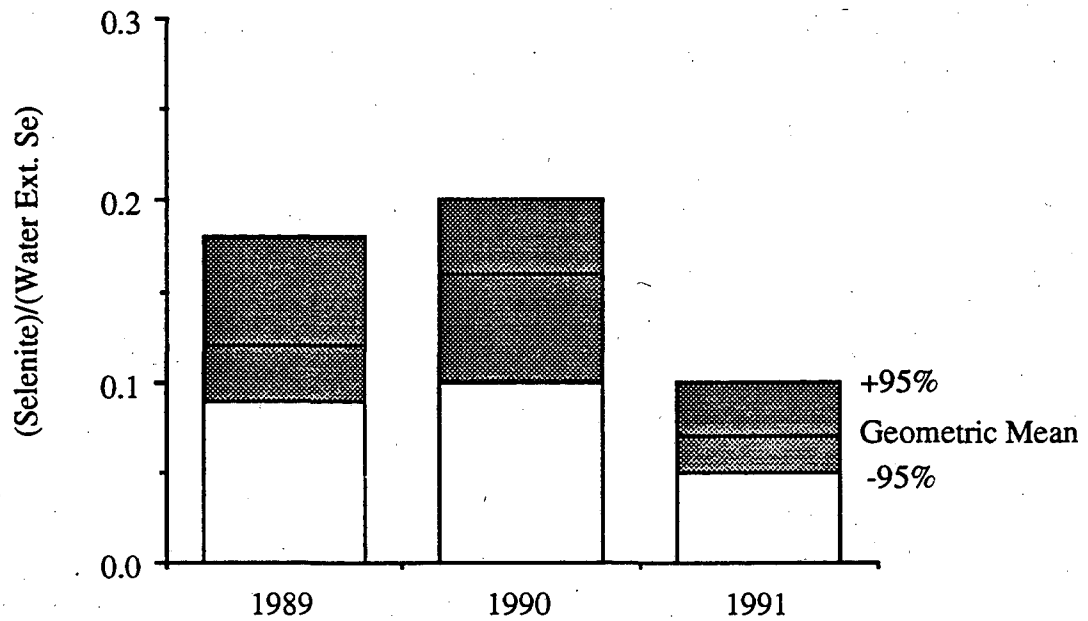

Figure 2.35. Geometric mean value for the ratio of selenite to water-extractable selenium concentrations in the top 15 cm of the soil profile. The ratio shows a significant decrease of 42% between 1989 and 1991, and a significant decrease of 58% between 1990 and 1991.

As indicated in Table 2.2, significant changes in the experimental data have not yet been detected in the total and water-extractable selenium inventories over the three-year monitoring period. The Kesterson soil environment is highly variable as previously indicated in Figure 2.38 and illustrated in Figures 2.39 and 2.40 where both total and water-extractable selenium concentrations range over three orders of magnitude. In order to further understand the distribution between the total and water-extractable fractions in predicting temporal trends, the ratio of water-extractable selenium to total selenium was analyzed. This ratio provides a more sensitive indicator of temporal changes as illustrated in Figure 2.41 where the range of values is less variable than those observed in Figures 2.38 and 2.39.

The fraction of the total selenium inventory that was water-extractable increased from 5% to 7% between 1989 and 1991 as observed in both Table 2.2 and Figure 2.34. While this demonstrates that only a small fraction of the total selenium inventory is currently mobile and available for plant uptake, it also supports thermodynamic predictions that the inventory will oxidize to more soluble and mobile species. The increase in this ratio is particularly notable in

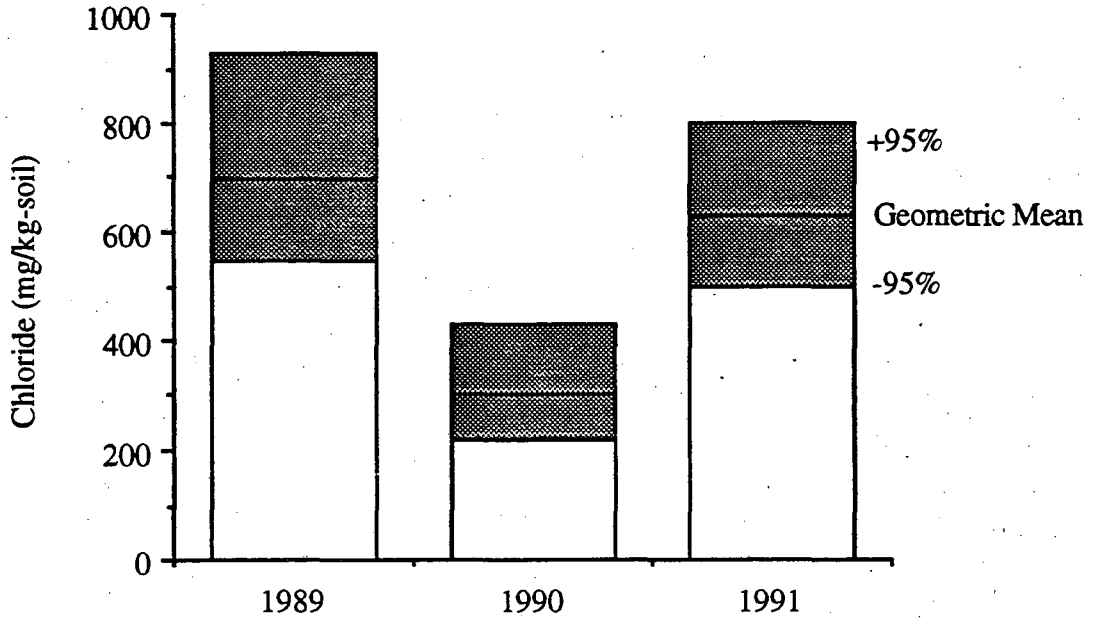

Figure 2.36. Geometric mean chloride concentrations in the top 15 cm of the soil profile. Chloride concentrations show a significant decrease of 60% between 1989 and 1990, and a significant increase of 56% between 1990 and 1991.

the open habitat where the ratio increased by 57% over the three-year period. This increase in the water-extractable fraction is consistent with process-oriented monitoring described by Tokunaga et al. (1991).

2.5.4. Temporal Trend due to Seasonal Cycles

In the analysis of the experimental data, it became evident that the sampling date relative to the seasonal cycle is an important variable. The significant year-to-year changes in sulfate and chloride concentrations, as well as in the ratio of selenite to water-extractable selenium detected in the data set are a reflection of seasonal leaching by infiltrating rainwater. The increase in both the selenite to water-extractable selenium ratio and the chloride concentration between 1989 and 1990, followed by the decrease between 1990 and 1991, are representative of the seasonal cycling of the soluble inventory (Figure 2.35 and Figure 2.36). Zawislanski et al. (1992) demonstrated that changes in water-extractable selenium concentrations mimic changes in chloride concentrations. It is therefore of interest to consider the influence of seasonal transport of species and the potential impacts of seasonal cycling on long-term trends. As noted previously, the

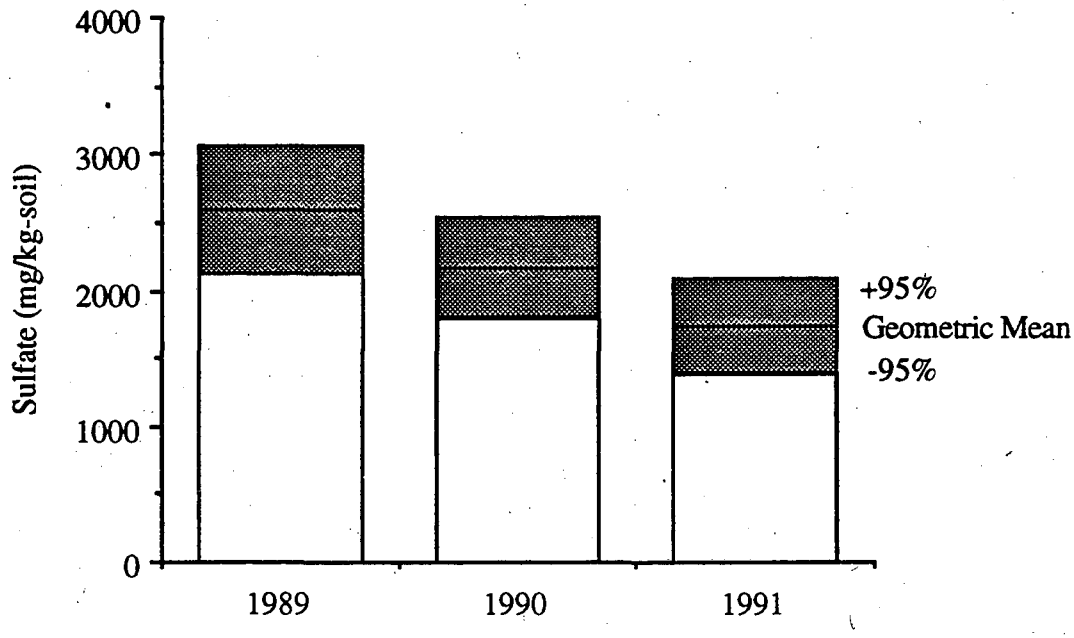

Figure 2.37. Mean sulfate concentrations in the top 15 cm of the soil profile. The sulfate inventory is significantly decreasing over the three-year monitoring period.

sampling dates for the soils over the three-year period were as follows: 1989 (May 8,9); 1990 (March 7); 1991 (Feb. 20, 26, 27). The heaviest precipitation period for each year as obtained from an on-site meteorological station were as follows: 1989-April; 1990-Jan., Feb.; 1991-March.

In 1989 and 1990, soil samples were collected after the heavy winter rains for that season. As demonstrated in Zawislanski et al. (1992), it can be assumed that the rainfall leached the salts (sodium chloride and sulfate) and the more soluble water-extractable species which had accumulated at or near the soil surface. Under oxidized conditions, selenate (the dominant fraction of the water-extractable selenium inventory) and chloride would be transported deeper in the profile. In contrast, selenite and sulfate, whose mobilities are limited by adsorption and precipitation respectively, are not driven as far into the soil profile by the winter rains. In addition, the lower redox potential favored by saturating the soils with rain water would tend to promote reducing selenate to selenite and possibly, in reducing microsites to elemental selenium. Such conditions would also lead to the reduction of a certain percentage of the water-extractable selenium inventory. In 1991, the samples were collected before the seasons heaviest rainfall and

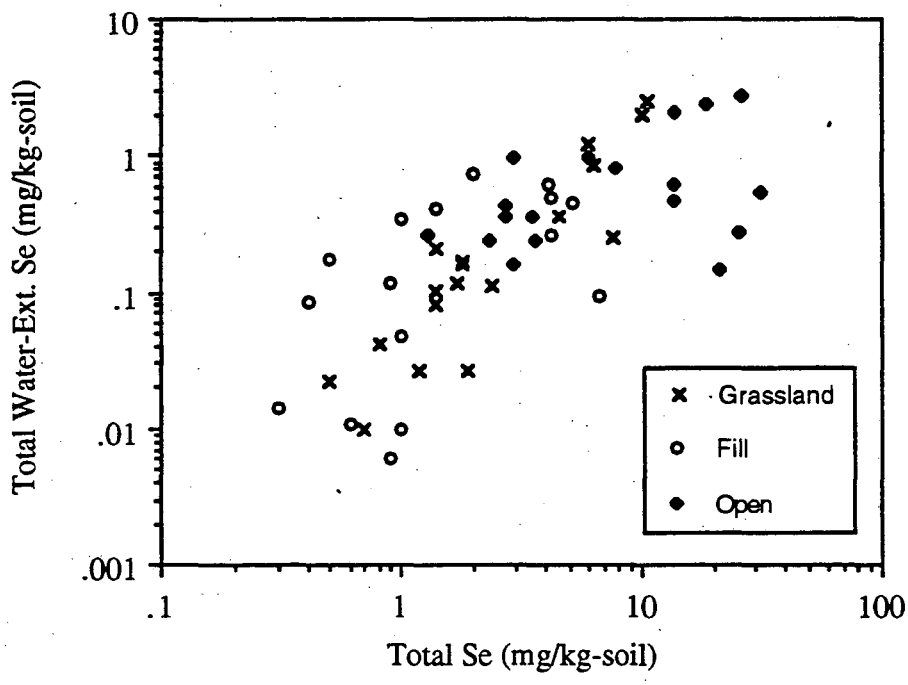

Figure 2.38. Distribution and range of selenium concentrations in the top 15 cm of the soil profile (1991) by habitat delineations.

therefore compared to other years the soils were drier. Under these conditions, selenate will be the prevalent selenium species and chloride will not yet have leached from surface soils by the annual rainfall. This scenario explains both the increase in chloride concentrations from 1990 and 1991 and also the decrease in the ratio of selenite to total selenium.

As indicated above, the cycling of chloride and water-extractable selenium concentrations are driven by the processes of physical redistribution which are due to seasonal leaching by infiltrating rainwater and evaporative reconcentration. On the other hand, the sulfate inventory decreases significantly over the three-year sampling period by 35% (Figure 2.37). Differences in the overall behavior of sulfate and chloride can be explained by solubility limitations on sulfate (e.g., gypsum and thenardite solubilities). Once transported deeper in the profile, sulfate may precipitate due to the transpirative concentration of solutes in the root zone. Chloride will remain mobile as a result of higher solubility limits and will be transported by evaporation back to the soil surface.

2.5.5. Discussion and Summary

In analyzing the data, it became evident that the trends observed in reservoir-wide data are analogs of processes described by more intensive sampling conducted by Tokunaga et al.

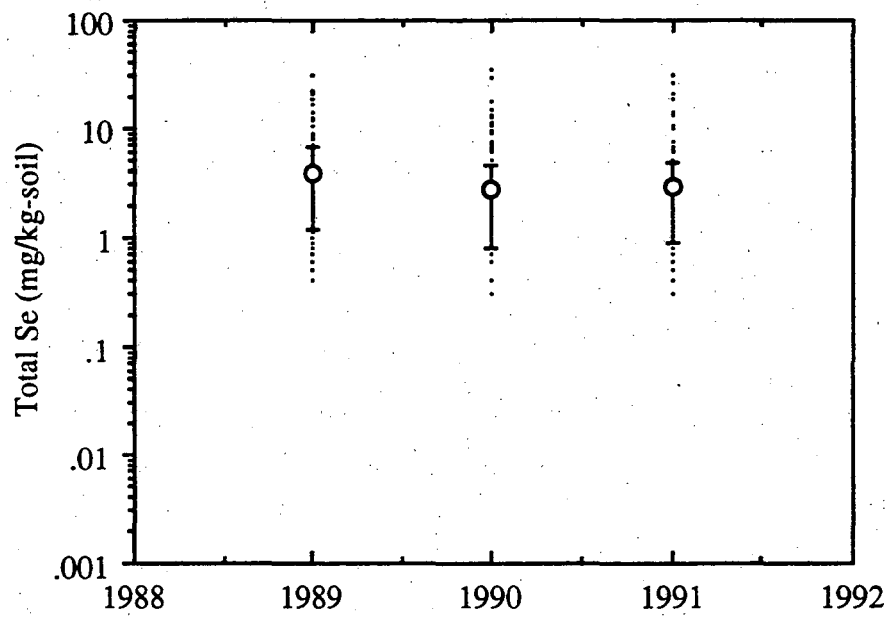

Figure 2.39. Range and geometric mean values of total selenium concentrations in the top 15 cm of the soil profile.

(1991) and Zawislanski et al. (1992) on smaller monitoring sites within the Kesterson Reservoir soil environment.

The fraction of the total selenium inventory in the top 15 cm that is water-extractable amounts to 7%, indicating that only a limited fraction of the total selenium inventory is currently mobile and available for plant uptake. However, as described in Tokunaga et al. (1991), bioavailable selenium is expected to increase slowly over time. The data collected here are consistent with these trends and confirm that increases are occurring slowly. Processes contributing to this evolution may include microbial transformations of organic and inorganic forms of selenium, cyclic oxidation and reduction of selenium resulting from seasonal variation in soil moisture content and rainfall infiltration, oxidation of soil organic matter, and physical redistribution resulting from root uptake of soil moisture and/or selenium.

Both seasonal and spatial variability make it difficult to detect changes in chemical concentrations over time. For example, process-oriented studies have demonstrated that water-extractable selenium concentrations, and conservative solutes such as chloride, are strongly influenced by the seasonal cycling of the inventory (Tokunaga et al. (1991) and Zawislanski et al. (1992)). This trend has also been observed in this data set. Chloride and selenium are

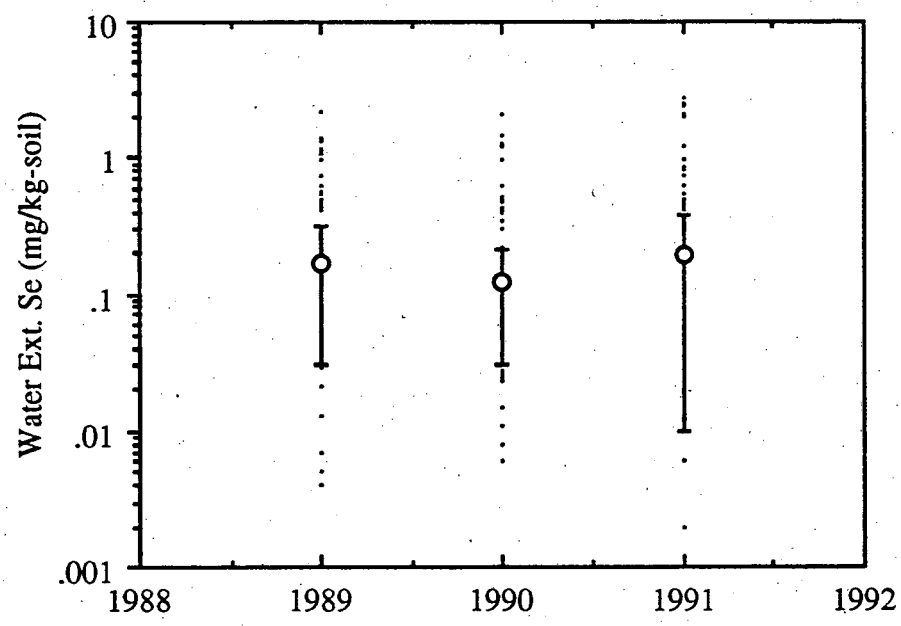

Figure 2.40. Range and geometric mean values of total water-extractable selenium concentrations in the top 15 cm of the soil profile.

readily leached down into the soil profile with winter rains, and are transported back to the soil surface by evaporative processes. In addition an oxidized environment is favored in the dry, summer months. Therefore, for the purposes of establishing long term trends it is essential that samples be collected at the same time of the year relative to the seasonal hydrologic cycle. Late in the summer, prior to the winter rains is the preferable time to collect samples at Kesterson.

The large spatial variability in the soil environment at Kesterson Reservoir may be attributed to such factors as habitat (vegetative) type, soil parent material, treatment/remediation history, land use, and biological activity. Given the experimental data set (162 total samples), the estimated mean value is within 18% of the actual mean value at a 95% confidence interval (Warrick and Nielson, 1980). To be within 5% of the correct value, at a 95% confidence level, requires 2200 samples. This is obviously an unrealistic sampling load, making it challenging to define the mean and detect small changes over time. As an example, as observed in Table 2.2, mean total selenium values reservoir-wide decrease from 3.9 to 2.9 mg/kg, or 26%, over the three-year period. However, this decrease is not significant. In order to detect a significant decline within the constraints of our data set, a 41% decline in total selenium concentrations is necessary. This may suggest that sampling on a yearly basis is too frequent

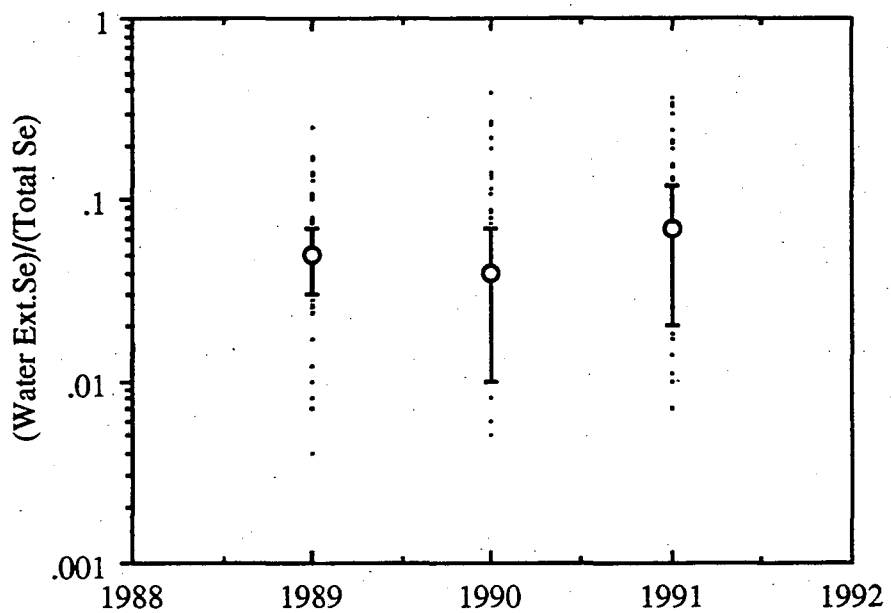

Figure 2.41. Range and geometric mean values of the ratio of water-extractable selenium to total selenium concentrations in the top 15 cm of the soil profile.

given the show rates of change. Sampling every two-to-five years may show significantly greater changes in the selenium inventory over time.

2.5.6. Conclusion

This chapter has described efforts to track the evolution of the selenium inventory in the top 15 cm of the soil profile at Kesterson Reservoir. With this data set we have demonstrated that changes in selenium concentrations will evolve slowly. No detectable changes have been observed in both total selenium and total water-extractable selenium concentrations. More careful examination of the ratio of water-extractable selenium to total selenium has indicated the gradual increase of the water-extractable component due to the progressive oxidation of the selenium inventory. This change is biologically important as it represents a significant increase in the more mobile and bioavailable fraction of the selenium inventory. This is consistent with process-oriented monitoring described by Tokunaga et al. (1991) and Zawislanski et al. (1992).

We also demonstrated the difficulty in tracking the evolution of slow time trends when the spatial environment of the study site is highly variable. In addition, we suggest the importance of the seasonal cycle on not only the movement of a contaminant within the soil

profile, but also on its distribution between extractable and solid phases. Complementary process-oriented monitoring described by Tokunaga et al. (1991) and Zawislanski et al. (1992) was extremely helpful in interpreting the results. A similar combination of process-oriented and synoptic type sampling is recommended for sites with similar monitoring objectives as described here.

3.0. Anticipated Soil Selenium Concentrations at Kesterson Reservoir

Sally M. Benson, Tetsu K. Tokunaga and Peter Zawislanski
Earth Sciences Division
Lawrence Berkeley Laboratory

Temporal trends from soil monitoring data collected at Kesterson Reservoir have been reviewed to shed light on anticipated concentrations of total and water-extractable selenium in surface and subsurface soils. Based on these data, a mass balance model for selenium has been developed and employed to evaluate the rate of leaching, remobilization and volatilization that has occurred since the Reservoir was dried out in 1987. Results from a series of calibration runs were then extrapolated 25 years in the future to forecast the evolution and redistribution of selenium within the soil profile. Projected water-extractable selenium concentrations within the 0.15 to 1 m depth interval were then used to drive a food-chain based risk-assessment model described in a separate report (CH2M Hill, 1992). Inventories of water-extractable selenium in the root zone increased in 4 of the 5 scenarios investigated. However, predicted values for the average concentration of water-extractable selenium in the root zone fall within the range of values observed at Kesterson today. Consequences of these projected increases on wildlife residing in and around Kesterson are addressed in CH2M Hill (1992).

3.1. Introduction

The work described herein was carried out at the request of the United States Bureau of Reclamation to assist in evaluating alternatives for continued management of the former Kesterson Reservoir, Merced County, California. From 1978 to 1986, Kesterson Reservoir was used for disposal of selenium-contaminated subsurface drainage water. The estimated 9000 kg of selenium delivered to Kesterson during this period accumulated largely in the surface-most 0.15 m of pond bottom sediments (Weres et al., 1989). By 1988, the Reservoir was dried out and the low-lying areas were filled with imported and local fill (soils and sediments). About 50% of the Reservoir was filled with an average thickness of 25 cm of fill. Since 1987, the inventory and distribution of the inventory within the soil profile[1] has been monitored. Today, as in 1987, the majority of the inventory is largely insoluble and concentrated in a thin detrital layer and the surface-most 0.15 m of soil. However, detailed monitoring of the distribution and speciation of the selenium inventory deeper in the soil profile indicates that a growing fraction of water-extractable selenium is potentially available for uptake into plants and the food chain.

[1] Henceforth the term soil profile is used to represent the top 2 m of Kesterson soils.

Concern about the long-term evolution of the selenium inventory and effects on biological exposure prompted this effort to predict trends in soil-selenium concentrations in areas not covered with fill material over the next 20 years. These projections are then used to drive a biological risk assessment model over the same 20 year period. This report describes the data base available to support these projections, the methodology used to predict time trends, the results of the predictions and finally, how these predictions have been incorporated into the biological risk assessment. The biological risk assessment was carried out by CH2M Hill and is described in a separate report (CH2M Hill, 1992).

There remains much to be learned before we can predict, from first principles, the behavior of selenium in Kesterson soils. A complex interplay of seasonally variable physical, chemical and biological processes cyclically transform selenium from one form to another, transport the soluble and gaseous forms within the soil profile and gradually dissipate the selenium inventory. Comprehensive understanding of the individual processes, rates and interplay between them is beyond the present understanding of the scientific community. For example, in spite of the intensive research carried out to date at Kesterson, even such information so basic as "What are the different forms of selenium present in the soil?" have only been answered partially.

Nevertheless, building on a foundation of information on biogeochemical cycling of selenium, we have learned much about how selenium behaves in the Kesterson environment and have developed a substantial data base from which we may extrapolate the time trends observed from 1987 to 1991, into the future. From intensive monitoring data, supported by laboratory and theoretical studies conducted by others and ourselves, we have identified three "phenomena" that appear to control the inventory and redistribution of selenium within the soil profile. These include 1) remobilization of insoluble selenium, 2) leaching of selenium from surface soils to deeper in the soil profile and 3) volatilization, which converts selenium to gaseous forms that are dissipated in the atmosphere. Undoubtedly these phenomena involve a whole suite of chemical, physical and biological processes that interact to produce the phenomena we are able to observe through monitoring the inventory and distribution of selenium within the soil profile. In spite of the inherent complexity, and for lack of a more rigorous framework for embarking on this endeavor, we build upon the monitoring data at hand to project the effects of these processes into the future.

3.2. Objectives

The objectives of this effort include the following:

- Synthesize data gathered from ongoing monitoring and research efforts at Kesterson regarding evolution of the selenium inventory;

- Develop a mass balance model for selenium in the grassland[2] and open[3] habitats that can be used to extrapolate observed 1987-92 time-trends into the future;
- Predict the average evolution of the current inventory and distribution of soil selenium in the grassland and open habitats over a 25-year period, beginning in 1987; and
- Through the above exercise, identify gaps in existing knowledge so as to prioritize future research efforts.

3.3. Soil Selenium Data Base from Kesterson Reservoir

Since 1987, intensive collection of soil and soil-water samples to determine selenium concentrations has taken place as part of a variety of monitoring and research activities at Kesterson Reservoir. These include the following:

- Soil selenium fractionation and speciation studies;
- Long-term soil and soil-water selenium monitoring in former Ponds 5, 6, 7, 8, 9, 10 and 11,
- Annual synoptic sampling of soil selenium at Kesterson;
- Volatilization experiments in former Ponds 2, 4 and 11; and
- Soil-Water-Vegetation management experiments in former Ponds 2, 5 and 7.

A description of relevant data collected during each of these activities and how they were used in this study is provided in the following sections of the report.

3.3.1. Soil Selenium Fractionation and Speciation Studies

As early as 1985 it was clear that most of the selenium delivered to Kesterson was converted from selenate to sparingly-soluble forms by microbial activity in the pond bottom sediments and uptake by aquatic flora (Weres et al., 1985). Since then several research efforts have attempted to identify the predominant species of selenium present in the soils (Weres et al., 1989; Zawislanski, 1990; Tokunaga et al., 1991). From these investigations, selenate, selenite and elemental selenium have been proposed as the major species of selenium present in the surface soils. In addition, selective extractions indicate that unidentified species of organically associated and organically bound forms may also form a significant fraction of the inventory. Information regarding each of the predominant forms of selenium in the soils is summarized briefly below.

---

[2] The grassland habitat is one of three major habitatats remaining at Kesterson following draining and filling the low-lying areas of the former Reservoir. Now, as in the past, the grassland habitat is vegetated with a combination of annual and perennial grasses (CH2M Hill, 1992).

[3] The open habitat is another of three major habitatats remaining at Kesterson following draining and filling the low-lying areas of the former Reservoir. Historically, the open habitat was vegetated with cattials. After the Reservoir was drained the cattials were disked into the soil. The open habitat is slowly being re-vegetated with a variey of annual and perenial plant species (CH2M Hill, 1992).

The selective extraction techniques used for this investigation are described in Tokunaga et al. (1991) and Weres et al. (1989). Five major pools of selenium are identified with these extraction techniques, including: water extractable selenate; water extractable selenite; adsorbed selenium; organically-associated selenium, and; refractory[4] selenium. Note that the selective extraction techniques employed to fractionate selenium into the pools defined below are not mutually exclusive and as such, there remains significant uncertainty with regards to the forms of selenium present. Nevertheless, the following summarizes our best understanding of the nature and distribution of selenium in Kesterson soils.

Selenate occurs predominantly in forms that are readily extracted from the soil with a 1:5 mass ratio of soil-to-water solution (henceforth referred to as water-extractable selenium). Comparisons between soil extracts and soil water solutions collected in situ with suction samplers suggest that nearly all the selenate is dissolved and freely transported within the soil profile and is available for plant uptake. Selenate comprises typically about 90% of the selenium in soil-water solutions. Minor amounts of selenate may also be present in adsorbed forms or co-precipitated with carbonate minerals in surface soils, organic detritus and salt crusts (Tokunaga et al., 1991; Zawislanski, 1990).

Selenite in Kesterson soils occurs in water-extractable, adsorbed and co-precipitated forms (Tokunaga et al., 1991; Zawislanski, 1990). Selenite typically comprises about 10% of the water-extractable fraction. However, the majority of selenite appears to be associated with adsorbed or co-precipitated phases that limit the mobility and availability of selenite (Weres et al, 1989; Tokunaga et al., 1991). In addition, a significant fraction of the organically associated selenium may occur as selenite adsorbed or otherwise incorporated with soil organic matter.

Elemental selenium is also believed to comprise a significant fraction of the selenium inventory in Kesterson soils. Elemental selenium is formed by microbial reduction of selenate or selenite (Geering et al., 1968; Doran, 1982; Oremland et al., 1989). A significant fraction of organically-associated selenium may be in the elemental form (Tokunaga et al., 1991). Elemental selenium is nearly insoluble in Kesterson soils and as such has extremely limited availability for plant uptake or transport.

Figures 3.1a, 3.1 b and 3.1c provide illustrative examples of the distribution of the various forms of selenium in Kesterson soils in 1990. Data presented represent conditions at Kesterson ranging from the cattail-habitat of former Pond 2 (open habitat), to the re-vegetated playa-habitat in Pond 9 (now considered grass-land habitat) to the grassland-habitat of Pond 11. In each case, fractionation data from two depth intervals are provided, the surface ten centimeters (0 - 0.1 m) and from 0.45 to 0.55 m.

While there is a wide range of variability in soil selenium concentrations and speciation in Kesterson soils, the following generalizations can be made. In the open and grassland habitats, the

---

[4] Note that the term "refractory" is operationally defined in tbis context as selenium that could not be extracted from the soils using the extaction methods that remove the other 4 fractions identified. Evidence from numerous sources suggest that this pool is largely elemental selenium (Weres et al., 1989; Oremland et al., 1989; and Tokunaga et al., 1991). Under the present conditions, this pool is nearly insoluble and under geochemically reducing conditions this pool may remain in its current form. However, under the oxiding conditions in the vadose zone at Kesterson, this pool is expected to slowly oxidize and become mobile and available for transport and plant uptake. Hence, the name "refractory" is used in the context of its current status rather than an indication of its future behavior.

surface-most interval contains typically greater than 50% "refractory" selenium. In this same interval, the water-extractable pool comprises from 2 to 5% of the total selenium inventory, most of which is selenate. The remainder of the selenium inventory in this interval is distributed between adsorbed and organically-associated forms.

Deeper in the soil profile, a much larger fraction of the total inventory is in water-extractable forms. For the three samples shown in Figure 3.1, from 40 to 60% of the selenium is present as water-extractable selenate. The remainder of the selenium is distributed amongst the adsorbed, organically-associated, and "refractory" pools, with large site-to-site variability.

These data also illustrate that the concentration of selenium in the 0.45 to 0.55 m depth interval is typically less than 1/10 the concentration in the surface ten centimeters. However, such large contrasts are not present in the water-extractable inventory. For example, as shown in both Figures 3.1b and 3.1c, water-extractable concentrations are nearly equal in these two depth intervals. In the open habitat, however, as illustrated by the sample shown in Figure 3.1a, the amount of water-extractable selenium in the surface-most 10 cm may be an order of magnitude greater than deeper in the soil profile.

The data provided in Figures 3.1a-3.1c, as well as data from previous studies (Weres et al., 1989; and Tokunaga et al., 1991) suggest that within the surface 10 cm there is a large pool of selenium that is currently in insoluble or immobile forms. Thermodynamic considerations indicate that selenate is the stable form of selenium in this environment and that eventually the speciation will shift in this direction (Geering et al., 1968; Doran, 1982; Elrashidi et al., 1987; and Weres et al., 1989; and Tokunaga et al., 1991). Specifically, we expect that some fractions, such as adsorbed selenite and organically associated selenium will be oxidized or mineralized and released into the soil water. Less is known about the stability of elemental selenium in this environment. From thermodynamic considerations, we expect that elemental selenium will eventually be transformed to selenite or selenate. However, the rate and mechanisms of these transformations remain uncertain. Bacteria capable of oxidizing elemental selenium have been identified (Saratchandra and Watkinson, 1981), but these specific bacteria have not been identified in Kesterson soils, nor is it certain that others may not act in a similar capacity. Slow abiological mechanisms of transformation may also be effective in long-term transformations. The complexity of the system is compounded by seasonal variations in redox conditions, populations of soil microorganisms, and soil moisture which act to periodically shift the thermodynamic status of the soil system towards more reducing conditions (Zawislanski, 1989; Ita and Benson, 1992).

Experiments are underway to accelerate the rate of transformations within Kesterson soils to determine the relative rate at which the presently immobile pools are oxidized to more mobile and available forms of selenium (Weres et al., 1989; Yee, 1990; Zawislanski and Zavarin, 1992). Results from these suggest that all fractions are potentially labile to varying degrees. Oxidation or volatilization of all soil selenium fractions have been observed when soils have been provided with adequate moisture, aeration

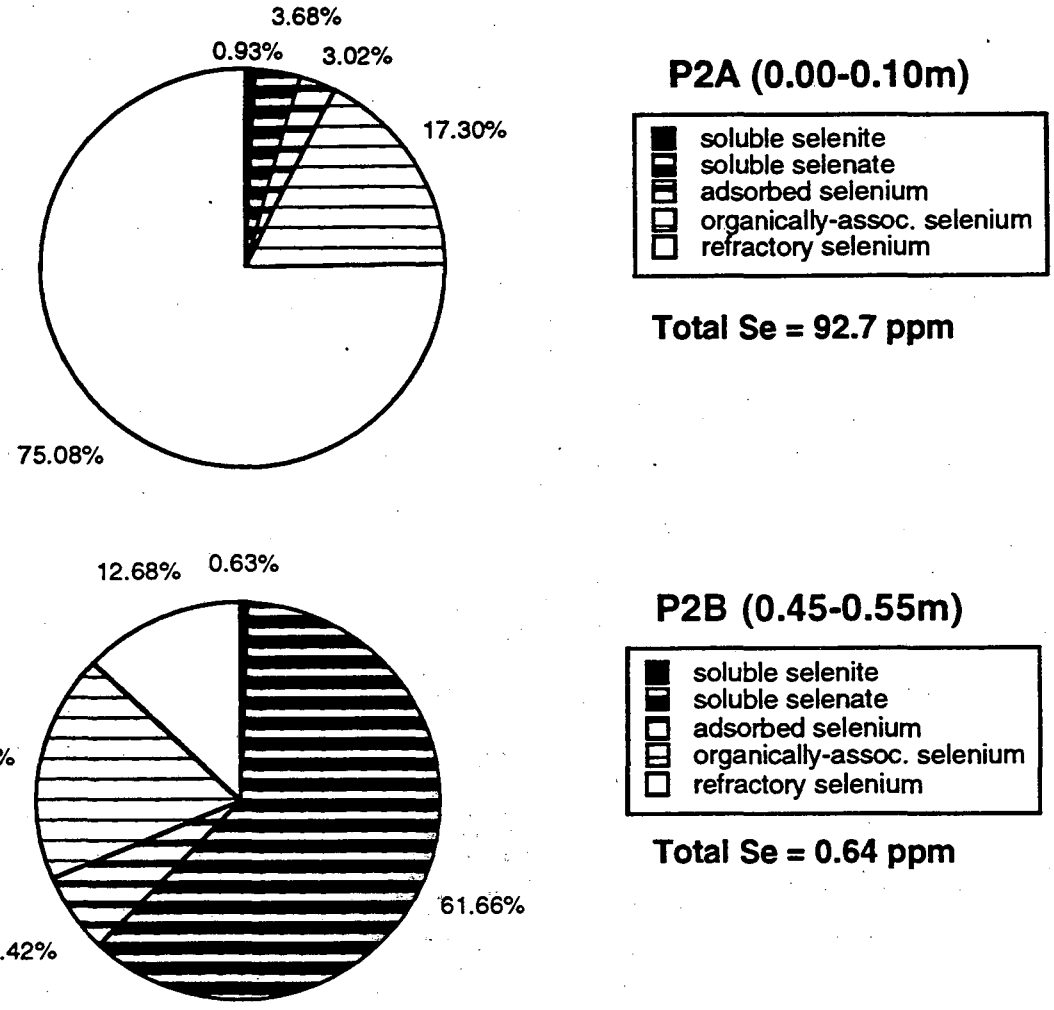

Figure 3.1a. Illustrative example showing the dominant forms of selenium in two Kesterson soils. These data were collected from former cattail habitat in Pond 2 (now open habitat) in November, 1990. Data illustrated in the top panel are from the surface soil (0 -0.10 m) and the lower panel from a sub-soil (0.45 - 0.5 m).

and a plentiful population of soil microorganisms. "Refractory fractions" in general are oxidized or volatilized at low rates compared to the other soil fractions. However, recent experiments conducted at slightly elevated temperatures (35 °C) have demonstrated oxidation of the "refractory" fraction from 12 to 22% over a 3-month period. Together, these data and previous investigations suggest that a large fraction of the selenium inventory at Kesterson is susceptible at times to oxidation and remobilization. Only

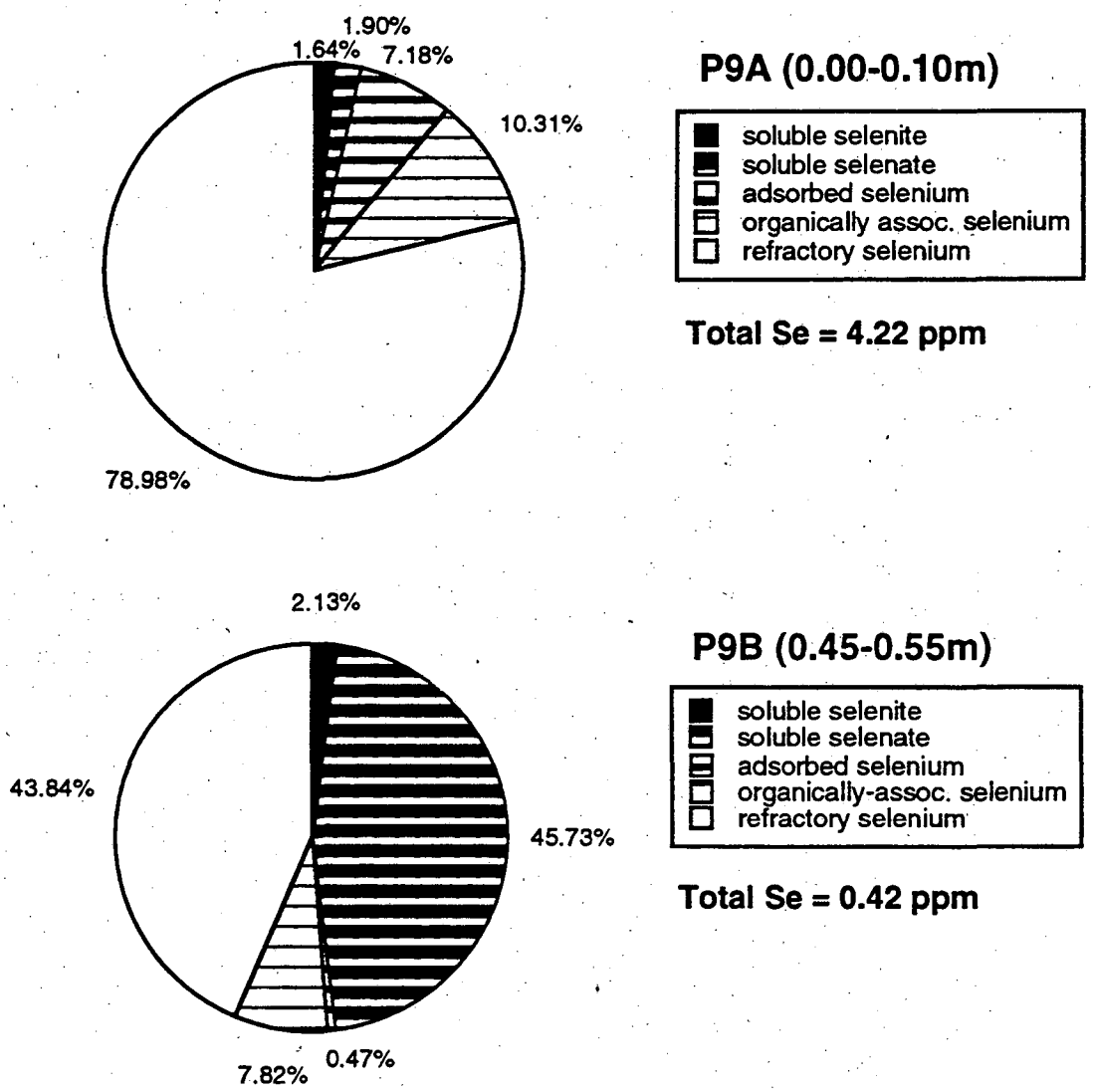

Figure 3.1b. Illustrative example showing the dominant forms of selenium in two Kesterson soils. These data were collected from re-vegetated playa habitat in Pond 9 (now grassland habitat) in November, 1990. Data illustrated in the top panel are from the surface soil (0 -0.10 m) and the lower panel from a sub-soil (0.45 - 0.5 m).

through detailed monitoring of soil-selenium concentrations will site-specific mechanisms and rate constants be obtained.

In the following sections, ongoing soil-selenium monitoring data will be described briefly and discussed in the context of how they are used in the current effort to extrapolate observed trends into the future.

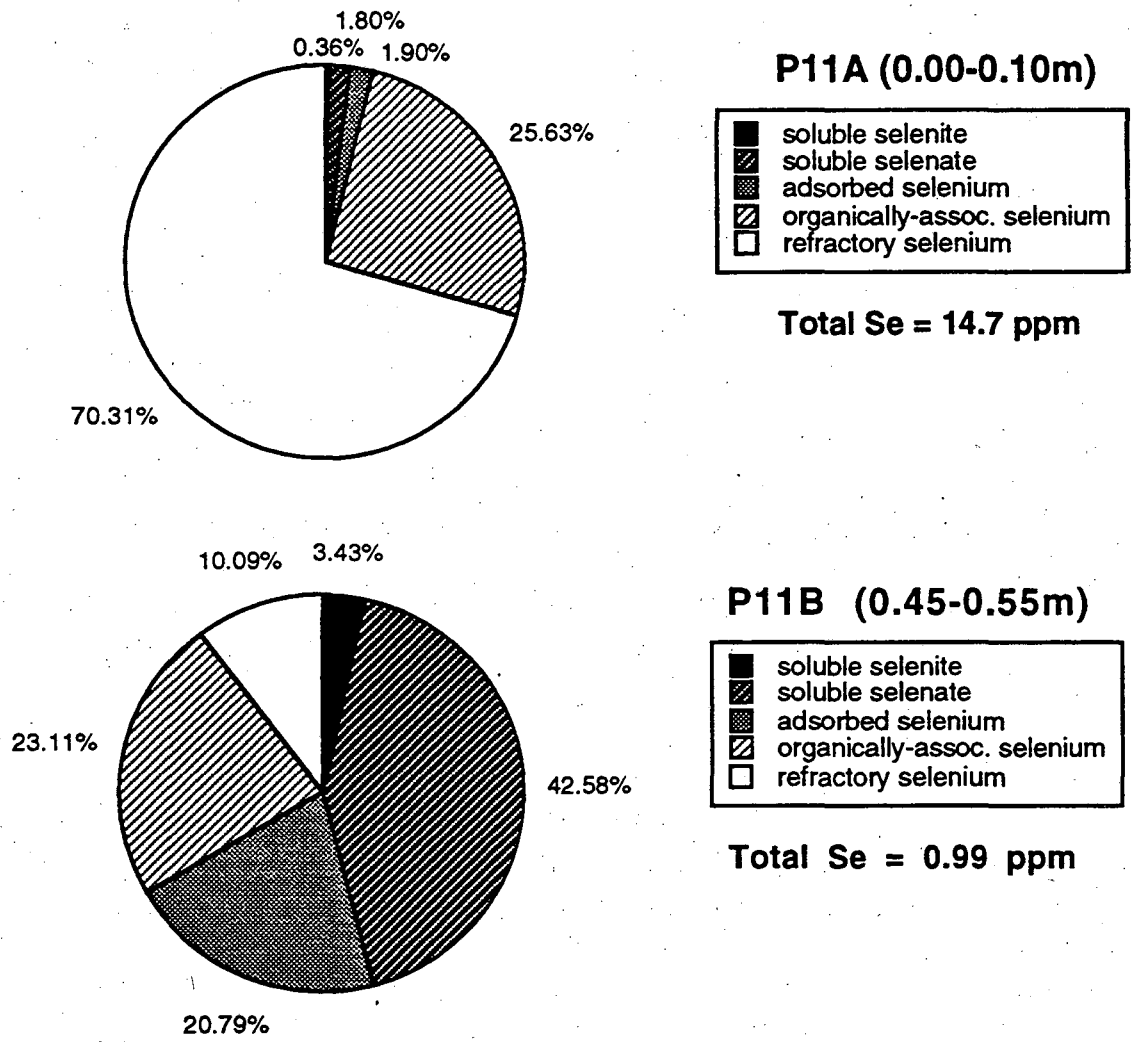

Figure 3.1c. Illustrative example showing the dominant forms of selenium in two Kesterson soils. These data were collected from grassland habitat in Pond 11 in November, 1990. Data illustrated in the top panel are from the surface soil (0 -0.10 m) and the lower panel from a sub-soil (0.45 - 0.5 m).

3.3.2. Long Term Soil and Soil-Water Selenium Monitoring

Beginning in 1987 several grassland and playa sites within Kesterson were instrumented with soil-water samplers, tensiometers and neutron probe access holes for monitoring selenium transport in the vadose zone (Long et al., 1990; LBL, 1988; 1990a,b). Soil water samples and extracts of soil cores from these plots have been obtained at regular intervals since this time. These sites have provided the foundation for our understanding of the physical and chemical "processes" taking place within the top 2 m of

Kesterson soils. Monitoring sites have been established in former Ponds 1, 2, 3, 5, 6, 7, 8, 9, 10, and 11. Data sets collected from two sites with the longest and most complete records are described below.

3.3.3. Pond 11

The test plot 11C is located in the south west corner of Pond 11 in an area covered with a dense and stable growth of salt grass (*Distichlis spicata*) that had been subject to seasonal flooding with incoming San Luis Drain water. The depth of the water table at the 11C test plot varies seasonally from a summer low of about 3 m to about 1.5 m in mid-winter. Detailed descriptions of all the monitoring data are provided in LBL (1988; 1990a; and 1990b) and Tokunaga et al. (1991). Two methods for tracking changes in the inventory and distribution of water-extractable selenium have been used in the 11C test plot 1) soil solution sampling with permanently installed vacuum extraction cups and 2) water-extracts from soil cores. Each method has its own particular set of advantages and disadvantages but together they provide a convincing record of the evolution of the selenium inventory at this site.

Electrical conductivities and selenium concentrations of pore waters collected from 1989 to 1991 with the vacuum-cup extraction system are shown in Figure 3.2a and 3.2b. These data illustrate two trends. First, overall concentrations of selenium and major ions (chloride, sulfate and sodium) have increased in the soil solution. Second, their distribution in the soil profile has shifted from being highest near the soil surface to being highest at about 1 m depth. These changes can be attributed to the following three processes: leaching of dissolved salts and selenium due to winter rains; evaporative and transpirative fluxes of chloride- and sulfate-rich groundwater into the root zone and; remobilization of the selenium inventory.

Similar information is available from the soil water extracts shown in Figures 3.3a and 3.3b. In 1988, water-extractable selenium concentrations were highest in the top 0.5 m of the soil profile. By the next year, water-extractable selenium concentrations nearly doubled in the upper 0.5 m and increased in the depth interval from 0.5 to 1 m. By 1991, surficial inventories declined to pre-1988 levels. This decrease was accompanied by a large increase in water-extractable selenium concentrations in soils from 0.5 to 1 m depth. Since there is little selenium in the groundwater, these changes must be caused by remobilization and leaching of the resident selenium inventory.

The extent of remobilization can be determined from the depth-integrated inventory of water-extractable selenium shown in Figure 3.3b. In 1988, the total inventory of water-extractable selenium was about 200 mg/m^2. By 1991, it more than doubled, increasing to about 500 mg/m^2. Figure 3.3b also illustrates that most of water-extractable selenium is located in the top meter of the soil profile and that the largest increases also occurred here.

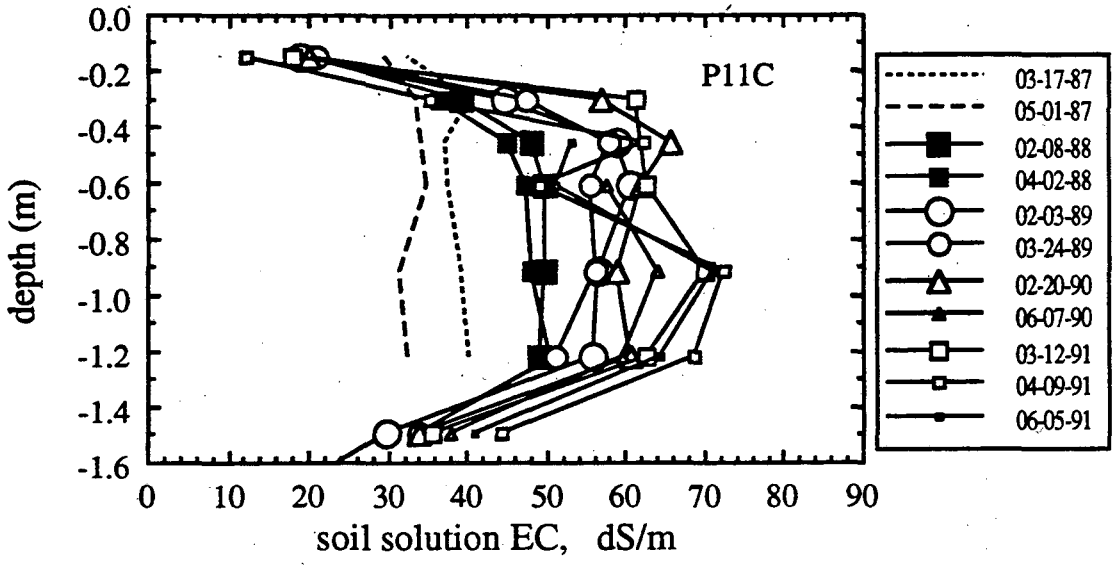

Figure 3.2a. Time trends in electrical conductivity (EC) of the soil solution at experimental plot 11C in the southwest corner of former Pond 11.

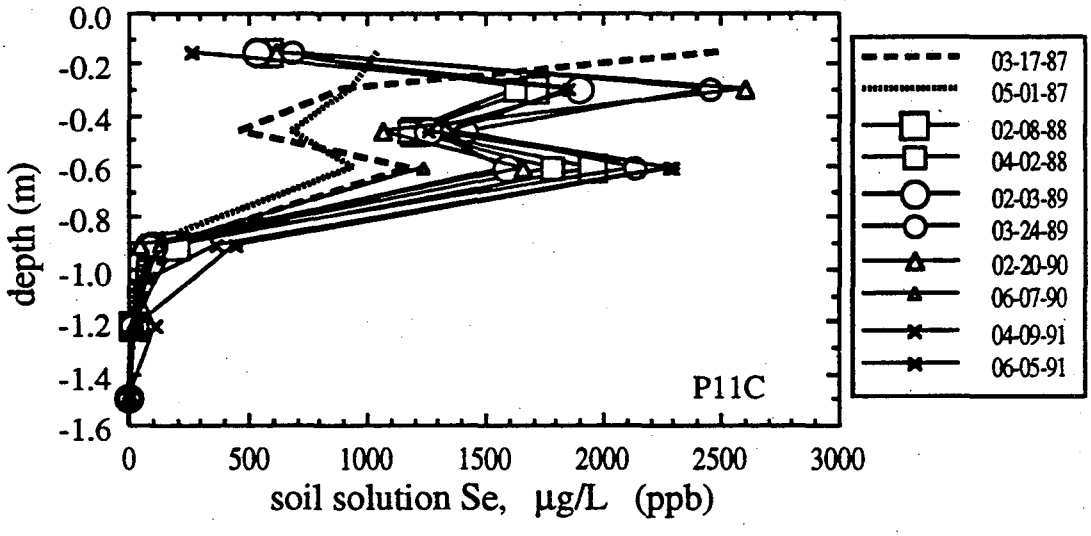

Figure 3.2b. Time trends in soil solution selenium concentrations at experimental plot 11C in the southwest corner of former Pond 11.

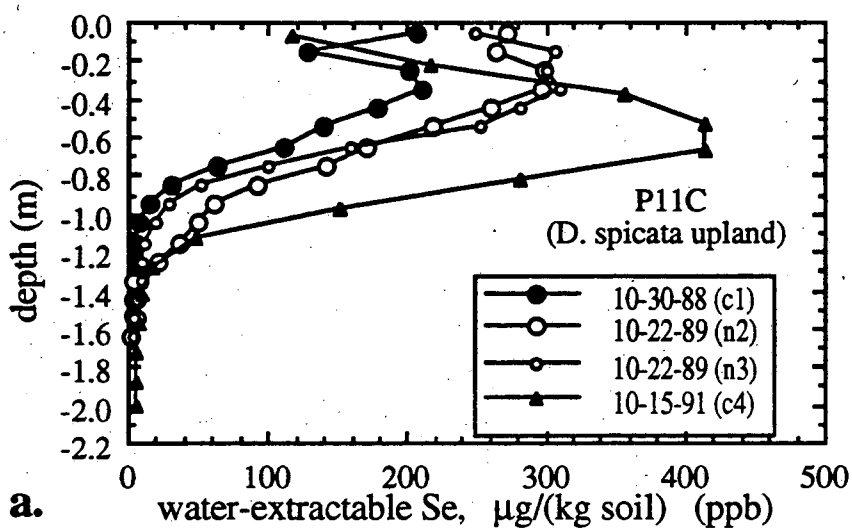

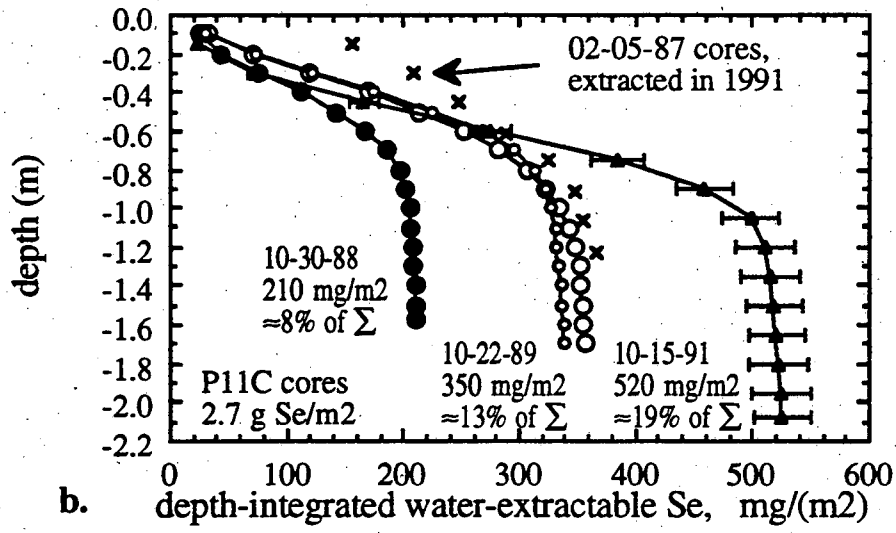

Figure 3.3a and 3.3b. Time trends in water-extractable selenium concentrations at experimental plot 11C in the southwest corner of former Pond 11. (a) water-extracted Se [mg/(kg-dry soil)] and (b) depth integrated water-extractable Se (mg/m^2).

3.3.4. Pond 8EP

In mid 1988 an experimental plot was developed in former Pond 8 (Plot 8EP) to evaluate the magnitude of evaporative fluxes of solutes in Kesterson soils. The Pond 8 test plot is located in a former playa that was frequently flooded with up to 50 cm of San Luis Drain water. Over the monitoring period, the plot was revegetated with *Bassia hyssopifolia*, a deep rooted annual. The test plot is located in the center of Pond 8 and detailed descriptions of the monitoring data are provided in LBL (1988; 1990a; 1990b) and in Zawislanski (1989).

Chloride and water-extractable selenium concentrations from a series of shallow soil samples (0 - 9 cm) are given in Figures 3.4a and 3.4b. These data illustrate the results of two important processes: 1) evaporative accumulation of salts and selenium during the summer months and 2) leaching during the winter rainy season. The net effect of these seasonal transport processes over the 3 1/2 year period is to reduce the chloride concentration by about 75% and the selenium content by 50%. Differences in the relative declines in chloride and selenium can be explained by remobilization of a fraction of the immobile selenium in the surface soils.

Depth profiles of water-extractable selenium concentrations over this same time period are provided in Figure 3.5. From 1988 to 1990, rapid increases in the inventory of water-extractable selenium are apparent, similar to those observed in the Pond 11 test plot. However, from 1990 to 1991 a different pattern emerges. Significant declines are observed from 0 to 20 cm and from 1.2 to 2 m. These can be attributed to a reduction of selenate to less mobile forms of selenium, presumably by creating reducing conditions due to water table rise and seasonal rainfall infiltration in the fine-textured soils present at this site. Although water-extractable selenium inventories remain higher than 1988 values, these data illustrate the importance of periods with wetter-than-average soil conditions on the behavior of the selenium inventory at Kesterson.

These data suggest that evolution of the selenium inventory will not take place in a monotonic fashion. Instead, year-to-year variations in leaching and remobilization rates are expected to occur due to external influences such as intensity and timing of winter rains, patterns of vegetation growth and succession, and diversity and abundance of soil microorganisms. The net effect of the interplay between these processes will become clearer as our window of observation increases.

3.3.5. Annual Synoptic Sampling of Soil Selenium at Kesterson Reservoir

Each year samples of the top 15 cm of soil are collected from 54 locations throughout Kesterson as a component of the ongoing biological monitoring program (LBL 1990a; 1990b). For sampling purposes, Kesterson is divided into three trisections: Trisection 1 includes all the former Ponds below Gun Club Road; Trisection 2 includes former Ponds 5, 6, 7 and 8; and Trisection 3 includes former ponds 9, 10, 11 and 12. Within each trisection, 6 samples are collected within each of the three habitats described previously (e.g., Fill, Grassland and Open).

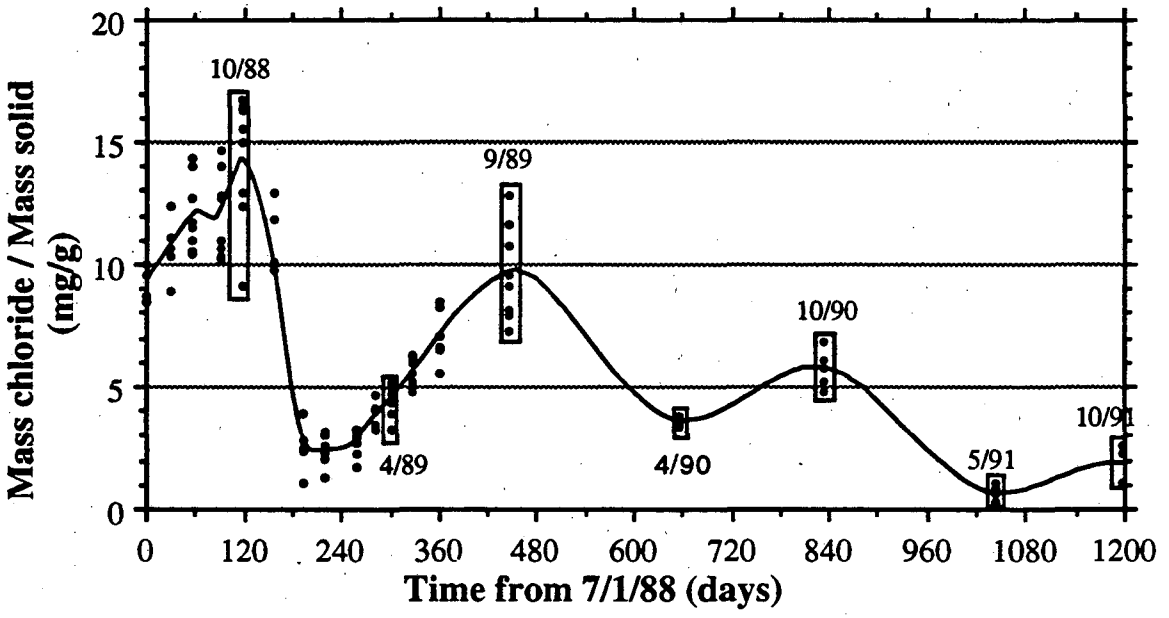

Figure 3.4a. Time trends in water-extractable chloride concentrations in the top 9 cm at experimental plot 8EP in the north east corner of former Pond 8.

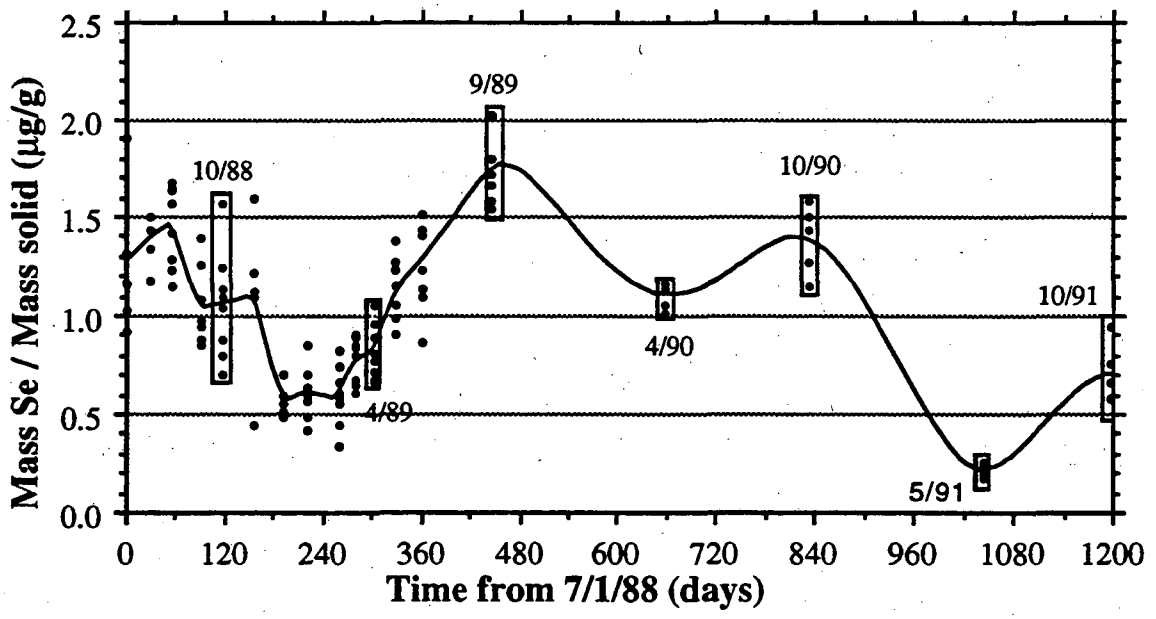

Figure 3.4b. Time trends in water-extractable selenium concentrations in the top 9 cm at experimental plot 8EP in the north east corner of former Pond 8.

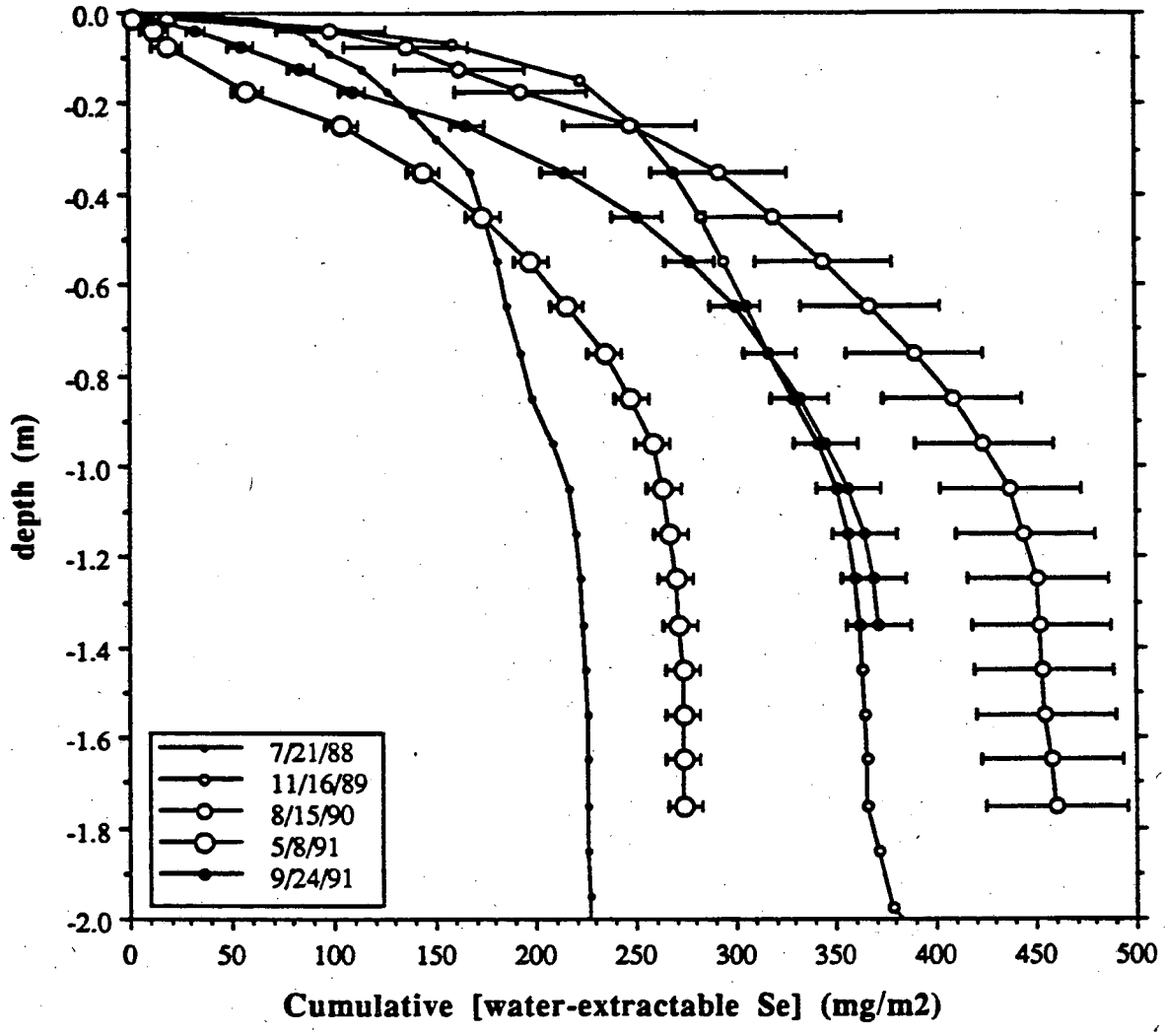

Figure 3.5. Time trends in water-extractable selenium concentrations at experimental plot 8EP in the north east corner of former Pond 8. Error bars represent cumulative error from three replicates to a depth of 1 m. No replicates are available below this depth.

Samples are analyzed for total selenium, water-extractable selenium, sulfate and chloride. Analysis of variance (ANOVA) was used to identify temporal trends in soil selenium concentrations[5].

[5] Fisher's PSLD method was used to determine ignificant differences in concentrations within year, tri-section and habitat ($P < 0.05$) (Mead, 1988). Log-transformed concentrations where used for ANOVA on all but the sulfate data because the concentration data were found to be log-normally distributed. Sulfate data were normally distributed and ANOVA was performed on the data as collected.

Because the samples are collected in the late-winter and early-spring, influences of seasonal leaching of salts and water-extractable selenium may be reflected in the data, as well as long term trends. Results from the sampling program are summarized in Table 3.1 and in Figures 3.6 through 3.8. Geometric mean concentrations are provided for each year's entire sample set. Similar trends are observed when the data is evaluated on a Trisection-by Trisection basis or on a habitat-by-habitat basis. For a detailed discussion of these data see Wahl (1992).

As shown in Table 3.1 and Figures 3.6, 3.7 and 3.8, statistically significant reservoir-wide changes have not occurred in the total and water-extractable inventories of selenium in the top 15 cm of soil over the three year monitoring period. Significant changes have, however, been observed in the ratio of water-extractable to total selenium, sulfate and chloride concentrations. These changes reflect the same processes observed in the more detailed long-term and process-oriented monitoring described previously.

Table 3.1. Geometric mean concentrations of total selenium, water-extractable selenium, sulfate and chloride in the top 0.15 m of soil from 54 samples collected annually as part of the biological monitoring program. Within a column, values sharing the same letters are not significantly different at the 95% confidence level.

Year	Total Selenium (mg/kg-soil)	Water Extractable Selenium (mg/kg-soil)	Ratio of Water Ext. to Total Selenium	Sulfate (mg/kg-soil)	Chloride (mg/kg-soil)
1989	3.9 A	0.17 A	0.05 A	2120 A	545 A
1990	2.7 A	0.12 A	0.04 A	1800 AB	220B
1991	2.9 A	0.19 A	0.07B	1380 B	500 A

The increase from 1989 to 1991 in the ratio of water-extractable to total selenium indicates a gradual remobilization of the selenium inventory. Significant year-to-year changes in sulfate and chloride concentrations are a reflection of seasonal leaching by infiltrating rainwater. While sulfate concentrations decline monotonically over the monitoring period, chloride concentrations decline from 1989 to 1990 and then increase from 1990 to 1991. Differences in temporal trends between sulfate and chloride can be explained by limits on the solubility of sulfate salts (e.g. gypsum and thenardite). Once transported deeper into the profile, sulfates may precipitate due to transpirative concentration of solutes in the root zone. Due to the much higher solubility limits, chloride salts will remain mobile and may be transported back to the soil surface by evaporation at the onset of the hot summer months.

3.3.6. Field-Measured Selenium Volatilization Rates at Kesterson Reservoir

Selenium may be transformed from aqueous inorganic and organic forms to gaseous forms (largely dimethylselenide) through microbial activity and plant transpiration (Doran, 1982; Frankenberger

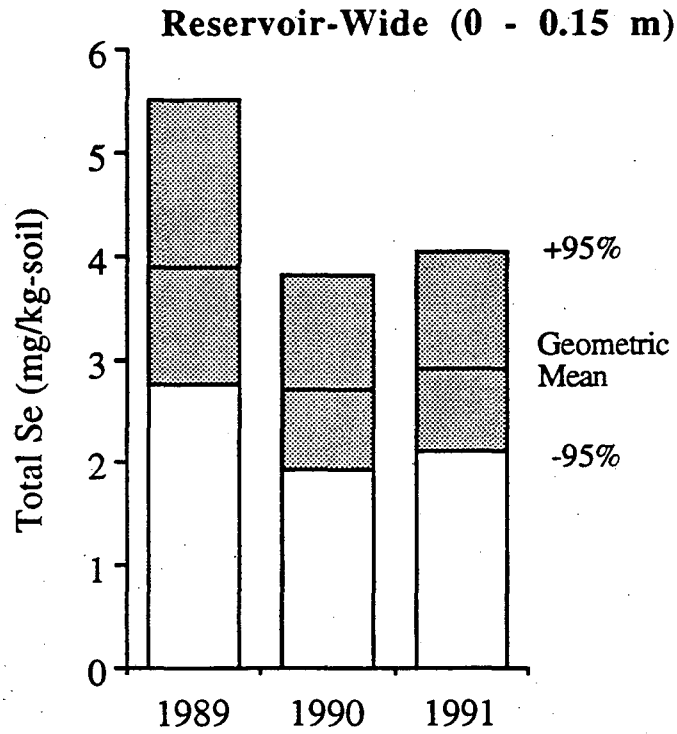

Figure 3.6. Geometric mean total selenium concentrations in the top 0.15 m of soil from 54 samples collected as part of the synoptic sampling for 1989, 1990 and 1991. Note that no significant changes in the inventory of total selenium in the top 0.15 m have been observed over this period.

and Karlson, 1988; Frankenberger, 1990). In soils, fungi appear to have the greatest capacity to volatilize selenium and do so as a detoxification mechanism. Whereas fungal volatilization of selenium may occur throughout the profile, it is most effective as a dissipation mechanism near the soil surface, where dimethylselenide can be transported to the atmosphere before it partitions into the soil-water or onto the surface of soil particles (Goldhammer and Alemi, 1990; Tokunaga, 1990). Plants may also contribute to selenium volatilization and may be comparatively effective for removing selenium from deeper in the soil profile (Terry et al., 1990; Biggar et al., 1990; ANR, 1992).

Although laboratory experiments demonstrate that microorganisms may volatilize, all of the selenium fractions identified in Kesterson soil, volatilization rates of elemental selenium are comparatively low (Yee, 1990; Doran and Alexander, 1977). In particular, we have demonstrated that in Kesterson soils where the water-extractable selenium has been removed, selenium is volatilized as effectively as in native, unaltered soils (Yee, 1990). However, recent data from volatilization experiments in former Pond 4 and with San Luis Drain sediments suggest that approximately 50 to 75% of the selenium is relatively resistant

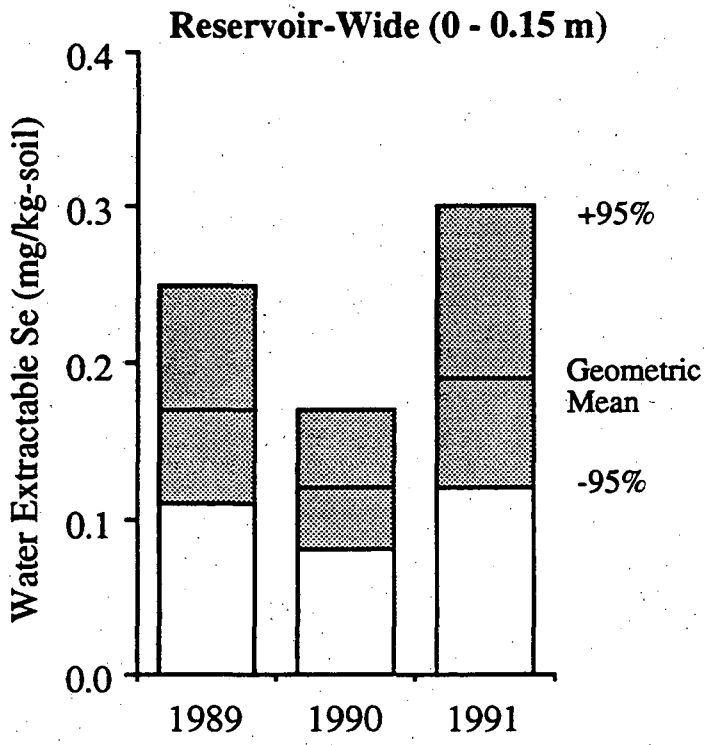

Figure 3.7. Geometric mean water-extractable selenium concentrations in the top 0.15 m of soil from 54 samples collected as part of the synoptic sampling for 1989, 1990 and 1991. Note that no significant changes in the reservoir-wide water-extractable selenium has been observed over this period.

to rapid (< 5 years) volatilization through microbial processes (W.T. Frankenberger, personal communication, 1992).

Rates of selenium volatilization have been measured as part of ongoing experiments aimed at stimulating volatilization rates through adding moisture and organic amendments to Kesterson soils. In each case, these experiments have been accompanied by measurement of volatilization rates in a nearby control plot where the soils have not been treated to stimulate volatilization rates. A summary of the field-measured volatilization rates from the control plots at these sites is provided in Table 3.2. In addition, volatilization data provided by Weres et al. (1989) are included in the table.

As shown, annually-averaged emission rates measured at Kesterson range from 0.4 to 3.5 $\mu g\ m^{-2}\ h^{-1}$. When normalized to the concentration of total selenium in the soils, volatilization rates fall in the range of 0.07 to 0.25 $(\mu g\ m^{-2}\ h^{-1})/(mg\text{-}Se/kg\text{-}soil)$. The corresponding annual depletion rates fall in the range of 0.3 to 1.0% of the total selenium inventory per year, with an average value of 0.6% per year. These low rates indicate that changes in the total inventory attributable to volatilization will be slow.

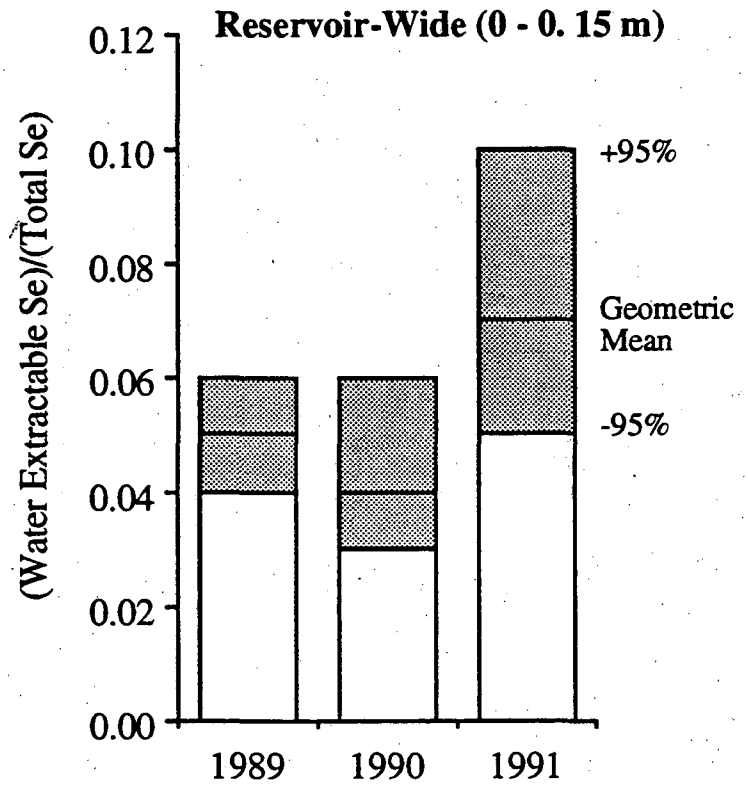

Figure 3.8. Geometric mean value for the ratio of water-extractable to total selenium concentrations in the top 0.15 m of soil from 54 samples collected as part of the synoptic sampling for 1989, 1990 and 1991. Note that a significant increase in this ratio was observed from 1989 to 1991 and from 1990 to 1991.

3.4. Expected Trends in Soil Selenium At Kesterson Reservoir

The combination of remobilization, leaching and volatilization are expected to create the following changes in the inventory and distribution of selenium in Kesterson soils over the next several decades:

- the total inventory of selenium in Kesterson soils will decline at an annual rate of approx imately 1% of the remaining inventory;
- water-extractable selenium in surface soils (0 -0.15 m depth) will be leached to deeper levels in the soil profile;
- water-extractable selenium inventories will most likely increase in the root zone in response to oxidation of selenium within this zone, as well as due to leaching of selenium from surface soils;
- the distribution of total selenium within the profile will change from being strongly concentrated near the soil surface to more evenly distributed within the upper 2 meters of soil;

Table 3.2. Summary of field-measured selenium volatilization rates from untreated soils at Kesterson Reservoir.

Location	Annually-averaged Emission Rate ($\mu g\ m^{-2}\ h^{-1}$)	Soil Selenium Concentration (mg/kg-soil)	Volatilization Rate Per Unit Soil Se Concentration ($\mu g\ m^{-2}\ h^{-1}$)/(mg/kg)	Corresponding Annual Depletion Rate (%/year)***
Pond 4 Test Plot[1]	3.5	39*	0.09	0.4
Pond 4 Test Plot[2]	2.6	39*	0.07	0.3
Pond 11 Test Plot[1]	0.8	3.7*	0.2	0.9
Pond 11 Test Plot[2]	0.4	3.7*	0.1	0.5
Pond 2 Test Plot[3]	4**	48.3	0.08	0.3
Reservoir Wide[4]	2	8.5	0.25	1.0
Average Value			0.13	0.6

*Median of initial values from the test plots (0 - 0.15 m depth interval).
**Estimated from measurements collected during August - October, 1991.
***Based on an estimated bulk density for surface soils of 1400 kg/m^3.

1 Frankenberger and Karlson, 1988.
2 Frankenberger, 1990.
3. ANR, 1992.
4. Weres et al., 1989.

- as a result of redistribution, total selenium concentrations will decline in the 0 -0.15 m depth interval and gradually increase at greater depths; total selenium concentrations are never expected to exceed the largest values heretofore observed at Kesterson;

- significant quantities of selenium will not be transported below 2 meters due to the chemically reducing conditions below the water table that favor immobile forms of selenium.

A schematic illustrating the net effect of the changes on the water-extractable selenium concentrations is presented in Figure 9. In the following section, the methodology for attempting to quantify the rate and extent to which these processes occur is described.

3.5. Predicted Changes in the Selenium Inventory and Distribution

To provide a more quantitative assessment of observed changes in the inventory and distribution of selenium in the soil profile over the past 5 years and to predict how these changes will continue into the future, a simple mathematical model has been developed and applied to the soil selenium data. The model tracks total and water-extractable selenium inventories in the top 2 m of soil and has been used to interpret existing data as well as to predict the range of possible future conditions. A detailed description of the approach, calibration and application of this model follows.

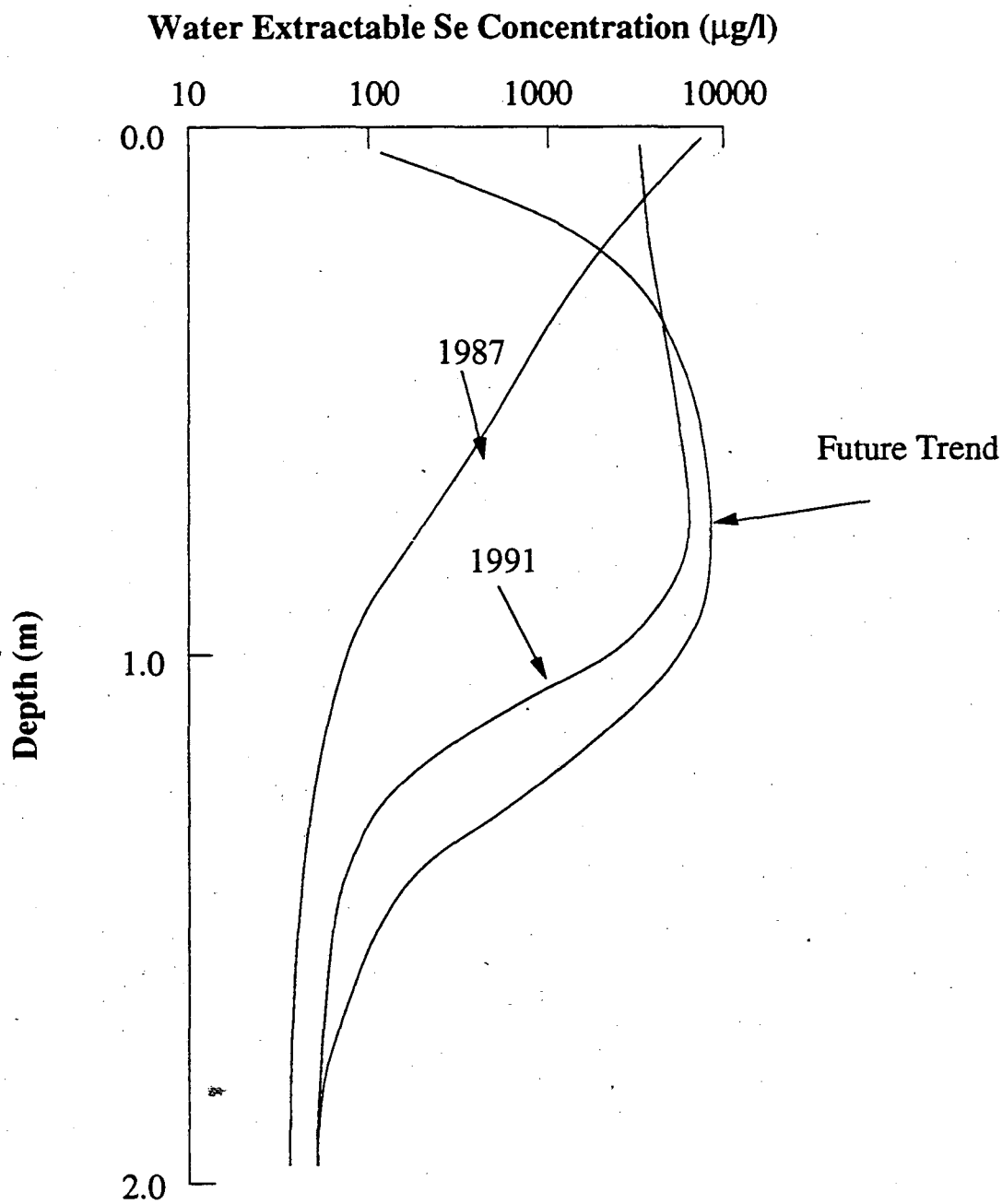

Figure 3.9 Schematic illustrating the distribution of water-extractable selenium concentrations in 1987, 1991 and under predicted future conditions.

3.5.1. Approach and Model Description

As illustrated in Figure 3.10, the top 2 m section is subdivided into three units for the purposes of tracking changes in the inventory: 1) from the soil surface to a depth of 0.15 m, 2) from 0.15 to 1 m and 3) from 1 to 2 m. Dividing the system into these three units was done primarily because:

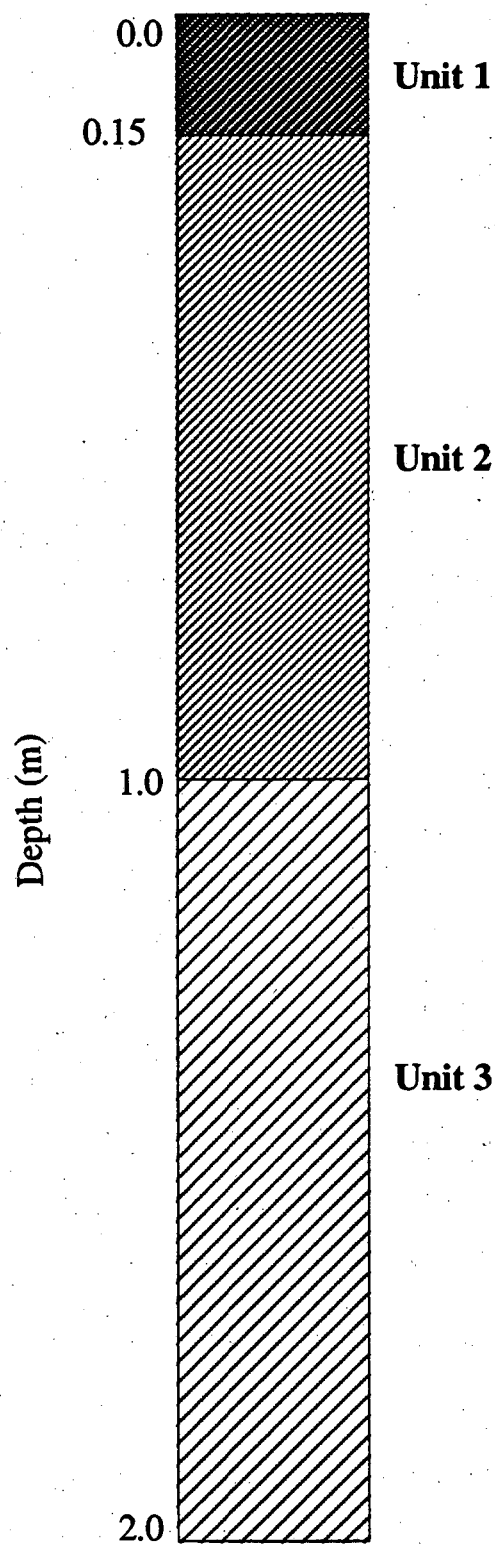

Figure 3.10. Illustration of the three subunits that the top 2 m of Kesterson soils have been divided into for model calibration and prediction.

- a relatively large data base is available to track changes in selenium concentrations in the top 0.15 m of soil;
- compared to deeper levels in the soil profile, the top 0.15 m of soil is most strongly in fluenced by microbial volatilization of selenium;
- concentrations of selenium in the top 0.15 m change dramatically in response to seasonal leaching and bare-soil evaporation (Ita and Benson, 1992);
- root uptake of soil moisture appears to be greatest in the depth interval from 0.15 to 1 m (LBL, 1988; 1990a, 1990b);
- below a depth of 1 m the soils are less affected by seasonal cycles in soil moisture content and by transport of solutes from surface soils, and consequently, are not expected to undergo rapid changes in selenium concentrations; and
- at Kesterson, the seasonal maximum depth to the water table, which occurs in the early fall, averages about 2.5 m below the ground surface.

The three "processes" that have been incorporated into the model are shown in Figure 3.11. These include selenium volatilization, leaching, and remobilization. As described earlier, these processes encompass a far more complicated interplay of physical, chemical and microbial processes that vary in importance throughout the year. Nevertheless, as a first approximation, these three processes can be used to describe the overall behavior of the system. As included in the model, the role of each of them is as follows.

Volatilization will transfer to the atmosphere a fraction of the selenium inventory from subunits within the system. For example, microbial volatilization is expected to remove selenium from the surface-most unit and plant volatilization from the root zone. The rate of volatilization is expressed in terms of the fraction of the total selenium inventory that is removed from each subunit per year. The quantity volatilized within a given year is calculated from

$$VOLI = VI*TII$$

where VOLI is the mass of selenium volatilized from unit I, VI is the volatilization rate for unit I and TII is the total inventory of selenium in unit I. Rate constants may be different for each subunit.

Leaching provides the mechanism for transporting selenium from one unit to another within the system. As currently included, leaching can only transport selenium deeper into the soil profile. This is in keeping with observations that rainfall infiltration transports selenium from the surface soils to depth. Very slow transport from unit 2 to unit 3 and from unit 3 to the groundwater system by molecular diffusion may also be mimicked by slow leaching rates. The leaching rate is expressed in terms of the percent of the water-extractable selenium inventory that is transported from one subunit to another over a 1 year period. Note that this is the net leaching that occurs over a one year period, not the maximum leaching that is observed immediately following the rainy season. The mass of selenium transported from unit I to unit J in a given year (LEACHIJ) is calculated by

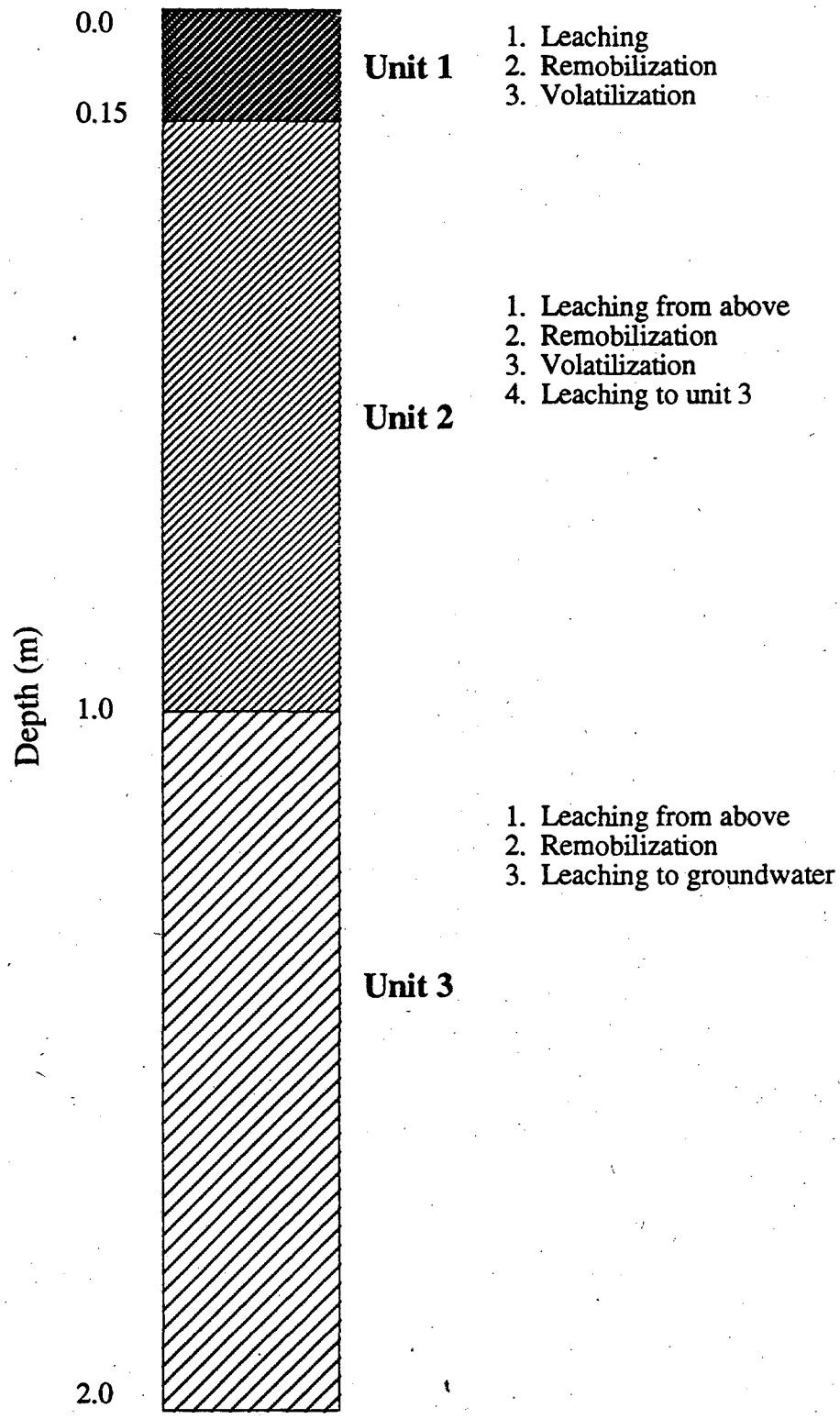

Figure 3.11. Illustration indicating the dominant processes affecting the selenium inventory within each of the three subunits of the model.

$$LEACHIJ = LIJ*EII$$

where, LIJ is the leaching rate from unit I to unit J, and EII is the inventory of water-extractable selenium in unit I. Rate constants may be different for each subunit.

It should be noted that the net transfer selenium from Unit 2 to Unit 1 is considered to be insignificant in this model. While this is a reasonable assumption as long as the inventory of selenium is greater in Unit 1 than in Unit 2, eventually, counter-diffusion of water-extractable selenium from deeper in the soil profile towards the soil surface may become significant. For the calculations described in this report, total selenium concentrations remain higher in Unit 1 than in the deeper units. Consequently, the assumption of no net transfer of selenium from Unit 2 to Unit 1 is a reasonable one.

The remobilization term accounts for increases in water-extractable selenium that occur due to oxidation or desorption of reduced forms of selenium, dissolution of selenium-bearing salts and decomposition of organic-matter-associated forms of selenium. Again, over the seasonal cycle, simultaneous or cyclical oxidation and reduction of selenium is expected to occur. Therefore, as with the leaching component, the rate constant associated with this "process" reflects the net effect of these competing processes over a year. The quantity remobilized within a given year is given by

$$REMOBI = RI*TII$$

where, REMOBI is the mass of selenium remobilized from unit I, RI is the remobilization rate for unit I and TII is the total inventory of selenium in unit I. Rate constants may be different for each subunit.

Rate constants for each of these processes were determined by calibrating the model with data from the long-term monitoring sites described above. Calibration, details of which are provided below, involved trial-and-error adjustment of remobilization and leaching rates from the subunits until the model results compared favorably with the measured data. Volatilization rates for units 1 and 2 (V1 and V2) were assigned a value of 1% per year, in keeping with field measured volatilization rates. Decreases in the inventory attributable to this small volatilization rate are not expected to be detectable for the 5 year period for which data are available. It was assumed that volatilization from unit 3 is negligible (e.g. V3=0).

3.5.2. Computational Procedure

The model uses an explicit time-stepping procedure to calculate yearly changes in the selenium distribution and inventory in the soil profile. A flow chart for the initialization and calculation procedure used by the model are provided in Figures 3.12 and 3.13. Model inputs include initial concentrations of total and water-extractable selenium and volatilization, leaching and remobilization rate constants for each unit. Model outputs include inventories and concentrations of water-extractable and total selenium for each subunit over time.

As shown in Figures 3.12 and 3.13, starting with the initial inventory of selenium, the model calculates the amount of selenium volatilized, leached and remobilized within each unit over a one-year period. After completing these calculations (see Figure 3.13), the model updates the inventories of water-

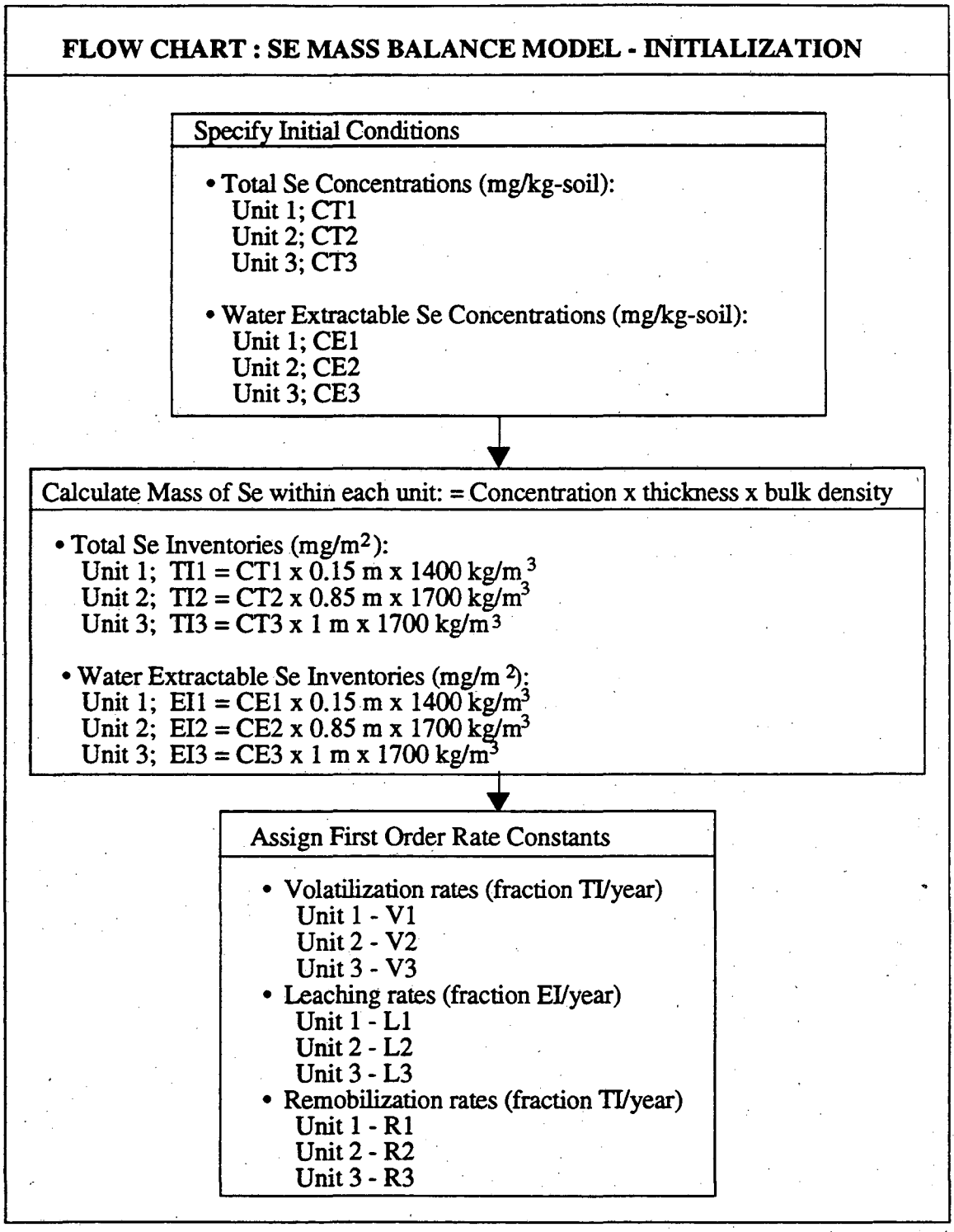

Figure 3.12. Flow chart for the mass balance model used to calibrate and predict the future behavior of selenium in Kesterson soils: data input and program initialization.

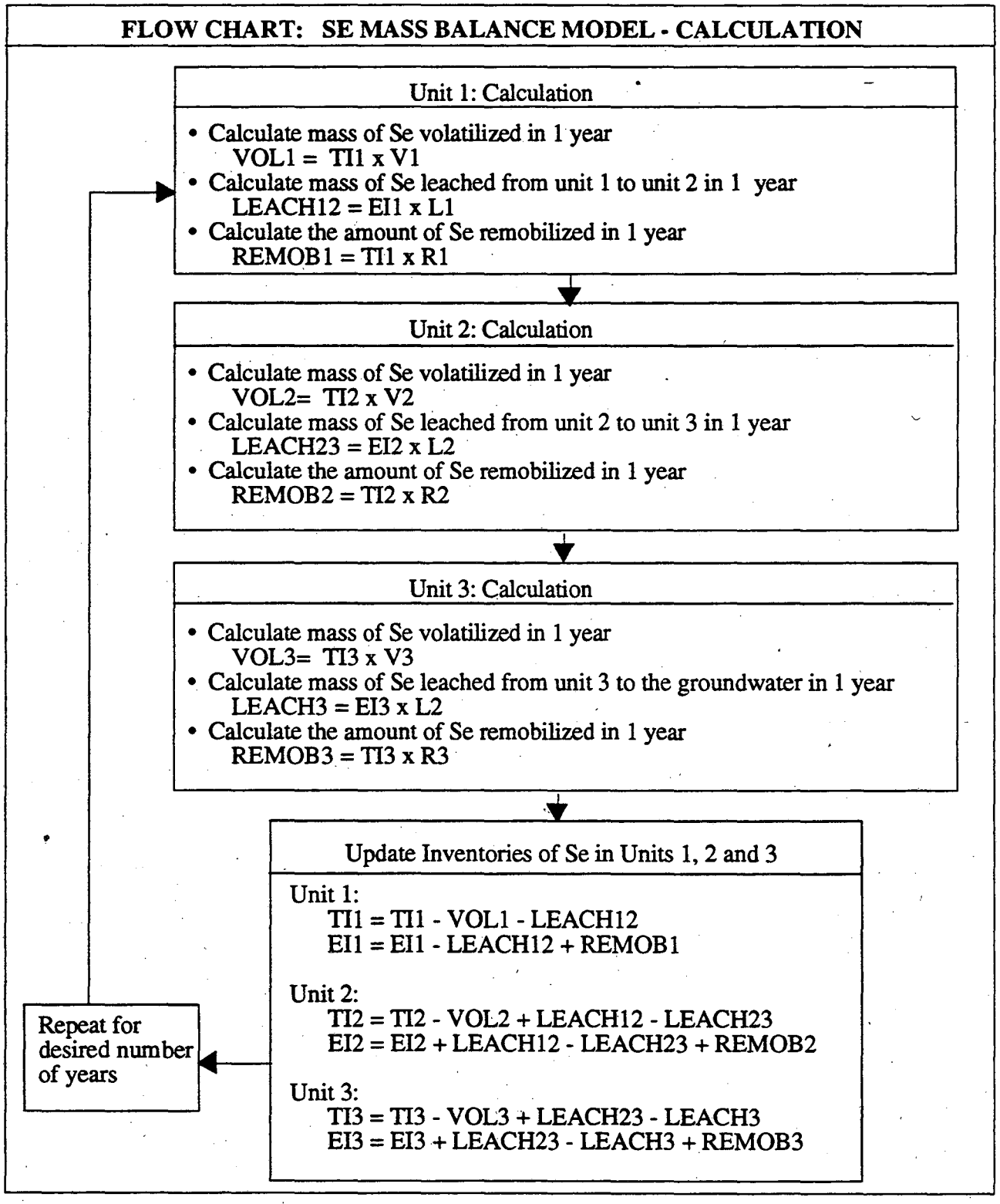

Figure 3.13. Flow chart for the mass balance model used to calibrate and predict the future behavior of selenium in Kesterson soils: calculation algorithm.

extractable and total selenium in the subunits. Having updated the inventories, the model repeats these calculations for the desired number of yearly intervals.

The computer program employed to carry out these calculations was written in the context of the EXCEL © spreadsheet environment.

3.5.3. Model Calibration Procedure

As described previously, there are several detailed data sets from which estimates of the rate constants can be obtained and consequently, the model calibrated. For the purpose of these calculations, initial conditions were assigned beginning with 1987 or 1988, depending on the availability of data. Specific pieces of information used for this purpose include the following:

- initial concentrations of total and water-extractable selenium and for the depth intervals from 0 to 0.15 m, 0.15 to 1 m, and 1 to 2 m;
- soil-solution selenium concentrations; and
- depth-integrated inventories of water-extractable selenium within each of the subunits and over the entire soil profile.

In calibrating the model the following procedure was used to establish a consistent method for obtaining rate constants. First, a lower limit for the leaching rate from the first to the second unit was determined by matching the rate of depletion of chloride from the surface-most unit. During this step, all other rate constants were set to zero. Having determined the leaching rate for Unit 1, the remobilization rate for that unit was then determined by increasing the rate from zero to the value required to approximately match the observed changes in its water-extractable inventory. Next, the remobilization rate for Unit 2 was increased until calculated and measured concentrations of water-extractable selenium were in reasonable agreement. If Unit 3 was only partially saturated for a majority of the year, its remobilization rate was increased up to a maximum of the value determined for Unit 2. If the calculated and measured values for water-extractable selenium for Unit 3 did not match well, the leaching rate from Unit 2 to Unit 3 was increased until the match was satisfactory. In general, because of the low concentrations of selenium in the 1 to 2 m interval, values for the leaching and remobilization rate constants for Unit 3 did not have a great influence on the rate constants for Units 1 and 2.

Due to the relatively slow rate constants and small percentage of the selenium inventory initially in extractable forms, changes in total selenium concentrations within the profile are not large enough to be quantified over the monitoring period and consequently were not used in the calibration procedure.

Detailed description of the calibration data from two sites are provided below.

3.5.4. Plot 8EP

Initial and subsequent concentrations of selenium over the period from 1988 to 1991 in plot 8EP are provided in Table 3.3. These were used to determine a set of leaching and remobilization rate constants that were consistent with the observed data. Rate constants were obtained by the calibration procedure

Table 3.3. Summary of soil selenium concentrations in Plot 8EP from 1988 to 1991.

Unit	Depth (m)	1988 Total Se (mg/kg-soil)	1988 Water-Extractable Se (mg/kg-soil)	1989 Water-Extractable Se (mg/kg-soil)	1990 Water-Extractable Se (mg/kg-soil)	1991 Water-Extractable Se (mg/kg-soil)
1	0.0 - 0.15	6.60	0.49	0.93	0.71	0.37
2	0.15 - 1	0.30	0.06	0.09	0.18	0.17
3	1 - 2	0.05	0.01	0.02	0.02	0.02

described above and are summarized in Table 3.4. Matches between observed and calculated concentrations of water-extractable selenium for the three subunits are shown in Figures 3.14, 3.15 and 3.16. As indicated in Table 3.4, annual remobilization rates in all surface-most units were on the order of 7% of the immobile inventory. Remobilization rate constants for Units 2 and 3 are zero, indicating that over the 3 year monitoring period no significant remobilization has occurred at depth in the soil profile. Examination of Figure 3.14 suggests that the low remobilization rate is attributable to a large amount of reduction that occurred during the 1990-1991 winter. This is consistent with the heavy rains that occurred during this period, the fine-textured nature of the 8EP soils and the relatively sparse growth of vegetation in this plot.

The leaching rate of 40% of the water-extractable inventory per year from layer 1 to layer 2 indicates that rainfall infiltration plays a major role in redistributing selenium within the soil profile. Only

Table 3.4. Summary of leaching and remobilization rate constants determined from Plot 8EP and 11C.

Depth Interval (m)	Leaching rate (fraction of water-extractable /year)	Remobilization rate (fraction of immobile/year)	Volatilization rate (fraction of total Se/year
Plot 8EP			
0.0 - 0.15	0.4	0.07	0.01
0.15 - 1	0.04	0	0.01
1 - 2	0.01	0	0
Plot 11C			
0.0 - 0.15	0.5	0.03	0.01
0.15 - 1	0.02	0.09	0.01
1 - 2	0.01	0.09	0

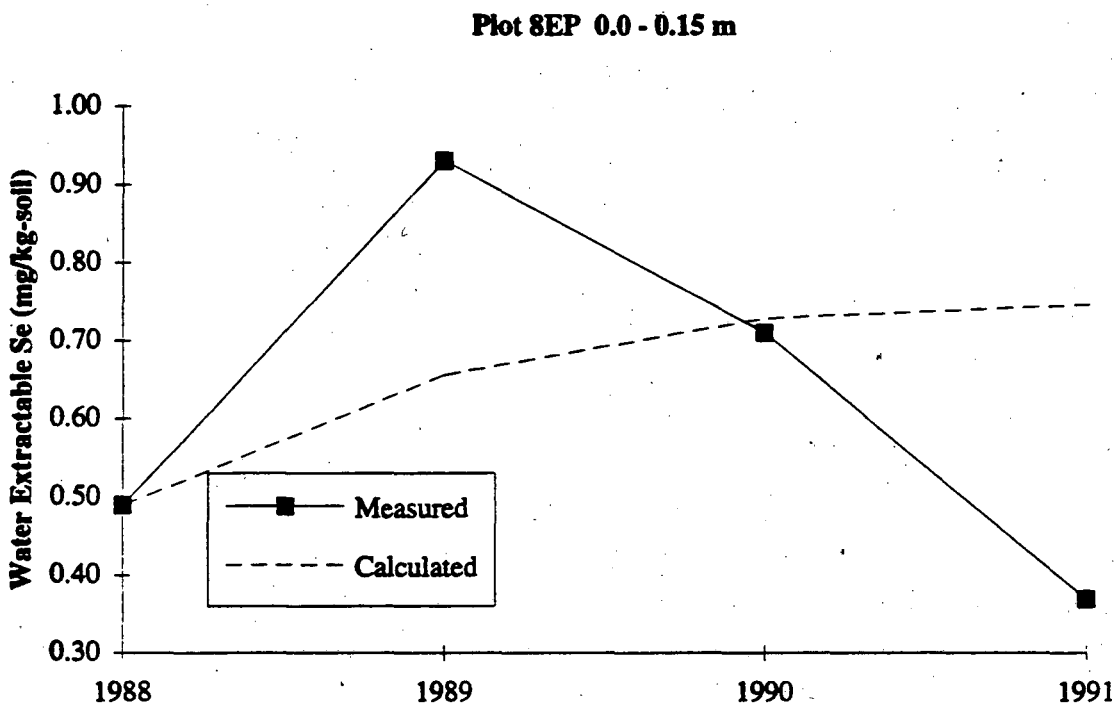

Figure 3.14. Comparison between measured and calculated water-extractable selenium concentrations in the top 0.15 m of soil at Plot 8EP.

a small amount of leaching from unit 2 to 3 appears to occur. This is consistent with field observations that leaching appears to be confined largely to the upper meter of the soil profile.

Matches between observed and calculated concentrations in Plot 8EP indicate that the major trends observed are represented reasonably well with the model. However, year to year variations are not reproduced accurately. This indicates that the rate constants, as implemented in the model are not constant over the three-year period. This can be explained in part by variations in quantity, intensity and timing of the rainy season, particularly for Unit 1. During 1989, the major rains occurred in mid-winter when the soils were nearly saturated from regional water-table increases. The combination of the high water saturation and a high water-table limits the effectiveness of leaching. In contrast, during 1990, the total rainfall was greater and perhaps more significantly, a series of large rainfall events occurred in mid-May, when the soils were drier and significant leaching was more likely to occur. As mentioned above, a sequence of heavy rains occurred in March 1991, leading to wetter-than-average soil moisture conditions.

The role of vegetation on the soil-moisture regime and transport of solutes may also contribute to annual variations in the rate constants. During the summer of 1989, no vegetation was allowed to grow in Plot 8EP. Thus, compared to the summer of 1990 when *Bassia* invaded the plot and transpired a large fraction of the soil moisture, the soil was relatively moist. Similarly, in 1991, the plot was only sparsely

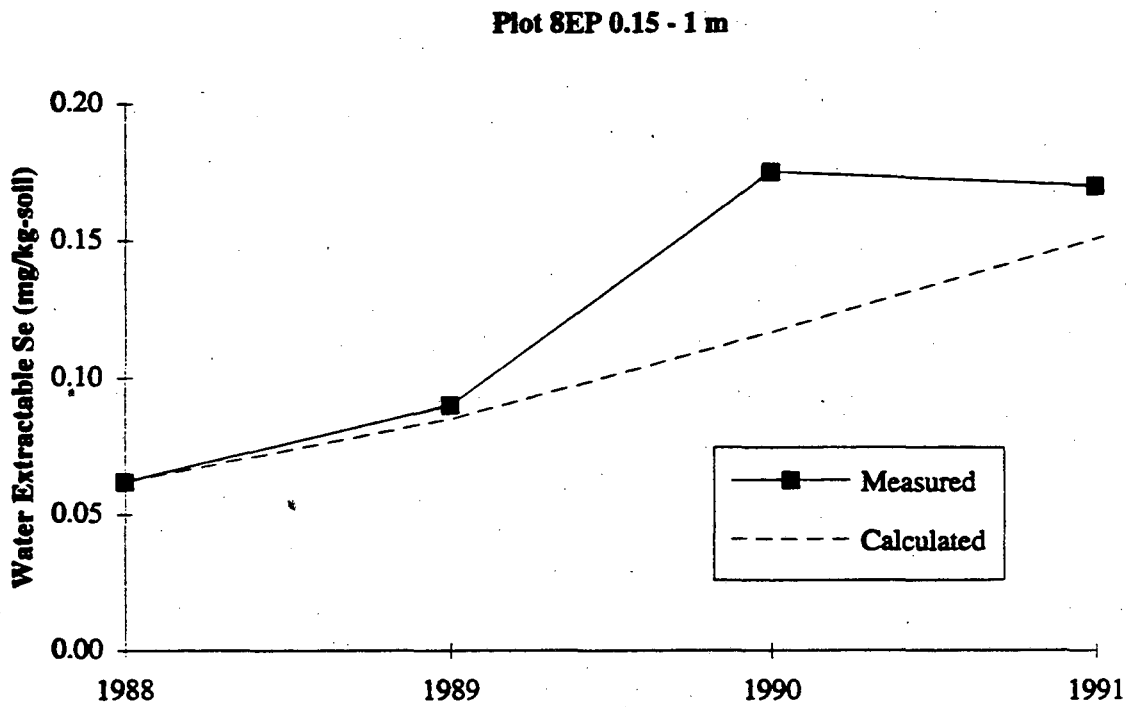

Figure 3.15. Comparison between measured and calculated water-extractable selenium concentrations in the depth interval of 0.15 to 1 m of soil at Plot 8EP.

vegetated. Higher moisture contents tends to maintain the reducing conditions that favors immobilization of selenium and limits the effectiveness of leaching.

3.5.5. Plot 11C

Initial and subsequent concentrations of selenium over the period from 1988 to 1991 in Plot 11C are given in Table 3.5. These were used to determine a set of leaching and remobilization rate constants that were consistent with the observed data. Rate constants were chosen by the calibration procedure described above and summarized in Table 3.4. Matches between observed and calculated concentrations of water-extractable selenium are shown in Figures 3.17, 3.18 and 3.19 for the three subunits. In addition, Figure 3.20 shows the match between the total inventory of water-extractable selenium in the top 2 m of soil. As indicated in Table 3.4, remobilization rates in all three units are on the order of 3 to 9% of the immobile inventory per year. The annual leaching rate of 50% of the water-extractable inventory per year from Unit 1 to Unit 2 again indicates that rainfall infiltration plays a major role in redistributing selenium within the soil profile.

In general, the matches between calculated and measured concentrations of selenium shown in Figures 3.17 through 3.20 are better for Plot 11C than they are for Plot 8EP. These good matches suggest that the rate constants determined by the calibration procedure are nearly constant over the 3-year period.

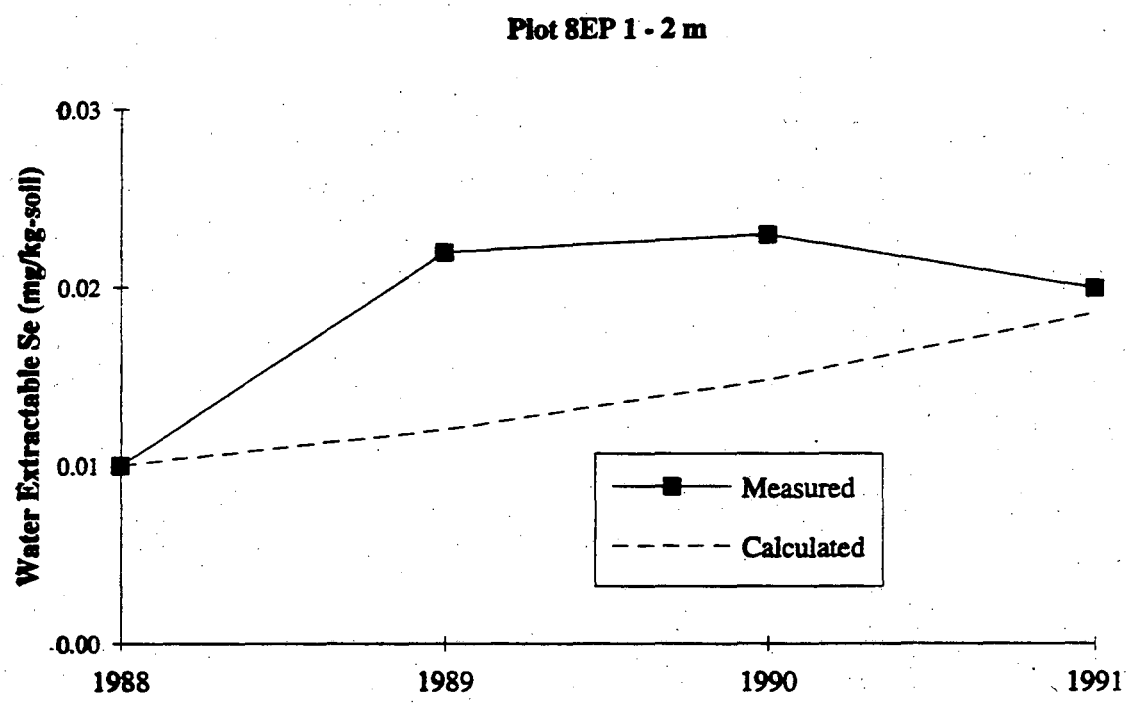

Figure 3.16. Comparison between measured and calculated water-extractable selenium concentrations in the depth interval of 1 to 2 m of soil at Plot 8EP.

Table 3.5. Summary of soil selenium concentrations in Plot 11C from 1988 to 1991.

Depth (m)	1988 Total Se (mg/kg-soil)	1988 Water-Extractable Se (mg/kg-soil)	1989 Water-Extractable Se (mg/kg-soil)	1990 Water-Extractable Se (mg/kg-soil)	1991 Water-Extractable Se (mg/kg-soil)
0.0 - 0.15	5	0.20	0.25	NA	0.11
0.15 - 1	0.9	0.11	0.19	NA	0.32
1 - 2	0.05	0.00	0.01	NA	0.02

NA - not available

This may be explained in part by the presence of a dense and stable growth of salt grass (*D. spicata*) in the test plot that persisted over the entire monitoring period.

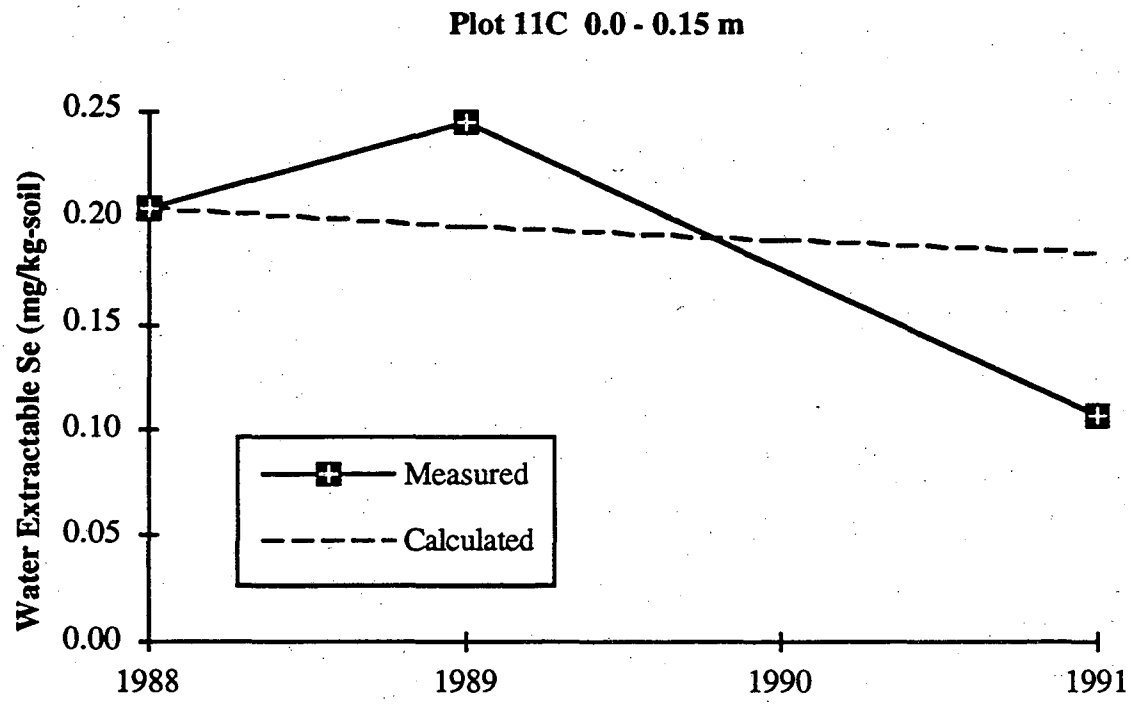

Figure 3.17. Comparison between measured and calculated water-extractable selenium concentrations in the top 0.15 m of soil at Plot 11C.

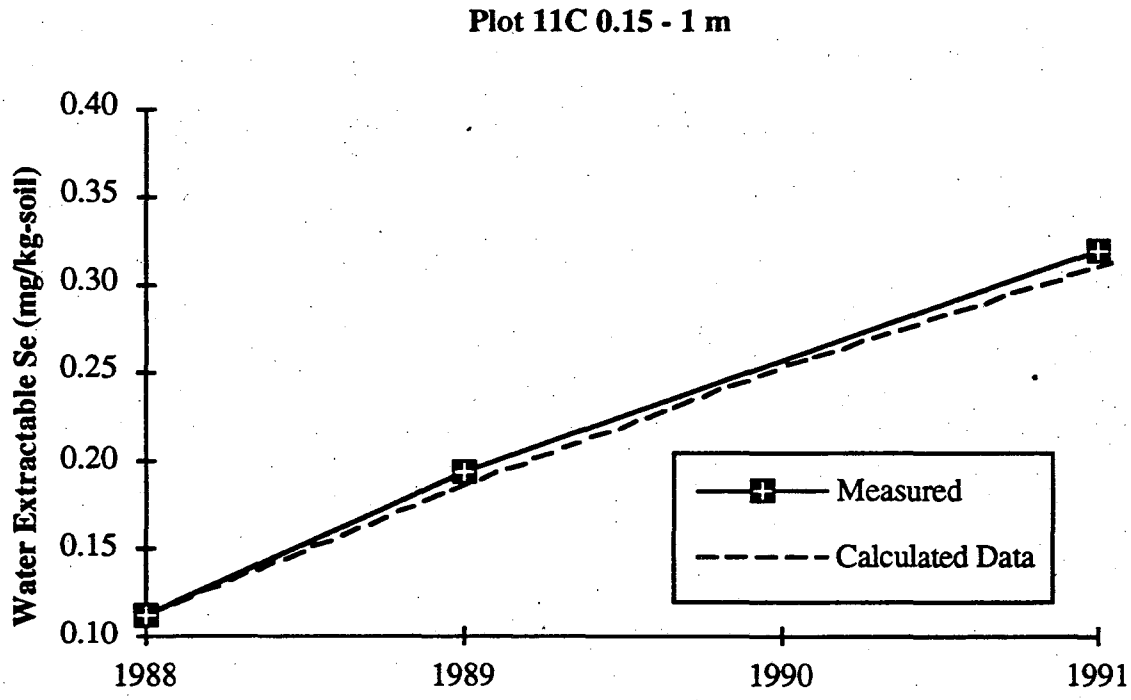

Figure 3.18. Comparison between measured and calculated water-extractable selenium concentrations in the depth interval of 0.15 to 1 m of soil at Plot 11C.

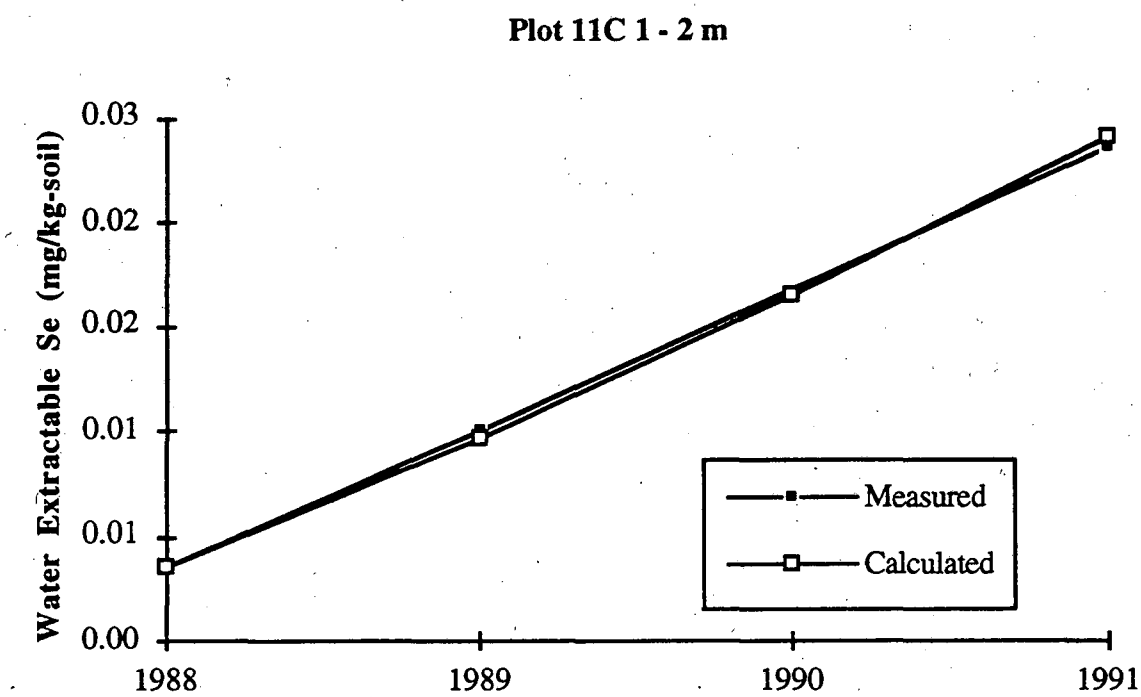

Figure 3.19. Comparison between measured and calculated water-extractable selenium concentrations in the depth interval of 1 to 2 m of soil at Plot 11C.

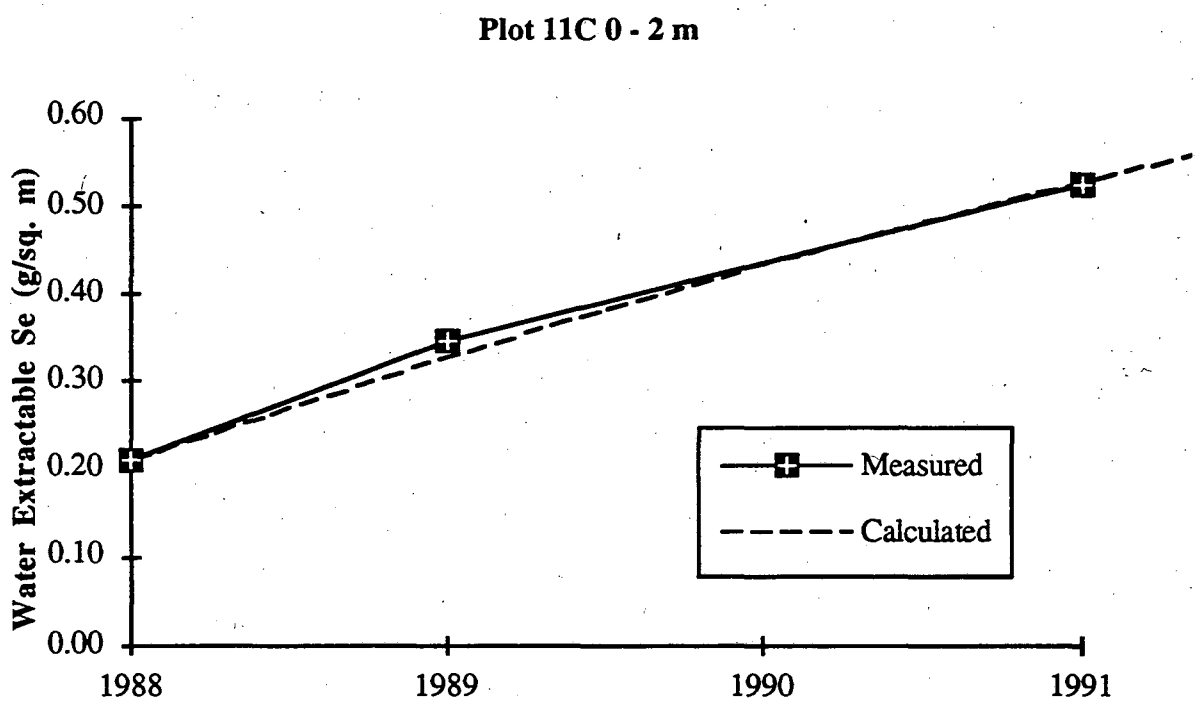

Figure 3.20. Comparison between measured and calculated inventories of water-extractable selenium in the top 2 m of soil in Plot 11C (note that inventories are expressed as grams of Se per m^2).

3.5.6. Prediction of Soil Selenium Concentrations for a Twenty-five Year Period

Using a range of rate constants determined from the calibration exercise described above, the model was used to forecast soil-selenium concentrations over a twenty-five year period beginning in 1987. Following a discussion of the initial conditions used in the model, calculated concentrations of water-extractable and total selenium are presented for 5 cases spanning the range of observed leaching, remobilization and volatilization rates.

Initial conditions listed in Table 3.6 are established based on the results of the Reservoir-wide sampling program described previously and from supplemental information gathered elsewhere at the Reservoir. For Unit 1, values for total and water-extractable selenium were taken directly from the 1989 Reservoir-wide sampling data (values were rounded to the nearest significant figure). It is assumed that these values remained essentially unchanged from 1987 to 1989. This assumption is consistent with the Reservoir-wide and profile monitoring investigations described previously.

For Units 2 and 3, initial conditions are estimated based on profile sampling described by Long et al. (1990), Weres et al. (1989), Zawislanski (1990) and Tokunaga et al. (1991). An estimated 20% (1800 kg) of the 9000 kg of selenium delivered to Kesterson from 1981 to 1986 is located in the depth interval of 0.15 to 1 m. If this inventory is distributed uniformly over this interval, the average selenium concentration will be approximately 0.25 mg/(kg-soil). Limited information is available for assessing the fraction of this inventory that was water-extractable prior to 1989. However, recent data indicate that about 50% is presently in water-extractable form (see Figures 3.1a to 3.1c). Observations of increasing concentration of water-extractable selenium in this depth interval over the past 4 years, combined with information provided in Tables 3.3. and 3.5, indicate that it is reasonable to assume that approximately 20% of this inventory was water-extractable in 1987, the first year that most of the Reservoir was dried out. The total and water-extractable selenium concentrations in Unit 3 were assumed to be 20% of the values assigned to Unit 2.

The calibration data presented in this report and additional unpublished calibration runs indicate that leaching and remobilization rates may vary over a wide range and from year to year. Given the range of soil properties, hydrologic parameters, depth to water table and vegetative cover, this is not surprising. No one set of conditions will be representative of the Reservoir as a whole. Also, in light of the short duration over which conditions have been monitored compared to the forecasting horizon, it is prudent to consider a range of likely scenarios. The five cases presented in this report are listed in Table 3.7 and were chosen to cover the spectrum of possible conditions. This list is by no means exhaustive, but results from these calculations span the range of a much larger set of cases that were investigated. Volatilization rates for Units 1 and 2 range from 0.001 to 0.02, leaching rates from 0.01 to 0.35 and remobilization rates from 0.01 to 0.10. Because of the small inventory of selenium in Unit 3, and slow leaching rate from Unit 2 into Unit 3, the results of the calculations are not very sensitive to the rate constants for Unit 3. For this

reason, the rate constants for Unit 3 were held constant at the following values: V3 = 0, L3= 0.01 and R3 = 0.

For the 5 cases listed in Table 3.7, predicted concentrations of water-extractable selenium in the top 0.15 m of soil are illustrated in Figure 3.21. As shown, temporal trends vary from monotonic decreases over the 25-year period (Case 4) to remaining nearly constant (Case 2), to increasing for a 4 to 10-year period before declining (Cases 1, 3 and 5). Most likely, there will be individual sites at Kesterson that will follow each of these trends.

Table 3.6. Initial conditions used to compute future trends in soil-selenium concentrations at Kesterson Reservoir.

Unit	Depth (m)	Total Se (mg/kg-soil)	Water-Extractable Se (mg/kg-soil)
1	0 - 0.15	4	0.2
2	0.15 - 1	0.25	0.05
3	1 - 2	0.05	0.01

Table 3.7. Initial conditions and rate constants used to compute changes in soil-selenium concentrations.

Case	Unit	VI (fraction of total inventory volatilized per year)	LI (fraction of water-extractable inventory leached per year)	RI (fraction of immobile inventory remobilized per year)
1	1	0.01	0.35	0.05
1	2	0.01	0.01	0.1
1	3	0	0.01	0
2	1	0.01	0.15	0.02
2	2	0.01	0.01	0.02
2	3	0	0.01	0
3	1	0.001	0.15	0.05
3	2	0.001	0.01	0.05
3	3	0	0.01	0
4	1	0.01	0.15	0.01
4	2	0.01	0.01	0.01
4	3	0	0.01	0
5	1	0.02	0.15	0.05
5	2	0.02	0.01	0.05
5	3	0	0.01	0

The ratio between the leaching and remobilization rates (LIJ*EII/RI*TII) is the primary factor governing temporal trends. Where this ratio is high, water-extractable selenium concentrations will remain the same or decrease over time (Case 4). Where this ratio is low, water-extractable selenium concentrations will increase until the inventory of total selenium is decreased substantially (Case 3). The reservoir-wide monitoring data of the top 0.15 m of soil presented previously, suggest that on-average, the concentration of water-extractable selenium has remained nearly constant over this period (see Table 3.1), thus indicating that the rate of selenium remobilization is nearly balanced by the rate of leaching.

For the 5 cases listed in Table 3.7, predicted concentrations of water-extractable selenium in soils from 0.15 to 1 m deep are given in Figure 3.22. Except for Case 4, water-extractable selenium concentrations increase over the entire 25 year period. The combination of leaching from Unit 1 and remobilization within Unit 2 governs the rate at which selenium concentrations increase within this unit. Note that although these calculations predict a significant increase in water-extractable selenium concentrations, even the maximum concentrations are less than, or equal to, concentrations presently observed at some Kesterson locations (for example, see Figures 3.1a and 3.1c).

Tracking the inventory of water-extractable selenium within the top 2 m of soil is another way of evaluating these calculations. As shown in Figure 3.23, except for Case 4, the inventory of water-extractable selenium in the top 2 m increases over the entire 25-year period. Increases in water-extractable selenium inventories are governed solely by remobilization rates. As indicated in Table 3.7, the range of remobilization rates within Units 1 and 2 span the range of values determined from the calibration procedure described previously. Ultimately, remobilization rates in Unit 1 will dominate the overall response because the majority of selenium resides within this unit. Total selenium concentrations are also calculated by the model. Temporal trends for total selenium in Units 1 and 2 are given in Figures 3.24 and 3.25. As shown, concentrations in the surface-most 0.15 m are expected to decline gradually over the entire period due to a combination of leaching, remobilization and volatilization. Total selenium concentration will decline most rapidly in locations with high leaching and remobilization rate constants (such as Cases 1, 3 and 5). Volatilization will only slowly contribute to depletion of the selenium inventory. Slow to moderate rates of depletion of the surficial inventory are consistent with the limited observations obtained during the Reservoir-wide monitoring program.

While total selenium concentrations decline in the upper unit of the soil profile, concentrations in the 0.15 to 1 m depth interval will remain the same or increase gradually (see Figure 3.25). High remobilization and leaching rates in Unit 1 cause the largest increases in selenium concentrations to occur in Unit 2 (Cases 1 and 3). Again, note that although significant increases are predicted, values still fall within the range of concentrations presently observed in some locations at Kesterson (see Figures 3.1a through 3.1c).

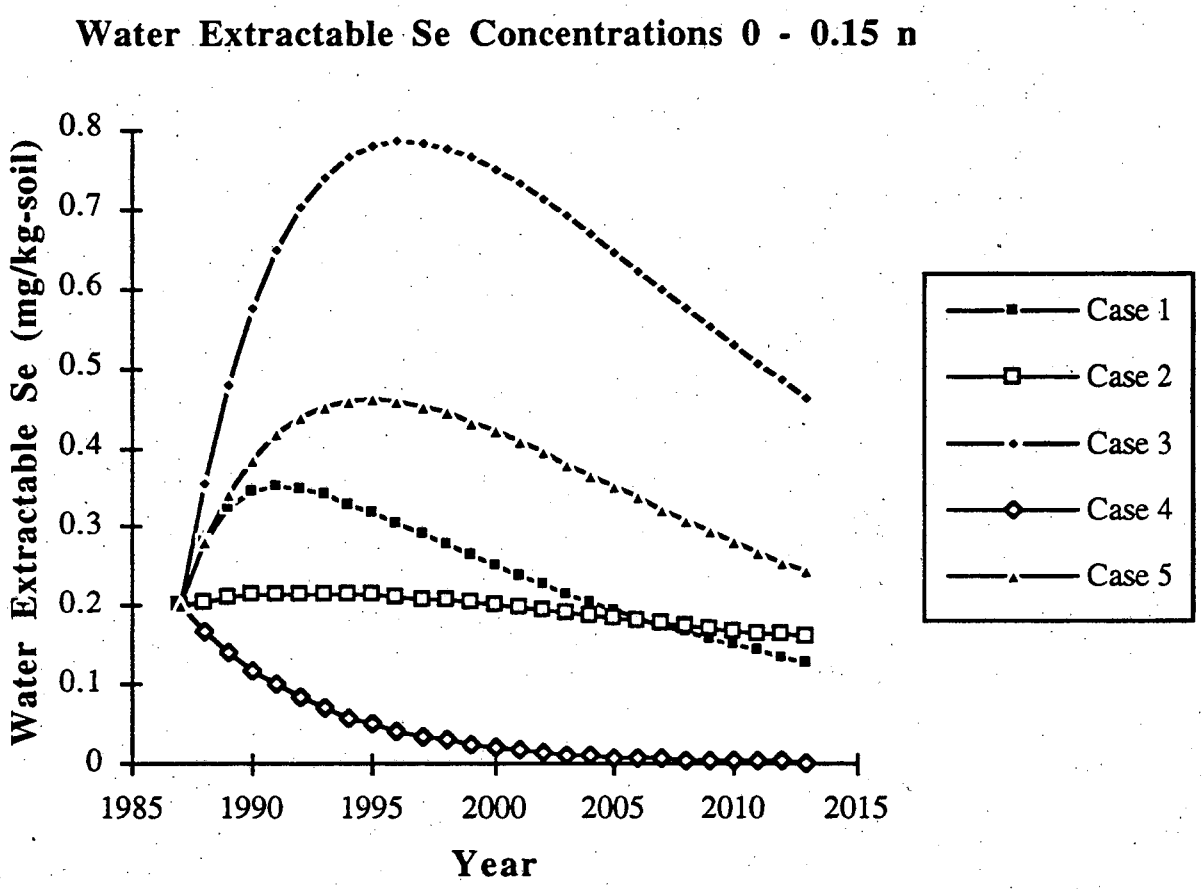

Figure 3.21. Predicted concentrations of water-extractable selenium in the top 0.15 m of soil at Kesterson Reservoir for the cases listed in Table 3.7.

Comparison between Figures 3.22 and 3.25 indicates that where remobilization rates are high (Cases 1, 3 and 5), within the next few years the majority of selenium in the 0.15 to 1 m depth interval will be in water-extractable forms. This suggests that the pool of selenium readily available for plant uptake will increase in the coming years. Implications of this prediction have been explored through the use of a computer model simulating the Kesterson food chain (CH2M Hill, 1992).

3.6. Use of Model Predictions for Biological Risk Assessment

Predicted water-extractable selenium concentrations in the 0.15 to 1 m depth interval were used to drive a food-chain-based biological risk assessment model (CH2M Hill, 1992). Motivation for choosing this depth interval, compared to the others, is based on observations from tensiometers and neutron-probe soil moisture measurements which indicate that *D. spicata* and *B. hyssopifolia* extract water most vigorously from this interval (LBL, 1988; 1990a; and 1990b). Unfortunately, there are limited Kesterson

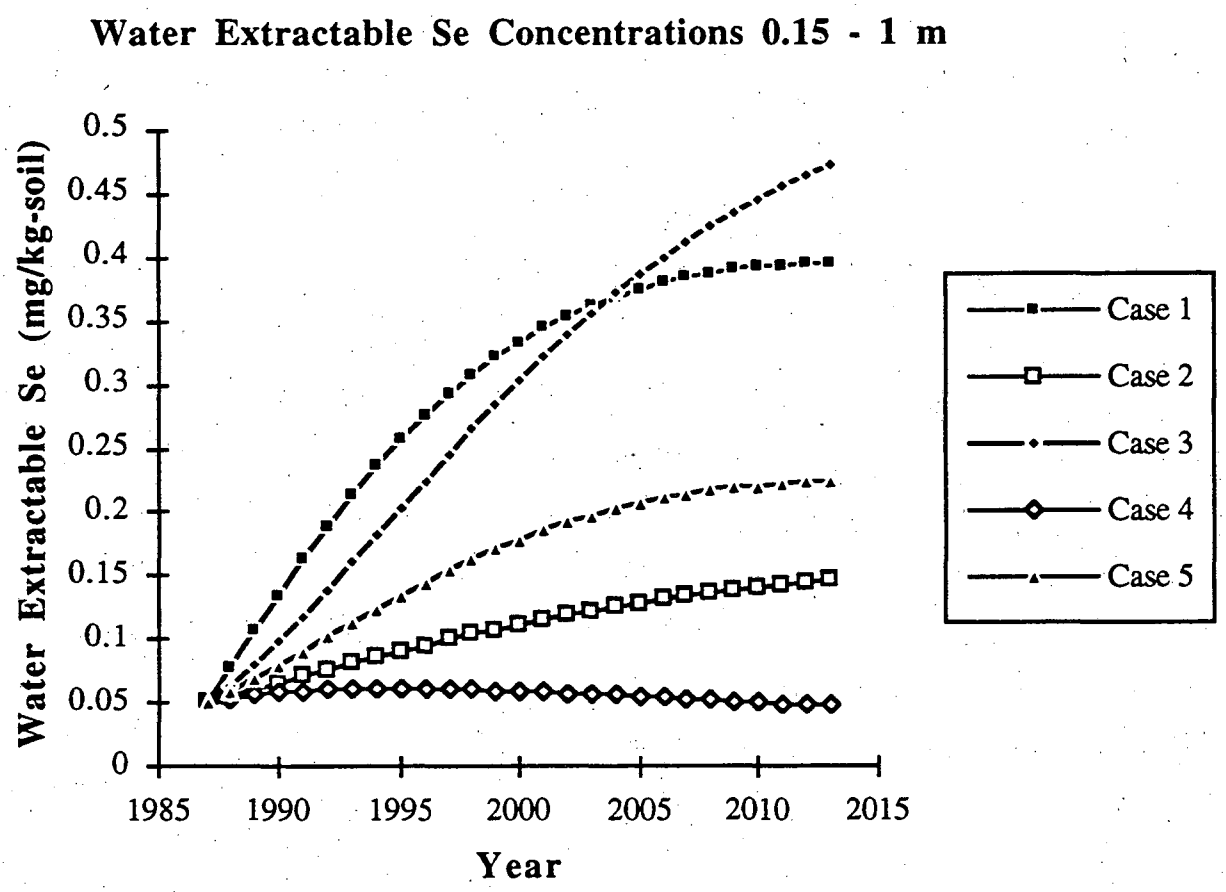

Figure 3.22. Predicted concentrations of water-extractable selenium in the depth interval from 0.15 to 1 m at Kesterson Reservoir for the cases listed in Table 3.7.

data providing correlations between concentrations of selenium in plant tissue and water-extractable selenium concentrations in this depth interval (Wu et al., 1990). Because of this deficiency, available data on correlations between water-extractable selenium in the 0 to 0.15 m depth interval and plant tissue selenium concentrations were adjusted to reflect sub-soil selenium concentrations. The adjustment involved assuming that sub-soil (0.15 to 1 m) concentrations of water-extractable selenium were on the order of 20% of those in the 0 to 0.15 m depth interval. Whereas this is a reasonable assumption shortly after Kesterson was dried out (Long et al., 1990), as time progresses, selenium concentrations in the sub-soil may increase towards or exceed surface soil concentrations. For this reason, we recommend that deeper soil samples be collected to improve these correlations and the rigor of this analysis.

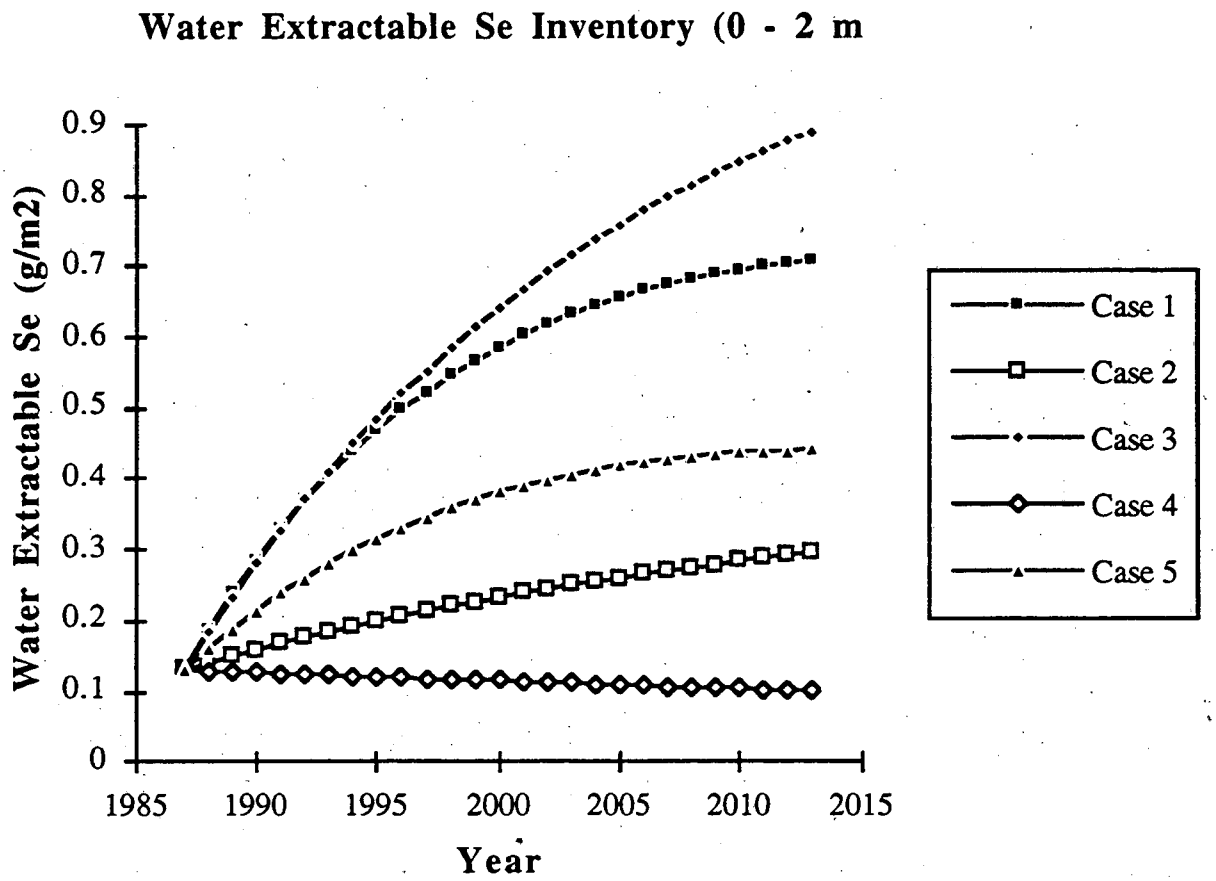

Figure 3.23. Predicted inventories of water-extractable selenium in the top 2 m of soil at Kesterson Reservoir for the cases listed in Table 3.5.

A limited subset of the 5 cases presented here were used in the risk-assessment model, including Case 1, Case 4 and Case 5. As illustrated in Figure 3.22, these 3 cases span the range of possible concentrations in this depth interval and as such, are considered to be representative of expected temporal trends.

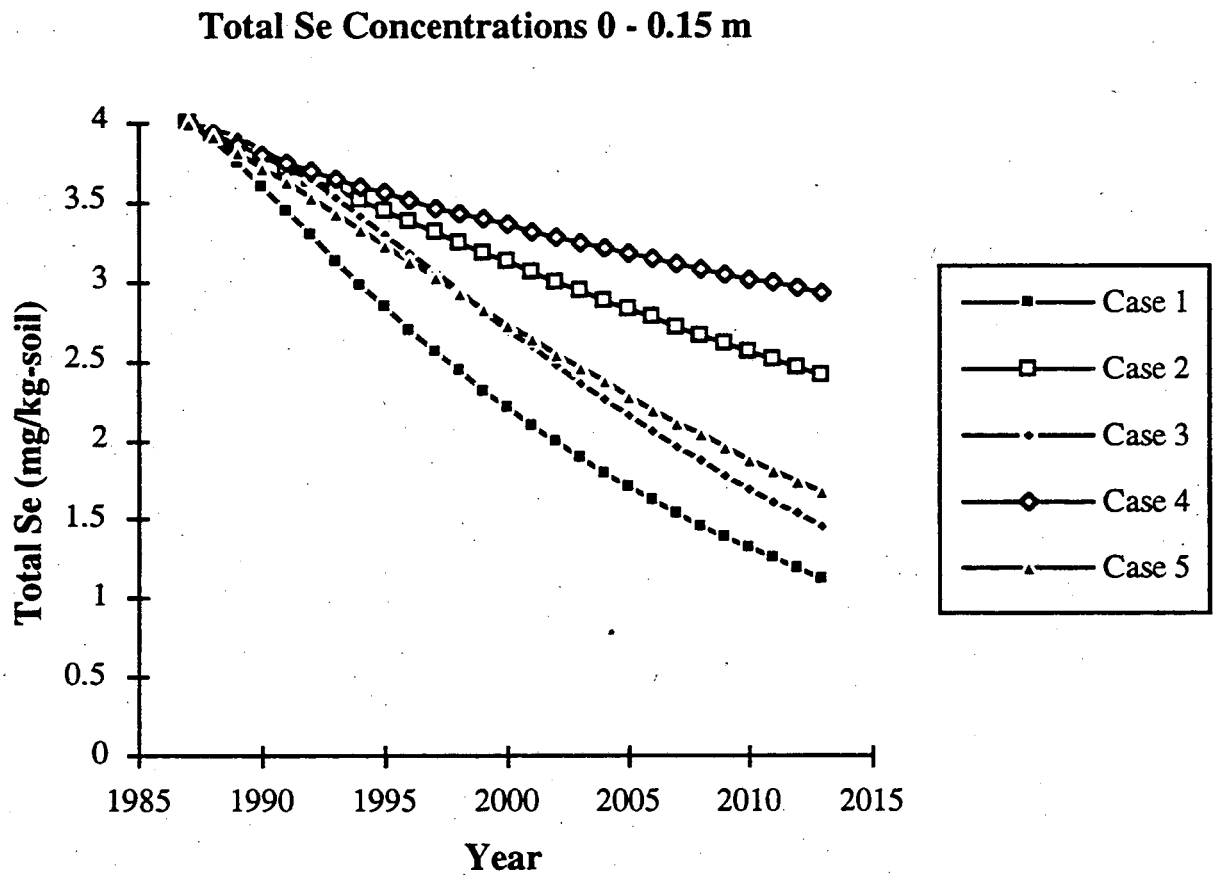

Figure 3.24. Predicted concentrations of total selenium in the top 0.15 m of soil at Kesterson Reservoir for the initial conditions and cases listed in Tables 3.6 and Table 3.7, respectively.

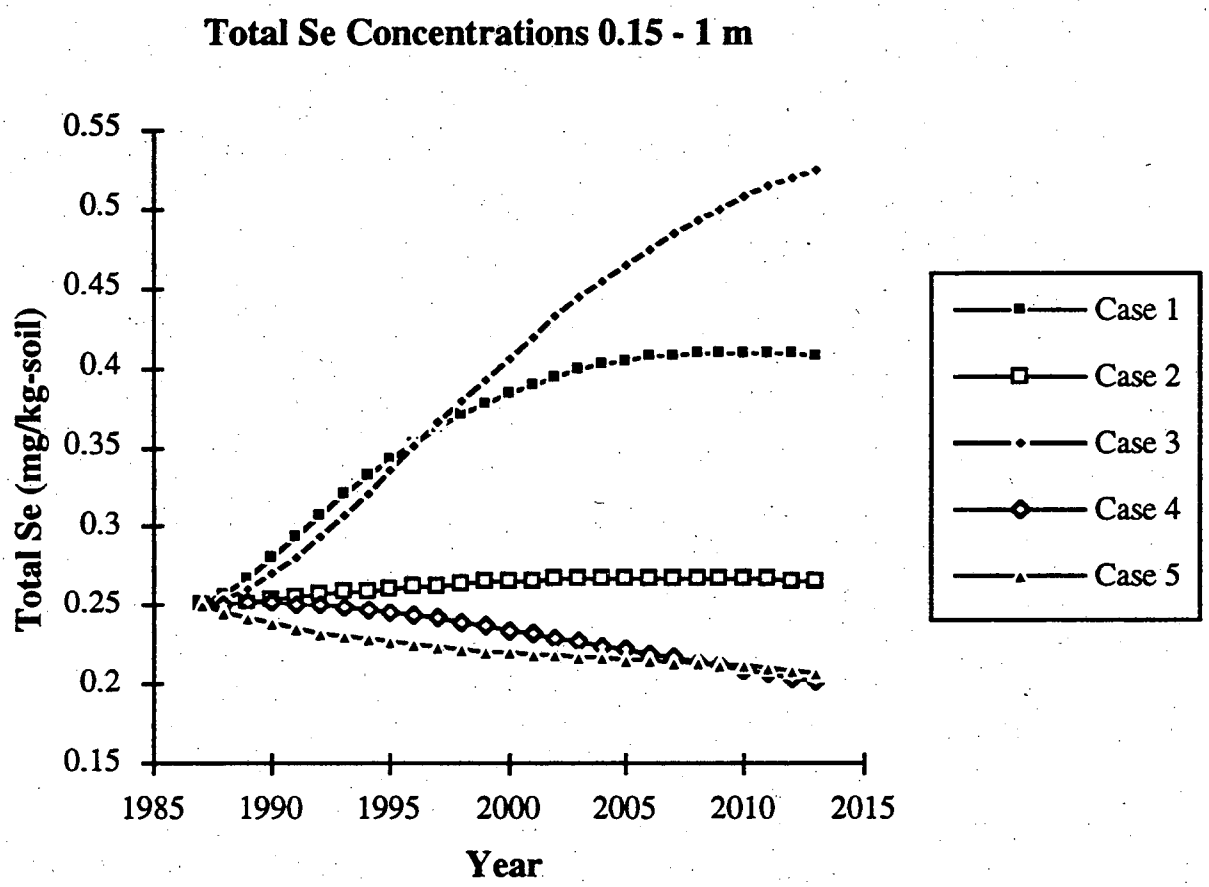

Figure 3.25. Predicted concentrations of total selenium in the 0.15 to 1 m depth interval at Kesterson Reservoir for the initial conditions and cases listed in Tables 3.6 and Table 3.7, respectively.

4.0. Offsite Migration of Selenium

Beginning in 1990, the former Freitas Ranch became available for soil and groundwater sampling to determine the extent of salt and selenium migration from Kesterson Reservoir. Two data sets have been collected, a soil sampling survey and a groundwater sampling survey. Both data sets demonstrate that selenium was not transported to any significant extent by groundwater movement or windblown particulates. However, salts and boron originating from Kesterson Reservoir have migrated several hundred meters from the Reservoir boundary, largely from groundwater transport. The results from the soil sampling are summarized in Section 4.1 and results from the groundwater sampling are summarized in Section 4.2.

4.1. Off-Site Soil Sampling (former Freitas Property)

Paul Johannis and Tetsu Tokunaga
Earth Sciences Division
Lawrence Berkeley Laboratory

4.1.1. Introduction

To better understand the extent of off-site migration of salts and trace elements, soil samples were collected from three transects on the former Freitas property and to the north on Kesterson National Wildlife Refuge adjacent to Ponds 2, 5, and 9 of Kesterson Reservoir in September of 1991. The transects (Figure 4.1a) were chosen in these areas to determine patterns in salinity, water-extractable boron, selenium, arsenic, and molybdenum caused by the ponding at Kesterson Reservoir, subsequent groundwater movement and windblown particulates.

As shown on Figure 4.1b the water table elevation decreases toward the northeast. Note that due to a surveying error, previous groundwater-contour maps prepared by USBR for the southern portion of the former Freitas property showed an incorrect groundwater gradient into Kesterson Reservoir. This problem has been corrected and all values reported here use the correct elevations.

The soil sampling transects were adjacent to wells drilled off-site between 1990-1991 for groundwater monitoring as shown in Figure 4.2. Also, just over a third of the soil sample points crossed over two previous ground conductivity surveys done by LBL in 1987 and 1988 (Goldstein et al., 1989). The ground conductivity survey showed that the saline plume was migrating about 5 to 50 m/yr, depending on location of EM readings. The survey also identified several anomalies with high electrical conductivity (EC) which were attributed to small topographic depressions and troughs. These same anomalies were seen in the EC of several of the soil water extracts taken throughout the study area. The (Goldstein et al., 1989) survey extended from Pond 1 out to Pond 5 (see Figure 4.7).

By matching up the soil survey points and the closest nodal readings from the EM equipment we attempted to show a correlation between the 1:5 soil-water extract electrical conductivity and the EM data. Figure 4.7 in Section 4.1.4 shows roughly where the intersects occur. Details of the comparison will be shown in an upcoming section.

Prior to this time, monitoring of lateral migration of salt and trace elements has focused on groundwater transport. Detailed soil sampling off-site had not been done to see if any of the trace elements mentioned above have migrated from Kesterson Reservoir into the Refuge to the east and north. Well samples are taken either monthly, quarterly, or semiannually through the Bureau of Reclamation's water-quality monitoring program of Kesterson and the surrounding area, and well samples were taken from the wells on the Freitas property when they were first installed by LBL in 1991.

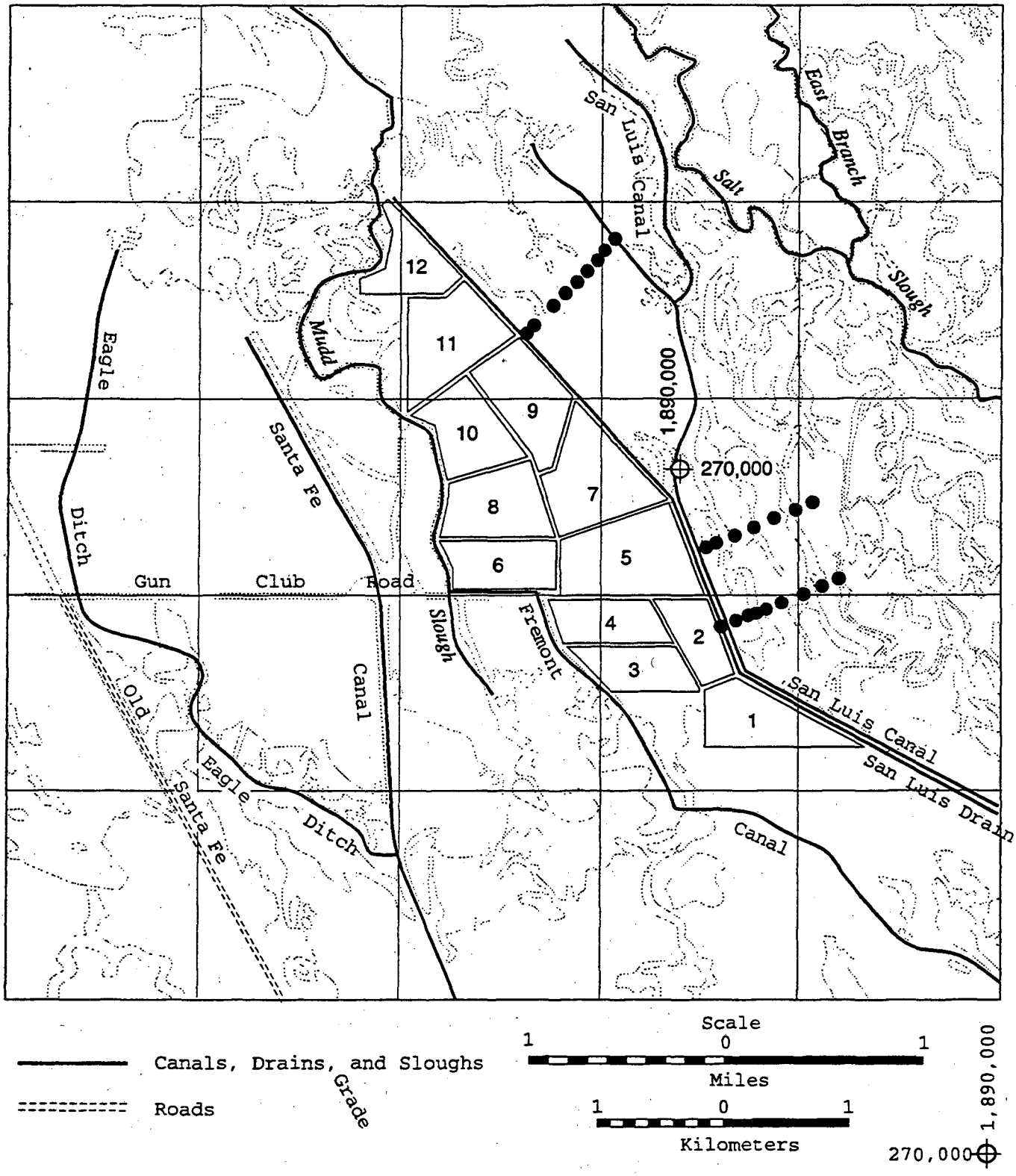

Figure 4.1a. Off-site soil sampling points.

XBL-921-6010

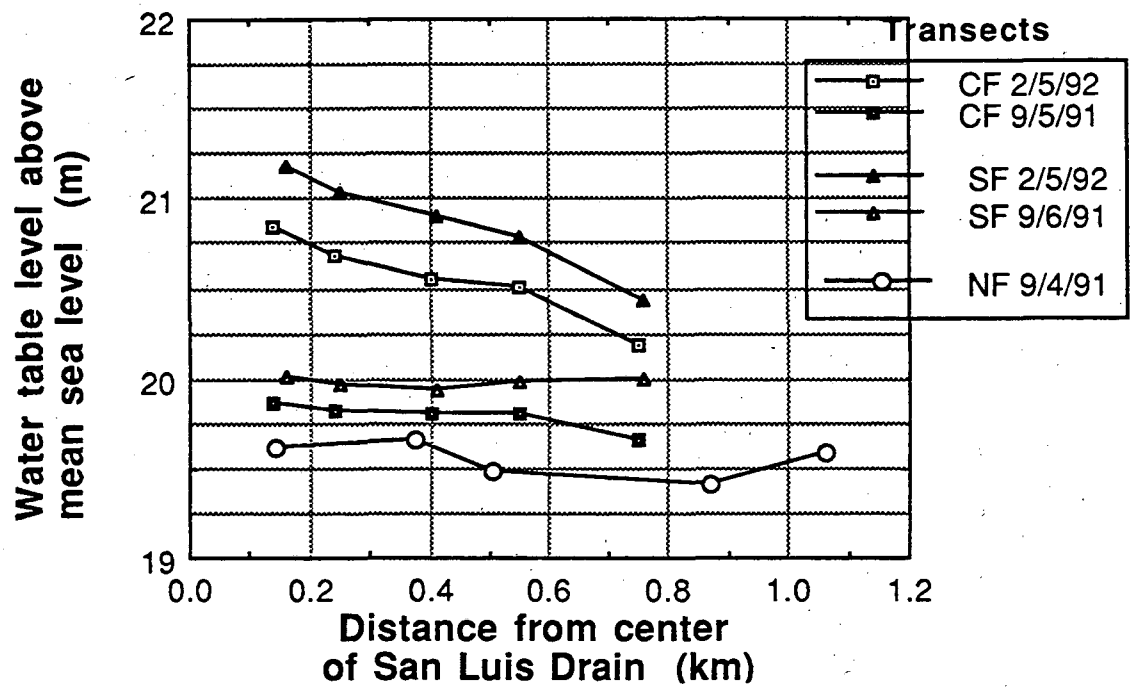

Figure 4.1b. Freitas Property water table levels (meters above mean sea level).

By establishing a basic reference data set for future soil and water sampling, time trends will be more easily understood. More detailed soil sampling may be desired in the future to alleviate the problem of spatial variability due to undulating topography, variable vegetation, and soil textural changes throughout the area of the transects.

4.1.2. Location, and Sampling Methods

4.1.2.1. Location

Placement of the three transects was designed to obtain the best overall view of off-site soil processes in reference to movement of trace element and major salts. The three transects paralleled wells that were placed off-site (southern transect: Fr 18-22, central transect: Fr24-28, northern transect: LBL 11-15). Two of the transects were placed adjacent to the southern ponds because these ponds were used more often for drainage disposal and had a greater opportunity for seepage and lateral migration. In addition the two transects in the south overlap the two ground conductivity surveys done in 1987 and 1988. Figure 4.7 shows the proximity of soil sampling points to EM transects. The origin of the third transect was placed north of the SLD, near the intersection to Ponds 9 and 11 to evaluate off-site migration to the northeast of the Reservoir.

The soil cores were named and numbered by transect. Figure 4.1 provides a map of the approximate sample locations and Table 4.1 below shows the naming sequence.

The spacing between soil samples was about 100 meters, roughly the same distance as between the wells. In some cases an extra sample point was placed in localized depressions or troughs to detect any unusual trends associated with topographic irregularities. The soil cores were placed close to the wells for comparison purposes. Soil cores were obtained out to a distance of one kilometer to sample soils with and without the influence of subsurface plume migration.

Table 4.1. Transect, point naming, and location.

Northern Transect Final (NF) location: perpendicular to P9 and P11	NF-1,NF-2.1,NF-2.2,NF-3,NF-4,NF-5, NF-6,NF-7,NF-8,NF-9,NF-10
Central Transect Final (CF) location: perpendicular to P5	CF-1,CF-2,CF-3,CF-4,CF-5,CF-6,CF-7
Southern Transect (SF) location: perpendicular to P2	SF-1,SF-2,SF-3,SF-4,SF-5,SF-6,SF-7,SF-8 SF-9

4.1.2.2. Field Methods

Soil cores were collected with the use of an hydraulically powered auger rig. Sampling depths varied form site to site because of the difficulty of obtaining a clean and thorough sample at each location. The sample tube size was 4 cm in diameter and 1.2 meters in length. Soils were sampled at the driest time of the year. Coring was extremely difficult in some cases. The gravimetric soil-moisture contents varied from approximately 2% up to 15% for the first 60 centimeters. See Figure 4.2a,b,c for profile depths and local water table level at the time of coring.

Vegetation was identified and estimated for percentage of cover at the different sampling points (see Tables 4.2.a–c.). A more detailed vegetation inventory would be useful during subsequent samplings. Topographic irregularities at sample location were also noted.

Soil samples were either sealed in plastic sampling tubes or in individual Ziplock brand freezer bags to retain moisture content. Samples were kept intact in the field unless the plastic tubing crimped, in which case the depth intervals of 0.20 m were broken up in the field.

4.1.2.3. Lab Methods

Upon arrival at the laboratory, soils were stored in humidified containers to retain the field moisture content. Soils cores were then cut into 0.20 m samples, homogenized and subsamples were oven-dried to determine soil moisture content as quickly as possible. 1:5 soil-water extracts were then

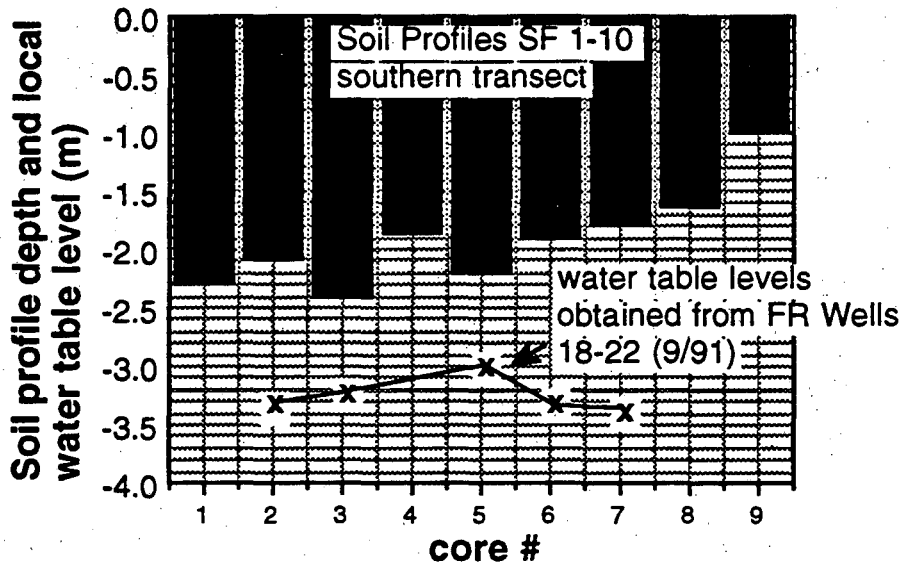

Figure 4.2a. Depth of soil sample and local water table (southern transect).

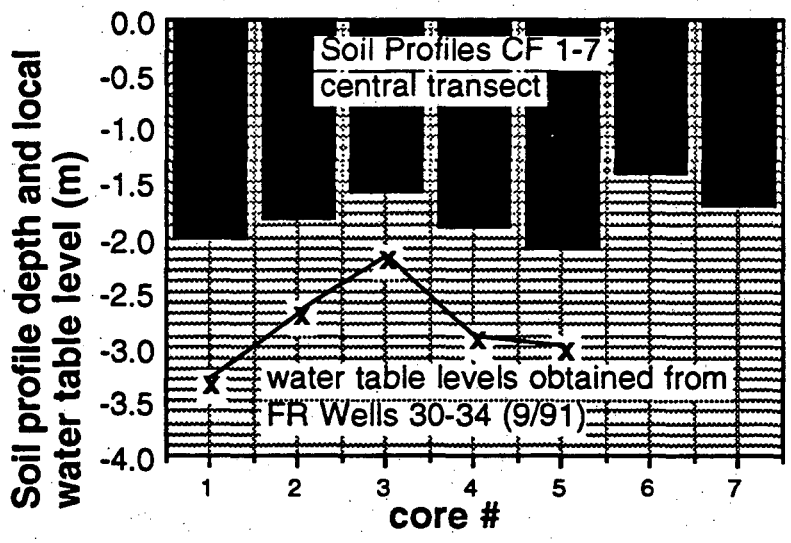

Figure 4.2b. Depth of soil sample and local water table (central transect).

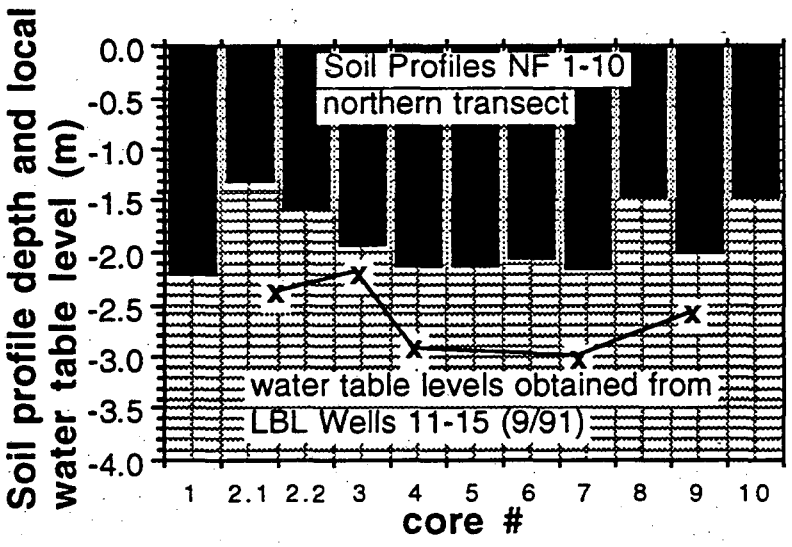

Figure 4.2c. Depth of soil sample and local water table (northern transect).

made and electrical conductivity and pH were then obtained. Samples were then analyzed for the trace elements listed in the introduction by either the inductively coupled plasma spectrometer (ICP) or atomic adsorption spectrometer (AAS). QA/QC samples were included to provide information on relative accuracy and precision of the analysis.

4.1.3. Trace Elements and Conductivity Evaluations

4.1.3.1. Electrical Conductivity Values

The data presented in Figures 4.3a–h show profiles of the 1:5 soil-water extracts EC's for each transect. Values range from less than 1 dS/m up to 8 dS/m for the majority of profiles. The northern transect is slightly higher in salinity than the other two transects. The graphs also show higher readings closer to the Reservoir in most samples than further to the east. There are several exceptions which can be attributed to the irregular topography. The last soil sample in the southern transect, SF-9, was taken in the bottom of a dry tributary to Salt Slough. There was approximately a 5 cm salt crust on the surface that contributed to the EC range of 40 to 85 dS/m. The water table was only about one meter from the surface at this point.

It should also be noted that the area around the northern transect was physically manipulated over the last several years by US Fish and Wildlife Service to improve their water delivery systems and to increase pond capacity within the seasonal wetland area (personal communication; D. Woolington USFWS, 1992). This manipulation could possibly explain the higher EC values found in NF-6 and NF-7 due to changing water table levels.

Table 4.2a. Southern transect. Plant identification and approximate cover (rough estimate).

				Sf-1	Sf-2	Sf-3	Sf-4	Sf-5	Sf-6	Sf-7	Sf-8
Chenopodiaceae (goosefoot)	*Suaeda*	*fructicosa*	sea blight,		1 plant						
Convolvulaceae	*Cressa*	*truxillensis*	alkali weed				50%				
Compositae (sunflower)	*Cotula*	*coronopifolia*	brass buttons				<1%				
	Lactuca	*serriola*	prickly lettuce				<2%				
Frankeniaceae (Frankenia)	*Frankenia*	*grandifolia*	alkali heath	sparse	<20% un	<25% un	20%	20%	20%		sparse
Leguminoseae	*Melitlotus*	*indica*			<1%						
Gramineae (Grass)	*Bromus*	*diandrus*	ripgut brome		<5%						
		mollis	soft chess		<40%		<5%	<1%	40%		
		tectorum	cheat grass		<5%						
ßπ	*Festuca*	*megalura*	foxtail fescue					<1%			
	Lolium	*multiflorum*	annual rye grass		<5%	<5%	<1%				
	Distichlis	*spicata*	saltgrass	dominant	<15% un	<5%un					abundant
	Hordeum	*jubatum*	foxtail barley					80%			
		leporinum	hare barley		<40%	<80%	<5%	10%	40%		
		stebbinsii?				<20%			10%		
Mixed grasses not identified				noted							scattered
*un = understory											

Table 4.2b. Central transect. Plant identification and approximate cover.

				CF-1	CF-2	CF-3	CF-4	Cf-5
Chenopodiaceae (goosefoot)	*Allenrolfea*	*occidentalis*	iodine bush		2 large shrubs			
	Suaeda	*fructicosa*	sea blight,		<10%			10 plants
Malvaceae (mallow)	*Sida*	*hederacea*	alkali mallow			≈3 plants		
Frankeniaceae (Frankenia)	*Frankenia*	*grandifolia*	alkali heath	10%	20%	10%	<5%	<10%
Gramineae (Grass)	*Festuca*	*megalura*	foxtail fescue	30%	20%		80%	15%
	Distichlis	*spicata*	saltgrass	5%	10%		<1%	<5%
	Hordeum	*leporinum*	hare barley	65%	40%	20%	25%	60%

Table 4.2c. Northern transect. Plant identification and approximate cover.

				NF-1	NF-2	NF-3	NF-7
Boraginaceae	*Heliotropium*	*curassavicum*	alkali heliotrope			10%	
Chenopodiaceae (goosefoot)	*Allenrolfea*	*occidentalis*	iodine bush			10%	10%
	Suaeda	*fructicosa*	sea blight, seep weed	5%			
	Bassia (Echinopsilon)	*hyssopifolia*	five-hook bassia		5%		
Convolvulaceae	*Cressa*	*truxillensis*	alkali weed			10%	
Frankeniaceae (Frankenia)	*Frankenia*	*grandifolia*	alkali heath	2%	5%		2%
Poaceae (Grass)	*Bromus*	*diandrus*	ripgut brome	5%			5%
		mollis	soft chess	5%			60%
	Distichlis	*spicata*	saltgrass		50%		
	Hordeum	*jubatum*	foxtail barley	5%	5%		
		leporinum	hare barley				
	Polypogon	*monspeliensis*	rabbitfoot grass				10%
	Sporabolus	*airoides*	alkali sacaton	60%			
Polygonaceae	*Rumes*	*crispus*	curly dock			10%	
Portulacaceae (purslane)	*Sesuvium*	*sessile*	lowland pursiane			10%	
Bare Soil			10%	30%			

No correlation was found between the groundwater EC and soil-water extract EC on the off-site samples. This is not unusual, because of the depth of the screened intervals in the monitoring wells and the depth of the soil samples only overlap at the very bottom of the soil sample.

4.1.3.2. Selenium

The levels of both soluble selenate and selenite shown in following graphs have concentrations that are just above the detection limit for selenium and most of them below the method limit of quantification (MLQ). The very low concentrations of water-extractable selenium and the lack of clear spatial patterns indicates that, as previously predicted, very little selenium was transported by groundwater from Kesterson to the adjacent properties. In addition, the low concentration suggests that transport of wind-blown particulates was not a major mechanism in selenium transport.

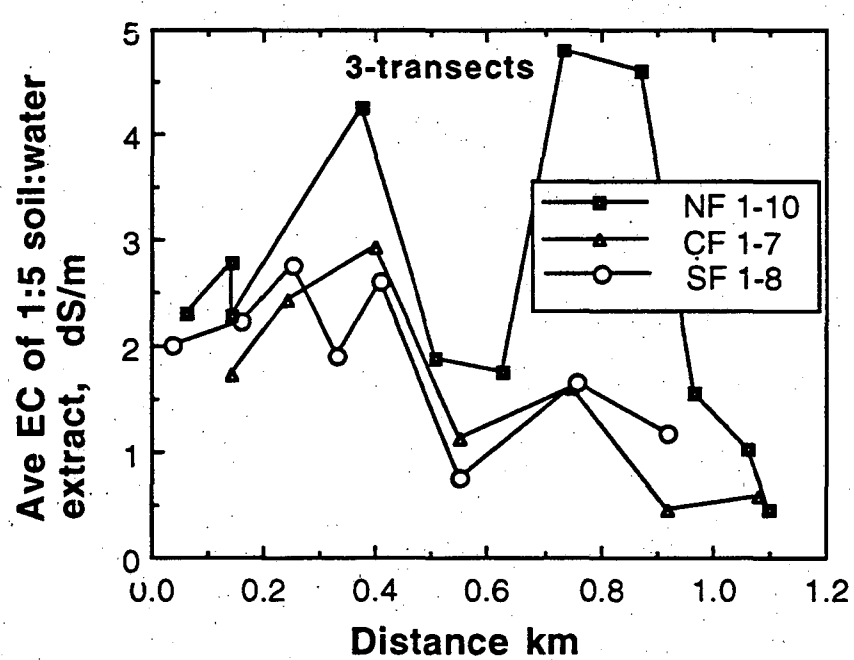

Figure 4.3a. Average electrical conductivities by transect from San Luis Drain outward along transects.

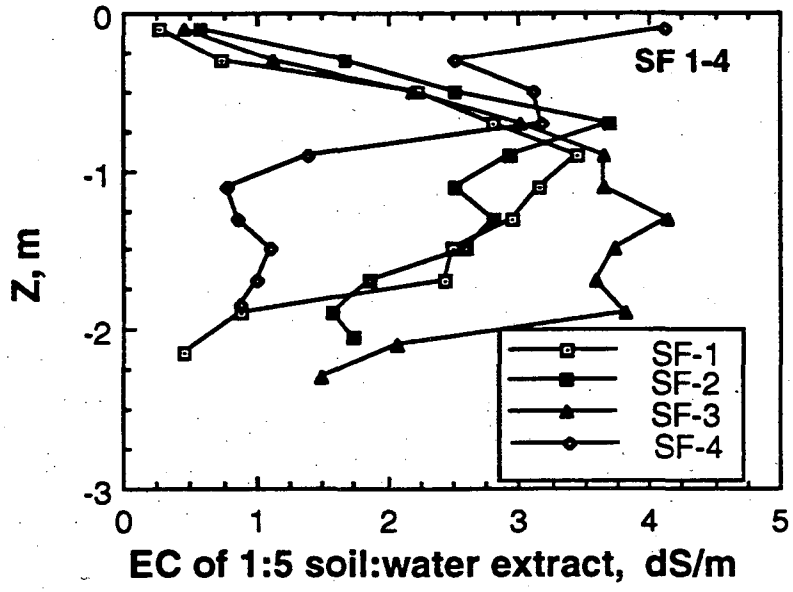

Figure 4.3b. Electrical conductivities for soil samples 1-4 (southern transect).

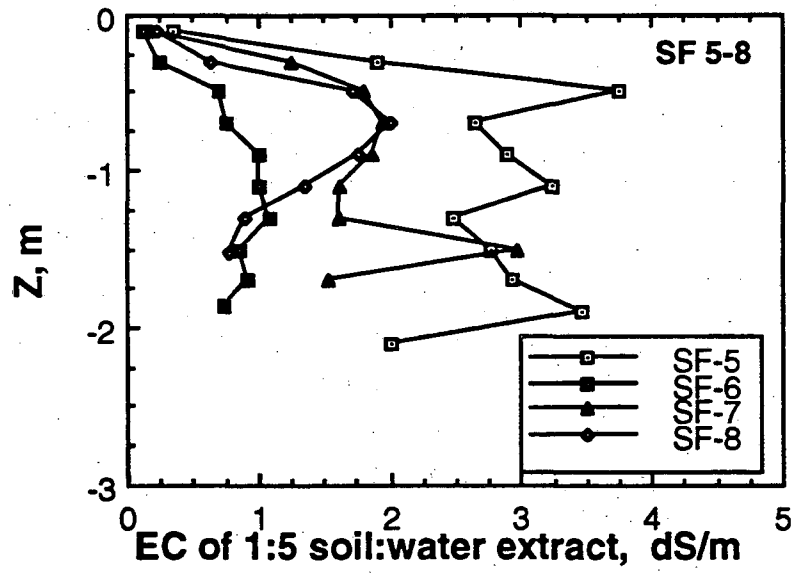

Figure 4.3c. Electrical conductivities for soil samples 5–8(southern transect).

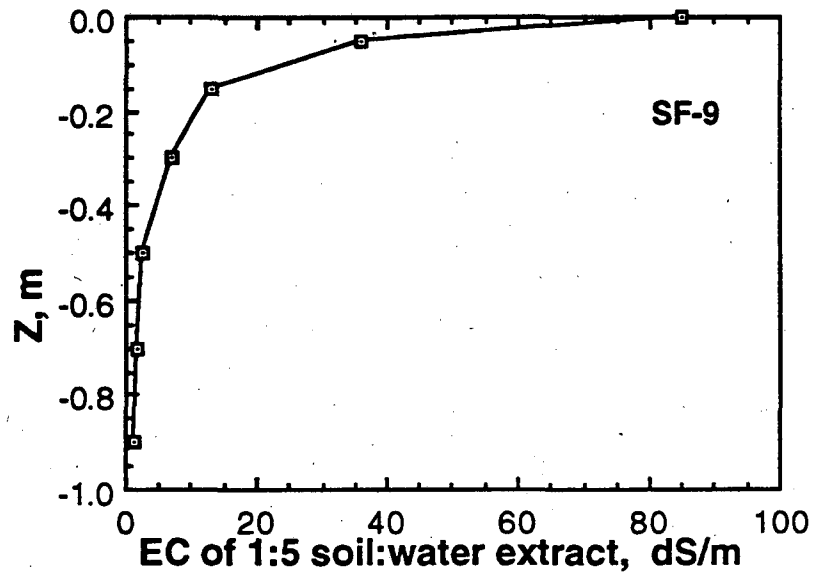

Figure 4.3d. Electrical conductivities for soil sample 9 (southern transect).

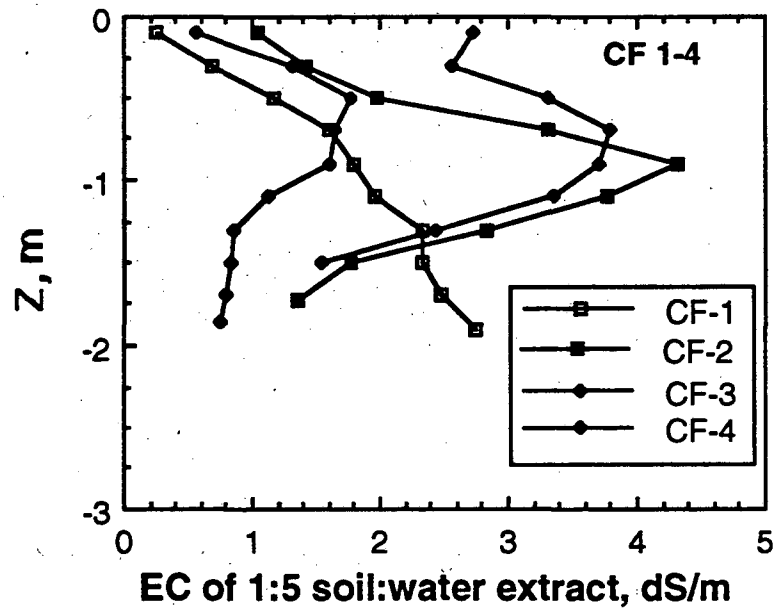

Figure 4.3e. Electrical conductivities for soil samples 1–4 central transect).

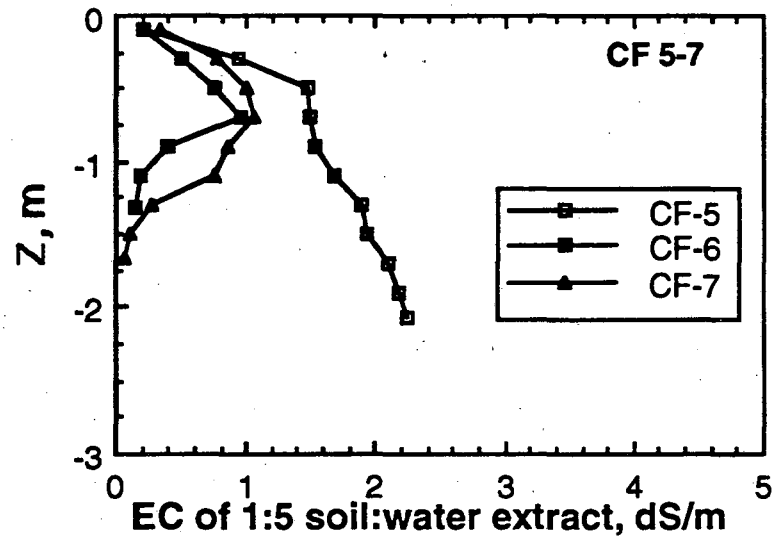

Figure 4.3f. Electrical conductivities for soil samples 5–8(central transect).

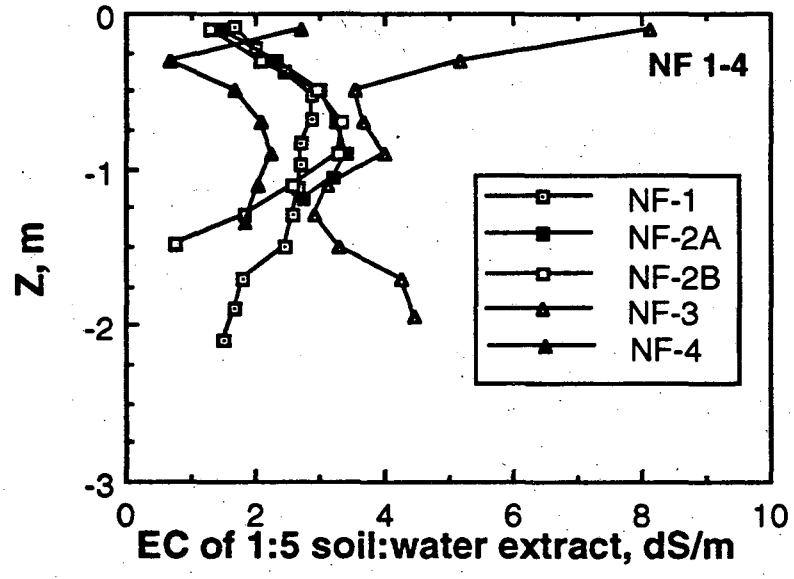

Figure 4.3g. Electrical conductivities for soil samples 1–4 (northern transect).

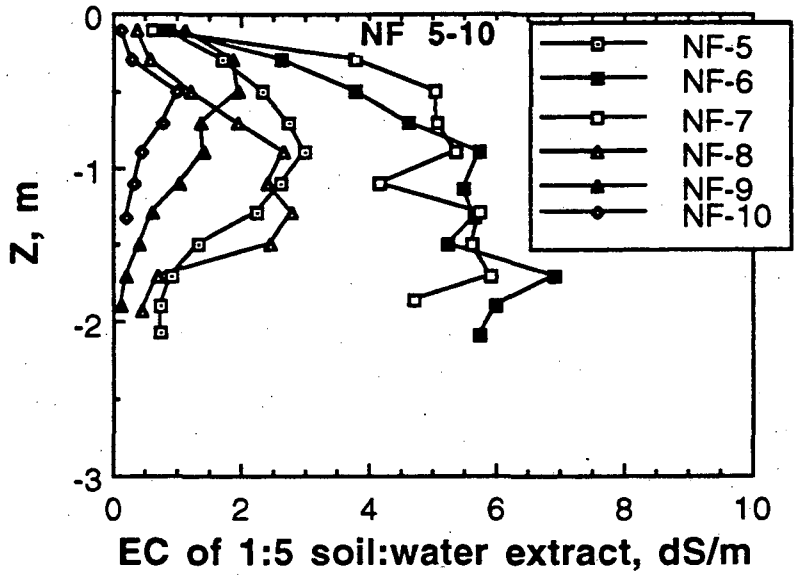

Figure 4.3h. Electrical conductivities for soil samples 5–10 (northern transect).

4.1.3.3. Boron

As predicted from previous reports, boron is the most mobile of all the trace elements transported to Kesterson via the San Luis Drain. As shown by the line graph of the three transects (Figure 4.5a–h) a definite trend can be seen with the transects going west to east. The moving front of the plume is approximately 300 plus meters from the Reservoir, which is consistent with previous estimates by Goldstein et al. (1989) and from the groundwater samples taken in 1990 and 1992 by LBL. Concentrations of boron drop to background levels for this area of the San Joaquin Valley at distances of greater than 300 m from the Reservoir. The levels of boron even though elevated are not unusual for this part of the San Joaquin Valley.

4.1.3.4. Molybdenum and Arsenic

All the samples were analyzed for water-extractable molybdenum and one transect was analyzed for water-extractable arsenic to detect unusual quantities or trends. Almost all samples were below the method limit of quantification for molybdenum on the ICP. The quantities shown in the following graphs are not unusual for arsenic concentrations in this part of the San Joaquin Valley. The variations seen between soil samples are correlated with textural differences in the soil. No systematic trends in the arsenic concentrations are apparent from the available data, suggesting that Kesterson Reservoir has not influenced arsenic concentrations in the area of study.

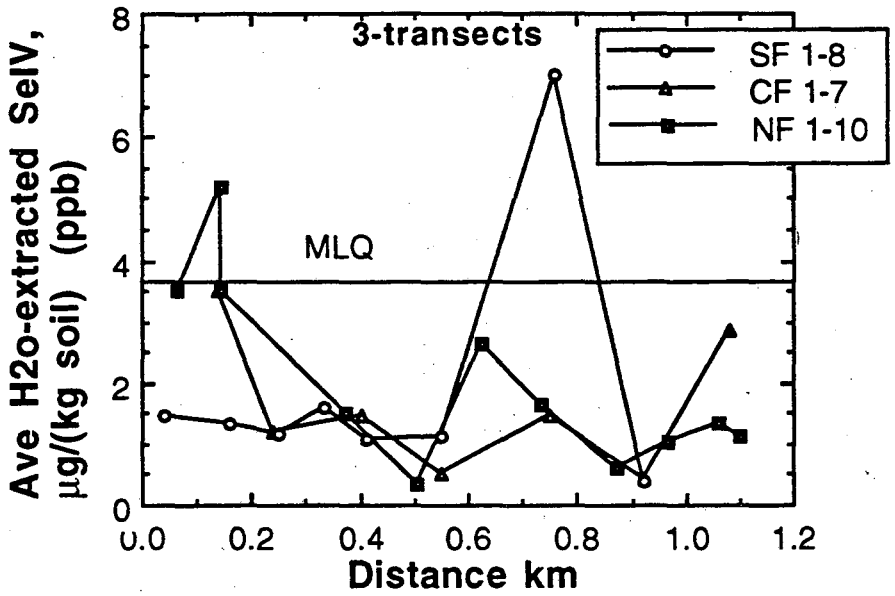

Figure 4.4a. Average water-extractable selenite concentrations (ppb) by transect from San Luis Drain outward along transect.

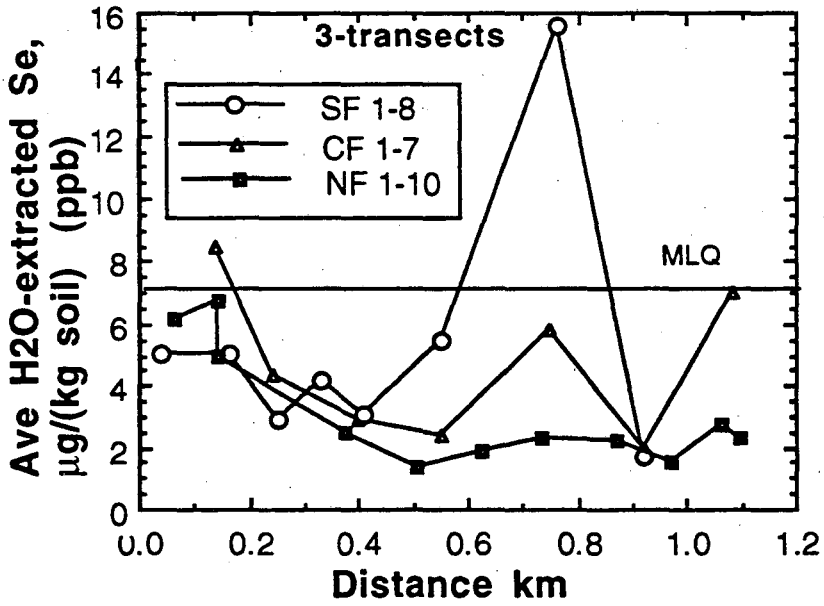

Figure 4.4b. Average water-extractable selenium concentrations (ppb) by transect from San Luis Drain outward along transect.

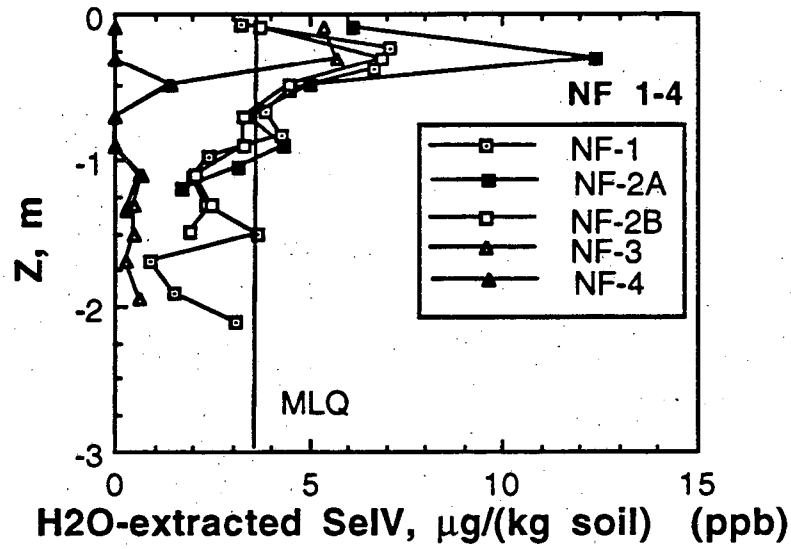

Figure 4.4c. Water-extractable selenite concentrations (ppb) soil samples 1–4 (southern transect).

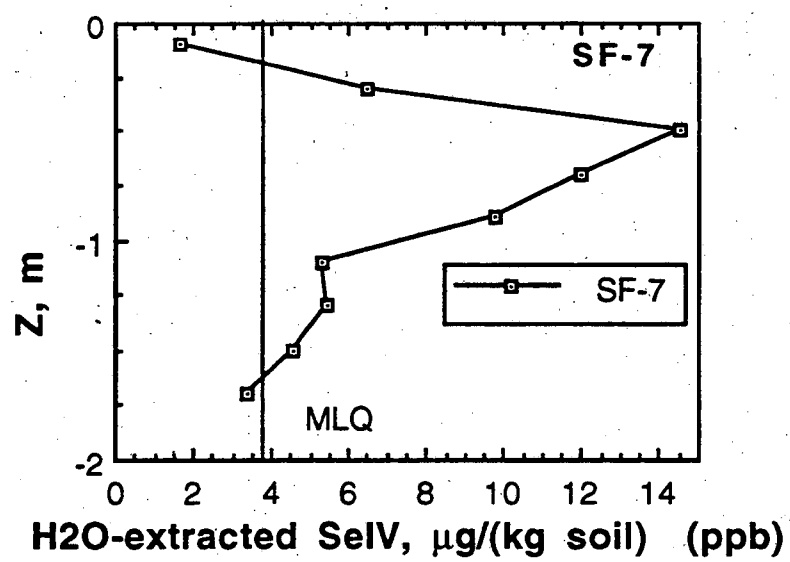

Figure 4.4d. Water-extractable selenite concentrations (ppb) soil sample 7 (southern transect).

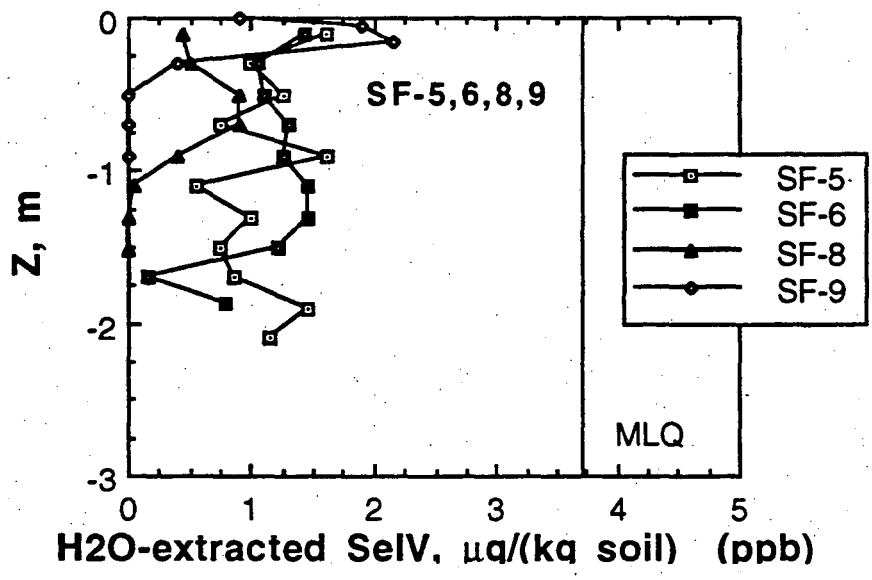

Figure 4.4e. Water-extractable selenite concentrations (ppb) soil samples 5–9 (southern transect).

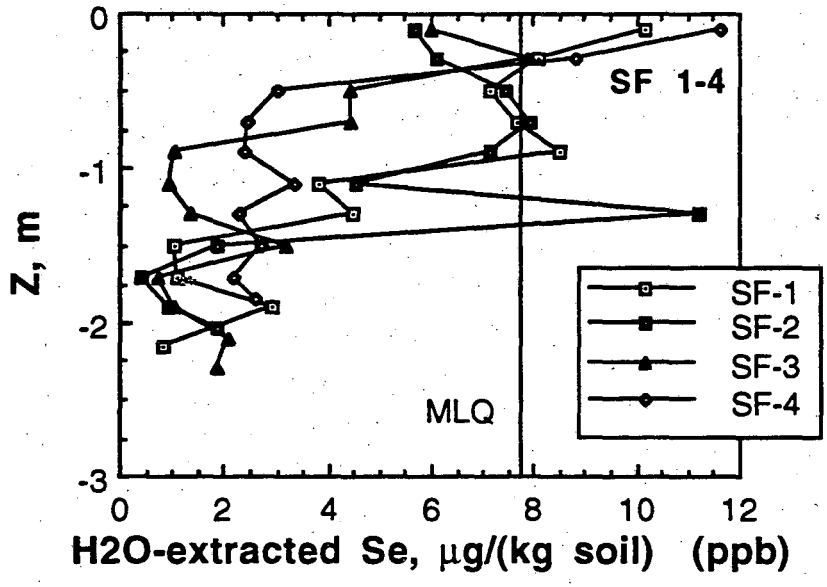

Figure 4.4f. Water-extractable selenium concentrations (ppb) soil samples 1–4 (southern transect).

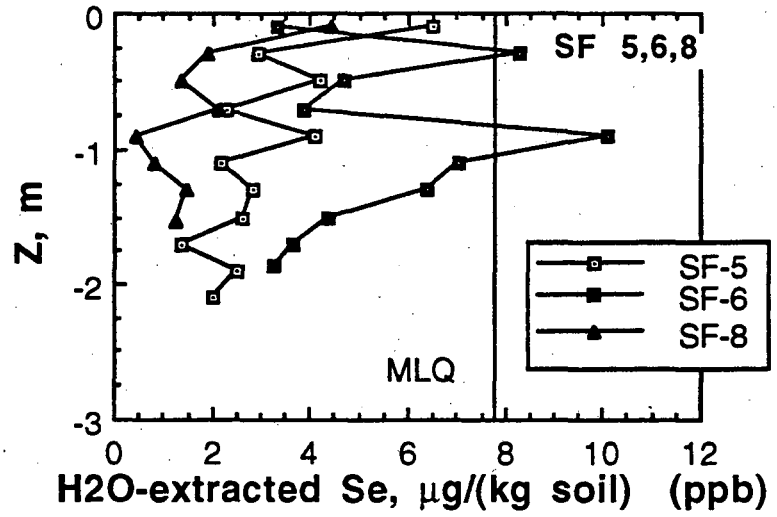

Figure 4.4g. Water-extractable selenium concentrations (ppb) soil samples 5–8 (southern transect).

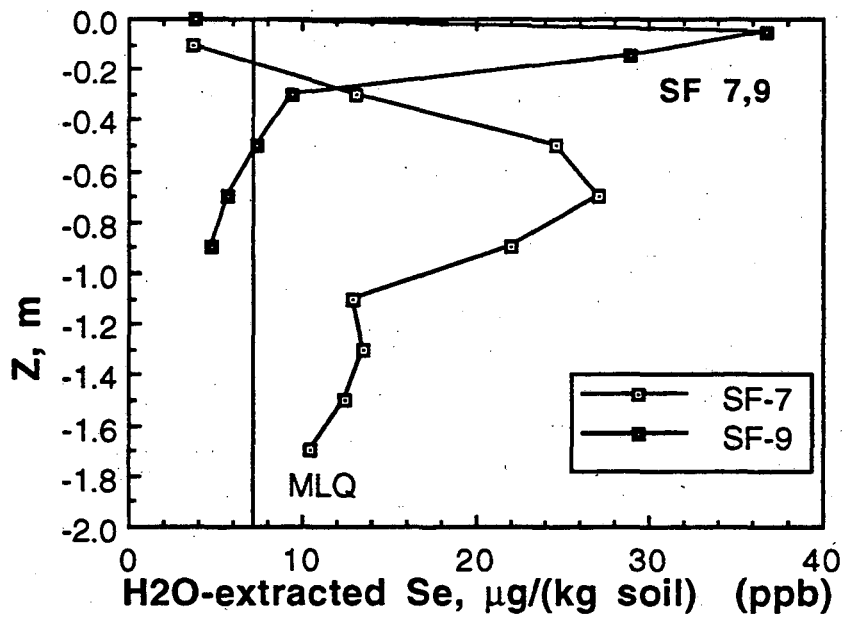

Figure 4.4h. Water-extractable selenium concentrations (ppb) soil samples 7 and 9 (southern transect).

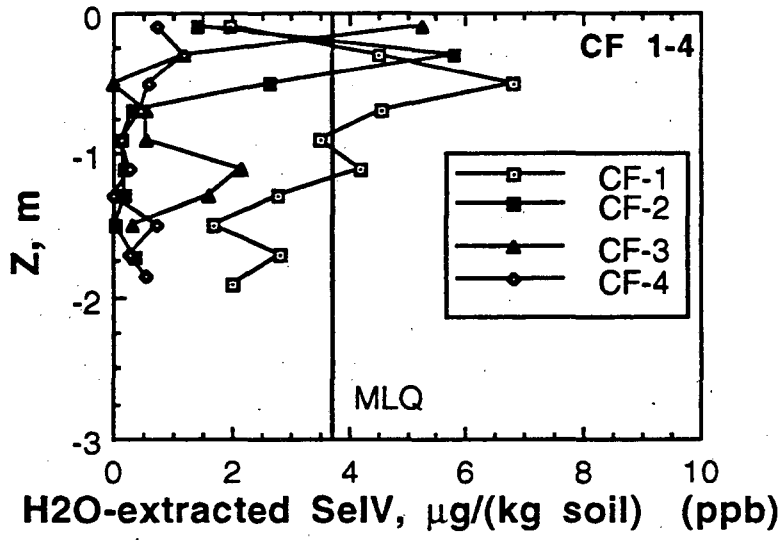

Figure 4.4i. Water-extractable selenite concentrations (ppb) soil samples 1–4 (central transect).

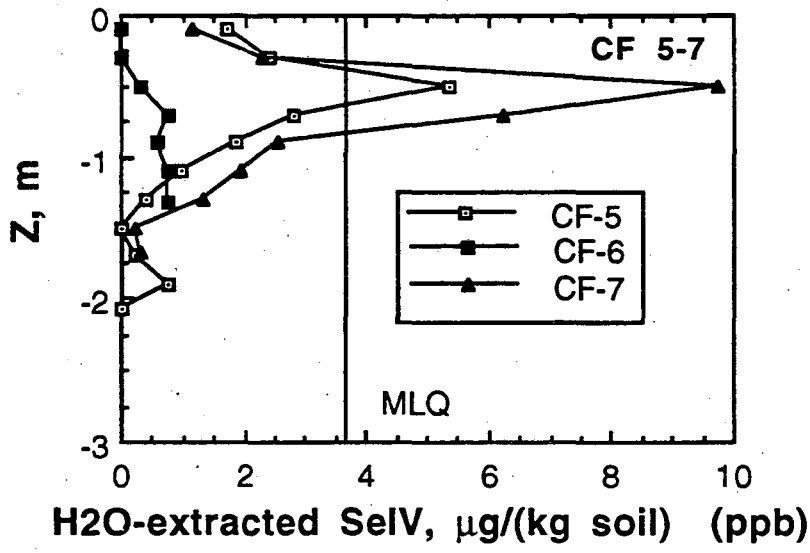

Figure 4.4j. Water-extractable selenite concentrations (ppb) soil samples 5–7 (central transect).

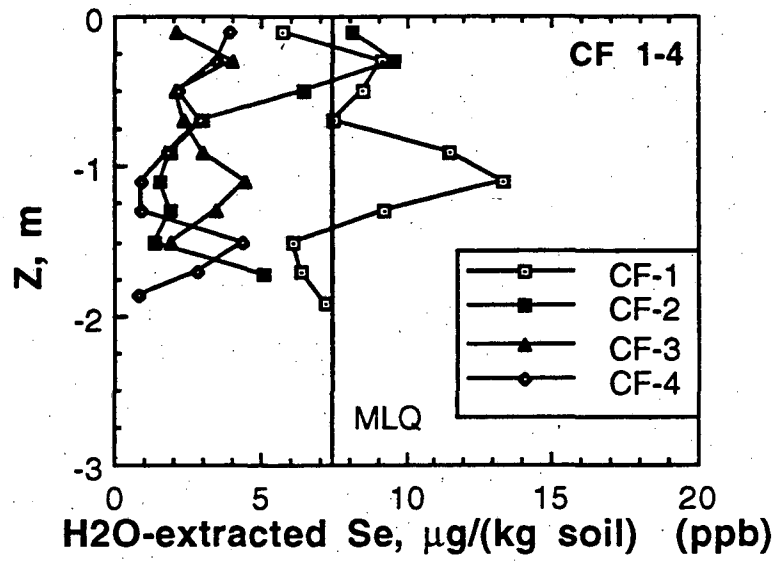

Figure 4.4k. Water-extractable selenium concentrations (ppb) soil samples 1–4 (central transect).

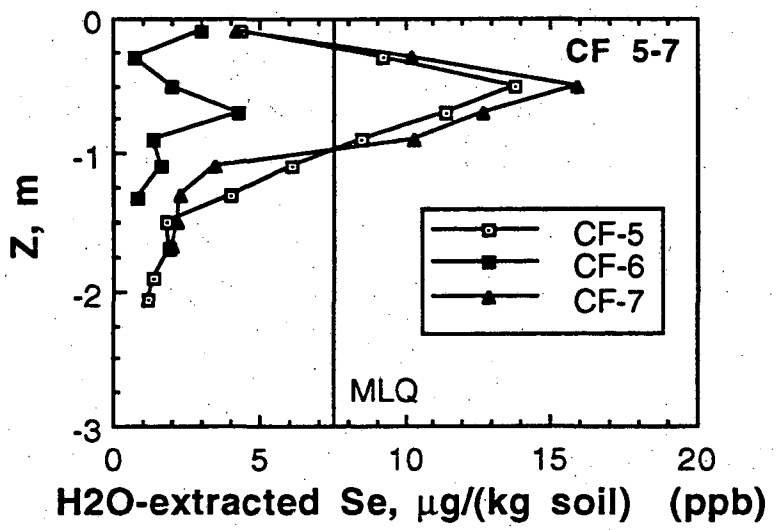

Figure 4.4*l*. Water-extractable selenium concentrations (ppb) soil samples 5–7 (central transect).

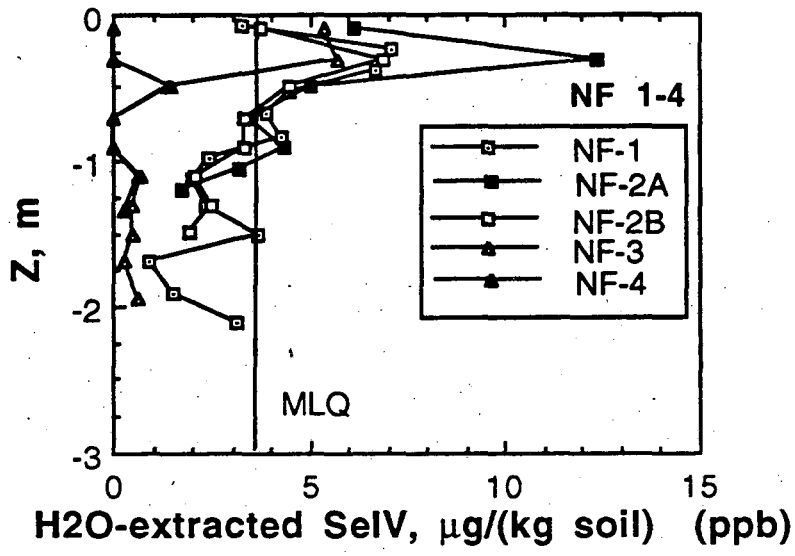

Figure 4.4m. Water-extractable selenite concentrations (ppb) soil samples 1–4 (northern transect).

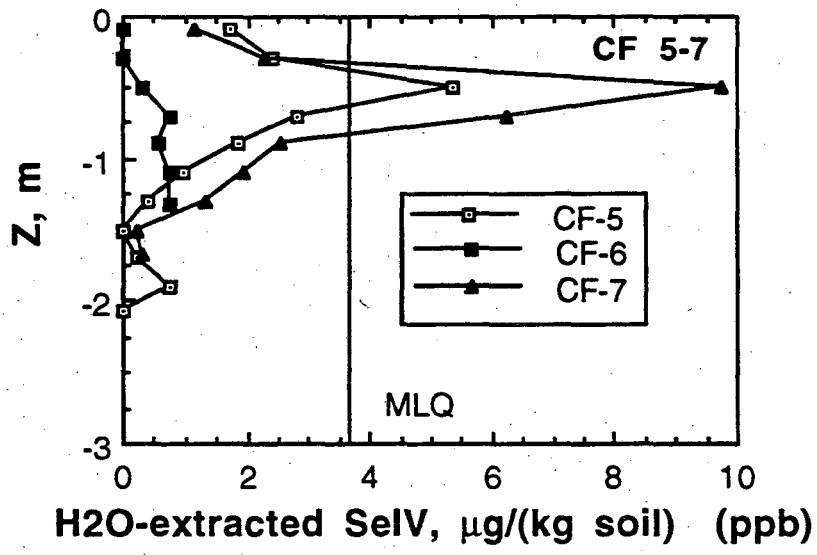

Figure 4.4n. Water-extractable selenite concentrations (ppb) soil samples 5–10 (northern transect).

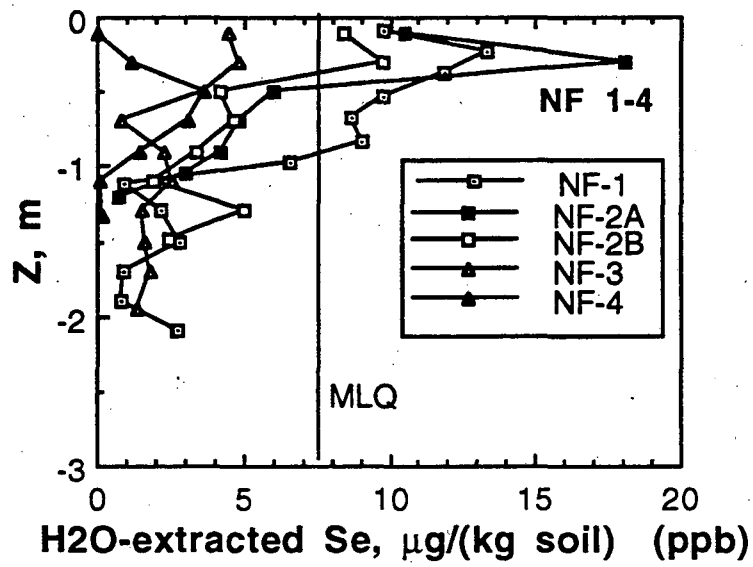

Figure 4.4o. Water-extractable selenium concentrations (ppb) soil samples 1–4 (northern transect).

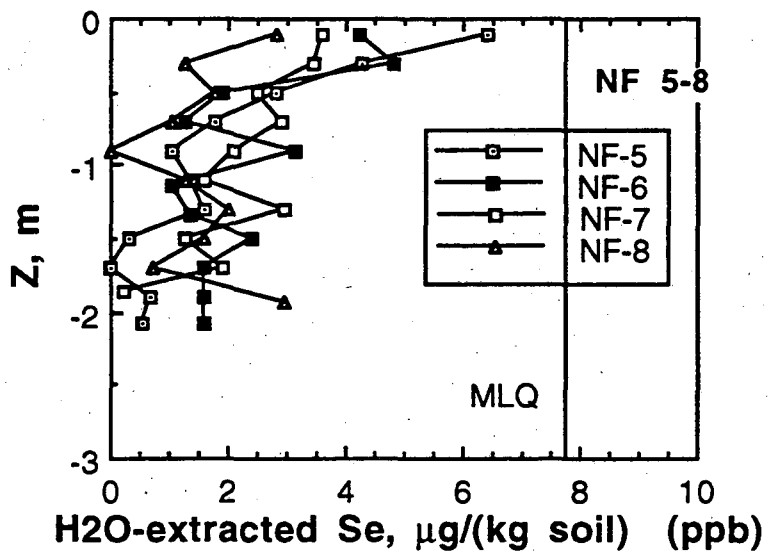

Figure 4.4p. Water-extractable selenium concentrations (ppb) soil samples 5–8 (northern transect).

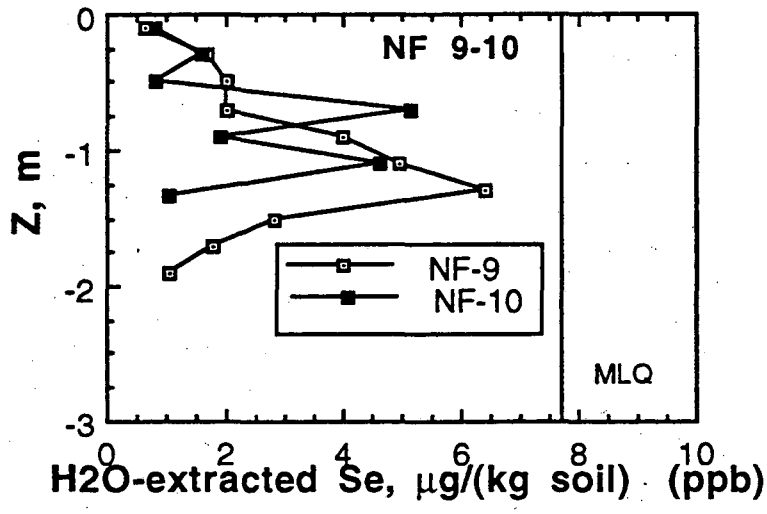

Figure 4.4q. Water-extractable selenium concentrations (ppb) soil samples 9 and 10 (northern transect).

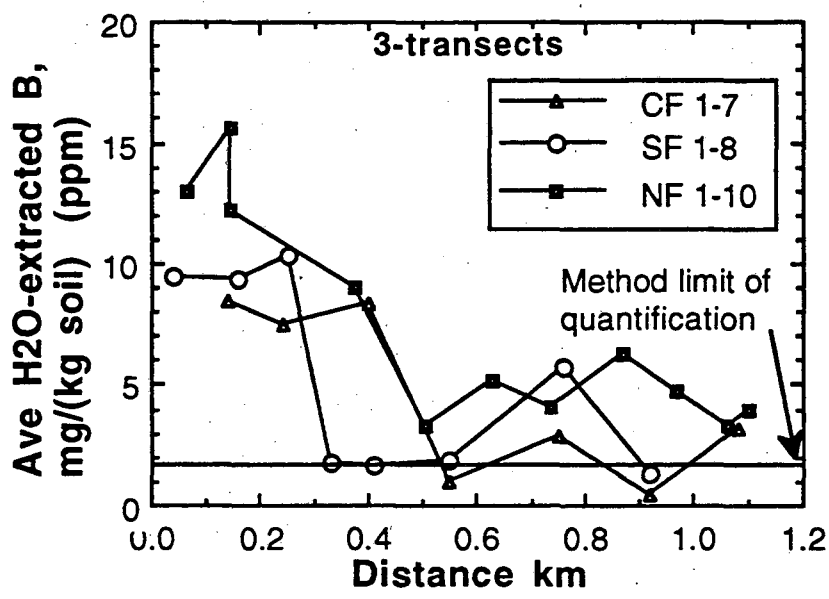

Figure 4.5a. Average water-extractable boron concentrations (ppm) by transect from San Luis Drain outward along transect.

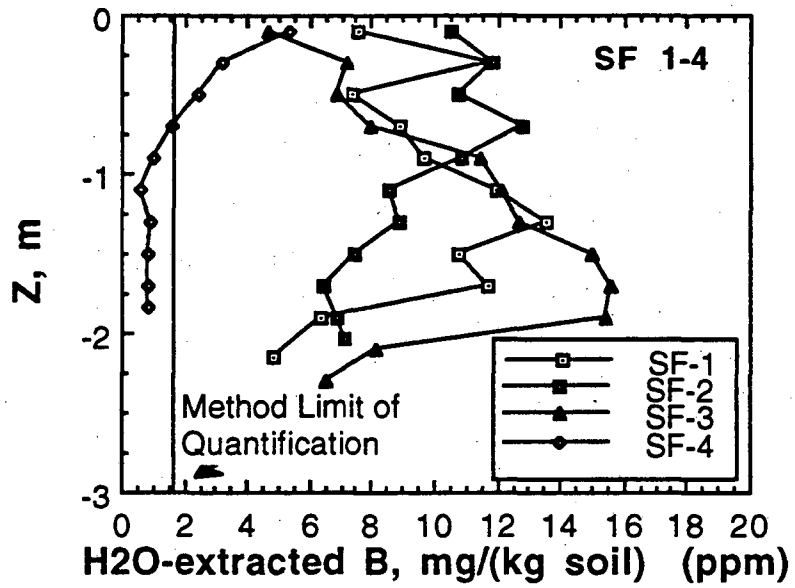

Figure 4.5b. Water-extractable boron concentrations (ppm) cores 1–4 (southern transect).

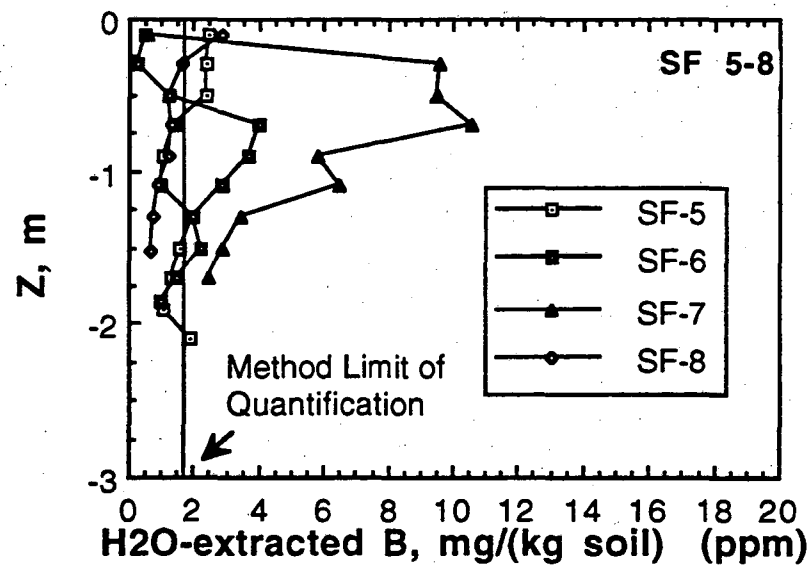

Figure 4.5c. Water-extractable boron concentrations (ppm) cores 1–4 (southern transect).

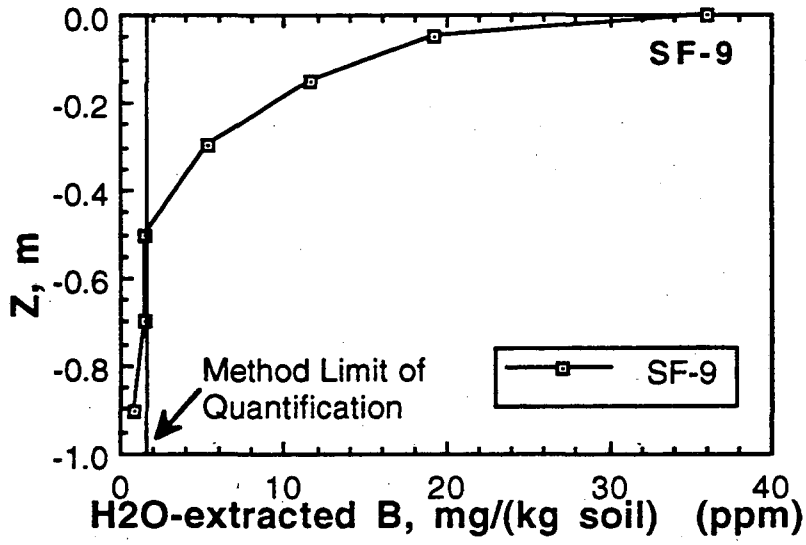

Figure 4.5d. Water-extractable boron concentrations (ppm) core 9 (southern transect).

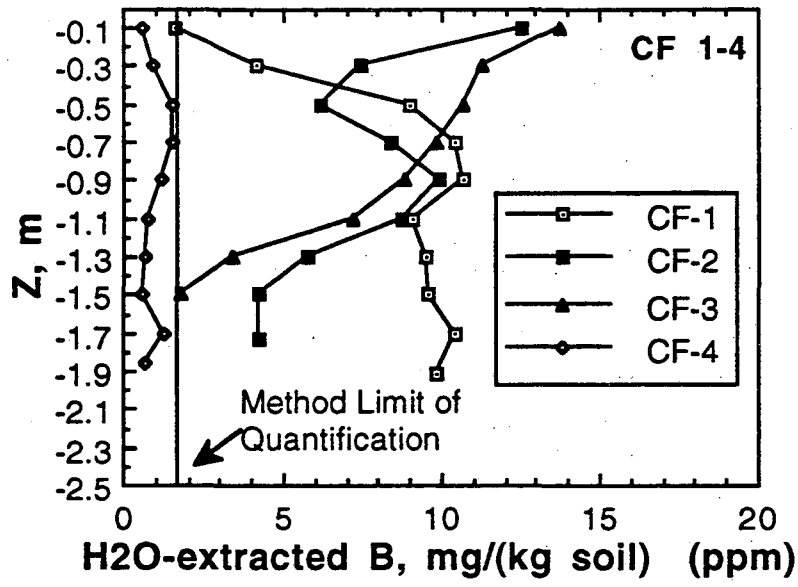

Figure 4.5e. Water-extractable boron concentrations (ppm) cores 1–4 (central transect).

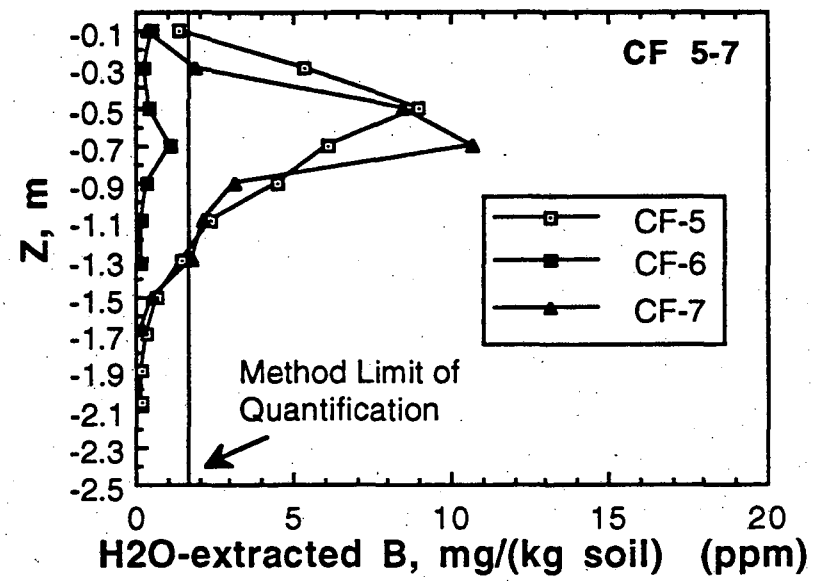

Figure 4.5f. Water-extractable boron concentrations (ppm) cores 5–7 (southern transect).

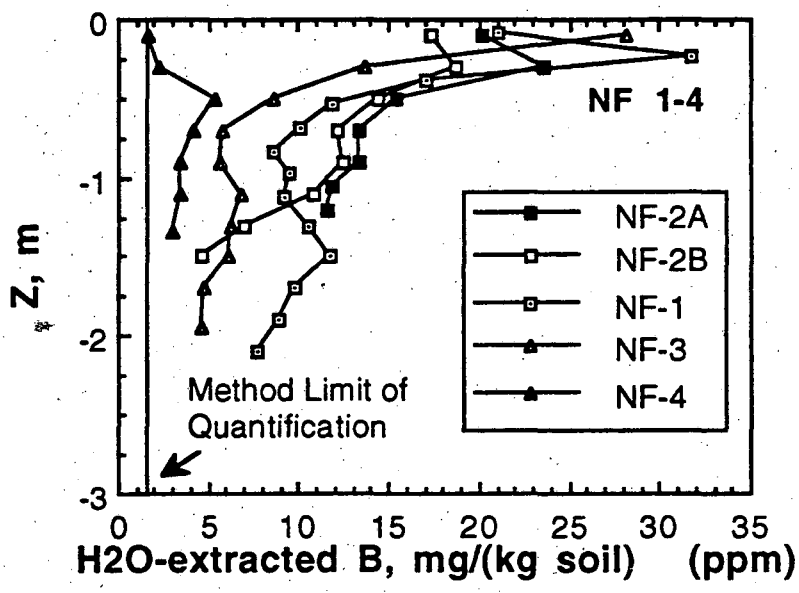

Figure 4.5g. Water-extractable boron concentrations (ppm) cores 1–4 (northern transect).

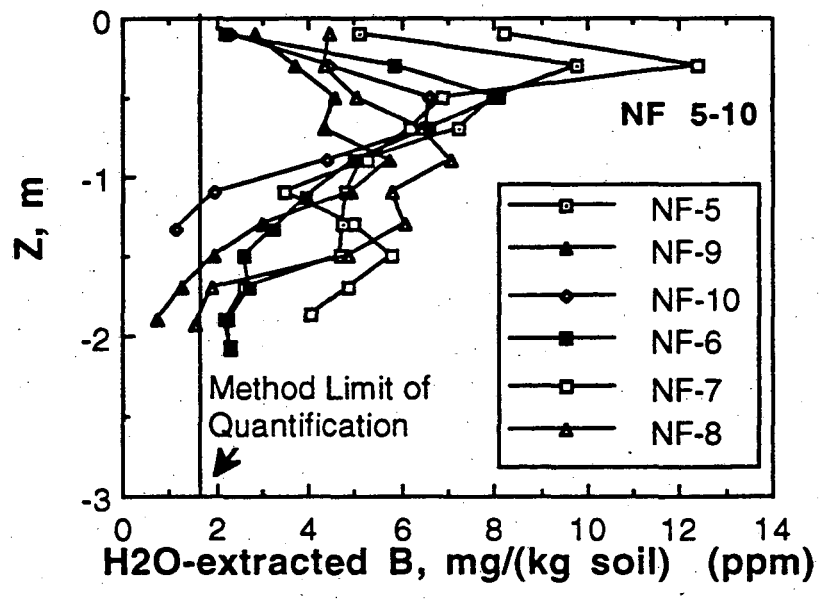

Figure 4.5h. Water-extractable boron concentrations (ppm) cores 5–10 (northern transect).

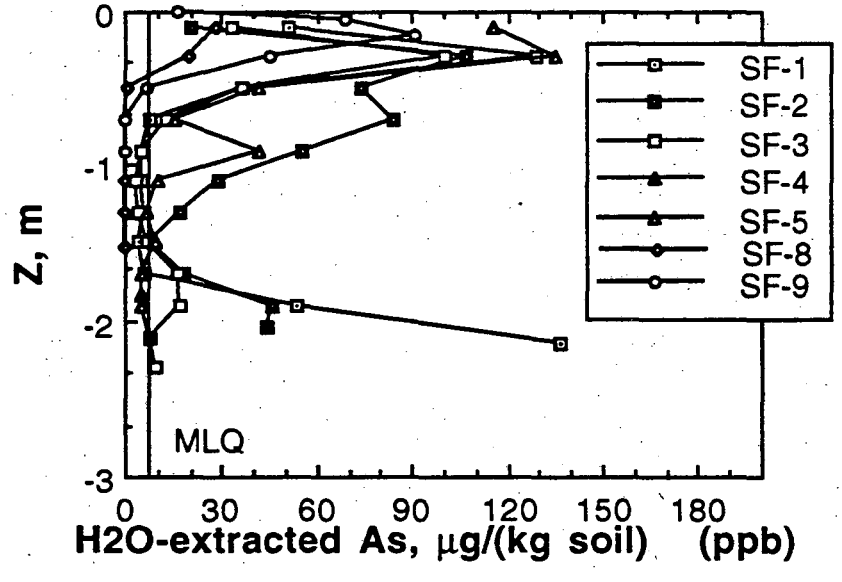

Figure 4.6a. Water-extractable arsenic concentrations (ppb) cores 1, 2, 3, 4, 5, 8, and 9 (southern transect).

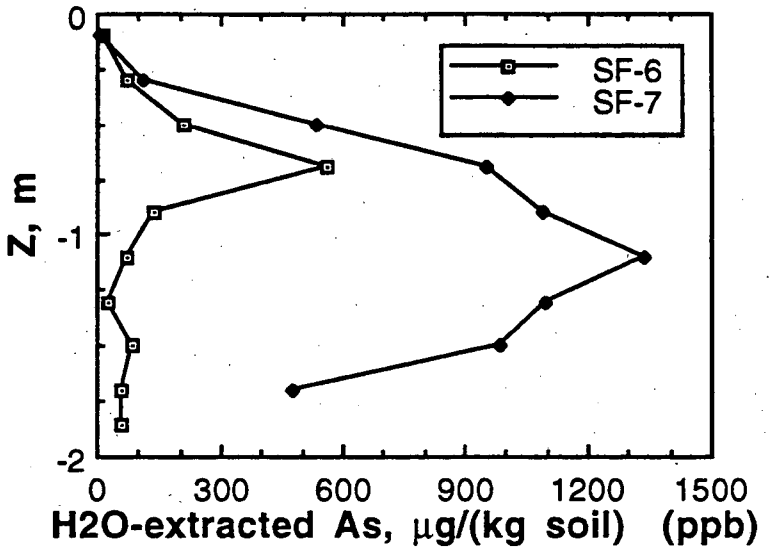

Figure 4.6b. Water-extractable arsenic concentrations (ppb) cores 6 and 7 (southern transect).

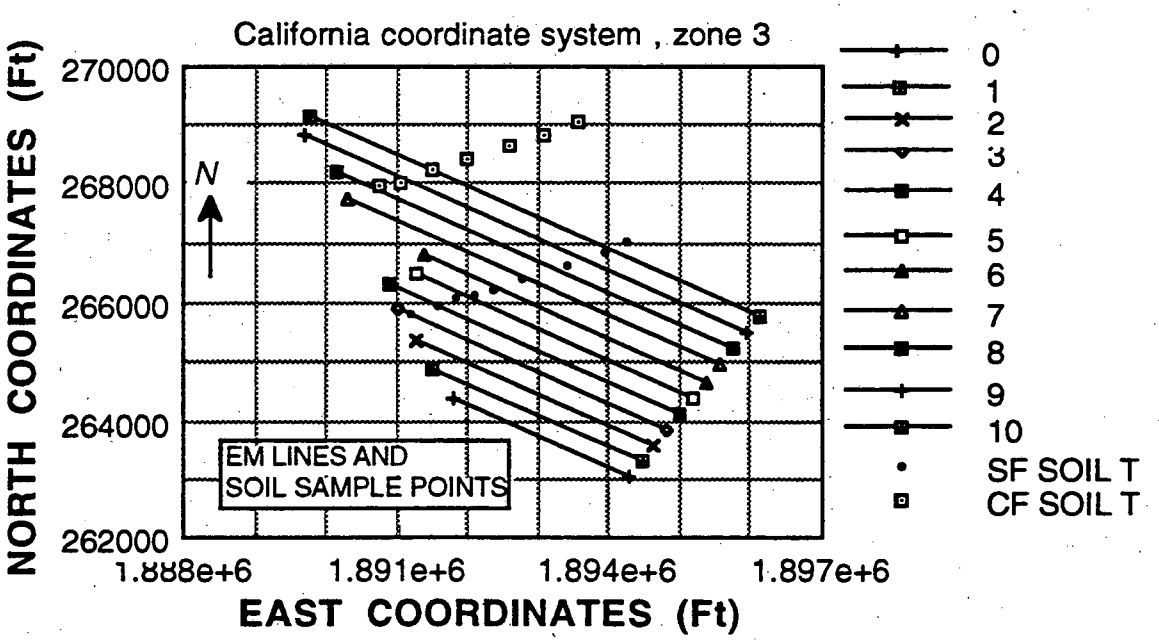

Figure 4.7. Location of soil sample points, (southern and central transects), and EM survey transects.

4.1.4. EC Comparison to 1988,1989–EM Survey

No correlation on a small scale was found between the EM survey data collected in 1989 and the average EC of the soil cores on the southern and central transects (Goldstein et al., 1989). Figure 4.7 shows the proximity of each of the soil sampling points to the EM transect lines. The lack of correlation could most likely be attributed to the spatial distance of the soil cores to the individual nodal points and to the very large differences in measurement volumes. The inaccuracy of actual locations of soil cores and nodal points could also add to the lack of correlation in data. To obtain a better correlation, many more sample points would be needed to account for the spatial variability. Even though there is no correlation between the two different data sets, the general trends of the two types of analyses are the same. The higher EC readings for the 1:5 soil water extracts are similar to the EM readings at approximately the same distances away from the San Luis Drain.

4.1.5. Conclusion

The data described here provide a baseline for future monitoring of salt and trace element composition of these lands. Concentrations of trace elements observed on the former Freitas Ranch were only slightly above the background concentrations of the area, hence they should not pose a significant risk to the wildlife.

The US Fish and Wildlife Service management plan for the Freitas Property calls for installation of 12 different water control structures and production wells within the property. A portion of the property will be made into permanent wetland with adjacent seasonal wetlands (D. Woolington, 1992, personal communication). Both surface and ground water will be used to flood these new wetlands. Historic groundwater flow patterns will change in response to these new management practices. Annual sampling of the wells will provide information on migration of salts and trace elements in response to these changes. Vegetation will also change as a result of new surface water management practices and the cessation of grazing (from when USFWS acquired the land spring 1991). The rough inventory of vegetation taken during the soil sampling may serve as a useful template to future vegetation sampling.

We recommend monitoring the area biannually to detect significant changes in the soil, vegetation, and ground and surface water salt loading and trace element concentrations.

4.2. Groundwater Quality on the Freitas Ranch

Sally Benson
Earth Sciences Division
Lawrence Berkeley Laboratory

Forty shallow wells were installed in the fall of 1990 to determine the extent of migration of salt, selenium and other trace elements through the groundwater system from Kesterson Reservoir to the adjacent Freitas Ranch. The majority of the wells were drilled to a depth of 7.87 m (25 feet) and screened over the bottom 1.52 m (5 feet). Well locations are shown in Figure 4.8. Twenty-nine of the wells were drilled along 6 transects perpendicular to the San Luis Drain (SLD). Along the transects, wells were drilled at distances of 100, 200, 300, 450 and 700 m from the SLD. Five additional wells were placed midway between these transects at a distance of 100 m from the SLD. Six wells drilled to a depth of 18.3 m (60 feet) were installed along the 6 transects at a distance of 100 m from the SLD. The bottom-most 1.52 m (5 feet) of these wells were screened.

Interpretations of both temporal and spatial trends in groundwater quality on the Freitas Ranch are provided below.

4.2.1. Groundwater Sampling and Chemical Analyses Program

Since these wells were drilled they have been sampled twice; first in December 1990 and again in May 1992. Groundwater samples were collected after pumping a minimum of three well volumes unless the well went dry during purging. In this case the well was sampled after one well volume was purged. Three samples were collected from each well during the first sampling period. Of these three samples, one was filtered, one was filtered and acidified with nitric acid, and one left unaltered. No significant differences were detected in the total selenium concentrations in these samples. Therefore, for the second sampling only two samples were collected and both were filtered in the laboratory prior to chemical analysis.

Total selenium and selenite concentrations were determined using atomic absorption spectroscopy (AAS). Methods for these analyses have been described in the LBL Quality Assurance Plan (1990). Boron concentrations were measured using Inductively Coupled Plasma (ICP). Quality assurance statistics for these and other chemical analyses are provided in the 1991-1992 LBL Kesterson Annual Report. Electrical conductivity was measured for the first sampling using a YSI field conductivity meter. A YSI model 35 meter was used to measure electrical conductivity during the second sampling period. Measured concentrations of total selenium, selenite, boron and electrical conductivities are provided in Table 4.3.

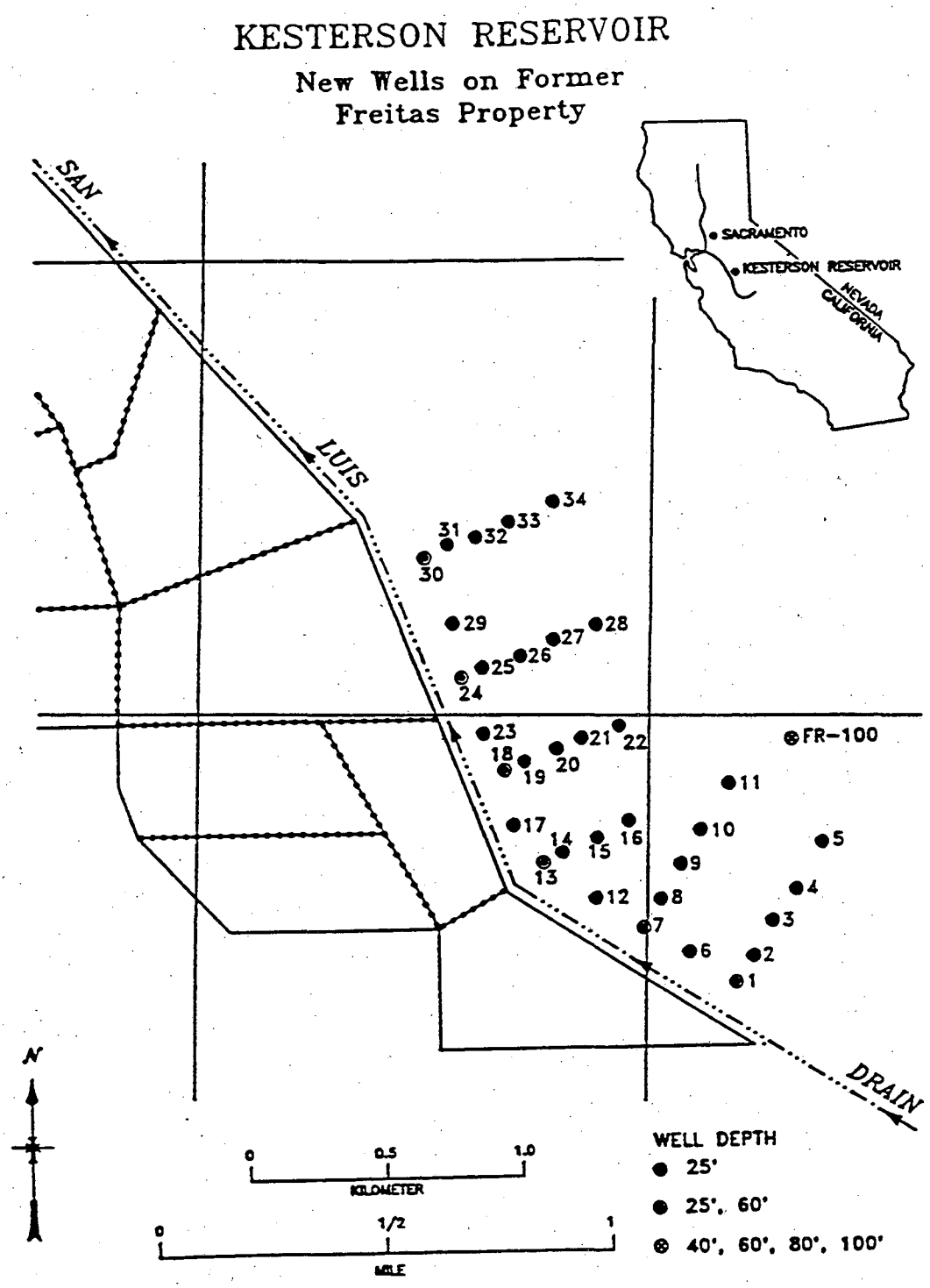

Figure 4.8. Map showing the location of monitoring ells on the Freitas Ranch.

4.2.2. Spatial and Temporal Trends in Groundwater Quality

Concentrations of boron and the electrical conductivity can be used to map migration of the agricultural drainage water discharged into Kesterson Reservoir. Electrical conductivity of drainage water typically ranged from 10 to 20 dS/m and boron concentrations averaged about 15 mg/L. Native groundwater in the area has electrical conductivity ranging from 5 to 10 dS/m and boron concentrations of less than 2 mg/L. Analyses of groundwater directly under the Kesterson ponds demonstrated that both boron and the major anions (chloride and sulfate) migrate without chemically interacting with the aquifer sediments. As such, both the electrical conductivity of the solution (a function of the major salts) and boron concentration can be used to track migration of agricultural drainage water under the former Freitas Ranch. However, because of the larger contrast between boron concentrations in drainage water and native groundwater, boron is a more sensitive indicator of drainage water migration.

Graphs showing the electrical conductivity and boron concentrations of groundwater from the 34 shallow wells are provided in Figures 4.9 through 4.12. Data are graphed along the 6 transects shown in Figure 4.8. Both the electrical conductivity and boron concentration decrease with distance from the SLD, demonstrating the extent of drainage water migration. Along all but the southernmost transect, concentrations return to background values at a distance of less then 450 m from the SLD. Along the southernmost transect, concentrations drop to background levels somewhere between 450 and 700 m from the SLD.

Figures 4.9 through 4.12 provide both 1990 and 1992 sampling data. Visual comparison illustrates that the concentrations of boron and electrical conductivities are very similar both years. To emphasize the difference between the two years, a graph of the ratio between the boron concentration at each well in 1992 and 1990 is shown in Figure 4.13. In locations where the boron concentrations have not changed, the ratio is equal to one. Where boron concentrations have increased, the ratio is greater than one and where they have decreased, the ratio is less than one. Although most ratios are close to one, 3 of the 5 wells indicate an increase in this ratio at a distance of 450 m from the SLD. Whereas this does not provide conclusive evidence for migration of the plume towards the northeast, this trend is consistent with slow migration of the leading edge of the drainage water plume.

Data from the 6 deeper wells (18.3 m deep) are provided in the bottom of Table 4.3. Electrical conductivities range from 5.9 to 15.2 dS/m and boron concentrations range from 1.2 to 17.8 mg/L. The wide range of values indicate that the depth to which drain water has migrated varies along the perimeter of the Reservoir. Boron concentrations in the range of 14.0 to 17.8 mg/L indicate the presence of undiluted drainage water at depths of 18.3 m in the vicinity of FR-13(A and B) and FR-18(A and B). Values ranging from 5.6 to 9.7 mg/L indicate the presence of mixture of drainage water and native groundwater. At FR-7(A and B), drainage water migration

Table 4.3. Tabulated values of electrical conductivity, selenite (SE(IV)), total selenium, and boron concentrations for wells on the Freitas Ranch.

Well	Depth (m)	EC (dS/m)	EC (dS/m)	Se(IV) (µg/L)	Se(IV) (µg/L)	Se Total (µg/L)	Se Total (µg/L)	B (mg/L)	B (mg/L)
Date		12/7/90	5/26/92	12/7/90	5/26/92	12/7/90	5/26/92	12/7/90	5/26/92
FR-1-B	7.87	13.6	10.7	0.7	0.8	1.0	1.7	16.9	14.8
FR-2	7.87	11.0	12.8	0.5	0.7	1.0	0.7	15.2	16.0
FR-3	7.87	13.8	12.7	0.5	0.5	0.7	1.1	13.5	15.3
FR-4	7.87	11.6	10.5	0.7	0.4	0.5	0.5	9.3	10.5
FR-5	7.87	4.6	4.5	0.6	0.5	LD	0.6	0.9	1.0
FR-6	7.87	14.5	11.8	0.5	0.5	1.8	1.0	17.6	13.0
FR-7-B	7.87	14.2	14.6	0.5	0.7	1.1	1.2	14.0	16.3
FR-8	7.87	6.5	5.9	0.7	0.4	0.1	0.4	1.4	1.9
FR-9	7.87	7.0	7.6	0.4	0.4	LD	0.4	0.5	1.0
FR-10	7.87	6.5	6.1	0.2	0.2	LD	0.2	NA	0.6
FR-11	7.87	8.5	7.4	0.8	0.2	0.2	0.4	0.5	0.7
FR-12	7.87	14.5	11.3	1.2	0.6	1.8	1.3	13.5	13.2
FR-13-B	7.87	18.0	16.9	0.7	0.5	1.1	0.7	14.6	17.9
FR-14	7.87	14.0	12.9	0.9	0.4	1.5	1.0	12.4	14.3
FR-15	7.87	13.0	11.7	0.4	0.6	0.7	0.6	9.5	11.2
FR-16	7.87	6.9	6.9	0.2	0.4	0.2	0.4	0.7	1.3
FR-17	7.87	11.0	11.4	0.8	0.6	0.9	0.6	6.5	8.5
FR-18-B	7.87	14.0	13.2	0.5	0.7	1.2	1.5	13.6	14.7
FR-19	7.87	14.0	12.9	1.0	0.7	1.3	1.1	12.4	13.8
FR-20	7.87	10.2	10.6	0.5	0.6	0.4	0.6	8.0	10.5
FR-21	7.87	6.1	6.3	0.4	0.5	0.1	0.5	1.3	2.1
FR-22	7.87	6.0	5.6	0.5	0.4	0.2	0.4	0.4	0.6
FR-23	7.87	13.5	12.5	0.5	0.6	0.9	0.9	13.6	13.6
FR-24-B	7.87	13.5	12.1	0.5	0.7	0.8	0.8	13.8	13.2
FR-25	7.87	12.8	10.1	0.7	0.6	0.7	0.7	12.5	10.0
FR-26	7.87	13.4	12.8	0.6	0.6	1.0	0.8	12.1	12.9
FR-27	7.87	20.0	21.6	0.4	0.5	5.5	0.5	2.9	2.2
FR-28	7.87	6.1	5.7	0.2	0.3	0.3	0.4	0.7	1.0
FR-29	7.87	13.4	11.6	0.6	0.6	1.0	0.9	12.6	11.7
FR-30-B	7.87	17.8	16.0	1.2	0.8	1.4	1.1	17.9	17.1
FR-31	7.87	8.5	7.4	0.9	0.5	3.0	1.3	1.5	1.8
FR-32	7.87	9.6	8.4	0.6	0.6	0.2	1.0	6.1	6.4
FR-33	7.87	6.7	5.8	0.4	0.4	0.1	0.4	0.6	1.0
FR-34	7.87	7.3	6.5	0.2	0.1	0.4	0.1	0.4	0.5
FR-1-A	18.3	NA	8.9	NA	0.5	NA	0.6	NA	8.5
FR-7-A	18.3	NA	5.9	NA	0.5	NA	0.6	NA	1.2
FR-13-A	18.3	NA	15.2	NA	0.6	NA	1.7	NA	17.8
FR-18-A	18.3	NA	12.5	NA	0.5	NA	1.0	NA	14.0
FR-24-A	18.3	NA	8.02	NA	0.4	NA	0.5	NA	5.6
FR-30-A	18.3	NA	12.5	NA	0.6	NA	0.6	NA	9.7

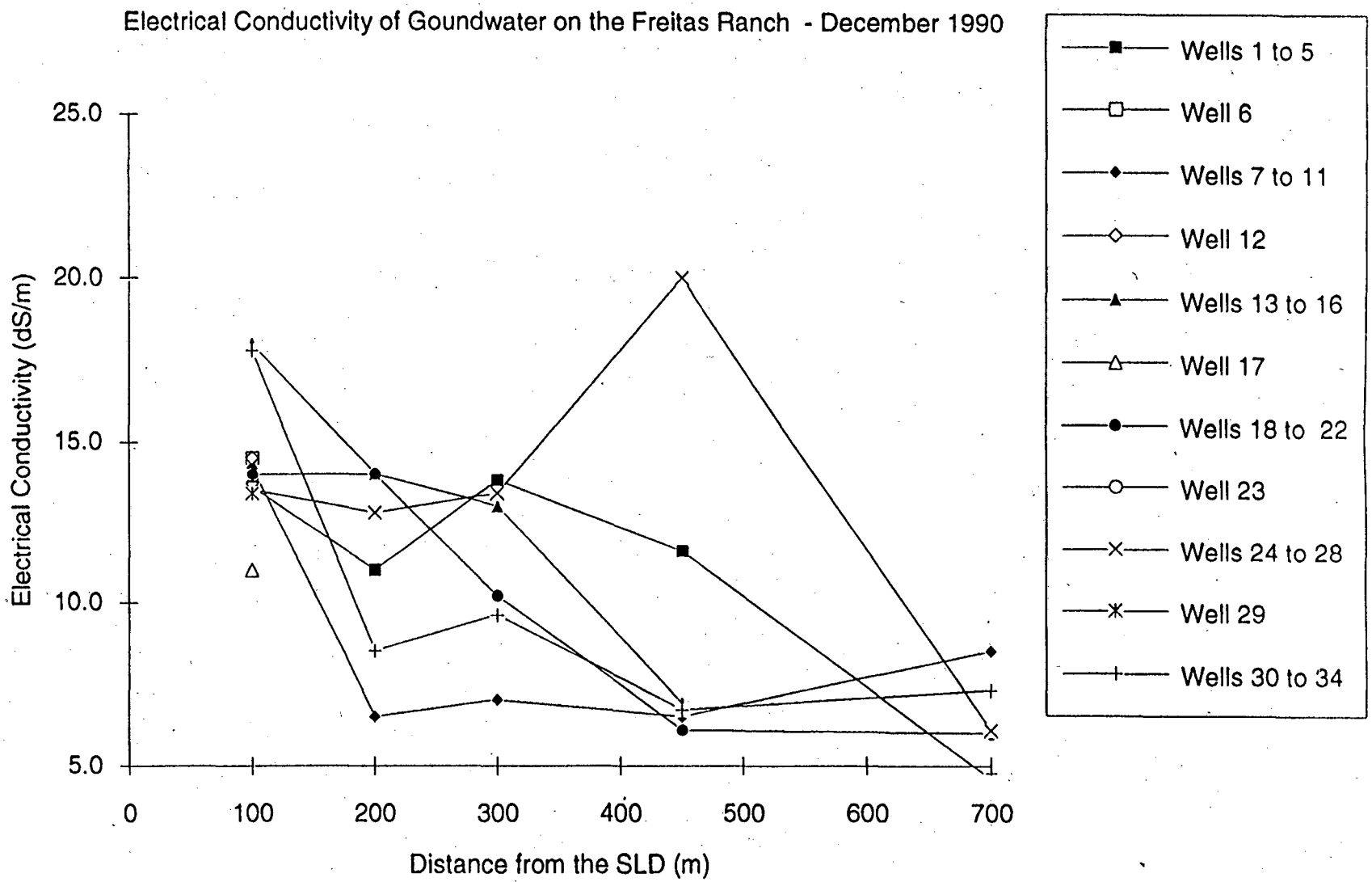

Figure 4.9. Electrical conductivity of groundwater along transects perpendicular to the San Luis Drain for December 1990.

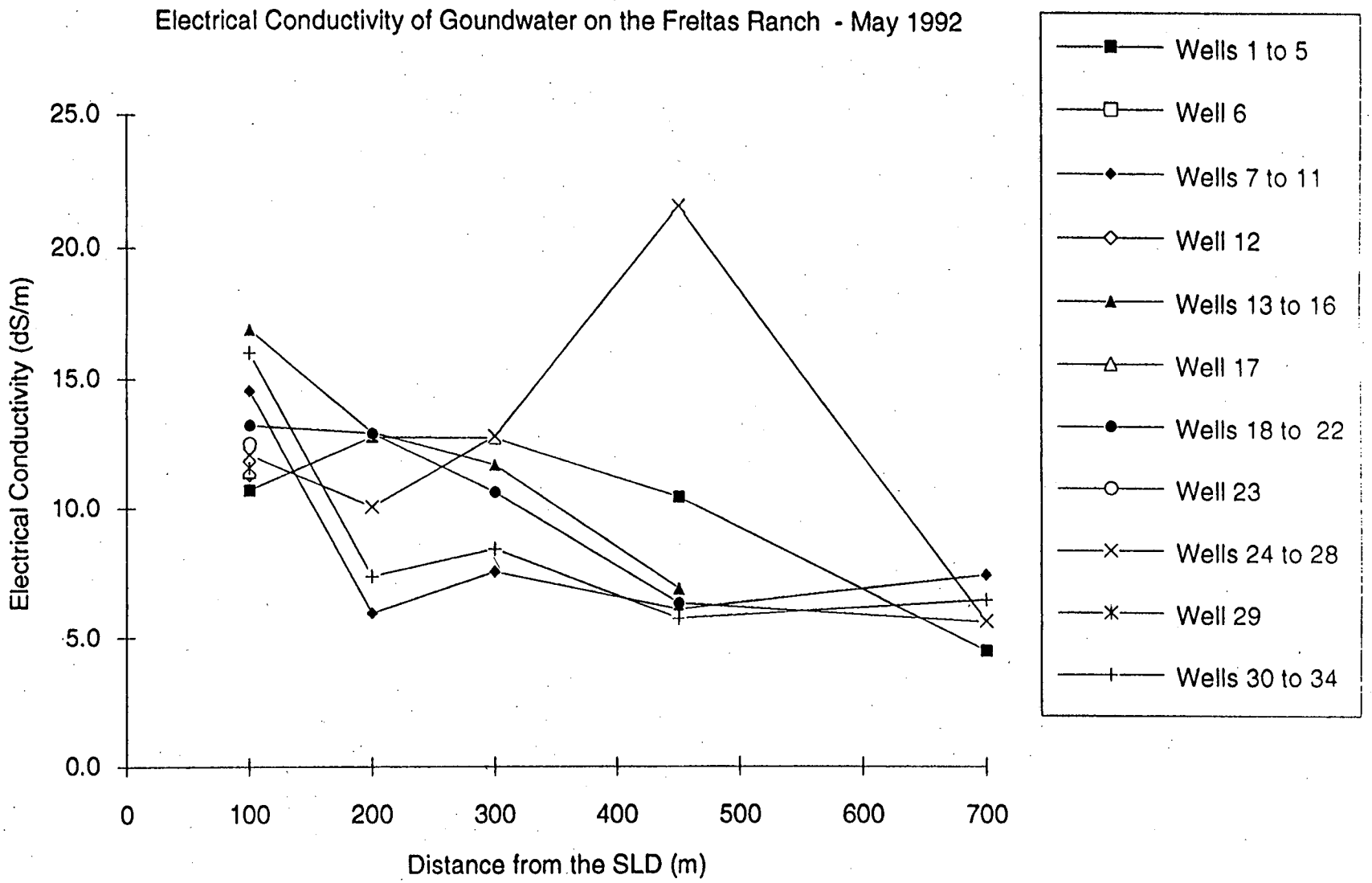

Figure 4.10. Electrical conductivity of groundwater along transects perpendicular to the San Luis Drain for May 1990.

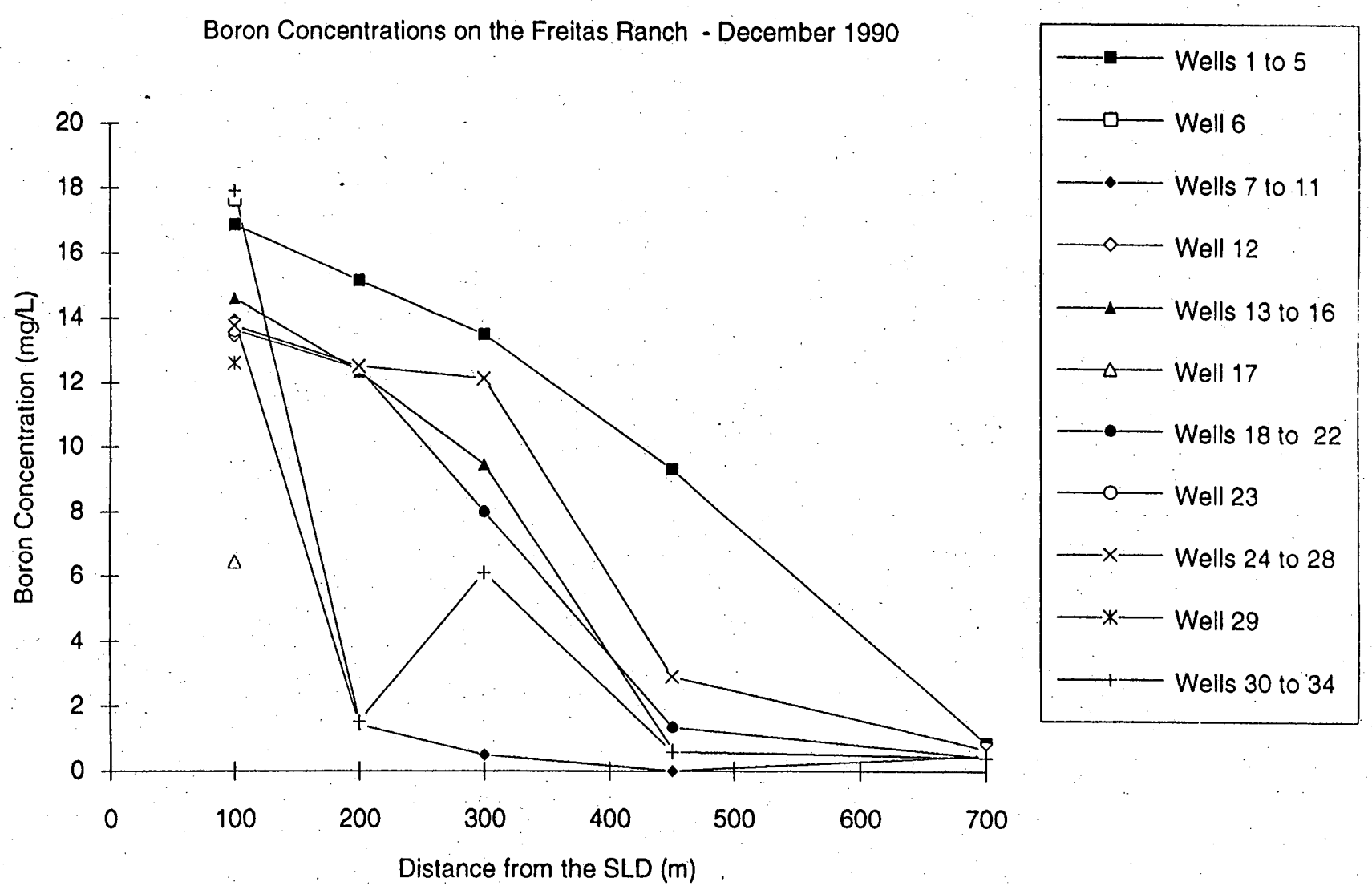

Figure 4.11. Boron concentrations in groundwater along transects perpendicular to the San Luis Drain for December 1990.

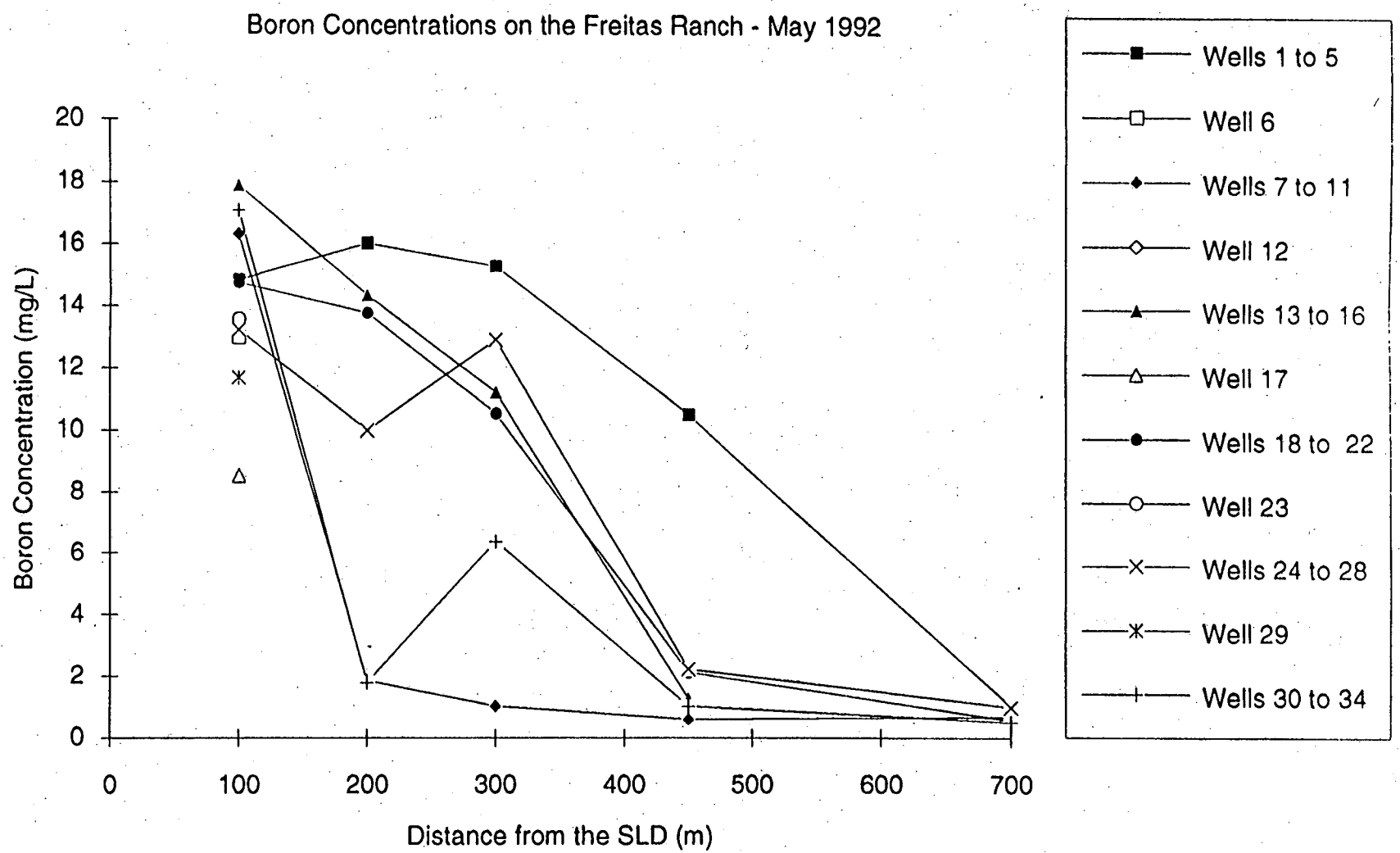

Figure 4.12. Boron concentrations in groundwater along transects perpendicular to the San Luis Drain for May 1990.

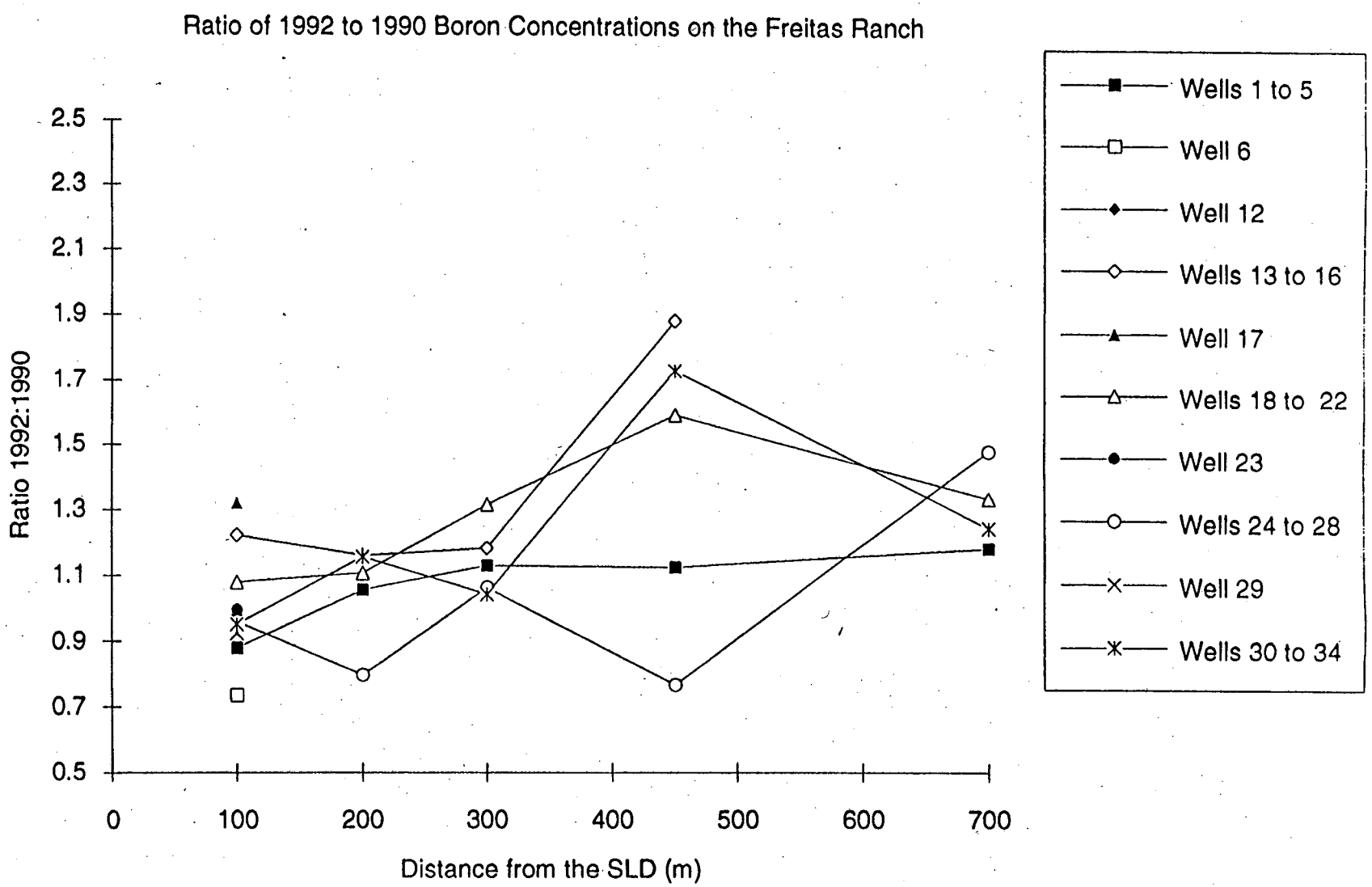

Figure 4.13. The ratio of the boron concentration in 1992 to the boron concentration in 1990 along transects perpendicular to the San Luis Drain.

is limited to depths of less than 17 m. These data are consistent with groundwater data collected from directly under the Reservoir, where the average depth of migration was about 20 m (Benson et al., 1991).

Total selenium and selenite concentrations were also measured in these wells. In 1990 total selenium concentrations were less than 6 µg/L and in 1992, less than 2 µg/L. Total selenium and selenite concentrations are provided in Figures 4.14 and 4.15, respectively. Data from both years are combined in these graphs. As illustrated, for both years the range of concentrations overlap. Total selenium concentrations decline from the range of 0.5 to 2 µg/L adjacent to the SLD to less than 1 µg/L at a distance of 700 m. Similar trends with lower concentrations are apparent from the selenite data shown in Figure 4.14. Although selenium concentrations in groundwater under the Freitas Ranch remain low, the nearly monotonic decline in selenium concentrations, coupled with stabilization of the majority of values at a distance of 450 m from the drain, suggest that elevated selenium concentrations are associated with drainage water migration from Kesterson Reservoir. Two exceptions to this pattern are found: wells FR-27 and FR-31. Both had elevated selenium concentrations (5.5 and 3 µg/L, respectively). However, boron concentrations are too low (2.9 and 1.5 mg/L) to indicate the presence of drainage water. Consequently, elevated selenium concentrations at the two wells were associated with local variations in the aquifer chemistry that is not associated with the presence of Kesterson Reservoir. Nevertheless, by 1992, selenium concentrations in both of these wells dropped to levels similar to those in surrounding wells.

4.2.3. Speciation of Selenium

The ratio of selenite to total selenium in the majority of samples ranges from 0.4 to 1, within 1992, with an average value of 0.8, indicating that the majority of dissolved selenium is in the selenite form. This is consistent with the presence of mildly reducing conditions in the aquifer, as have been observed and documented in previous analyses of the local groundwater (White et al., 1991).

4.2.4. Recommended Monitoring Plan

The presence of elevated concentrations of boron and high electrical conductivities clearly demonstrate the presence of a plume of brackish water associated with seepage and migration of drainage water from Kesterson. The low concentration of selenium within this plume attests to the effectiveness of biologically mediated reduction and immobilization of selenium, thereby, assuaging fears of large scale migration of harmful concentrations of selenium in the shallow groundwater system. Nevertheless, due to the close proximity to Kesterson Reservoir, and periodic observation of elevated concentrations of selenium in groundwater directly under Kesterson, prudence dictates continued collection of groundwater quality data under the former Freitas Ranch. For this reason, we recommend annual sampling of the array of groundwater

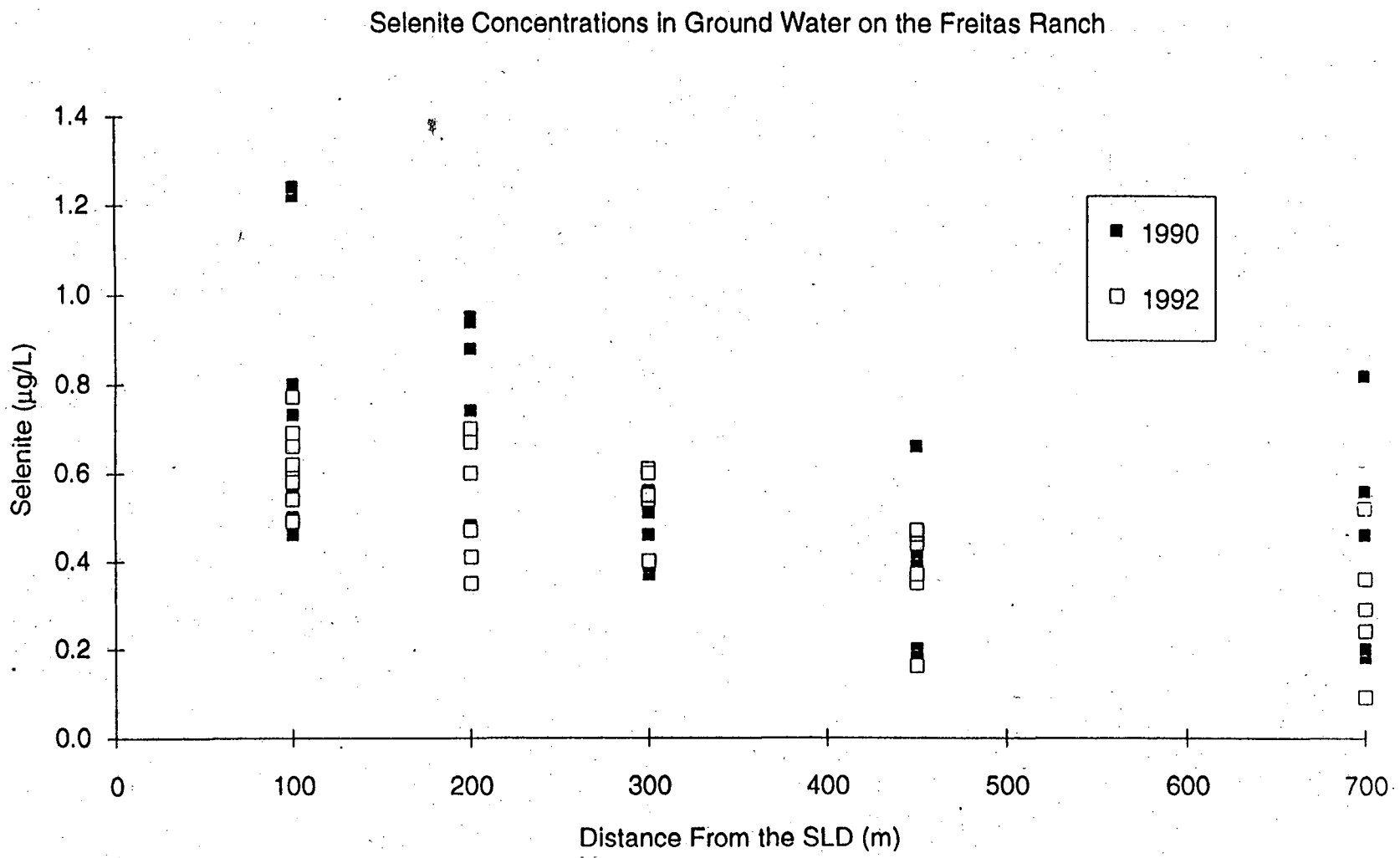

Figure 4.14. Concentrations of selenite in groundwater for both 1990 and 1992, plotted as a function of distance from the San Luis Drain.

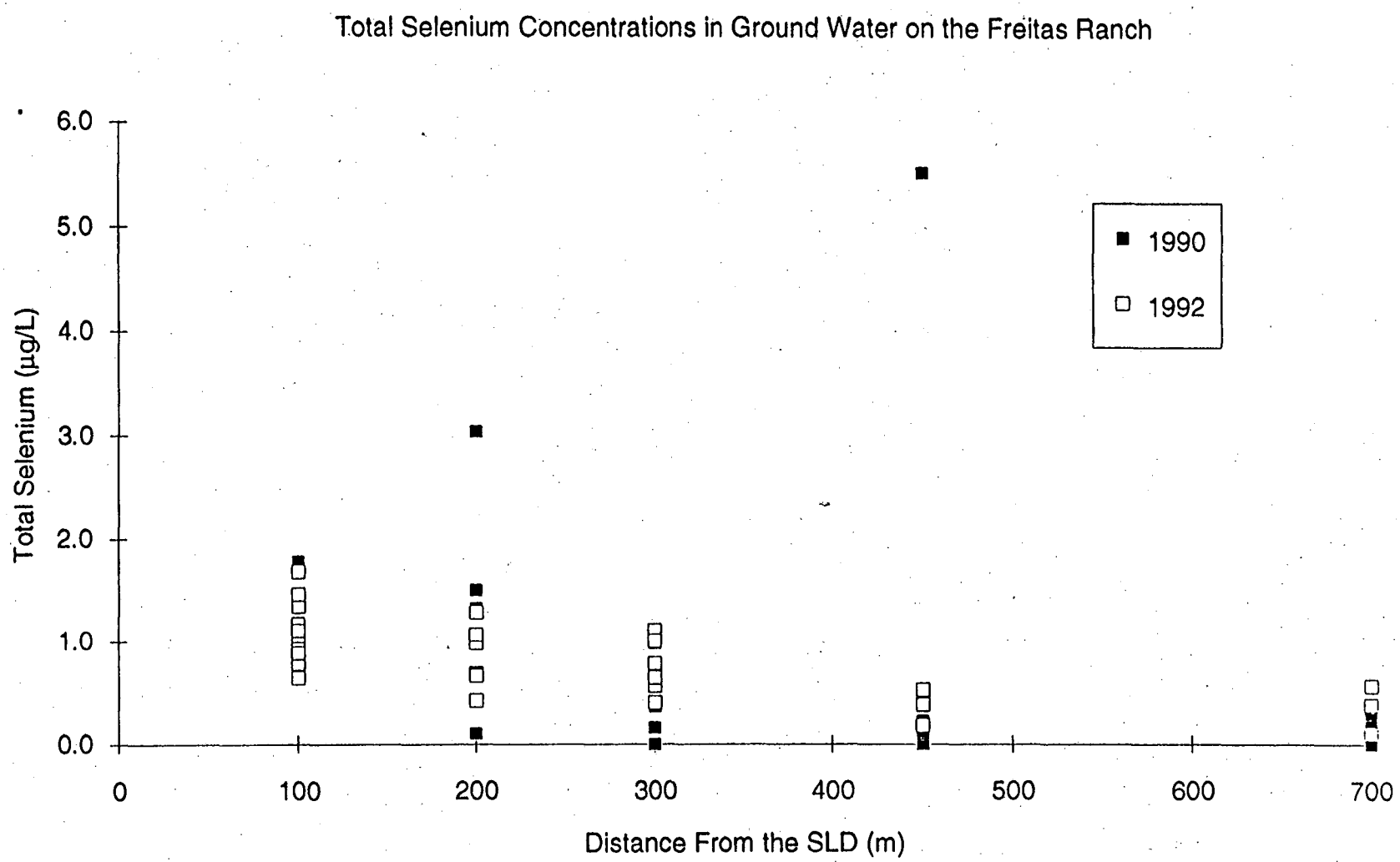

Figure 4.15. Concentrations of total selenite in groundwater for both 1990 and 1992, plotted as a function of distance from the San Luis Drain.

monitoring wells described here. Sampling could be carried out when associated activities pose the least interference with the wildlife habitat, such as in early August. At a minimum, groundwater samples should be analyzed for total selenium, boron, nitrate, sulfate and chloride concentrations.

4.2.5. Summary

Groundwater samples collected on two occasions, over a one and one-half year period, demonstrate the presence of a plume or brackish drainage water that migrated under the Freitas Ranch while Kesterson Reservoir was in operation. The plume extends an average distance of about 400 m from the San Luis Drain. As expected, selenium has not migrated along with this plume to any significant extent, though selenium concentrations immediately adjacent to Kesterson are slightly elevated with respect to local background concentrations. The majority of the selenium is present in the selenite form which is consistent with the presence of mildly reducing conditions in the aquifer. Little to no changes in the location of the plume were noted between sampling events. However, small but measurable increases in the concentration of boron were observed at a distance of about 450 m from the San Luis Drain, suggesting very slow migration of the leading edge of the plume.

5.0. Pond 2 Pilot Scale Microbial Volatilization Study: Soil Monitoring

Peter Zawislanski
Earth Sciences Division
Lawrence Berkeley Laboratory

Microbial volatilization is a potential remedial measure to decrease the selenium inventory at Kesterson Reservoir. Past studies in both the field and the laboratory suggest that a significant percentage of the selenium inventory may be removed in this fashion. The objectives of this study include the quantification of selenium losses and a test of a pilot-scale design which in the future may be used in other parts of the reservoir.

The site chosen for this study is a 2 acre plot in the northern end of Pond 2, an area which was very frequently flooded during the operation of the Reservoir and supported primarily cattail vegetation. Preliminary soil sampling in this plot in November 1989 revealed some of the highest selenium concentrations in the Reservoir: mean [selenium] in the top 15 cm (5 samples) was 291 ppm; in the 15 to 30 cm interval it was 27.3 ppm. Furthermore, the same soil intervals were found to be less saline than average (1:10 soil:water extract electrical conductivities linearly normalized to field water content ranged from 23 dS/m to 69 dS/m). In preparing this plot for the study, cattail remains on the soil surface were incorporated into the top 20 cm or so of soil by disking and rototilling. The plot was then divided into four subplots, each being reserved for a particular treatment: irrigation only (I), irrigation and disking (rototilling) (ID), disking (rototilling) only (D), and control or no treatment (C) (Figure 5.1). An 11.6 meter buffer zone was set up between the irrigated and non-irrigated plots in order to prevent irrigation water from falling onto the disked plot. Losses of selenium in the soil are being monitored by annual sampling along selected transects and semi-annual (originally quarterly) sampling in randomly selected subplots. There are 10 such subplots (5 by 5 meters in size) in each treatment. Along with total selenium analysis (performed by CSU Fresno), subsets of these samples are being analyzed for water soluble selenium. Emissions of gaseous selenium are being monitored (by UC Davis) every two weeks (less frequently in the winter). Monitoring of the soil for potential short-term and long-term leaching of selenium deeper into the profile is being conducted. In order to determine how much of the near-surface selenium is actually lost to volatilization, it must be known how much was displaced by irrigation water below the sampled interval. Tensiometers and neutron probe measurements give short term indications of over irrigation. All these efforts will aid in constructing a selenium mass balance in the vadose zone and estimating selenium losses due to volatilization. An overview of plot management and results of vadose zone monitoring are presented herein.

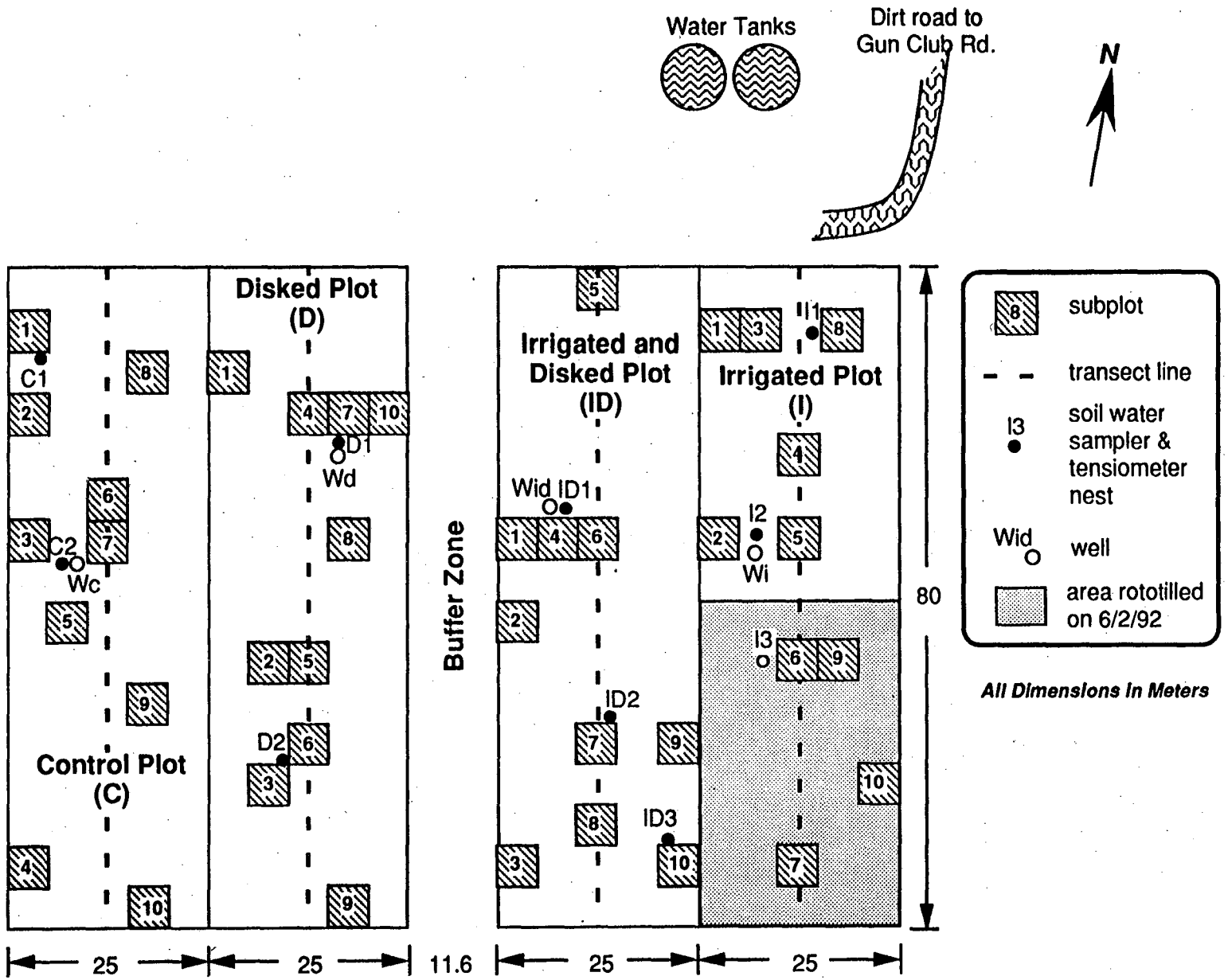

Figure 5.1. Pond 2 (Pilot Scale) Volatilization Site (P2VS).

5.1. Irrigation, Rototilling, and Rainfall

The I and ID treatments are irrigated every week during the spring, summer, and fall months and every two weeks in the winter when bi-weekly rainfall is less than 10 mm. Due to low evaporation rates during the winter, less frequent irrigation suffices. The only influx of water to treatments D and C comes from rainfall, most of which is restricted to a 3-month period between December and March (see Figure 5.2). Over the first year of the experiment, the total water influx into the irrigated treatments was roughly 2.5 times greater than into the non-irrigated treatments (Figure 5.3). However, during warm and hot months, when selenium volatilization is likely the highest, the non-irrigated treatments receive almost no water, except for the occasional spring shower.

The ID and D treatments are rototilled every two weeks, roughly to a depth of 15 cm. During the winter months, rototilling is much less frequent because the soil is often too moist. Rototilling serves to aerate the soil and also cut down and incorporate any plants.

5.2. Soil Monitoring

The soil monitoring system was installed in July 1990. There are a total of 10 nests of tensiometers and soil water samplers, three in each of the irrigated plots and two in each of the other two plots. The locations of these devices were chosen to coincide with locations of both soil and gas sampling (see Figure 5.1). Soil water samples and tensiometer readings are taken on a monthly basis. In addition, readings will are taken strategically, relative to irrigation and

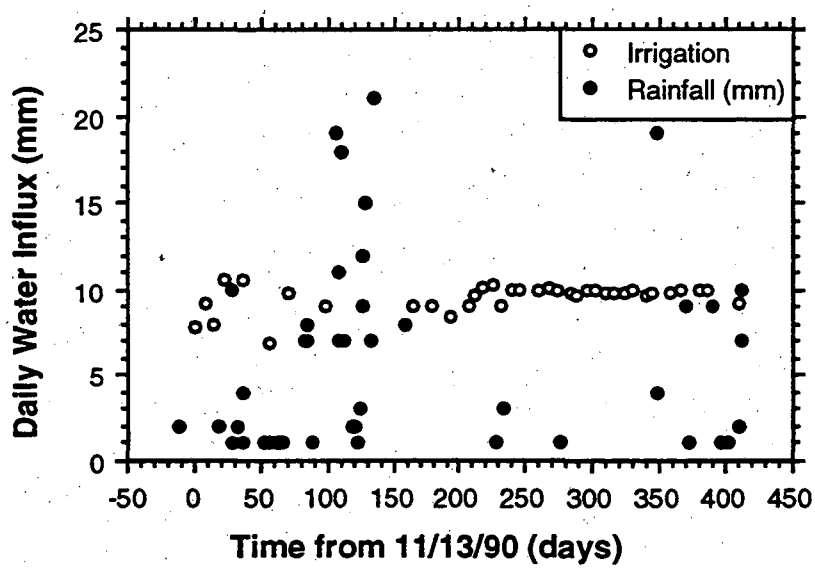

Figure 5.2. Irrigation and rainfall in plot P2VS between 10/90 and 12/91.

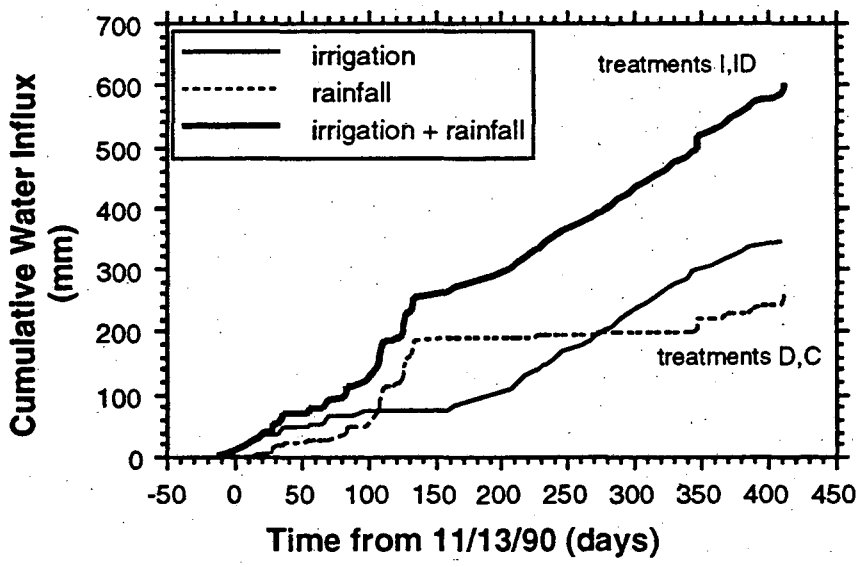

Figure 5.3. Cumulative irrigation and rainfall in plot P2VS between 10/90 and 12/91.

rainfall events. Each nest consists of 4 tensiometers and 4 soil water samplers with porous cups at the following depths: 0.43 m, 0.60 m, 0.80 m, and 1.00 m. All of the instruments are buried at least 30 cm below the soil surface in order to allow disking machinery to pass over the soil. Tubing is routed 1 meter away from the tensiometers and soil water samplers to a common standpipe through which the samplers are sampled and the tensiometers are read. There are 4 wells, one in each treatment. These penetrate to an average depth of 2.8 m. Wells are sampled on a quarterly basis. They are also used as neutron probe access holes. Neutron probe readings are taken at monthly intervals.

5.2.1. Soil Moisture Conditions

The soil moisture regime in plot P2VS is affected by irrigation, rototilling, rainfall, evaporation, transpiration, and the rise and fall of the water table. Tensiometer data through the end of 1991 reveal a relatively "flat" hydraulic head profile in most nests during most of the year, with head ranging roughly from -1 m to -3 m, suggesting that bare soil evaporation is not particularly significant compared to other plots in the Reservoir (Figures 5.4 through 5.7). This may be explained by the presence of loose organic material on the soil surface, which acts as a mulch. Hydraulic head in all treatments increased following rainfall events in January, February, and March of 1991. Also, the slope of the hydraulic head profile reversed, indicating a downward flux of water due to rainfall infiltration. This pattern changes abruptly upon the invasion of the irrigated and control plots by plants (primarily *Bassia*, Russian thistle, and clover) in the late spring of 1991. The ID and D plots remained free of vegetation due to rototilling. The

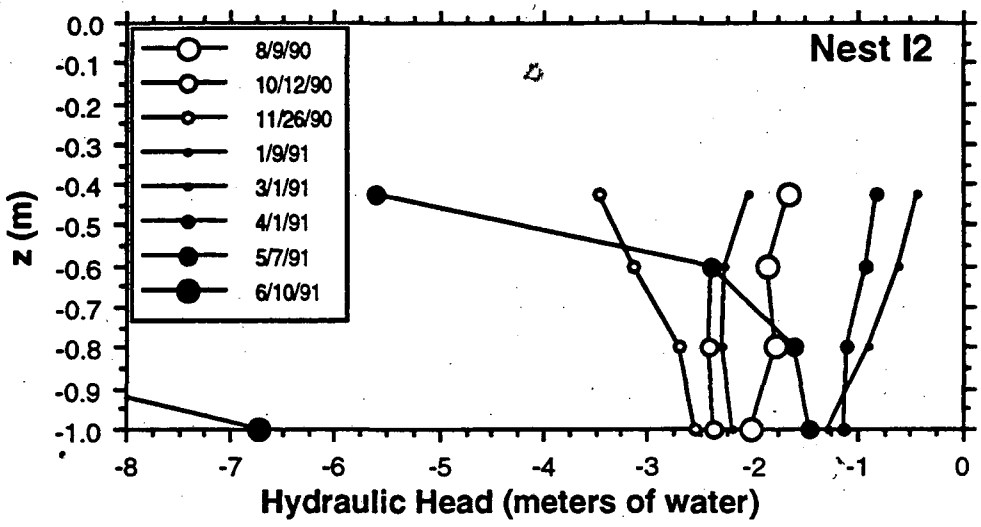

Figure 5.4. Hydraulic head distribution in the irrigated treatment as measured by tensiometers in nest I2. Hydraulic head was beyond the measurable range for the remainder of 1991.

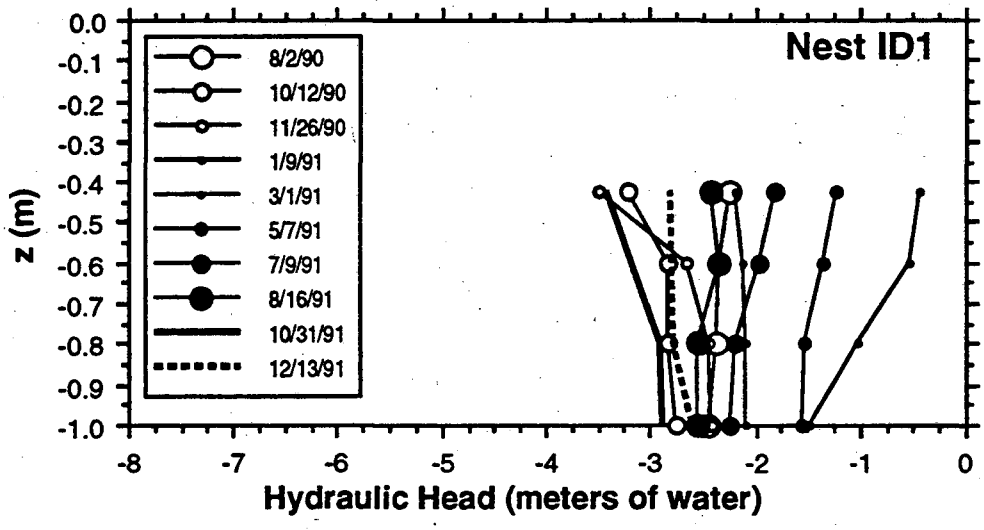

Figure 5.5. Hydraulic head distribution in the irrigated/disked treatment as measured by tensiometers in nest ID1.

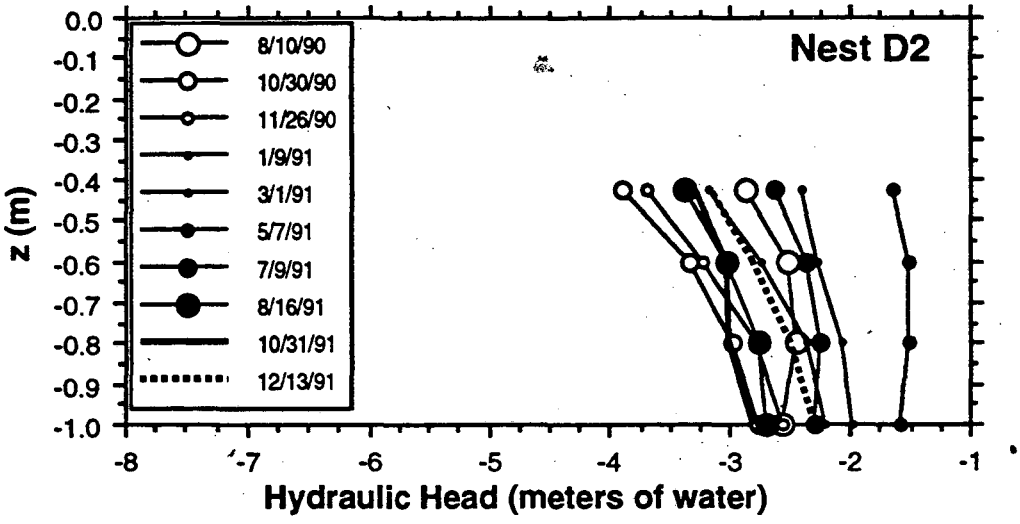

Figure 5.6. Hydraulic head distribution in the disked treatment as measured by tensiometers in nest D2.

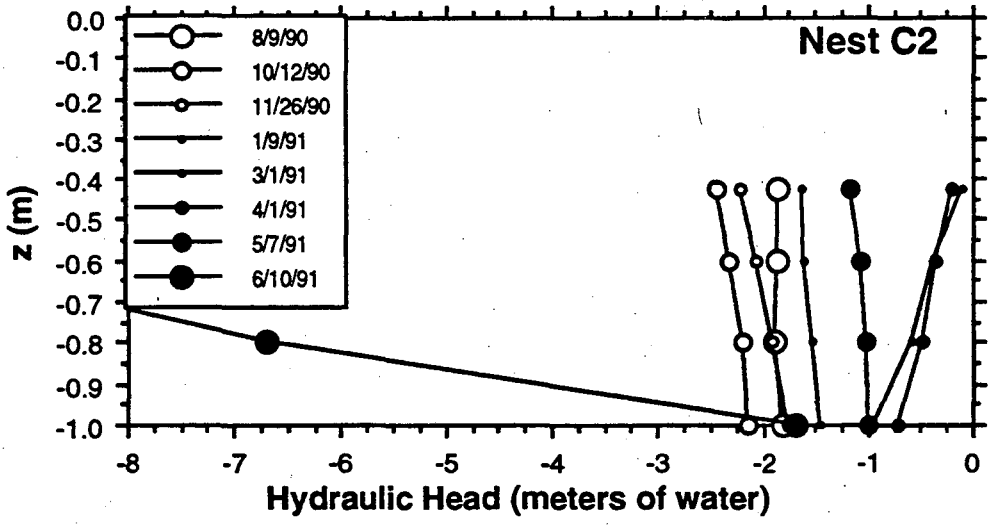

Figure 5.7. Hydraulic head distribution in the control treatment as measured by tensiometers in nest C2. Hydraulic head was beyond the measurable range for the remainder of 1991.

effect of plants was to drastically reduce the hydraulic head (reduce moisture content) in the root zone. This is clearly seen in Figures 5.4 and 5.7 between 4/1/91 and 6/10/91. Between 6/91 and 12/91, soil water potentials were beyond the range measurable by tensiometry.

The trends described above were also observed in soil moisture content as determined via neutron probe measurements. The instrument used was an Am-241/Be-source HydroProbe, manufactured by CPN Corp. (Model 503 DR). The probe was lowered into PVC wells, one in each treatment; readings were taken at 15 cm intervals, down to the water table. From direct counts of slow neutrons, volumetric moisture content was estimated using a regression based on an "average" Kesterson soil. Therefore, moisture content values should be considered as relative values for the observation of moisture changes. As shown in Figures 5.8 through 5.11, in soil profiles in treatments which were kept devegetated, temporal variations in moisture content occurred primarily within the top 0.5 m and in sandy layers close to the water table (between the depths of 2.3 m and 1.5 m), due to sand's low water retention. It should be noted that despite not being irrigated, the soil profile in the D treatment did not dry out significantly over summer months, most likely due to the presence of a 15-cm low density mulch layer produced by rototilling. On the other hand, significant changes in moisture content occurred in both the irrigated and control plots, due to the presence of plants. This change is especially apparent between readings taken on 5/7/91 and 7/11/91, when plant growth was most rapid. Moisture content in all treatments began to increase in 12/91, both at the surface due to rainfall infiltration and at the bottom of the profile, due to the rise of the water table. Although rainfall infiltration penetrated to approximately 1 m in all treatments (Spring 1991), water from irrigation was generally contained within the topmost 0.15 m. Net changes over the twelve month period (12/90 to 12/91) were not significant in the disked treatments (ID, D), while in the non-disked plots (I and C) were that of a profile-averaged decline in moisture content of approximately 60% and 30% respectively. The relatively higher moisture content in the Control plot vs. the Irrigated plot is due to a shallower water table in C. Changes in moisture content within the top 0.30 m were of the same order of magnitude in those two treatments.

5.2.2. Groundwater Level Fluctuations

In agreement with measurements made throughout Kesterson Reservoir, groundwater levels fluctuate seasonally, in relation to the flooding of surrounding lands. These fluctuations affect the soil moisture conditions and subsequently the plant biomass. Depths to the groundwater table measured at four wells, one in each treatment, are shown in Figure 5.12 (see Figure 5.1 for relative locations of wells). As seen in Figure 5.12, the water table is shallowest in the control treatment. This is primarily due to the slight slope of the ground surface from east to west within the experimental plot. After normalization for ground surface elevation, water table

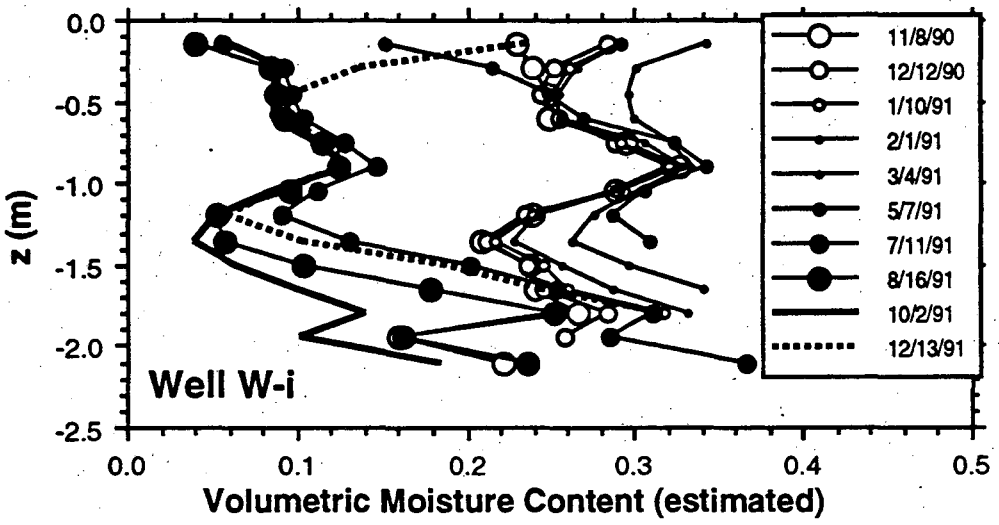

Figure 5.8. Volumetric moisture content as estimated via neutron probe measurements, as a function of depth in well W-i, irrigated treatment.

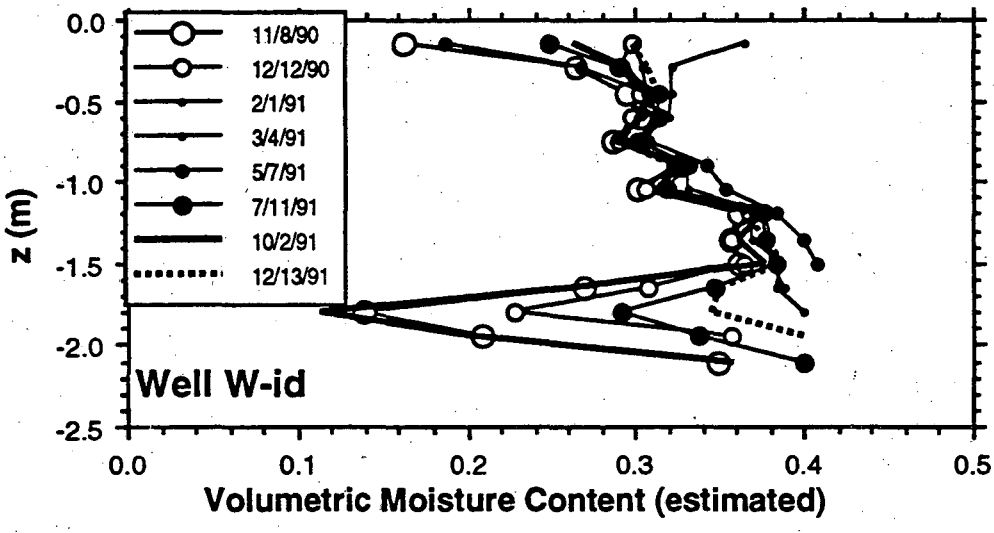

Figure 5.9. Volumetric moisture content as estimated via neutron probe measurements, as a function of depth in well W-id, irrigated/disked treatment.

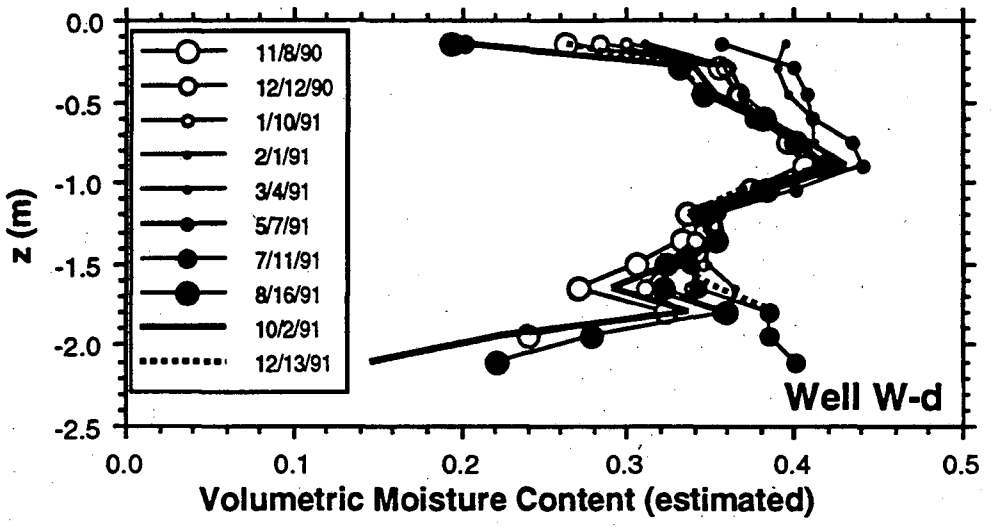

Figure 5.10. Volumetric moisture content as estimated via neutron probe measurements, as a function of depth in well W-d, disked treatment.

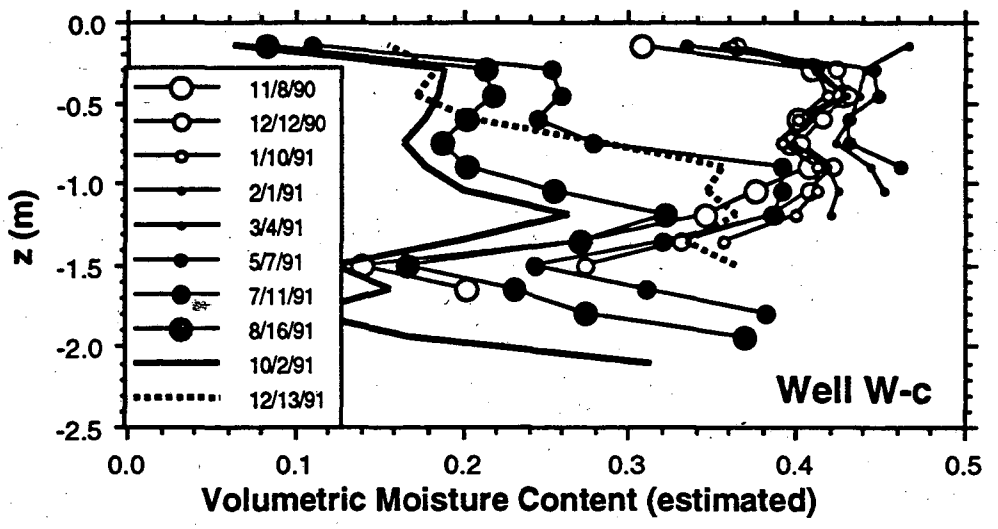

Figure 5.11. Volumetric moisture content as estimated via neutron probe measurements, as a function of depth in well W-i, irrigated treatment.

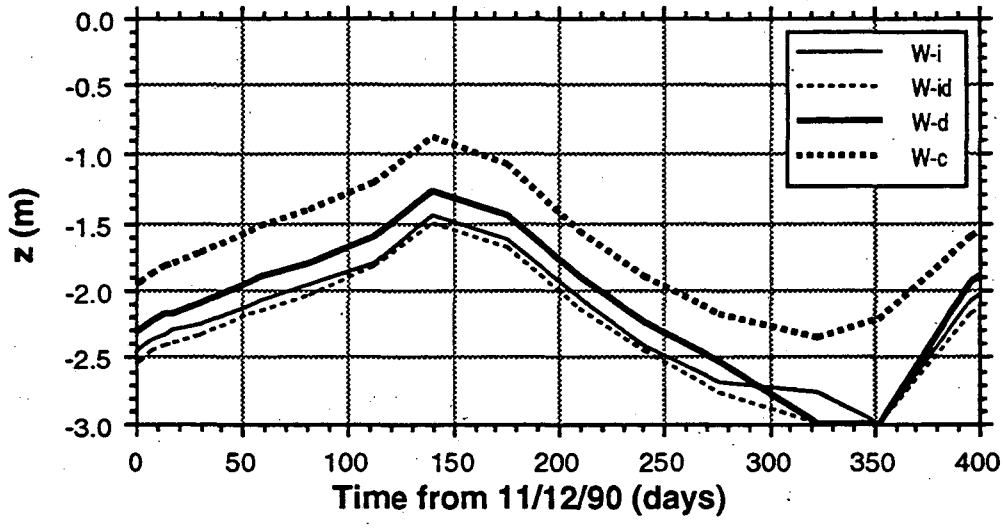

Figure 5.12. Depths to the water table relative to the soil surface in wells W-i, W-id, W-d, and W-c.

elevations relative to sea level are roughly equal throughout the plot, except for the end of summer when water levels drop further in treatments D, I, and ID, than in C (Figure 5.13).

5.3. Soil and Soil Water Selenium and Salt Distribution: Time Trends

Soil and soil water sampling are being conducted on a periodic basis. Soil water is sampled at four depths (0.425, 0.60, 0.80, and 1.00 m) via suction cup lysimeters, distributed around the site in ten nests. Samples are filtered through a 0.45 μm filter, prior to analysis for total dissolved selenium using ICP and EC determination. Samples in which selenium concentrations are below the nominal quantification limit for ICP are analyzed using HGAAS. Soil samples are collected using a tractor-mounted Giddings rig. Two different categories of soil samples are taken. An annual N-S transect is taken through the middle of each treatment in July. Samples are taken every 3 m along these lines and down to the depth of 0.60 m, in 0.15 m increments. Soil from the transects is extracted using a 1:5 soil:water extract and extracts are analyzed for total soluble selenium via HGAAS. Also, twice a year, 10 subplots within each treatment are sampled. Soil is cored to 0.60 m in 0.15 m increments, except for 30% of the subplots in which an additional two increments, 0.60-0.90 m and 0.90-1.20 m, are taken. Five such cores are taken in each subplot and composited by depth. All soil samples are extracted for total selenium via an acid digest and analyzed via HGAAS by the Engineering Research Institute, C.S.U. Fresno. A subset of the 1990 and 1991 transect samples was re-analyzed using XRF by Robert Giauque of LBL. See Figure 5.1 for sampling locations.

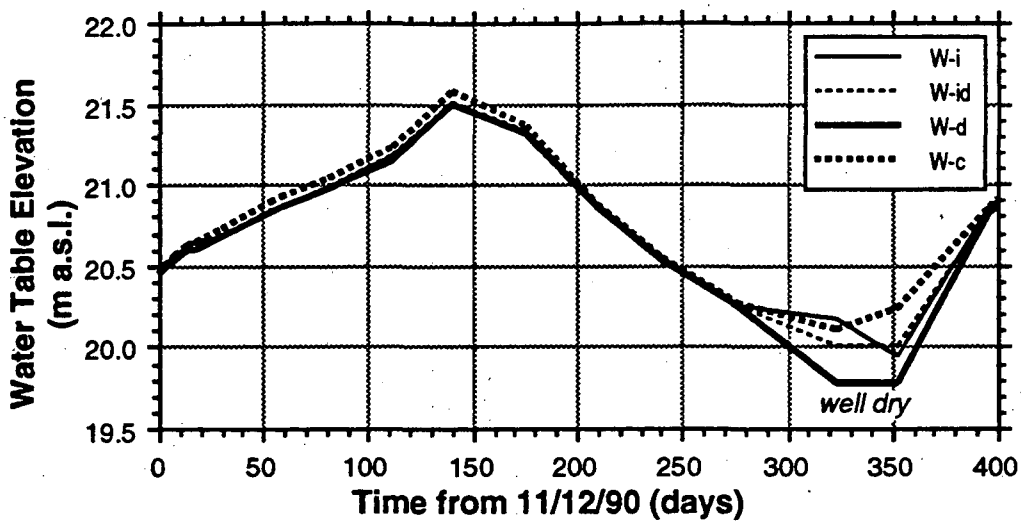

Figure 5.13. Water table elevation relative to mean sea level in wells W-i, W-id, W-d, and W-c.

5.3.1. Soil-Se Along N-S Transects: Spatial and (Early) Temporal Distribution

Data from the July 1990 and July 1991 transects are presented herein. Total selenium distributions along the four transects (I, ID, D, and C) at four depths (0-15 cm, 15-30 cm, 30-45 cm, and 45-60 cm) are shown in Figures 5.14-5.17. The depth interval of nominally the greatest interest is 0-15 cm because of the highest selenium concentrations and the favorable conditions for fungal growth. Within this interval, the average total selenium concentration was 50 ppm, with transect soils from the I treatment being high above that average at 97.8 ppm in July 1990. Between July 1990 and July 1991, total selenium concentrations apparently declined in the irrigated treatment by 21% and in the irrigated/disked treatment by 18%. These declines were not spatially uniform. For example, between the 60 m and 80 m mark in the ID transect, there were no significant changes from year to year. The reasons for these inconsistencies is not clear. There were no significant changes in total selenium concentrations in the 0-15 cm interval in treatments D or C.

Concentrations in the 15-30 cm interval averaged 15 ppm in July 1990, with a great deal of variability in the C treatment due to what appears to be displaced soil in the northern end of the plot. Concentrations in the 30-45 cm and 45-60 cm intervals averaged 5.7 ppm and 2.8 ppm respectively. In many of the subsurface transects, total selenium concentrations appear to have dropped, for example, in transect ID 30-45 cm, the average concentration declined from 4.1 ppm to 2.6 ppm between July 1990 and July 1991. Such trends are somewhat unexpected based on

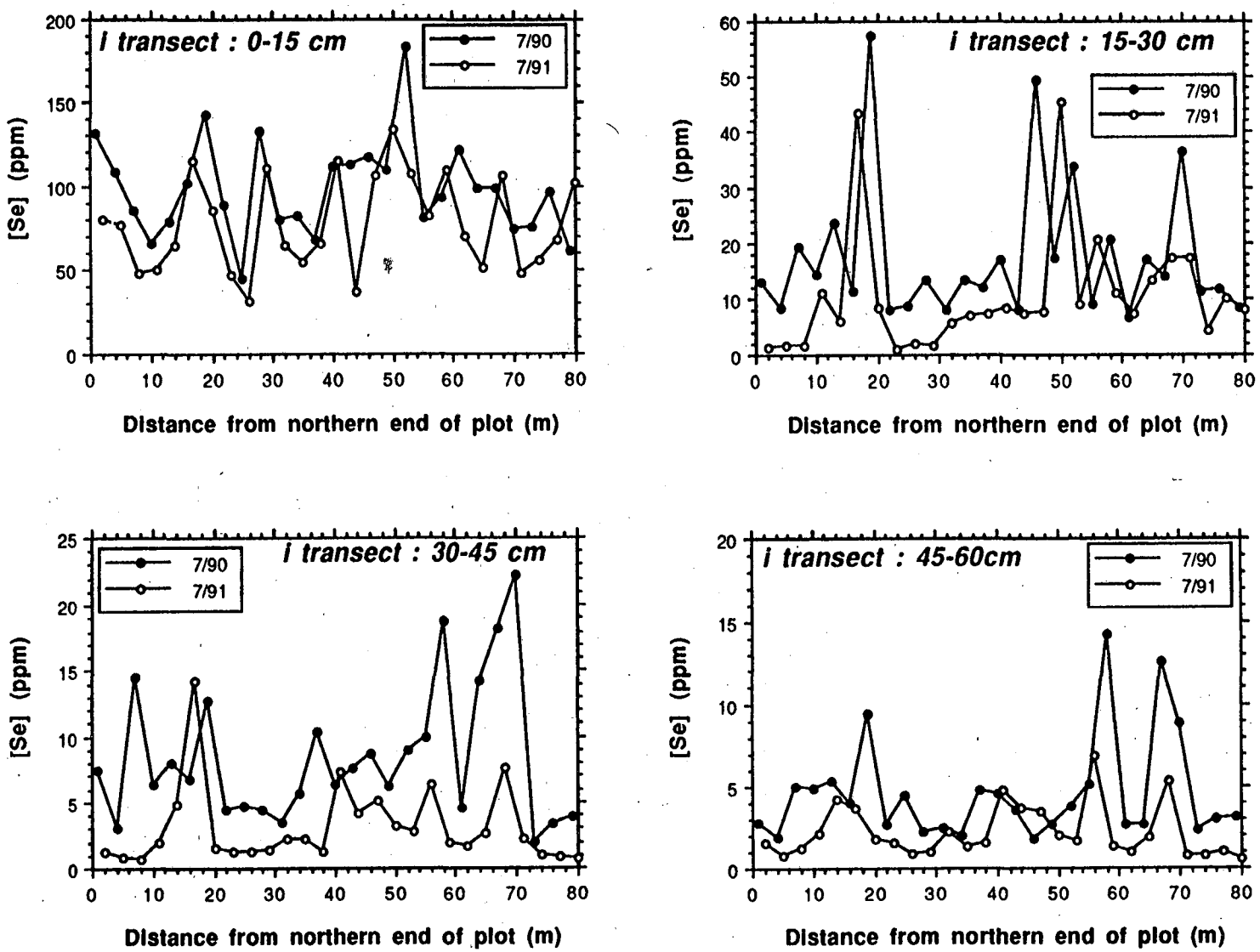

Figure 5.14. Total soil selenium in the irrigated treatment along a roughly N-S transect, 7/90 and 7/91.

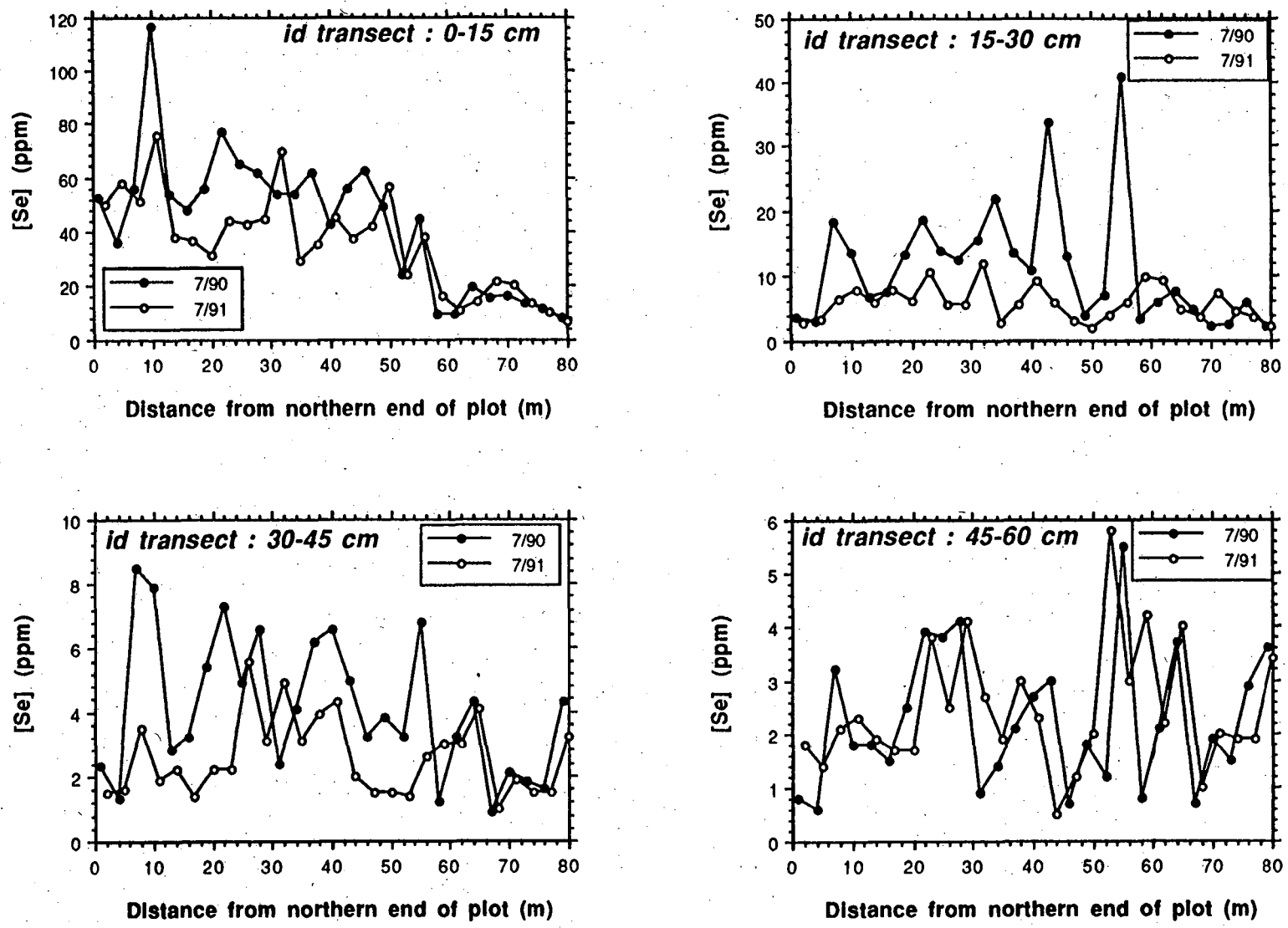

Figure 5.15. Total soil selenium in the irrigated/disked treatment along a roughly N-S transect, 7/90 and 7/91.

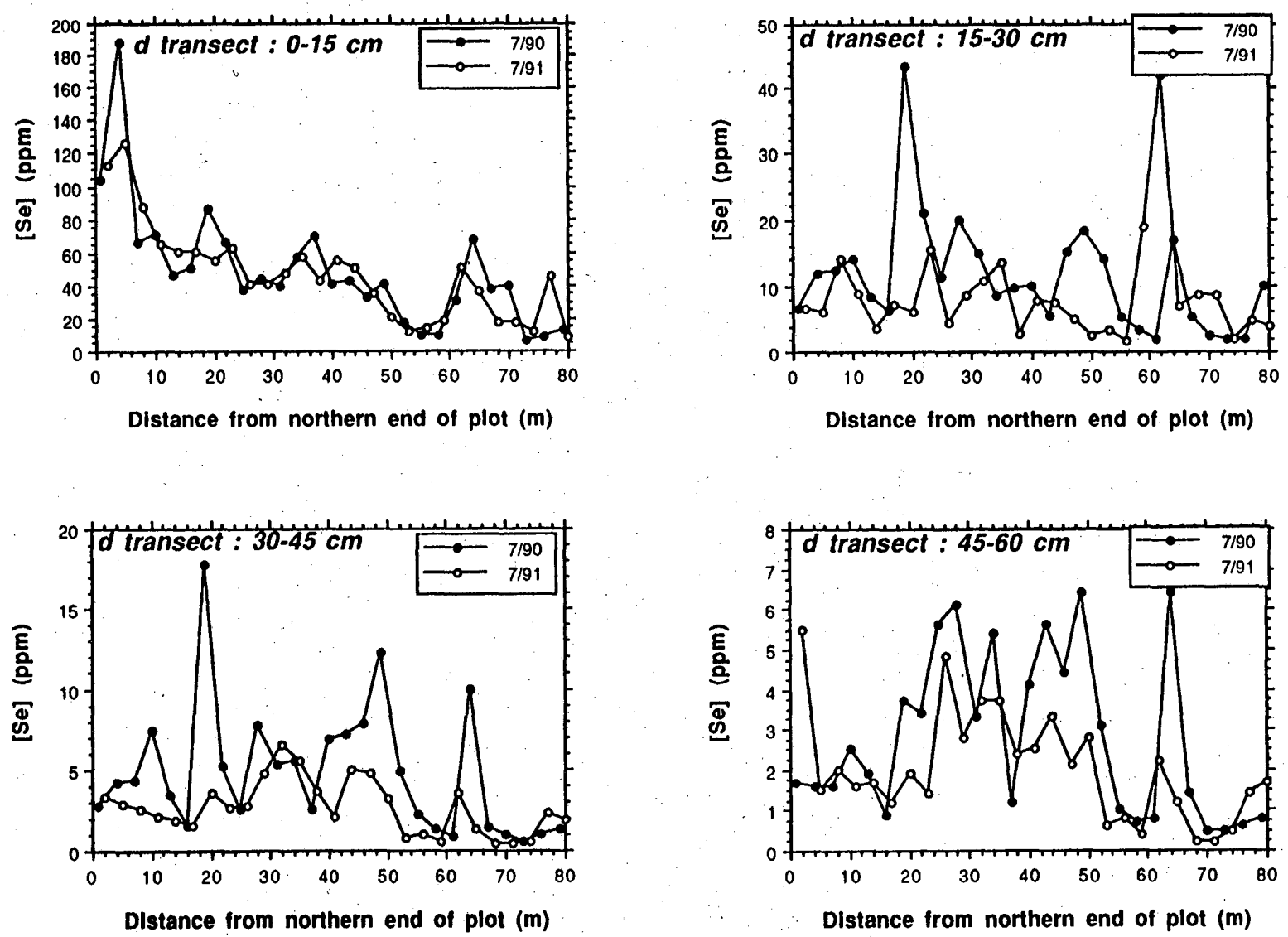

Figure 5.16. Total soil selenium in the disked treatment along a roughly N-S transect, 7/90 and 7/91.

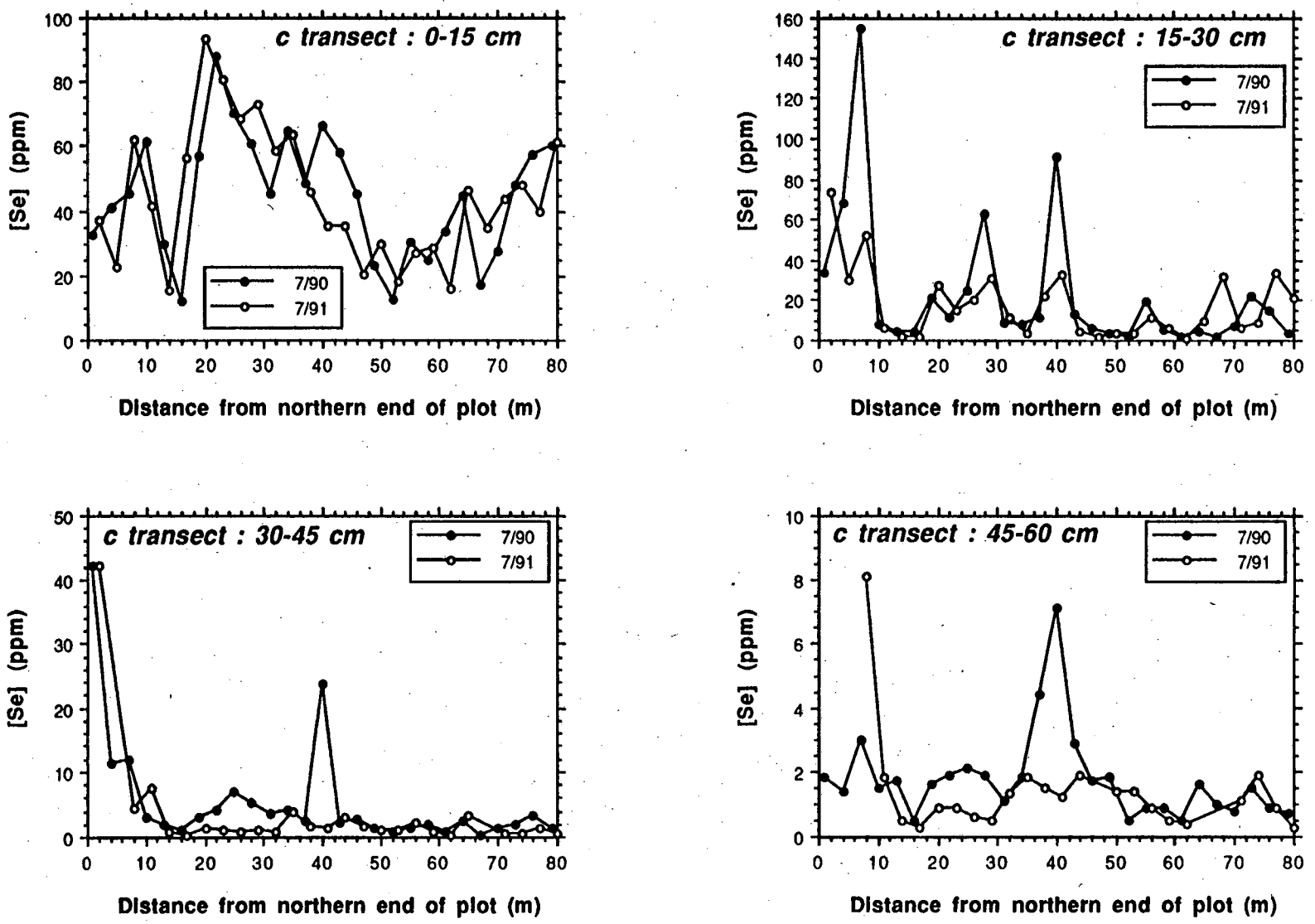

Figure 5.17. Total soil selenium in the control treatment along a roughly N-S transect, 7/90 and 7/91.

data from other experimental plots. However, what may be a distinguishing feature of this plot are the rather high concentrations of dissolved selenium, as observed via soil-water sampling (see Section 5.3.3.). The movement of high concentrations of selenium in soil water deeper into the soil profile due to rainfall infiltration may be partly responsible for declines in total selenium between 15 and 60 cm.

The amount of selenium available to water transport is seen in results of 1:5 soil:water extracts depicted in Figures 5.18-5.20 (data from treatment D is currently being processed and will be presented at a later time). Water-extractable selenium in the 15 to 60 cm intervals falls mostly in the 1 ppm to 4 ppm range with a few outliers as high as 15 ppm. Thus, the flushing of this water-extractable selenium below 60 cm in the soil could explain some of the subsurface declines in total selenium. However, total selenium decreases in the 0-15 cm intervals in the I and ID treatments were on the order of 10 to 20 ppm and cannot be explained in this fashion. Water-extractable selenium concentrations did not decline significantly in the 15 to 60 cm intervals. This does not negate the above hypothesis, because subsequent to flushing of selenium out of this interval, more reduced forms are likely to be reoxidized to water-extractable species after the soil profile dries out.

5.3.2. Plot-wide Soil-Se Distribution Based on Subplot Data

Data collected from subplots in September 1990 was compiled to generate spatial distribution maps of total selenium which are shown in Figures 5.22 and 5.23. In the 0-15 cm interval there are four major "features" in the total selenium distribution: three "highs," one in the middle of the irrigated treatment, one in the northeast corner of the disked treatment, and one on the northwest edge of treatment C and a "low ridge" which runs roughly SW-NE throughout the entire plot. These features correlate well with the topographic contours of the plot (Figure 5.21), that is, areas of higher selenium usually correspond to lower elevation and vice versa. This can be explained by the fact that the lower areas would have been ponded over longer periods of time than the topographic highs. One other interesting feature is the very good correlation between high selenium in the 45-60 cm interval in the central portion of the C treatment and by far the lowest elevation in the entire plot. This suggests that past ponding in this region, whether due to flooding or rainfall, resulted in the flushing of high concentrations of selenium deep in the profile.

5.3.3. Temporal and Spatial Trends in Soil-Water Selenium and Salts

Soil-water samplers (suction-cup lysimeters) were used to observe the movement of solutes in soil water. Data from one selected nest of samplers in each treatment are presented in Figures 5.24-31. Soil-water selenium concentrations and EC over the period of 8/90 to 4/92 in nest i2 (irrigated treatment, see Fig.5.1 for locations) exhibit a fairly typical trend (Figure 5.24, 5.25). Selenium profiles prior to 3/91 are increasing toward the soil surface. Subsequent to late

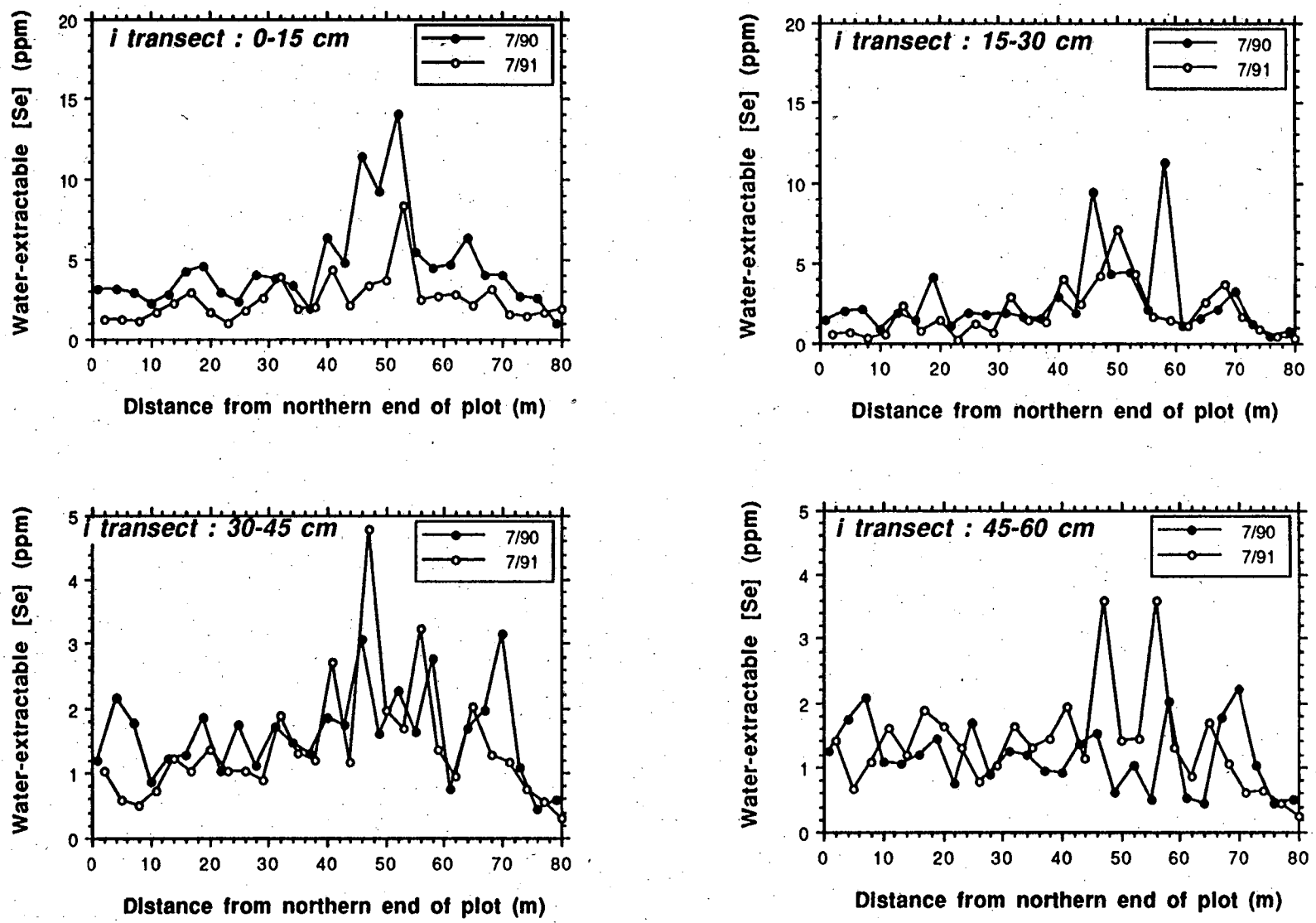

Figure 5.18. Water-extractable selenium (from 1:5 soil:water extracts), normalized to soil mass, in the irrigated treatment along a roughly N-S transect, 7/90 and 7/91.

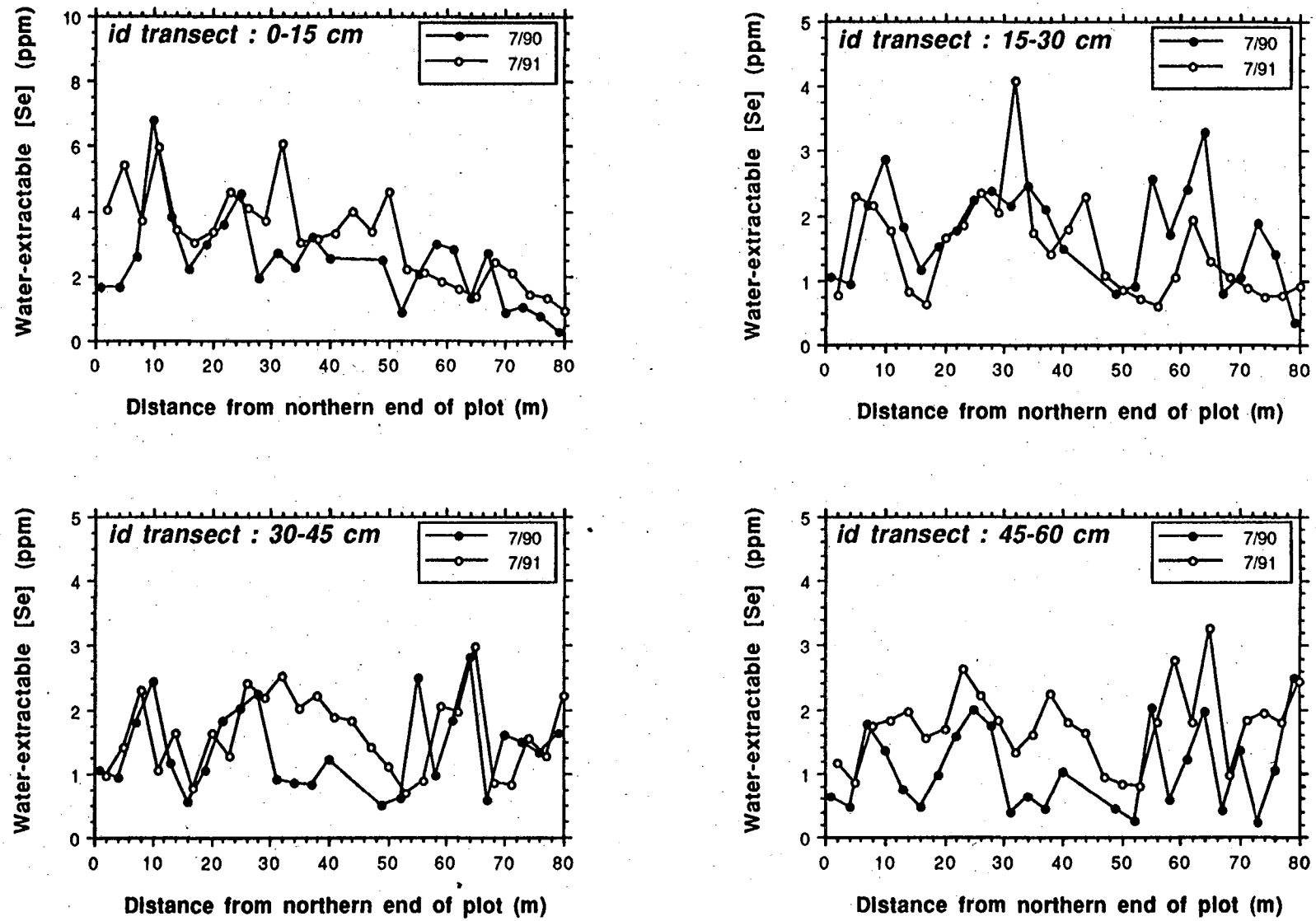

Figure 5.19. Water-extractable selenium (from 1:5 soil:water extracts), normalized to soil mass, in the irrigated/disked treatment along a roughly N-S transect, 7/90 and 7/91.

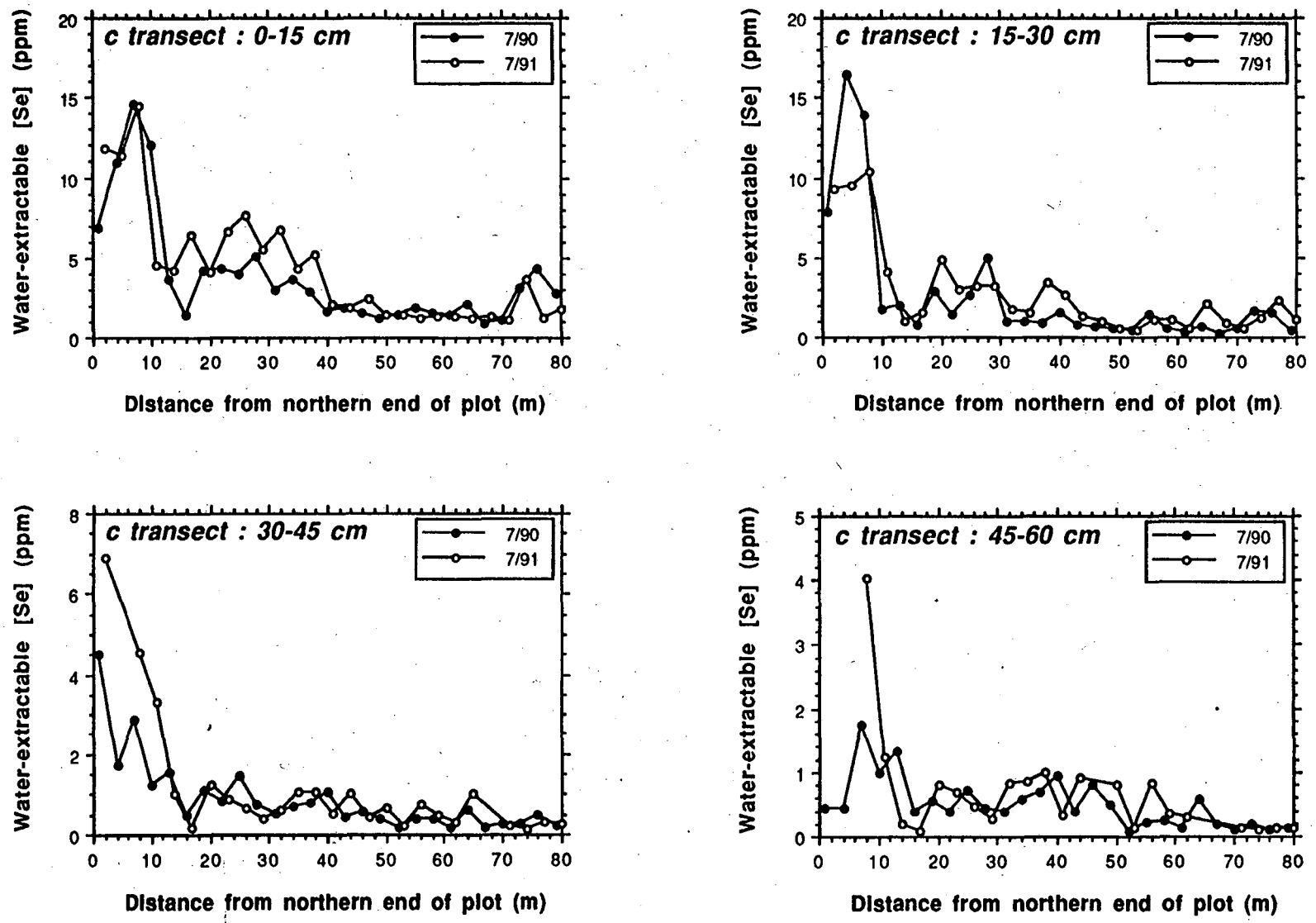

Figure 5.20. Water-extractable selenium (from 1:5 soil:water extracts), normalized to soil mass, in the controlled treatment along a roughly N-S transect, 7/90 and 7/91.

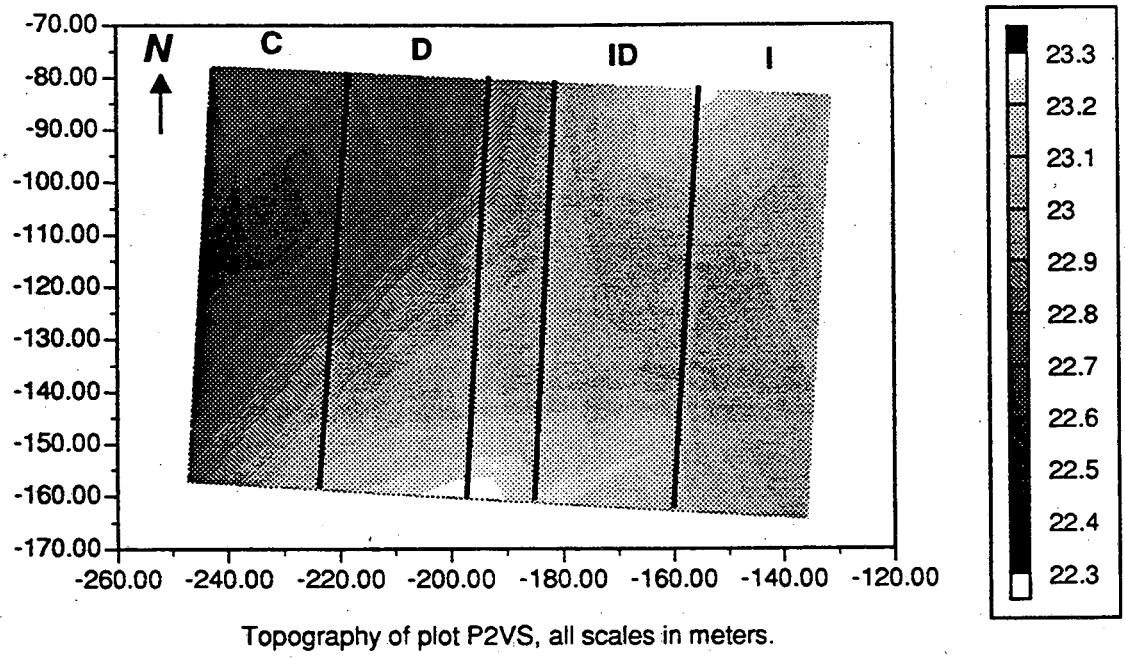

Figure 5.21. Results of survey of soil surface of plot P2VS.

February and early March rains, a significant redistribution of both selenium and salts below the depth of 40 cm was observed.

Both selenium and salts were flushed below a depth of 1 m. The last sample in the I treatment was taken on 5/9/91. Subsequent to that date the soil was too dry, primarily due to the invasion of that part of the plot by plants. However, based on the 5/91 data, it appears that soil water containing around 5 ppm of selenium was displaced into the 0.80 to 1.00 m interval and below. Even more significant changes in soil-water selenium were observed subsequent to early spring rains in 1992. It appears that most of the selenium and salts dissolved in the root zone were flushed below the 1 m depth. For example, selenium concentration at the 0.425 m decreased from about 4500 ppb in 12/91 to about 500 ppm in 4/92. The corresponding decrease in EC was from about 12.5 dS/m to about 6 dS/m.

Similar trends are observed in data from nest id1, representing the irrigated/disked treatment (Figures 5.26, 5.27). Due to the absence of plants in this treatment, samples of soil-water are available throughout the year. Therefore, a comparison may be made between concentrations in 8/90 and 8/91, which shows a large displacement of selenium from the 0 to 0.4 m depth interval to the 0.6 to 1.0 m interval. This is also seen, though not as dramatically, in the EC data. As in nest i2, early spring 1992 rains caused even more selenium displacement deeper

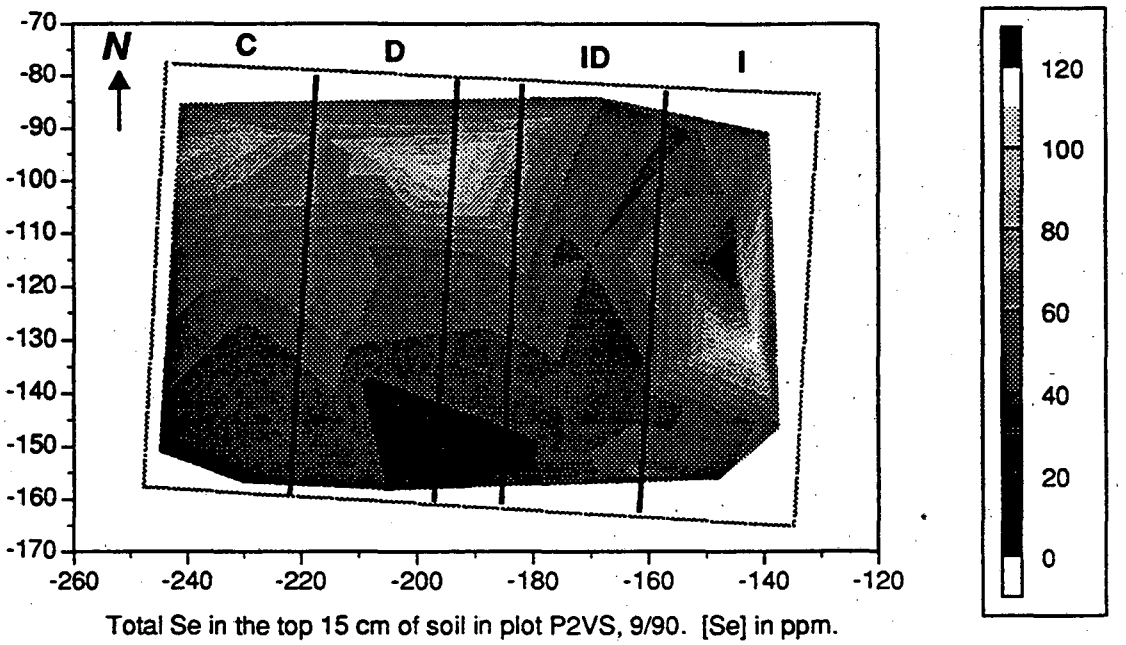

Total Se in the top 15 cm of soil in plot P2VS, 9/90. [Se] in ppm. Grid in meters.

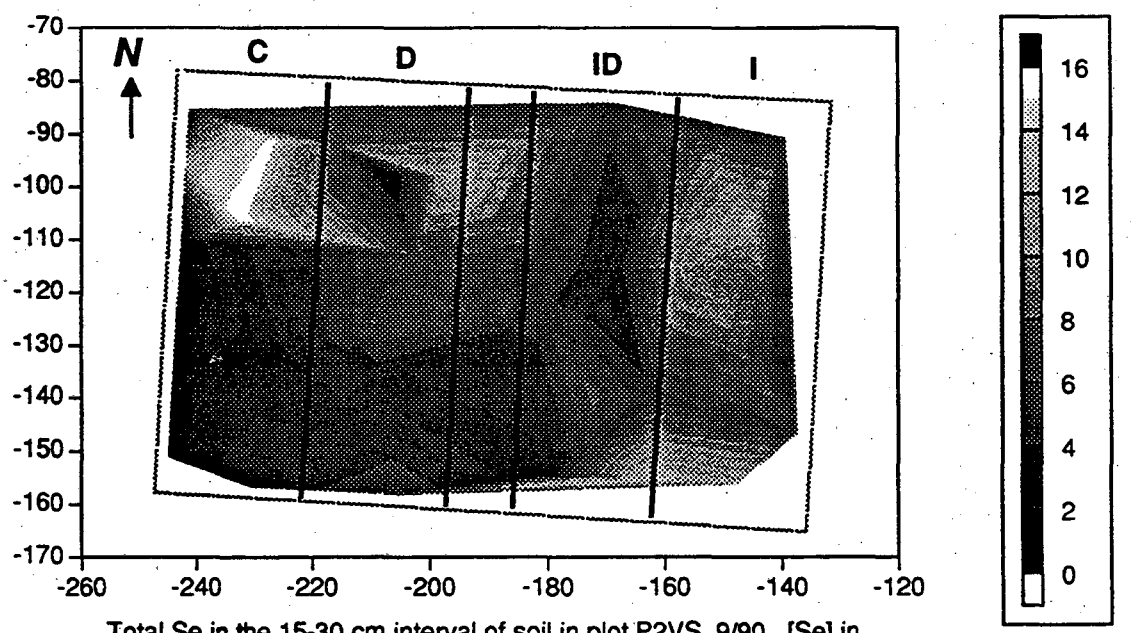

Total Se in the 15-30 cm interval of soil in plot P2VS, 9/90. [Se] in ppm. Grid in meters.

Figure 5.22. Contour maps of total selenium in the 0-15 cm and 15-30 cm depth intervals, based on subplot data from 9/90.

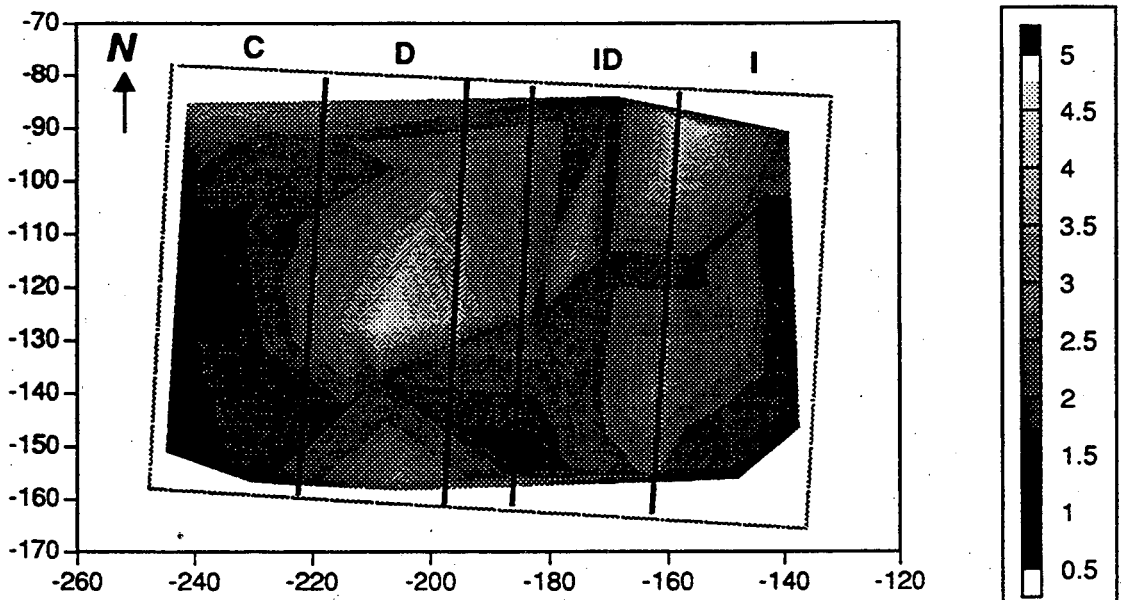

Total Se in the 30-45 cm interval of soil in plot P2VS, 9/90. [Se] in ppm. Grid in meters.

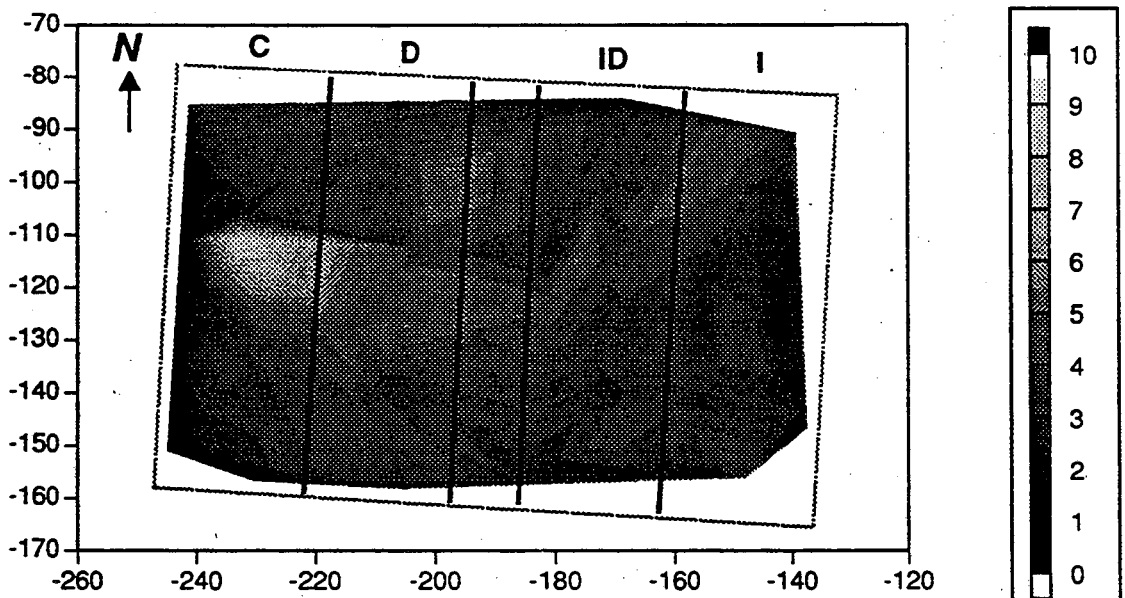

Total Se in the 45-60 cm interval of soil in plot P2VS, 9/90. [Se] in ppm. Grid in meters.

Figure 5.23. Contour maps of total selenium in the 30-45 cm and 45-60 cm depth intervals, based on subplot data from 9/90.

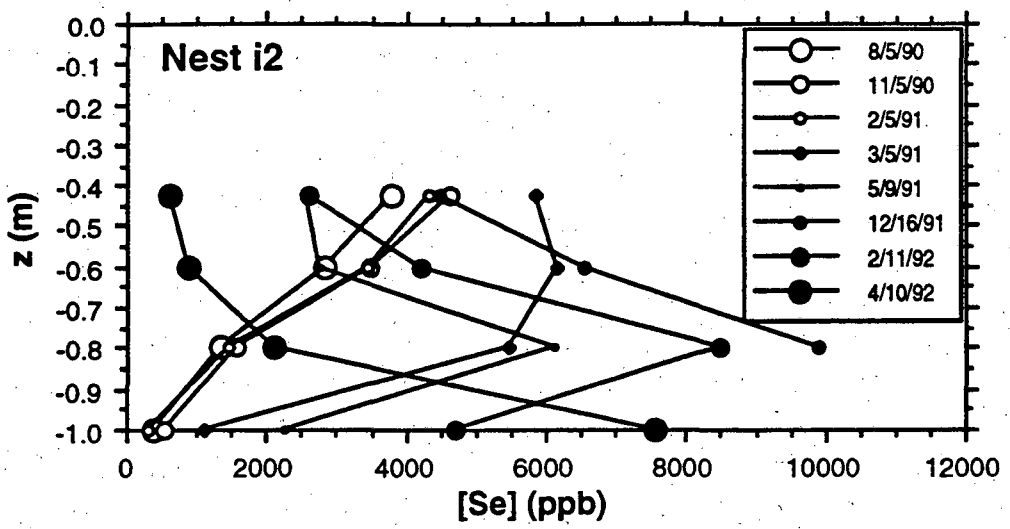

Figure 5.24. Soil-water Se, as sampled via soil-water samplers in nest i2, irrigated treatment.

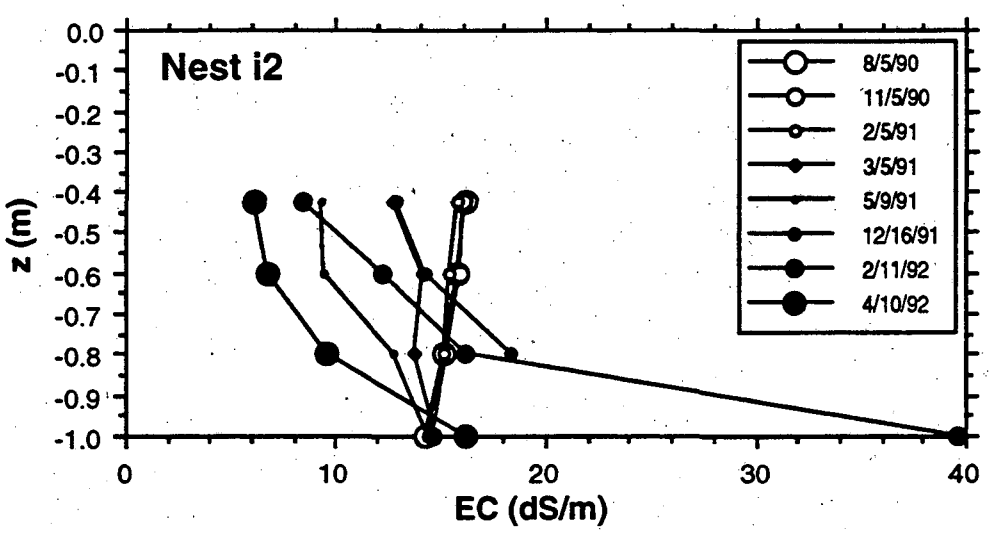

Figure 5.25. Soil-water EC, as sampled via soil-water samplers in nest i2, irrigated treatment.

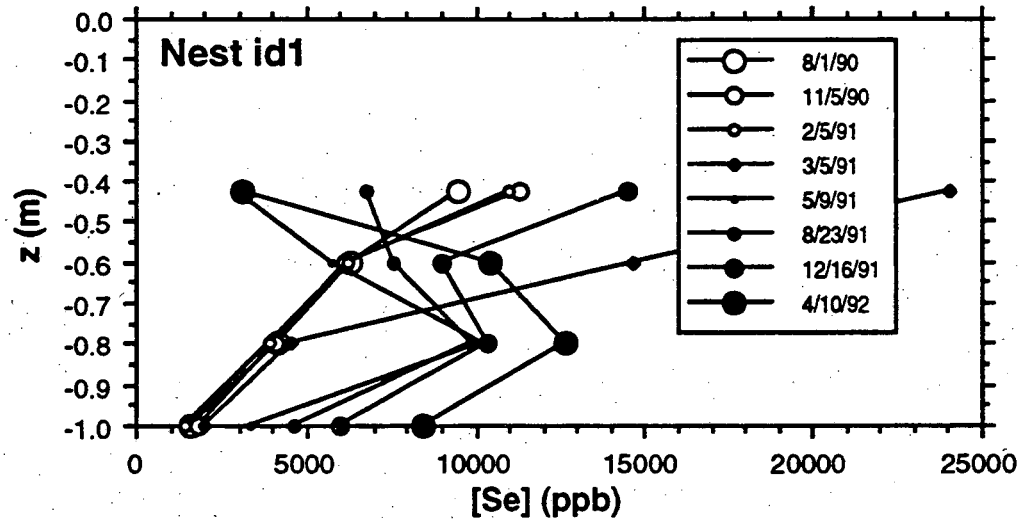

Figure 5.26. Soil-water Se, as sampled via soil-water samplers in nest id1, irrigated/disked treatment.

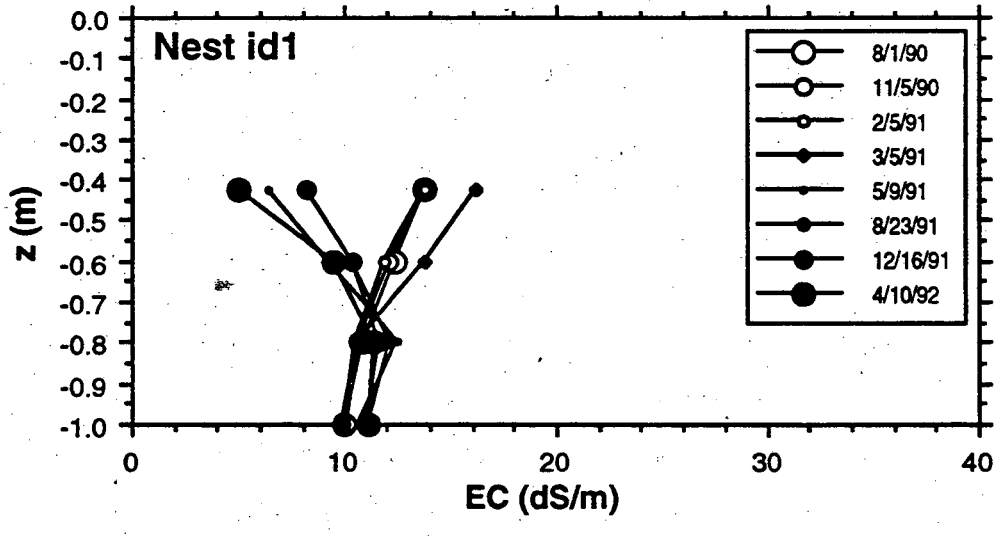

Figure 5.27. Soil-water EC, as sampled via soil-water samplers in nest id1, irrigated/disked treatment.

Downward flushing of solutes was also observed in the D treatment (Figures 5.28, 5.29). As seen in data from nest d2, there was an increase in the spring of 1991 in selenium concentrations at depths of 0.425 m and 0.60 m of around 5 ppm. Once again, this selenium was flushed down from overlying soil intervals. Further displacement occurred after spring 1992 rains, when selenium concentrations on the order of 2 ppm where flushed below the depth of 1 m. Similar, but less pronounced trends are also seen in EC data; changes in EC are more subtle due to the small vertical variations of salt concentrations in the soil profile.

Movement of solutes in treatment C, as observed through data from nest c2, is shown in Figures 5.30 and 5.31. Once more, there is extensive flushing of selenium and salts below the depth of 1 m. For instance, a net 6 ppm increase was observed between 8/90 and 6/91 at the 1 m sampler. It needs to be noted that samples from 2/11/92 were taken prior to the major rainfall events of the season and selenium concentrations and EC reflect a distribution caused by plant-root extraction of soil-water and the consequent salinization of the root zone. Also, the very low selenium concentrations on 4/10/92 are in part due to soil water flushing (as seen in the EC data) and in part due to selenium reduction. This nest is in an area of the plot which was ponded for several weeks each year following major storms.

5.4. Conclusions

Several comments need to be made about the correlation of soil-water sampler data and declines of total selenium in the bulk soil. First, data from soil-water samplers is often more representative of macropore concentrations rather than bulk soil concentrations of solutes. However, since both selenium concentrations and EC generally display trends which are consistent over periods of weeks to months, there is sufficient data to state that changes in dissolved selenium of up to 5 to 10 ppm have occurred in the soil profile of this plot. These changes are the result of downward flushing of soil-water by infiltrating rain water and redistribution of solutes due to plant-root water extraction (the latter applies to treatments I and C only). When translated to bulk selenium concentrations, these changes are on the order of 2 to 3 ppm and can account for much, but not all of the decline in total selenium in soil intervals below 15 cm. Clearly, this process cannot account for declines in total selenium in the 0 to 15 cm interval as observed in treatments I and ID. Data from soil samples taken in July 1992 (transect), and October 1991 and 1992 (subplots) will likely shed much light on the rates of selenium dissipation from surface soils in this plot. These samples are currently being processed and the data should be available within the next six months.

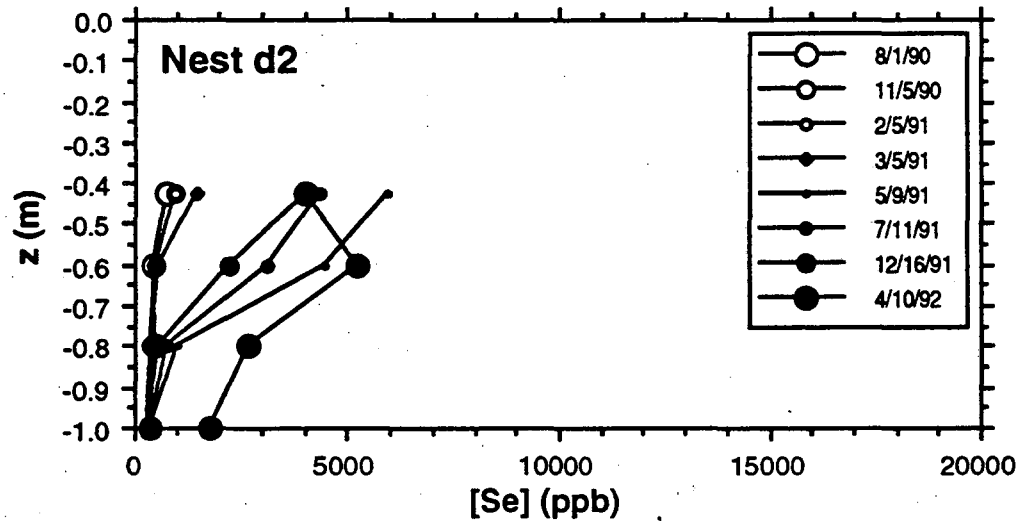

Figure 5.28. Soil-water Se, as sampled via soil-water samplers in nest d2, disked treatment.

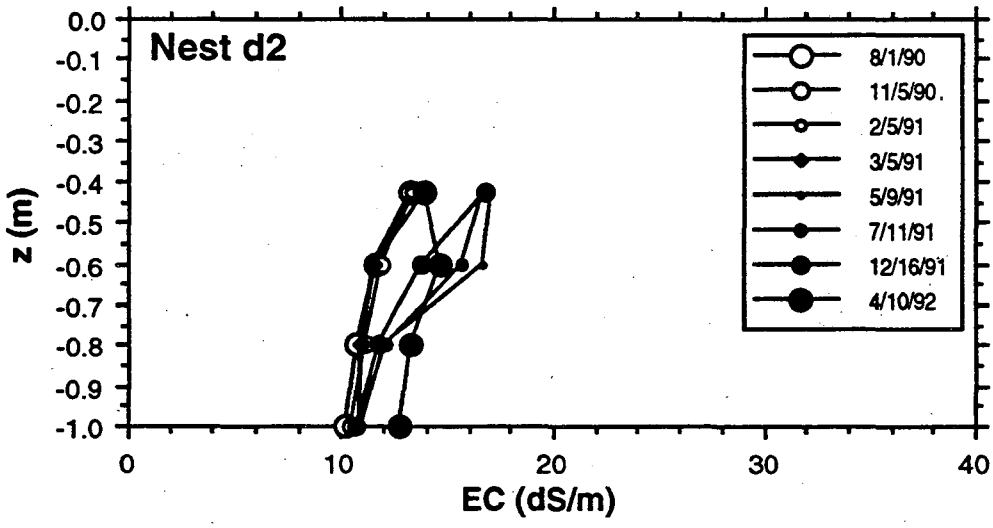

Figure 5.29. Soil-water EC, as sampled via soil-water samplers in nest d2, disked treatment.

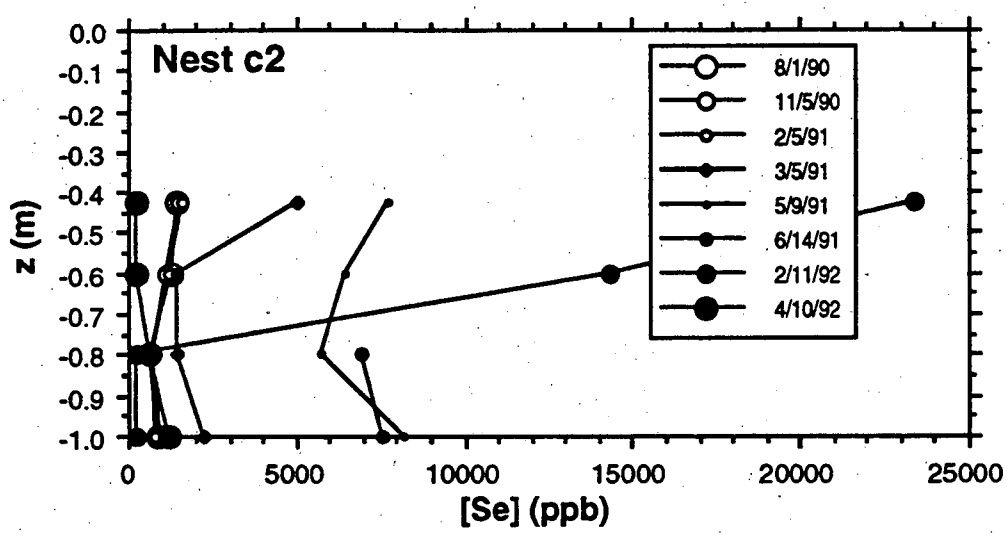

Figure 5.30. Soil-water Se, as sampled via soil-water samplers in nest c2, control treatment.

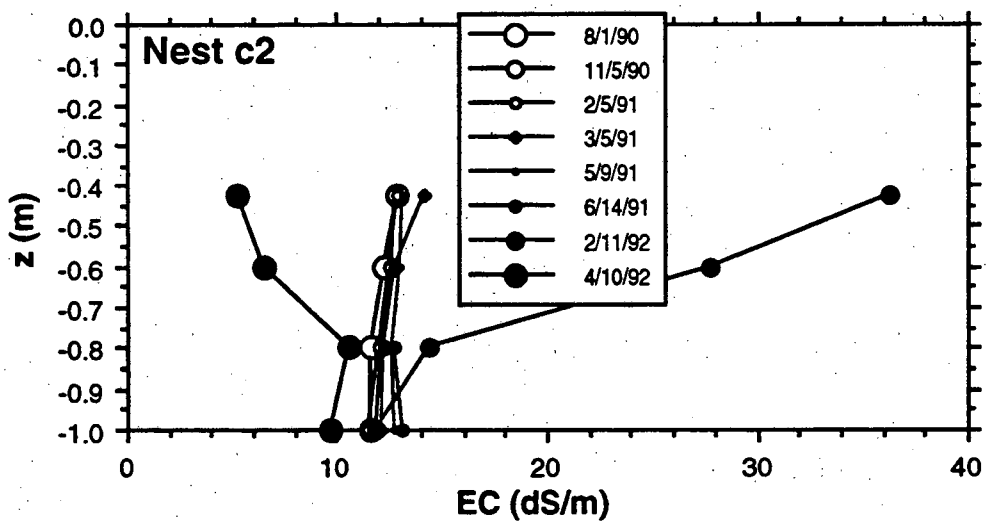

Figure 5.31. Soil-water EC, as sampled via soil-water samplers in nest c2, control treatment.

6.0. Laboratory Accelerations of Soil Selenium Transformations

Peter Zawislanski and Mavrik Zavarin
Earth Sciences Division
Lawrence Berkeley Laboratory

The future mobility and availability of selenium at Kesterson Reservoir will depend on changes in selenium speciation. Currently, selenium occurs predominantly in insoluble or minimally soluble forms (see e.g. LBL, 1990a,b). The oxidizing conditions which now prevail above the water table suggest that much of the inventory of selenium is in disequilibrium. (Under oxidizing conditions, selenium is expected to occur as highly soluble selenate at equilibrium.) It would be advantageous to gain an understanding of selenium transformation rates in order to predict future conditions at Kesterson Reservoir. Unfortunately, such rates are slow under field conditions, so slow in fact that year-to-year changes are sometimes too small to detect against the background of spatial variability and given the available analytical capabilities. Therefore, a laboratory experiment is currently underway in which rates of selenium transformations are accelerated relative to field rates. Soils from three Kesterson environments (cattails, saltgrass, playa) have been sampled, homogenized, and are being incubated in the laboratory under controlled conditions. Increased temperature is being used to accelerate selenium transformations.

Both theoretical considerations and laboratory data have shown that chemical and biochemical reaction rates are strongly dependent on temperature. Generally, it is considered that an increase of 10°C will increase reaction rates 2- to 3-fold (Reference). This rule-of-thumb should only be applied over a small range of temperature variations, especially when dealing with biological systems. Microorganisms from warm environments, or mesophiles, usually cannot tolerate temperatures in excess of 45°C (Brock, 1970). Therefore, even though an increase in temperature from 15°C to roughly 40°C will significantly increase microbial activity and related biochemical reactions, a further increase will result in a drastic slowing down and eventual death of the microorganism (Figure 6.1). The factor by which reactions are accelerated due to a 10°C rise in temperature, called Q_{10}, cannot be known a priori. Furthermore, the complexity of reactions taking place in a soil precludes the definition of a unique Q_{10} value. For the purpose of this experiment, a Q_{10} of 2.5 will be assumed.

6.1. Field-Sample Collection and Preparation

Soils for this experiment were collected from sites in three ponds on November 30th, 1990: Pond 2, a cattail area in the buffer zone of the P2VS plot; Pond 9, a predominantly *Bassia* vegetated playa

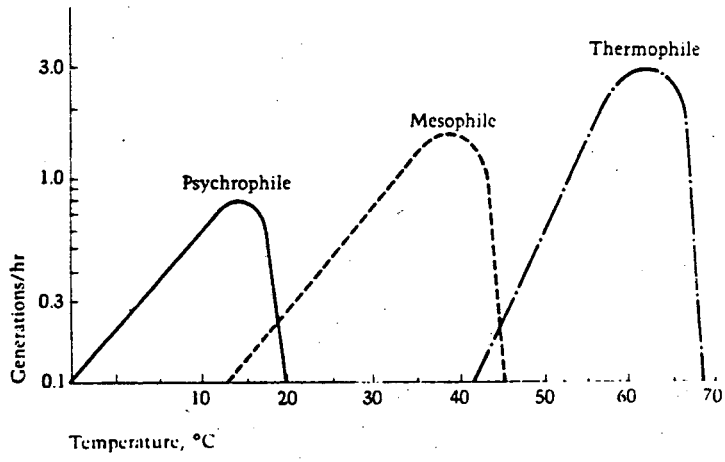

Figure 6.1. Relative growth rates of psychrophiles, mesophiles, and thermophiles as a function of temperature (from Brock, 1970).

between experimental plots P9C and P9D; and Pond 11, a saltgrass-covered area between plots P11S1 and P11S $^1/_2$. These three areas were identified as representing three of the four primary environments at Kesterson Reservoir. The fourth, filled environment, was not included in this experiment due to the fact that most of the selenium in the fill material is already in selenate form and in relatively low concentrations. Two soil intervals, 0.00-0.10 m (labeled "A") and 0.45-0.55 m (labeled "B") were sampled, in order to include both surface and subsurface soils in this experiment. Roughly 0.02 m^3 (5 gal) of soil was collected for each interval from each site. Samples were subsequently homogenized (by Brian Adkins, January 1991) to pass a 4.75 mm-mesh sieve. Field moisture content and moisture release curves (curve of water saturation vs. pressure) were determined for each soil at a dry bulk density of 1.0 gcm^{-3}. The table below summarizes these data (moisture release curves were measured using pressure cells).

Table 6.1. Gravimetric moisture content and moisture release curve of P2A,B, P9A,B, and P11A,B soils

Matric Potential	Gravimetric Moisture Content					
	P2A	P2B	P9A	P9B	P11A	P11B
Field Conditions	0.122	0.210	0.051	0.220	0.074	0.110
0 bar	0.65	0.55	0.48	0.82	0.63	0.60
-0.3 bar	0.365	0.217	0.210	0.491	0.312	0.202
-5 bar*	0.206	0.149	0.123	0.354	0.167	0.138

*5 bar values of gravimetric moisture content were slightly higher at the beginning of the experiment and were later refined

6.2. Experiment Design

The experiment consists of three separate but related parts. Subsamples of each soil (400 g in a 600 ml glass beaker), in duplicate, are subjected to different sets of conditions, which are combinations of three temperatures and two to four moisture contents (15°C, 25°C, 35°C; 0.3 bar, and 5 bar, plus 0 bar and air-dry). These variables were chosen to accelerate both microbial and chemical activity under high moisture and low moisture conditions. It is expected that biochemical reactions involving selenium will be accelerated to varying degrees in the three temperature environments. The average annual temperature at Kesterson Reservoir is around 15°C (15.2°C in 1988/1989). Therefore, reaction rate in soil kept at 15°C were used as a reference for comparison to reaction rates at two higher temperatures. In the 25°C environment, reactions should occur roughly 2.5 times faster. In the 35°C environment, the rate of these reactions should be roughly 6.25 (2.5 × 2.5) times higher. The differences in relative moisture content will predominantly have an effect on microbial activity, including microbial volatilization of selenium. It needs to be stressed that although this is a laboratory experiment, under controlled conditions, no effort is being made to distinguish between selenium speciation changes via chemical vs. biochemical reactions (except for microbial volatilization). Besides being difficult to make experimentally, this distinction is rather indeterminate in nature.

In Part I, a subsample of each soil, in duplicate, is subjected to six different sets of conditions, which are combinations of three temperatures and two moisture contents (15°C, 25°C, 35°C; 0.3 bar, and 5 bar). The rationale behind the choice of these temperatures is given above. The moisture contents chosen for this experiment are reasonable endpoints of a moisture content range in the field. Under extremely dry conditions during the summer, the matric potential in surface soils may be more negative than 5 bar, but on an annual average, this is not likely. Subsurface soils may experience a regime wetter than that equivalent to 0.3 bar matric potential, but this again is not likely over an annual period.

In Part II, a subsample of each surface soil ("A"), in duplicate, is subjected to varying temperature and moisture conditions. These variations have been designed to mimic seasonal changes at Kesterson Reservoir. Four "seasons" are introduced at 5-week intervals (due to elevated temperatures, a 5-week period is nominally equivalent to a 3-month period in the field.) Details of soil sample treatment are given in Table 6.2.

Part III consists of three sub-parts, α, β, and γ. In each of these experiments, a subsample of each surface soil ("A"), in duplicate, is subjected to constant temperature (either 25°C or 35°C), and widely varying moisture conditions. In part α, matric potential is allowed to fluctuate between 0 bar and 5 bar, in part β, it fluctuates between 0 bar to air-dry, and in part γ, it fluctuates between 0.3 bar and 5 bar. This experiment will help predict long-term effects of moisture fluctuations at the soil surface, including the effects of periodic flooding.

Table 6.2 Schedule for soil treatment in Part II.

Season	$T_{mean, field}$	$T_{mean, lab}$	P_{init}	P_{final}	Comments
Summer	23.4°C	35.0°C	5 bar	air-dry	Not watered for 5 weeks, after initial moistening
Fall	15.3°C	25.0°C	air dry	5 bar	5 bar reached after 3 weeks and maintained for 2 more
Winter	6.0°C	15.0°C	5 bar	0.3 bar	Held at 5 bar until 3rd day; brought to 0 bar on 8th day, allowed to dry to 0.3 bar and maintained for remainder
Spring	16.0°C	25.0°C	0.3 bar	5 bar	Brought to 0 bar on 7th day and allowed to dry to 0.3 bar over 2 weeks; maintained at 5 bar for remaining two weeks

6.3. Environmental Control

This experiment is being conducted in temperature-controlled chambers. The 15°C chamber is an incubator capable of both heating and refrigeration and is therefore very efficient and precise: diurnal temperature fluctuations rarely exceed ±0.5°C. The 25°C environment is maintained in an incubator capable of heating only. Therefore, on occasions when room temperature rises above 25°C, so does the temperature in this incubator. Such days are rare (see Fig. 6.2). When room temperature is less than 25°C, the temperature in the incubator is maintained within ±0.5°C. The 35°C chamber is a convection oven. It is slightly affected by diurnal variations in room temperature and has an effective precision of ±1.0°C. Temperature in all three chambers is closely monitored and adjusted as necessary.

Moisture content is controlled to within ±5% of the desired value by small additions of distilled water. Moisture content uniformity is maintained by periodic mixing of soil in the beakers and by injecting water not only from the surface but also via small holes in the soil, thereby wetting the soil up from the bottom. The 25°C and 35°C chambers have built-in fans which circulate and exchange air. The volume of the 15°C incubator is much larger than the volume of the samples inside of it and does not have a fan, but is opened daily to allow for air exchange.

6.4. Sampling, Extraction, and Analysis

Table 6.3 summarizes the schedule for the subsampling and extraction of soils in all three parts of the experiment.

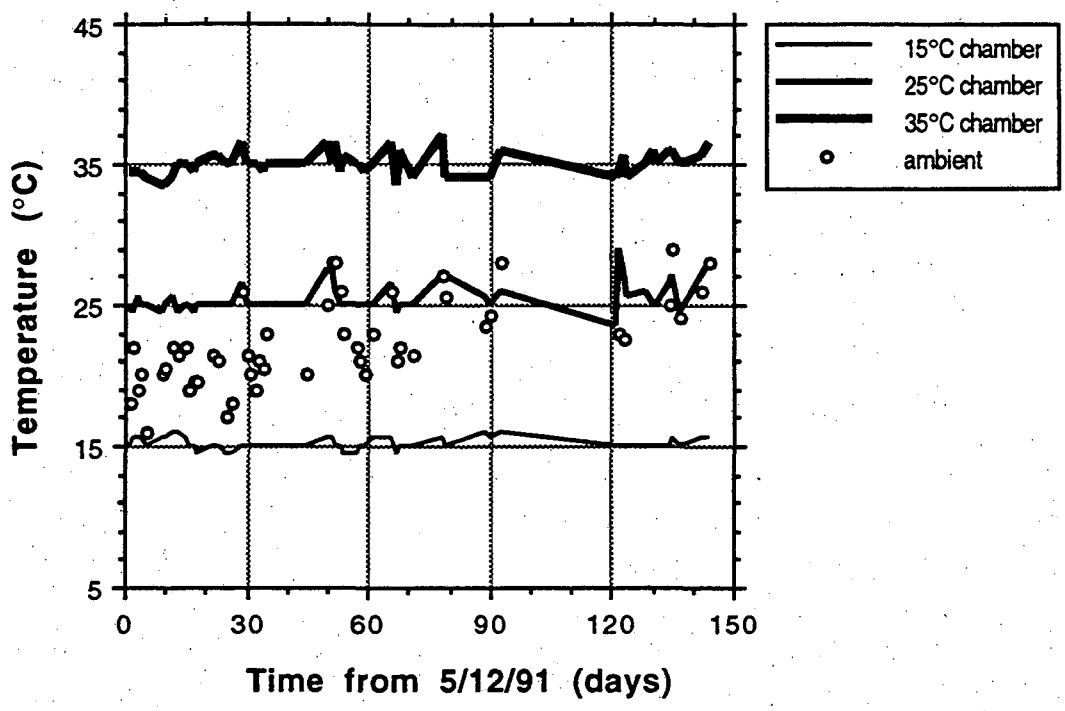

Figure 6.2. Incubator and room temperature over the first 144 days of the experiment.

Table 6.3. Sampling and extraction frequency for incubated soils

PART	Sampling Frequency	Frequency of DW Extract	Frequency of PO_4 Extract	Frequency of NaOH Extract	Frequency of Total Acid Digest
I	13 wks (quarterly)	13 weeks	13 weeks	13 weeks	26 weeks
II	20 wks (1 "lab-year")	20 weeks	20 weeks	20 weeks	20 weeks
III	6 months	26 weeks	26 weeks	26 weeks	26 weeks

DW extract = distilled water extract, 1:5 soil:water, 1-hour on shaker table, filtered.

PO4 extract = Na_2HPO_4 extract, 1:20 soil:Na_2HPO_4, 0.001M, 24-hour on shaker table, filtered.

NaOH extract = NaOH extract, 1:10 soil:NaoH, 0.02M, in 85°C bath for 2 hours, shaken for 5 minutes every 30 minutes, filtered. Sequential after phosphate extract.

Total Acid Digest = 110°C HNO_3 and 30% H_2O_2 wash followed by repeated washes with 6M HCl at 110°C; 8M urea added, then filtered. Final dilution - 1:200 soil:extractant.

Note: The frequency of sampling and extraction may be reduced if periodic changes are not significant.

The distilled water extract will liberate a readily available fraction of selenium. The phosphate extract will also liberate the readily soluble fraction as well as most of the adsorbed selenium; both extractions will tend to dissolve salts which may contain selenium. For this and other reasons, these

The distilled water extract will liberate a readily available fraction of selenium. The phosphate extract will also liberate the readily soluble fraction as well as most of the adsorbed selenium; both extractions will tend to dissolve salts which may contain selenium. For this and other reasons, these extractions are not unique and the results should be considered to be approximations of selenium fractions in soil. The sodium hydroxide extract will liberate organically-bound selenium. Again, the same proviso of non-uniqueness applies. The total acid digest is a fairly good approximation of total selenium in a soil.

6.5. Initial Selenium Speciation

All of the above extractions were performed on homogenized bulk samples of each soil. Water extracts (WX), phosphate extracts (PO4X), and total acid digests (TAD) were done in triplicate; sodium hydroxide extracts (NaOHX) were done in duplicate. In all extracts, except for the TAD, field-moist soil was used; air-dry soil was used for the TAD. Based on these extracts, selenium speciation was estimated, and broken down into "soluble" selenite, "soluble" selenate, "adsorbed" selenium (predominantly selenite), "organically-associated" selenium (on average 60% selenite/40% selenate), and "refractory" selenium, which refers to the fraction which was not extracted by any other method but TAD. The results are shown in Figures. 6.3 through 6.5, where selenium fractions are shown as percentages of the total inventory. The main feature of this fractionation is the predominance of refractory selenium in surface soils (P2A:75%; P9A:79%; and P11A:70%), and soluble selenate in subsurface soils (P2B:62%; P9B:46%; and P11B:43%). Organically-associated selenium is the second-most common form in all soils except for P9B, where the inventory is almost split between soluble and refractory selenium. As expected, surface soils have higher total selenium concentrations than subsurface soils, by 1 to 2 orders of magnitude, with soil P2A having by far the most total selenium, 92.7 ppm. Table 6.4 summarizes concentrations of all fractions.

6.6. Results of Quarterly Sampling - Part I

Soils from Part I were sampled subsequent to three months of incubation. Three months of real time at 25°C are nominally equivalent to 7.5 modelled months; three months of real time at 35°C are nominally equivalent to 19.8 modelled months (assuming a Q_{10} of 2.5). Each soil sample was homogenized and subsampled. All soils were water-, phosphate-, and hydroxide-extracted. TADs were not performed since changes in total selenium over this relatively short time interval were not likely to be detected. However, air-dried subsamples of soils were preserved for potential future extractions. Figures 6.6. through 6.11 contain a summary of extraction results. All values are normalized to dry soil mass. Each data point is a mean of two replicate extractions.

The most noticeable changes are observed in soil P2A (Figure 6.6), with results being virtually the same for both moisture regimes (0.3 bar and 5 bar). An increase with temperature of water soluble selenate is observed, with concentrations peaking at around 19 ppm at 35°C. This is roughly a 5.5-fold increase relative to the initial concentration. At the same time, adsorbed selenium concentrations declined with

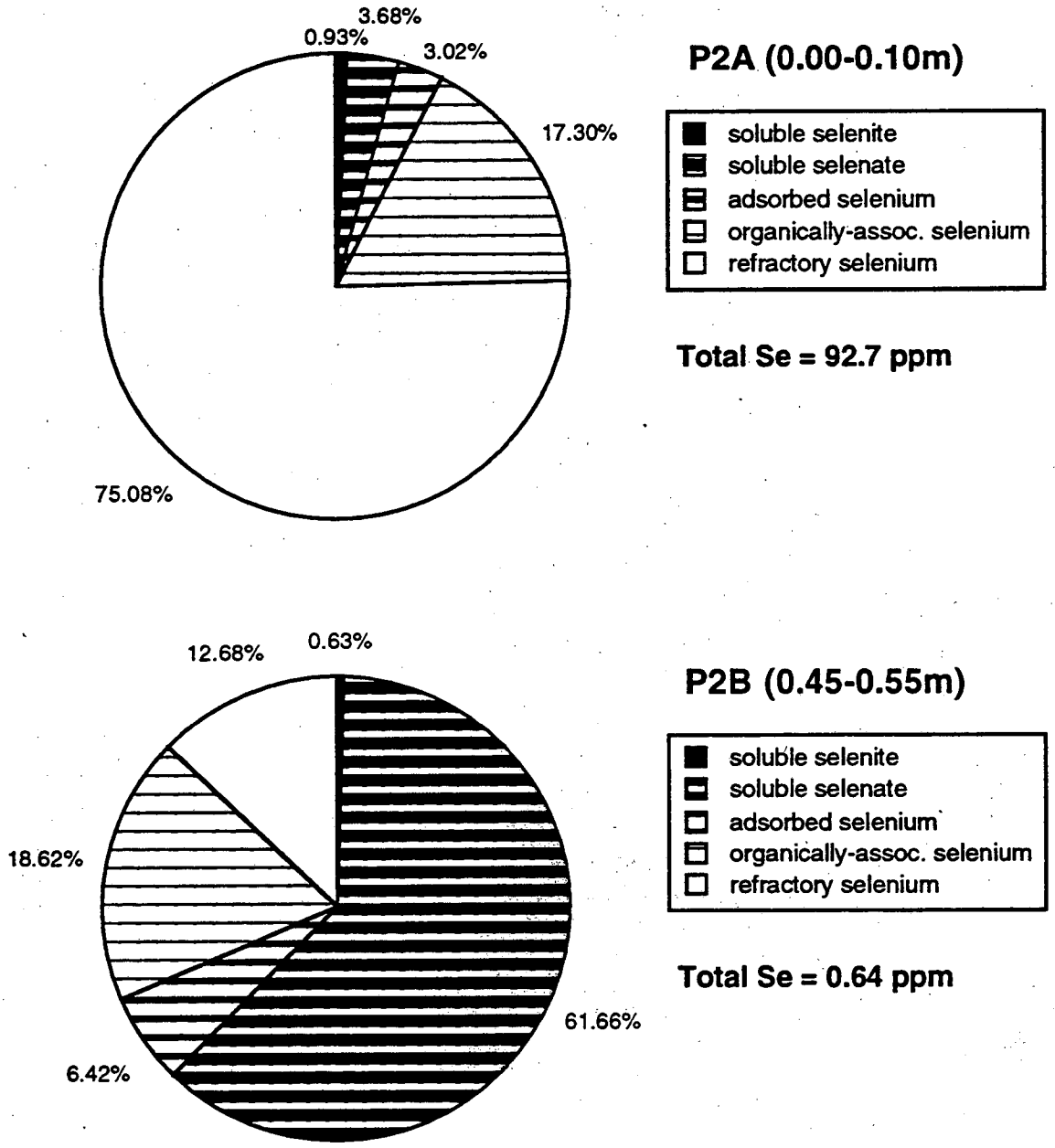

Figure 6.3. Initial fractionation of selenium in soils from plot P2VS: P2A - 0.00-0.10 m and P2B - 0.45-0.55 m.

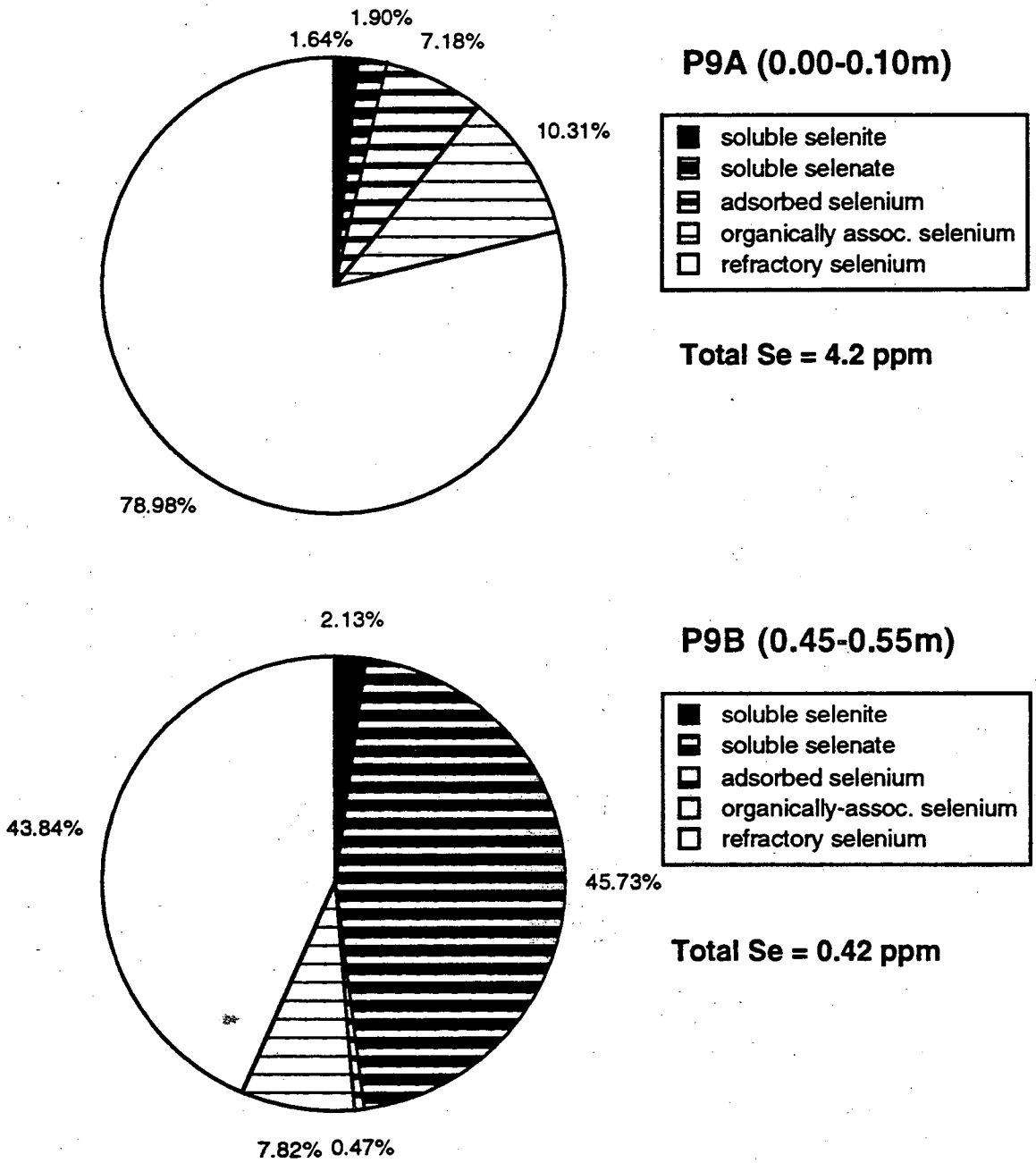

Figure 6.4. Initial fractionation of selenium in soils from plot P9TM: P9A - 0.00-0.10 m and P9B - 0.45-0.55 m.

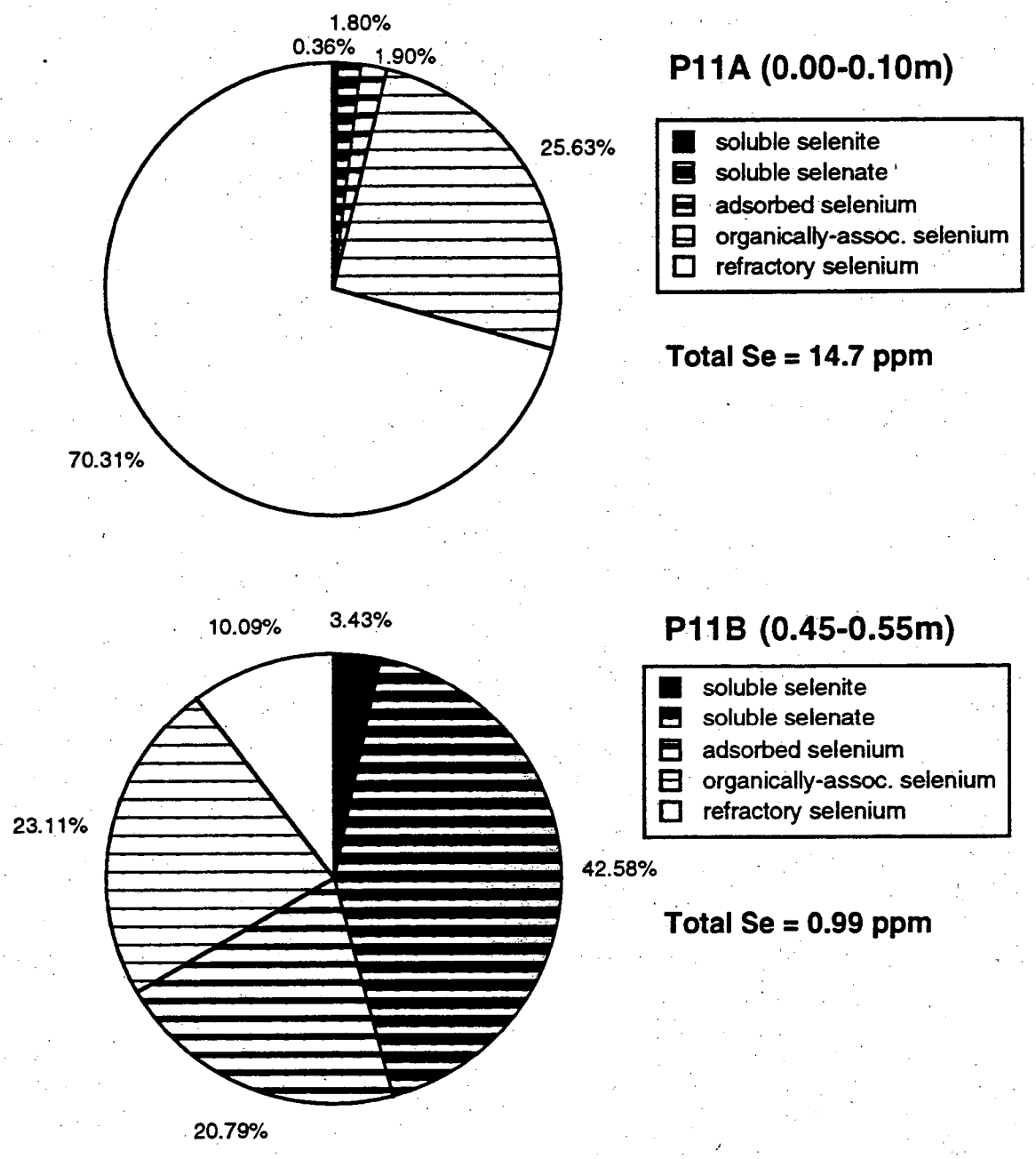

Figure 6.5. Initial fractionation of selenium in soils from plot P11TM: P11A - 0.00-0.10 m and P11B - 0.45-0.55 m.

Table 6.4. Initial selenium fractionation in soils (all values in ppm)

Fraction	P2A	P2B	P9A	P9B	P11A	P11B
Se(IV)	0.859	0.004	0.069	0.009	0.053	0.034
Se(VI)	3.41	0.394	0.080	0.193	0.265	0.422
Se(ads)	2.80	0.041	0.303	0.002	0.279	0.206
Se(org)	16.0	0.119	0.435	0.033	3.77	0.229
Se(refr)	69.6	0.081	3.33	0.185	10.3	0.100
Se(total)	92.7	0.640	4.22	0.421	14.7	0.992

temperature by roughly 30% (0.3 bar) to 90% (5 bar). Even though there are fluctuations in organically-associated selenium, there is no clear trend and variations may be due to a larger uncertainty in organic selenium determination. There appear to be no changes in water-soluble selenite concentrations. Given the small absolute changes in other selenium fractions, approximately 90% of the soluble selenate increase must be due to the oxidation of a more refractory fraction. This corresponds to an oxidation of 14 ppm of the initial 69.6 ppm of the refractory selenium fraction of 35°C.

A slight decline in water soluble selenate was observed in soil P2B (Figure 6.7) . There is no obvious explanation for a decline of the soluble, more oxidized fraction. The apparent changes in organic selenium could be an artifact of soil variability and analytical uncertainty. No clear trends emerge from data from soil P9A (Figure 6.8), at either moisture content, with the exception of an apparently significant upward trend in water soluble selenate at 5 bar. In soil P9B (Figure 6.9) there appears to have been a decrease in soluble selenate from the initial concentration. However, since selenate concentrations at the three temperatures and two moistures contents are not significantly different from each other, it is possible that the initial sample may not have been representative of the bulk soil. Otherwise, there are no other significant trends.

Significant increases in water-soluble selenate concentrations were observed in P11A soils, at 35 °C, with patterns being similar for both moisture contents (Figure 6.10). Selenate concentrations increased from the initial 0.265 ppm to roughly 1.5 ppm. Adsorbed selenium concentrations appear to have dropped to zero. There is no clear trend in organically-associated selenium concentrations, which range from roughly 4 ppm to 5.3 ppm. Since the increase in selenate is within range of organic-selenium concentration variations, it is not possible to determine whether the additional soluble selenium came from the refractory pool.

An upward trend in soluble selenate and concentrations is observed in P11B silts (Figure 8.11). There was also a slight decline in adsorbed selenium. The significance of these changes will become apparent with future sampling and analysis.

6.7. Results of Quarterly Sampling - Part II

Subsamples of soils in Part II were taken on 10/4/91, after 20 weeks under varying conditions which were outlined in Table 6.2. These were water-, phosphate-, and hydroxide-extracted. A total acid digest was also performed, but results of analysis are not yet available. Results of the three extracts are shown in Figure 6.12. In soil P2A, there were increases in both the water-soluble selenate fraction and the organically-associated selenium and a decrease inadsorbed selenium. The magnitude of the changes falls between the Part I results at 15°C and 25°C for this soil (compare with Figure 6.6). In soil P9A, there were decreases in all fractions, except the organically-associated selenium which registered an increase. Except for the "adsorbed" selenium fraction, these changes are within the range of "noise" observed in Part I for this soil (compare with Figure 6.8). Finally, there were small increases in all fractions except for soluble selenite in soil P11A. This suggests the liberation of a small but significant fraction of the refractory selenium. All these results are preliminary.

6.8. Summary

Given the short duration of the experiment thus far, making any firm conclusions would be premature. However, trends which can be easily identified (P2A and P11A), are those of soluble selenium increase and the concurrent oxidation of the refractory pool. In Part I, an approximately 5.5-fold increase in selenate was observed in both P2A and P11A soils at 35°C, which corresponds to the oxidation of 22.4% and 12.0% of the refractory selenium inventory, for P2A and P11A respectively. Such changes were not observed in other soils, possibly due to relatively lower organic matter contents, if one assumes that microbial activity is critical in oxidation of refractory selenium. Also, a decline in adsorbed selenium is observed in most soils, potentially indicating a shift toward selenate.

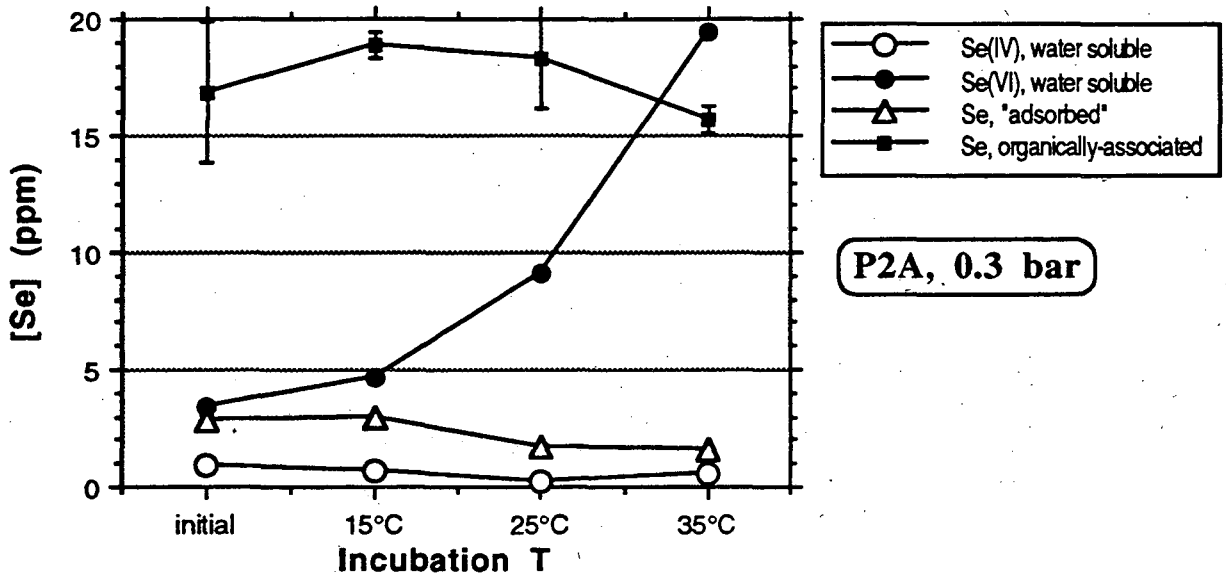

Figure 6.6a. Changes in selenium speciation in soil P2A, at 0.3 bar, initial extracts vs. extracts after 3 months of incubation. Error bars denote one standard deviation.

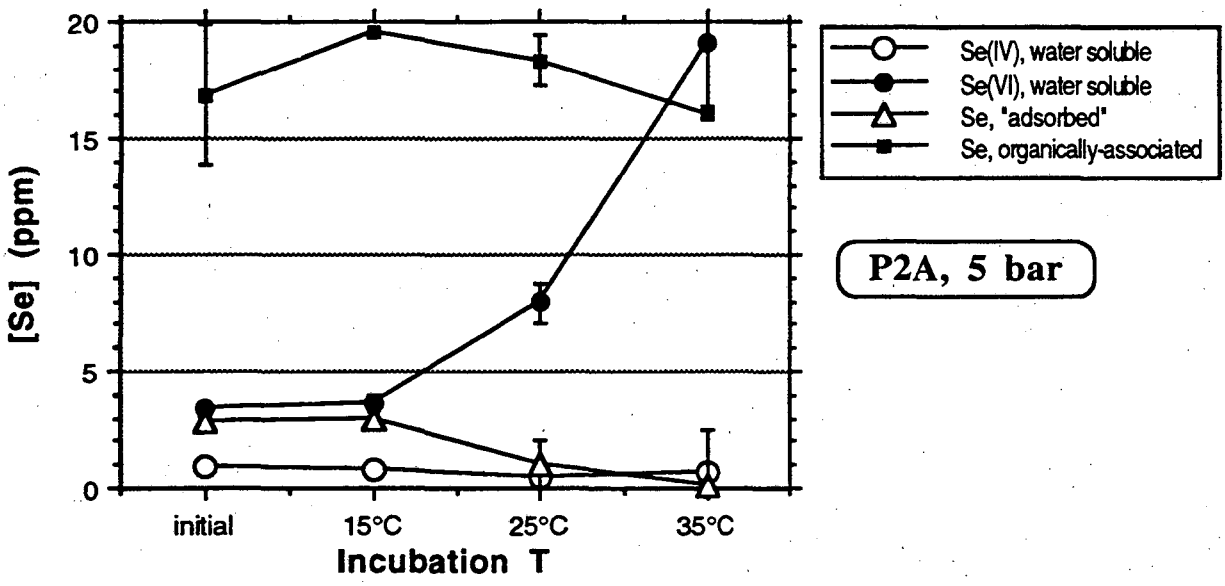

Figure 6.6b. Changes in selenium speciation in soil P2A, at 5 bar, initial extracts vs. extracts after 3 months of incubation. Error bars denote one standard deviation.

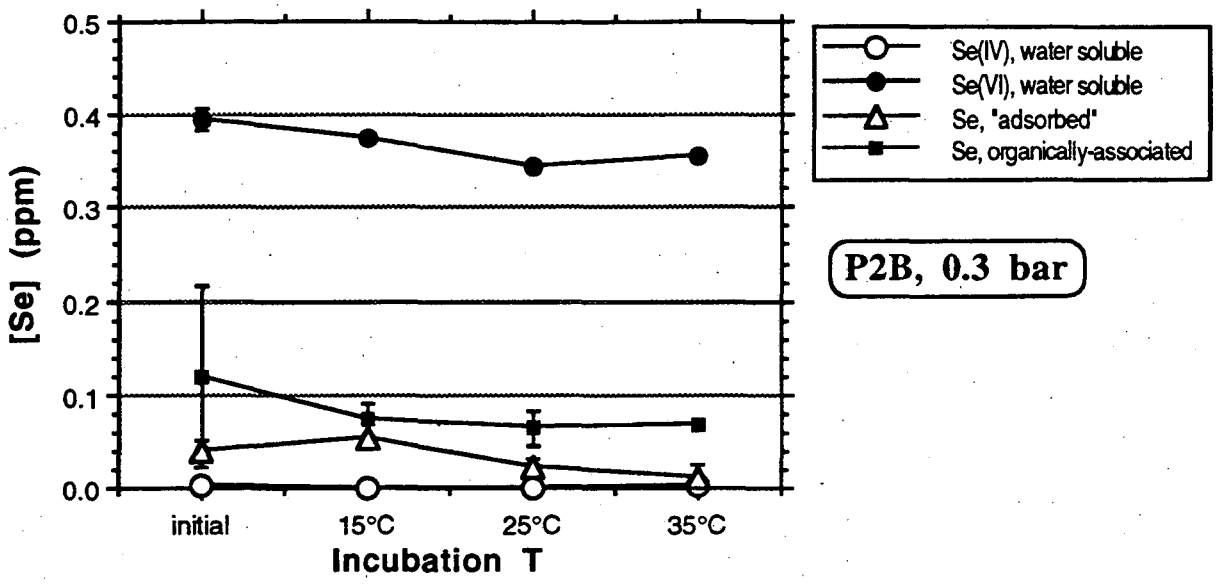

Figure 6.7a. Changes in selenium speciation in soil P2B, at 0.3 bar, initial extracts vs. extracts after 3 months of incubation. Error bars denote one standard deviation.

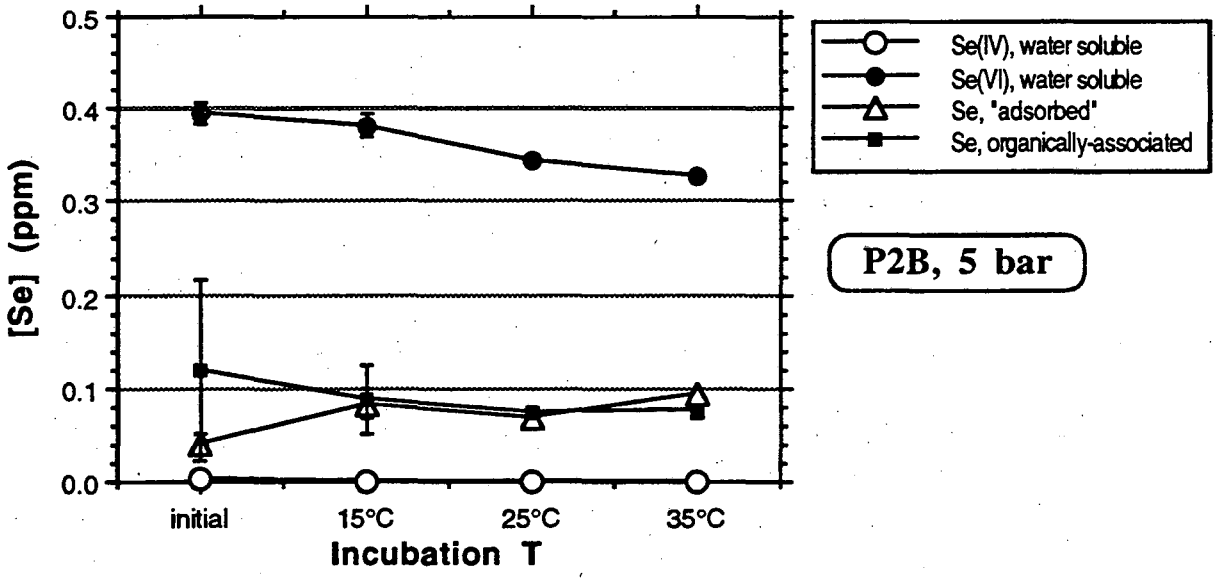

Figure 6.7b. Changes in selenium speciation in soil P2B, at 5 bar, initial extracts vs. extracts after 3 months of incubation. Error bars denote one standard deviation.

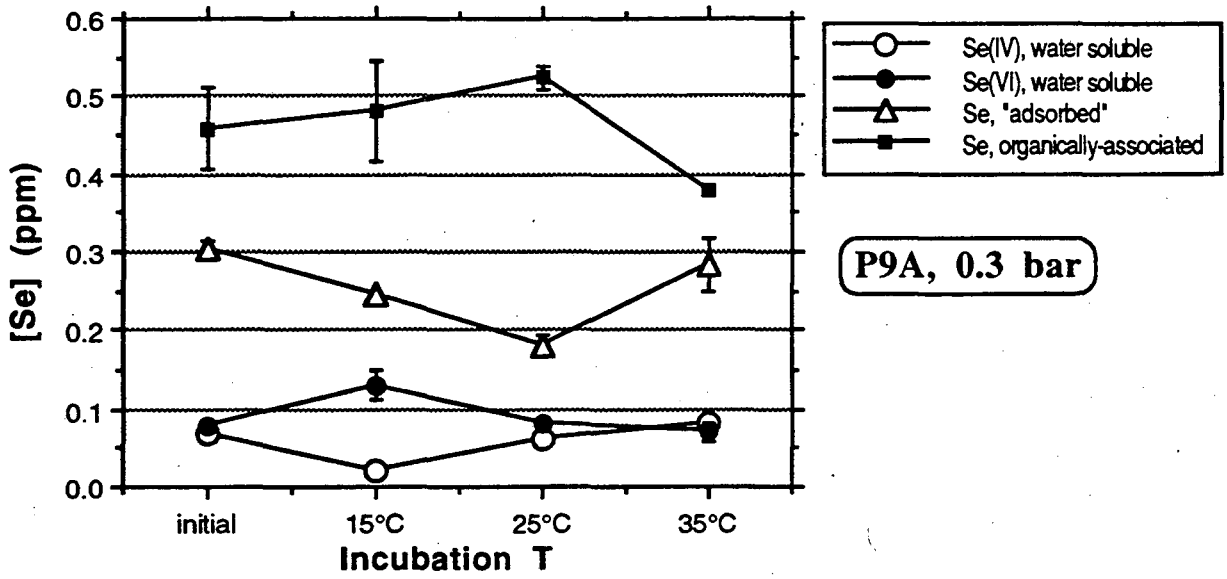

Figure 6.8a. Changes in selenium speciation in soil P9A, at 0.3 bar, initial extracts vs. extracts after 3 months of incubation. Error bars denote one standard deviation.

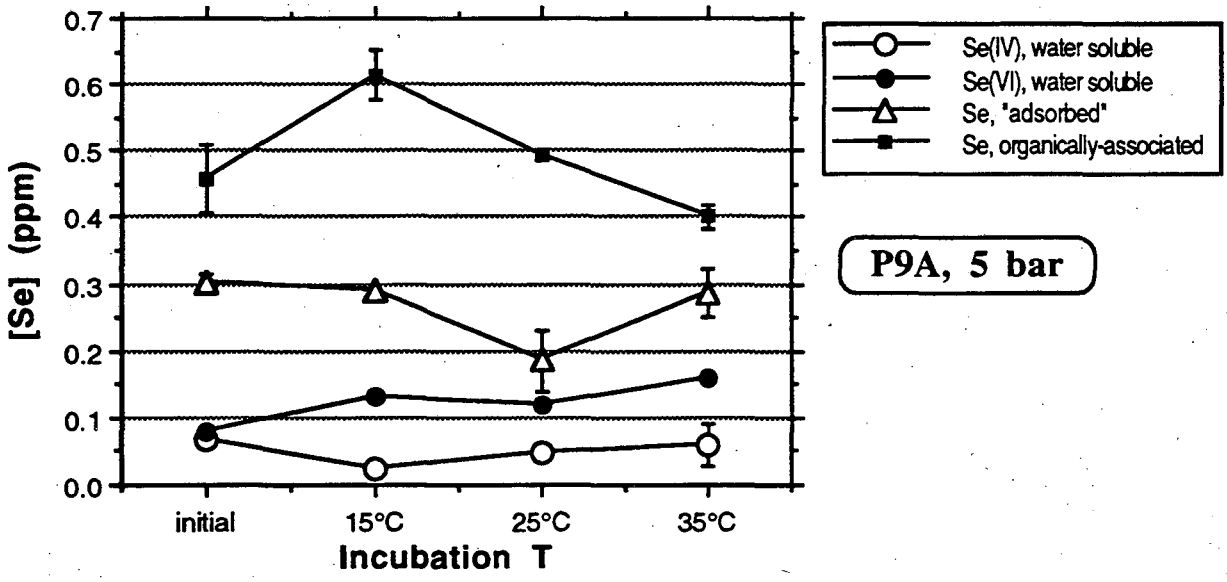

Figure 6.8b. Changes in selenium speciation in soil P9A, at 5 bar, initial extracts vs. extracts after 3 months of incubation. Error bars denote one standard deviation.

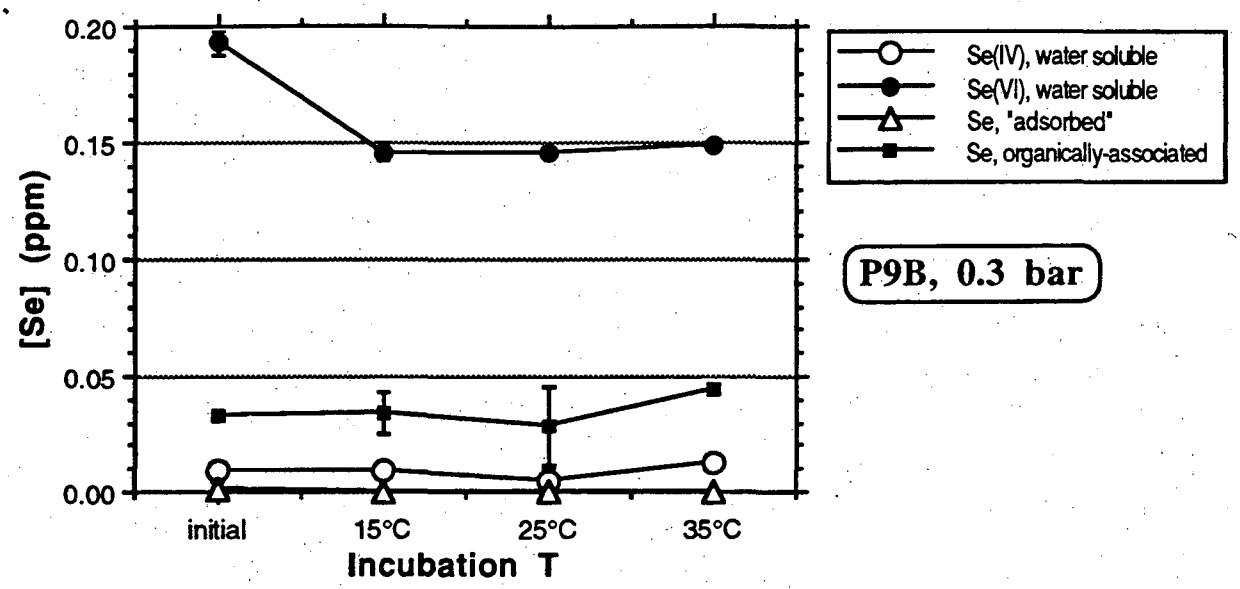

Figure 6.9a. Changes in selenium speciation in soil P9B, at 0.3 bar, initial extracts vs. extracts after 3 months of incubation. Error bars denote one standard deviation.

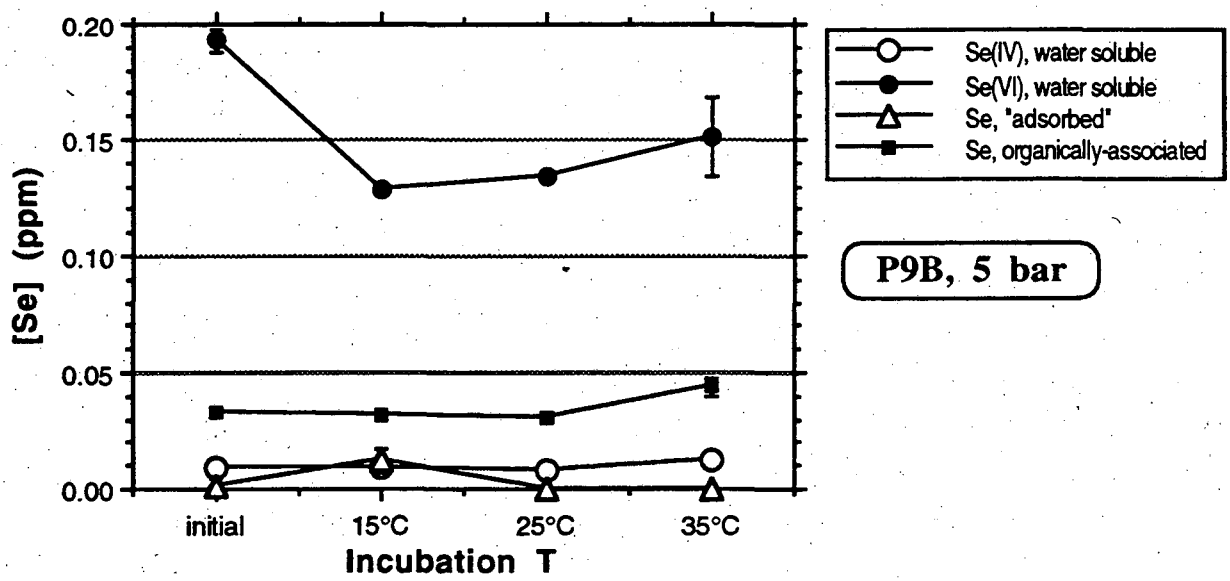

Figure 6.9b. Changes in selenium speciation in soil P9B, at 5 bar, initial extracts vs. extracts after 3 months of incubation. Error bars denote one standard deviation.

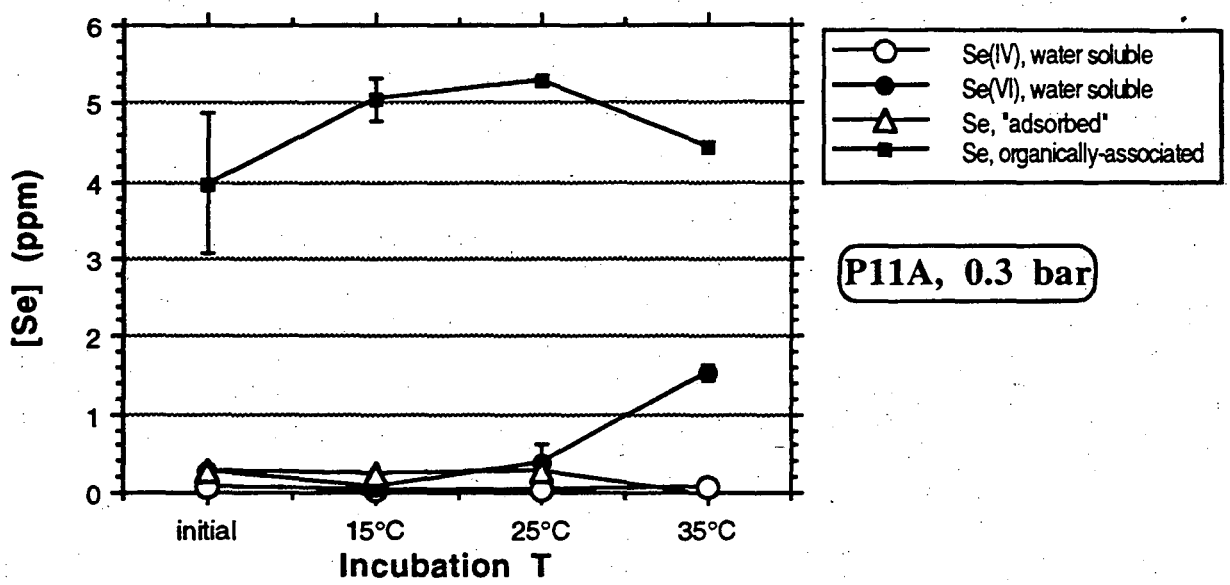

Figure 6.10a. Changes in selenium speciation in soil P11A, at 0.3 bar, initial extracts vs. extracts after 3 months of incubation. Error bars denote one standard deviation.

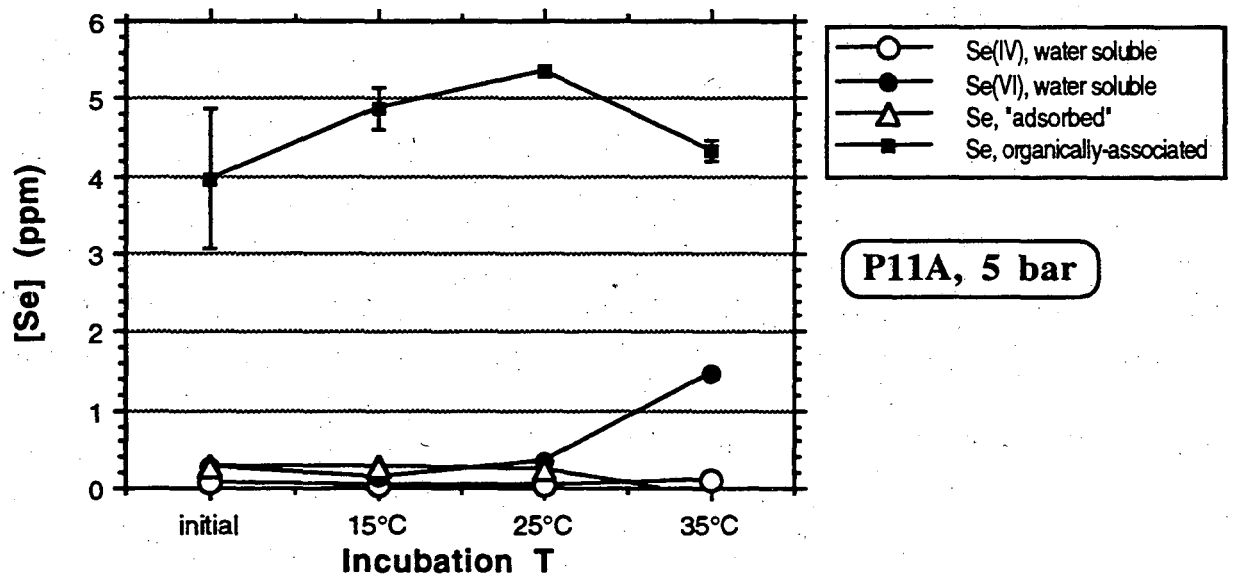

Figure 6.10b. Changes in selenium speciation in soil P11A, at 5 bar, initial extracts vs. extracts after 3 months of incubation. Error bars denote one standard deviation.

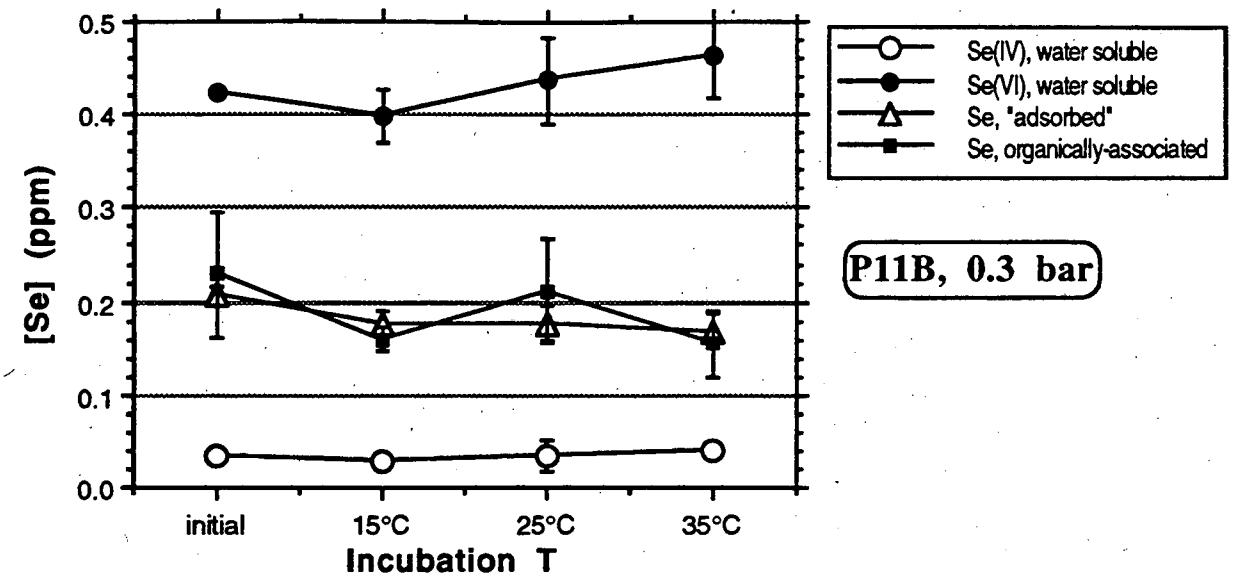

Figure 6.11a. Changes in selenium speciation in soil P11B, at 0.3 bar, initial extracts vs. extracts after 3 months of incubation. Error bars denote one standard deviation.

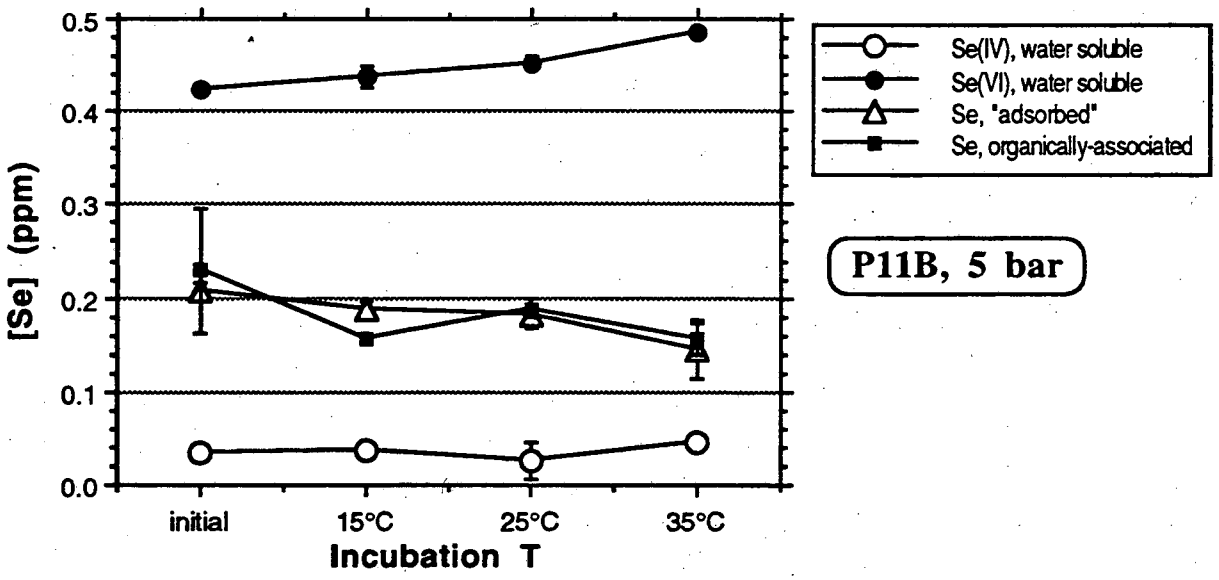

Figure 6.11b. Changes in selenium speciation in soil P11B, at 5 bar, initial extracts vs. extracts after 3 months of incubation. Error bars denote one standard deviation.

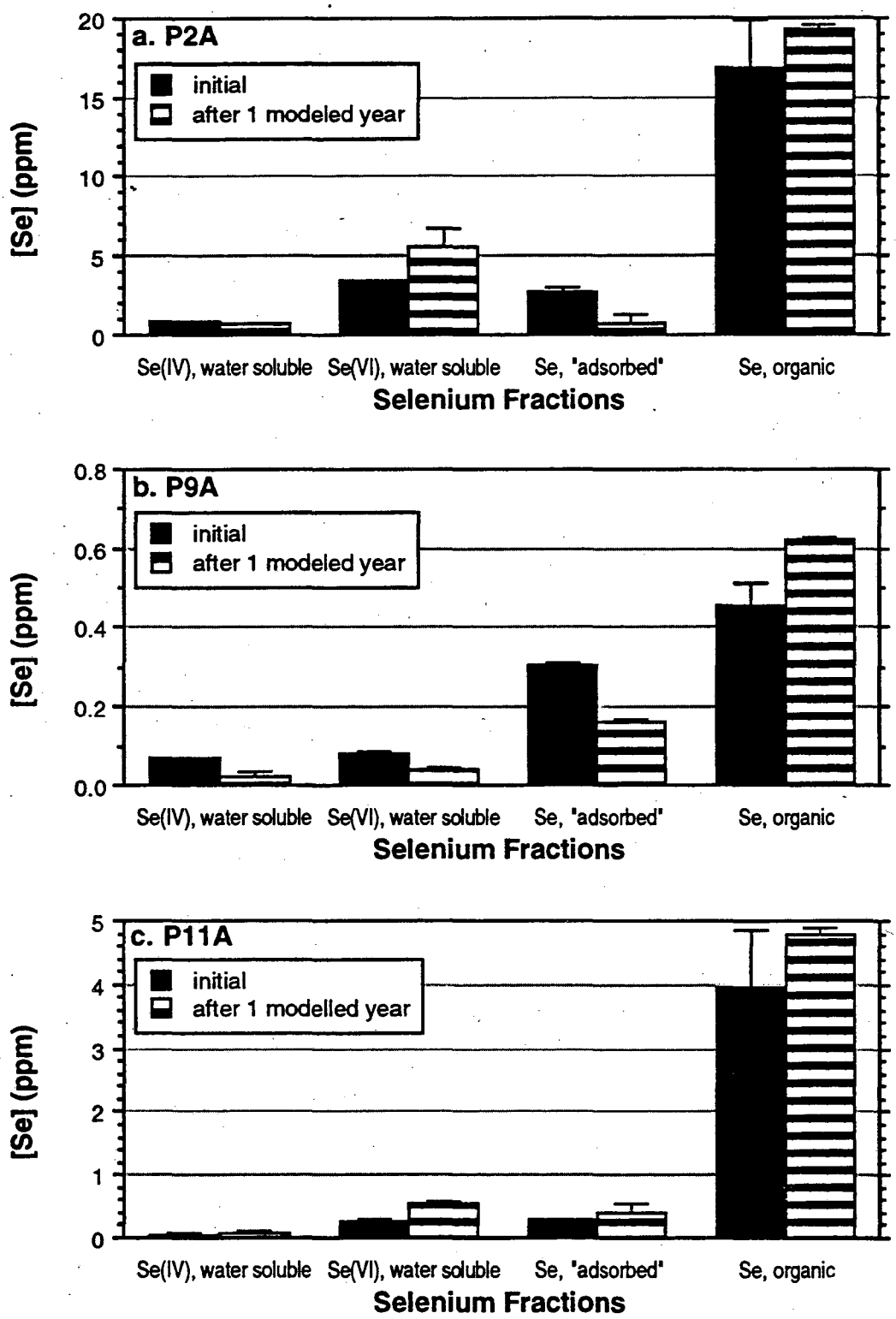

Figure 6.12. Changes in selenium speciation in Part II, initial extracts vs. extracts after 1 "modeled" year, or 20 real weeks.

7.0. Water Quality in Winter 1992 Ephemeral Pools

Tetsu Tokunaga and Paul Johannis
Earth Sciences Division
Lawrence Berkeley Laboratory

Considerably higher than average rainfall at Kesterson Reservoir during February 1992 resulted in the formation of a large number of relatively persistent ephemeral pools. While the 1982 to 1992 average February rainfall at Kesterson Reservoir is 59 mm, the February 1992 rainfall amounted to 151 mm (USBR, Kesterson Reservoir weather data). Most of this precipitation occurred on 2-12-92 when 77 mm was recorded in the CIMIS weather station located in Pond 5. (The USBR rain gauge overflowed at 52 mm.) Prior to February, the 1991-1992 rainfall (90 mm) was below the average cumulative precipitation (July through January) of 122 mm (USBR data, 1982 to 1992). The cumulative 1991-1992 rainfall from July through February of 241 mm is 33% greater than the average cumulative annual rainfall for these months (181 mm, USBR data). Summaries of Kesterson Reservoir rainfall data collected since 1982 appear in Figures 7.1a and 7.1b.

Unlike previously observed periods of ephemeral pool formation at Kesterson Reservoir, rainfall was considerably above average for February 1992, and served as the sole source of surface water. Our previous experience with monitoring ephemeral pools differed in two ways. Prior to covering of much of the Reservoir with fill soil in the summer of 1988, ephemeral pool water quality reflected a mix of runoff from permanently flooded pools, soil water displaced upwards by water table rise, and rainfall. Ephemeral pools sampled in 1987 and 1988 (Tokunaga and Benson, 1992) provided water quality information relevant for these pre-fill conditions. Ephemeral pool water samples collected since filling, but prior to the February 1992 storms, have been limited to short term pools because of below-average rainfall. Thus the 1992 rains provided the first opportunity to monitor water quality over moderately long periods in large, post-fill ephemeral pools.

In the first section, data on pool water quality immediately following the major February 12, 1992 rain storm will be presented. In the second section, time trends in ephemeral pool water selenium concentrations and salinity (EC) will be presented. Brief discussions follow both sections.

7.1. Water Quality in Ephemeral Pools Shortly After the Feb. 12, 1992 Rain

Prior to the major rainfall event on Feb. 12, 1992, only minor ponding of rain water was observed. After the major storm event, an estimated 50% of the Reservoir experienced

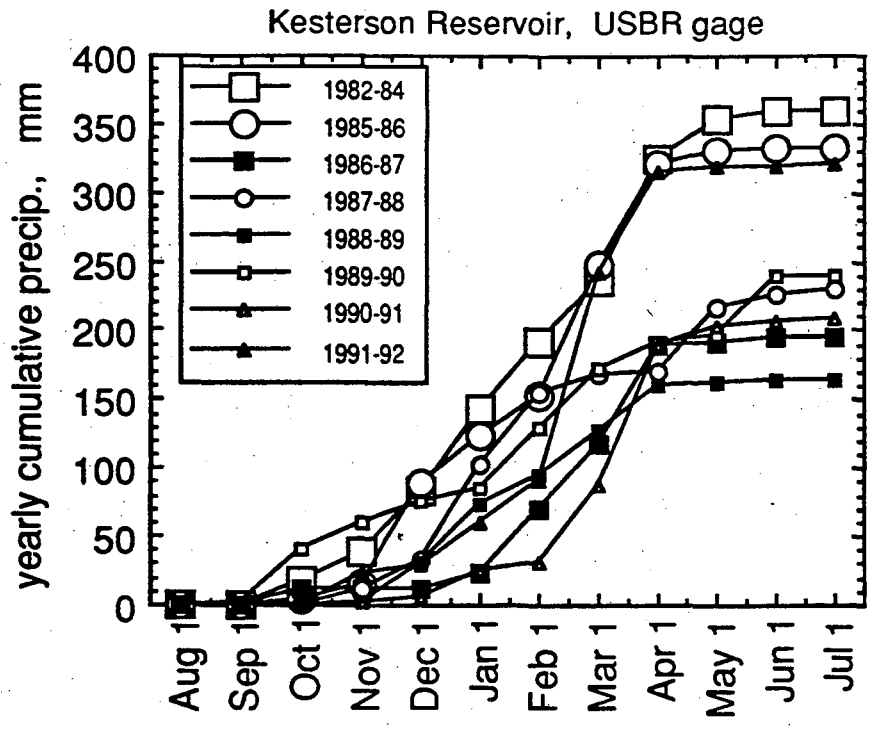

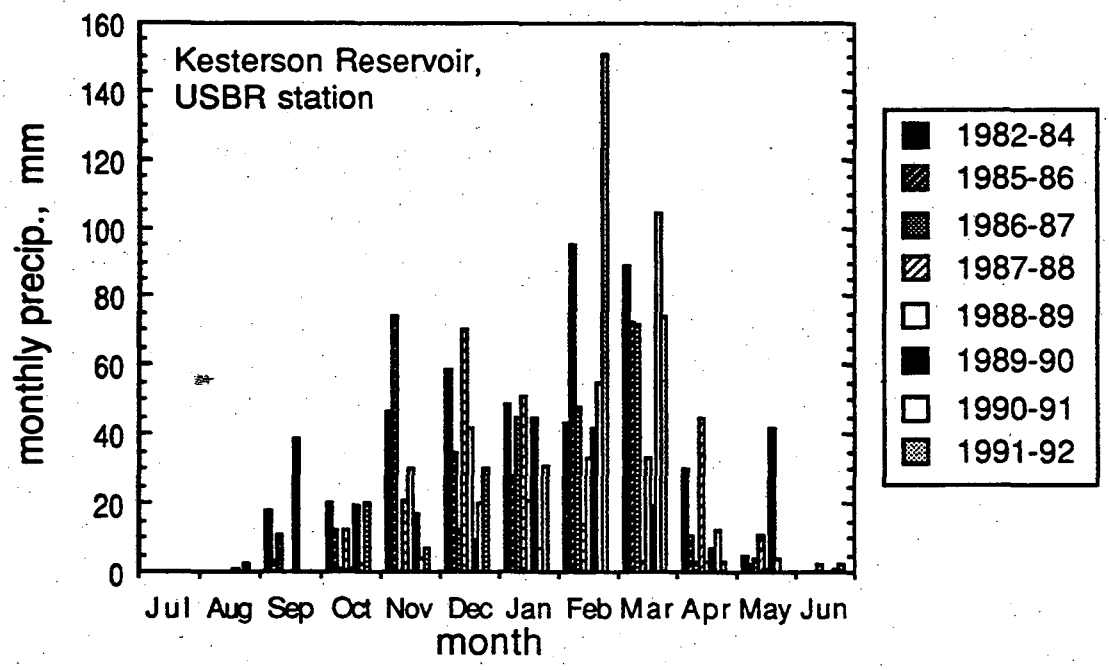

Figure 7.1. (a) Yearly cumulative rainfall at Kesterson Reservoir. The data are primarily from the USBR weather station, supplemented with CIMIS records. (b) Monthly total rainfall at Kesterson Reservoir.

ponding for some period of time. In this section, water quality data from surface water samples collected within 9 days after this storm are presented. Sampling during this period was relatively intensive, and provides data from a range of ponding environments.

7.1.1. Data

Table 7.1 provides a listing of the surface waters sampled shortly after the 2-12-92 storm. Included in the table is information on sampling locations, surface soil (original Kesterson soil or fill), site vegetation, estimated ponded area and ponding depth, electrical conductivity, pH, and total dissolved Se. (A key to abbreviations used in the vegetation column is provided at the end of the table.) In Figure 7.2, the selenium concentrations are shown distributed according to general locations, primarily by pond number. Also included in this figure are selenium concentrations measured in Mud Slough and Fremont Canal, and in pools formed along the perimeter of the Kesterson Reservoir ponds.

In Figure 7.3, data on 94 samples collected only from the Kesterson Reservoir ponds are plotted in terms of probabilities of exceeding particular concentrations of selenium. This plot was constructed by arranging data in increasing order of selenium concentrations, and assigning equal probabilities to each sample concentration. With this assumption, the probability of exceeding a particular concentration of selenium simply becomes equal to the fraction of samples with concentrations greater than this reference value. It should be noted that a better way of generating this type of probability function would take into account the individual pool sizes. However available estimates of pool sizes are poor and are not suitable for quantitative use. Histograms of selenium concentrations in these surface waters are presented in Figures 7.4a and 7.4b. In Figure 7.5, selenium concentrations in the ephemeral pool waters are plotted against their corresponding EC values. The diagonal line labeled "drain water line" represents the nominal relation between selenium concentrations and EC values in the case that a seleniferous pre-closure Kesterson Reservoir pond water is either diluted or evaporatively concentrated. The line represents

$$[\text{Se, } \mu\text{g/L}] = 25*(\text{EC, dS/m}) \ .$$

This relation probably predicts a slightly higher than average relation between the original Kesterson Reservoir selenium concentrations and EC values. A coefficient of 20 in the above equation gives closer to average correlations. The slightly higher slope used in the line was intended to provide an upper envelope for comparisons described in the following section.

7.1.2. Discussion

Very rough correlations between ephemeral pool selenium concentrations and Kesterson Reservoir pond number appear in Figure 7.2. Selenium concentrations in ephemeral pool waters

Table 7.1. Summary of surface water samples collected between February 15 and February 21, 1992.

Feb.15-21,'92 KR Pools

COMMENTS	POND #	SURFACE WATER SAMPLING LOCATION	soil	vegetation	date	approx. area m2	approx. depth mm	EC dS/m	pH	total Se µg/L (ppb)
representative data on	off-site	Fremont Canal, south of Pond6	NA	NA	2/16/92	NA	NA	3.030	7.1	23.7
surface waters sampled in and	off-site	Mud Slough at Pond 10 (near LBL site P10GC)	NA	NA	2/15/92	NA	NA	2.300	7.0	7.6
around Kesterson Reservoir on										
Feb. 15, 16, 20, and 21 '92.	off-site	S border of Pond 1, (near gauge cover)			2/21/92			0.537	7.3	1.0
The main rainfall event occured	off-site	S border of Pond 1			2/21/92			0.434	7.2	0.5
on Feb. 12, 1992 (77mm =3.0")	off-site	S border of Pond 1			2/21/92			0.464	7.3	0.8
	off-site	S-SE border of Pond 1, near well KR 52			2/21/92			0.466	7.2	0.4
	off-site	W border of Pond 1		Bh, Ds, Fg	2/21/92	30	60	0.375	7.2	0.6
	off-site	W border of Pond 3			2/21/92	1500		2.840	7.4	1.6
	off-site	W border of Pond 4			2/21/92	2000		1.832	7.3	0.9
	off-site	pool between Mud Slough and LBL P10GC, west			2/15/92	80		5.020	7.6	1.6
	off-site	pool between Mud Slough and LBL P10GC, central			2/15/92	7		5.530	7.2	0.5
	off-site	pool between Mud Slough and LBL P10GC, east			2/15/92	32		0.902	7.1	0.1
	off-site	v. deep pool between Ponds 6 and 8, and Mud Slough			2/16/92	50		3.700	7.8	1.0
	1	west-central	ffff?	Ds, Sk, ag	2/16/92	150	100	0.109	7.4	0.0
	1	LBL site UZ5	KR, and fill	Bh, Sk, ag	2/21/92	400	400	0.180	7.2	0.6
	1	NW of UZ5	ffff	ag, Ml, Bh, Sk, Sf	2/21/92	140	60	0.279	7.1	0.4
	1	south-central	ffff		2/16/92			0.106	7.1	0.0
	1	SE corner, ~10 m NW of UZ3 ("rwp 1C"?)	ffff	Ml, Bh	2/21/92	200	100	0.373	7.2	7.5
	1	SE corner, LBL site UZ3	KR	Tl, Bh	2/16/92	50	300	0.466	6.7	17.5
	1	E-side, 150 m NW of UZ3, 25 m W of SLD	ffff	Bh, ag	2/16/92	150	70	0.134	7.0	1.8
	1	NE corner, flooded secondary road	ffff	-	2/16/92	500	100	0.298	6.8	4.9
	1	rwp 1H	ffff	Ml, Ec, ag	2/21/92	130	70	0.209	7.2	0.3
	1	~30 m W of rwp 1H	ffff	Ml, ag, Ec	2/21/92	180	70	0.224	7.1	0.7
	1	LBL site UZ6, S-central area of Pond 1	KR		2/21/92	30	400	0.089	7.2	0.5
	2	SE area, 100 m N of P1, 30 m W of SLD	KR	Tl	2/16/92	300	120	3.450	6.6	141.3
	2	NE area, 100 m S of GCR, 30 m W of SLD	KR, and fill	-	2/16/92	500	50	0.154	7.4	2.5
	2	west-central, staked as "P2C (9)"?	?	Bh, Sf	2/16/92	200	120	0.230	7.1	2.5
	2	2VS plot D, north end	KR	Tl, algae	2/21/92	64	50	0.520	7.6	54.3
	2	2VS west of instrument nest C1	KR	Bh, Tl, algae	2/21/92	400	50	0.540	7.7	14.8
	2	2VS south of instrument nest C2	KR	Bh, Tl, algae	2/21/92	400	150	0.430	7.3	9.2
	3	NE area, rwp 3B	ffff		2/21/92	40		0.550	7.2	2.6
	3	NE area, ~20 m SW of rwp 3B	ffff	Bh, Ks, Sf, algae	2/21/92	400		0.406	7.3	1.6
	3	NE area, ~15 m N of rwp 3B	ffff		2/16/92	100		0.384	7.0	3.3
	3	NE area, rwp 3D	ffff		2/16/92	100		0.236	6.9	2.2
	3	NE area, rwp 3E	ffff	sparse(Bh, Ks, Sf, algae)	2/21/92	150		0.422	7.3	1.9
	3	NE area, rwp 3F	ffff	sparse(Bh, Ks, Sf, algae)	2/21/92	400		0.375	7.2	2.5
	3	N-NE area, ~ 15 m SE(SW?) of well LBL 36	ffff		2/16/92	500	100	0.252	6.8	1.5
	3	in N- side ditch (near Pond 4)	KR	Bh	2/21/92		150	0.853	7.0	20.0
	3	N-central, in ditch near well KR 105	filled ditch	Bh	2/21/92			0.649	7.0	17.5
	3	NE of ditch	ffff	Bh, Ks, Fg	2/21/92	200	100	1.135	7.0	26.4
	3	N-central, near well KR 105	KR	Bh	2/21/92	250	80	0.959	7.0	6.8
	3	NW	KR?	Al, Ao, Bh	2/21/92	10000		1.023	7.1	13.4
	3	NW corner	KR		2/21/92			1.014	7.2	13.0
	3	W-central edge	ffff		2/21/92			1.196	7.1	14.5
	3	SW corner	KR	sparse Ct	2/21/92	2000	70	1.646	7.2	11.3
	3	N of well KRD3S2, along S side	ffff	Bh	2/21/92	500		1.115	7.2	8.4
	3	SE area	KR	Fg, Bh, Ss, Ml, Sk	2/21/92	200		0.502	7.2	4.4

Feb.15-21,'92 KR Pools

COMMENTS	POND #	SURFACE WATER SAMPLING LOCATION	soil	vegetation	date	approx. area m2	approx. depth mm	EC dS/m	pH	total Se µg/L (ppb)
	4	S-central, 18 m W of P3-P4 ditch	KR?	Bh, Ss	2/21/92	100		0.787	7.2	6.3
	4	70 m W of P3-P4 ditch	fill	Al, Bh	2/21/92	300	100	0.658	7.2	2.8
	4	160 m W of P3-P4 ditch	fill	ag, Bh	2/21/92	300	70	0.453	7.3	1.5
	4	240 m W of P3-P4 ditch	fill	Al, Bh	2/21/92	1000	90	0.645	7.2	2.7
	4	SW area, ~ 60 m NE of corner	fill	sparse (Bh, Fg, ag)	2/21/92	1000	150	1.932	7.1	20.5
	4	SW area, near W edge	fill	Al	2/21/92			0.558	7.2	4.7
	4	~30 m S of UCR test plot	KR	(former Tl) Bh	2/21/92	300		0.370	7.3	2.3
	4	UCR test plots	KR	none	2/21/92			0.638	7.4	19.4
	4	E of UCR plots, LBL soil site P4X	KR	in Tl near ag	2/21/92	2000	250	1.976	6.9	74.8
	4	N edge, ~ 70 m SW of P5 CIMIS station	fill		2/21/92			0.421	7.1	2.9
	5	S side, across GCR from P4X	KR	Bh, Tl	2/21/92	2000	300	0.858	7.1	23.7
	5	SE area, LBL SB1	KR	Tl	2/21/92	10	150	1.812	7.2	162.1
	5	SE area, LBL SB2, NW of SB1	KR	Tl, Bh	2/21/92	900	250	0.737	7.1	41.1
	5	SE area, LBL SB3, NW of SB2	fill	Bh	2/21/92	200	50	0.206	7.4	1.1
	5	central area of Pond 5, LBL SB4, NW of SB3	fill	Bh	2/21/92	100	50	0.380	7.3	2.2
	6	LBL 1 ft excavation test plot P6S12	excav. KR	none, (+ algae film)	2/21/92	65	180	1.350	7.1	120.0
	6	LBL 0.5 ft excavation test plot P6S6,	excav. KR	Bh, (Ds, Fg)	2/20/92	20	50	1.182	7.6	10.0
	6	LBL (KR soil) ephemeral pool 6PC	KR	Ds, Ct, Bh, Ks, ag	2/20/92	300	300	0.716	7.1	11.0
	6	fill area, ~ 50 m W of 6PC	fill	Bh, ag	2/20/92	4000	120	0.377	7.0	3.5
	6	NE area, "rwp 6B"	fill		2/16/92	250	100	0.213	6.8	1.0
	6	SE area near gate	fill		2/16/92	400	100	0.526	6.7	11.6
	6	SW area	fill	Ds, Fg, ag, Ct, Bh, Sf	2/16/92	500	70	0.366	7.2	3.0
	6	NW area	fill	Ds, Ct	2/16/92	5000	170	0.623	6.9	7.6
	8	~0.6 km E of Mud S., ~0.3 km W of Pond 9, 50 m S of P	fill	Ds, Bh, Ec	2/16/92	400	70	0.220	6.7	1.6
	8	LBL site 8EP area average	KR	Bh, ag (sparse)	2/21/92	320	600	0.320	7.0	1.0
	8	~75 m NE of plot 8EP	KR	Bh, ag (sparse)	2/21/92	25	100	0.738	7.4	5.6
	8	~75 m NE of plot 8EP	Fill	ag, Bh (sparse)	2/21/92	25	100	0.630	7.4	4.9
	8	~50 m SW of plot 8EP	KR		2/21/92	5	150	0.466	7.5	1.6
	8	between 8EP & KR103	KR,Fill		2/21/92	300	100	0.753	7.5	5.5
	8	by well KR103	KR	Bh, ag (sparse)	2/21/92	100	100	0.918	7.5	8.7
	9	N area, LBL monitoring sites P9D,C,R	KR	Bh, Ks	2/15/92	2500	150	0.251	6.9	2.2
	9	S-central, access road to LBL site 9BE	fill	Bh, Sf	2/16/92	400	100	0.153	6.9	0.7
	9	LBL site 9BE	KR	Bh	2/21/92	150	1000	0.103	7.5	0.0
	9	"P9-H"	fill		2/16/92	1000	100	0.121	6.9	0.0
	9	S area, LBL pool 9PC	fill (re-disked)	Bh, ag	2/16/92	1500	100	0.618	6.6	7.5
	9	E area,	fill	Bh, ag, Ds	2/16/92	3000	100	0.228	6.8	2.5
	9	10m east of plot 9BE	fill	Grasses	2/21/92	100's	50	0.265	7.4	0.0
	9	10m west of plot 9BE	fill	Grasses	2/21/92	100's	50	0.303	7.5	0.1

Feb.15-21,'92 KR Pools

COMMENTS	POND #	SURFACE WATER SAMPLING LOCATION	soil	vegetation	date	approx. area m2	approx. depth mm	EC dS/m	pH	total Se µg/L (ppb)
	10	LBL monitoring site P10G, fully flooded	KR, trough	Ct, Ds, ag	2/16/92	1500	600	0.960	6.6	19.0
	10	rwp L, west-central Pond 10 fill	|||	Ml, ag, Ec	2/15/92	30	30	0.074	7.0	0.0
	10	rwp I, west-central Pond 10 fill	|||		2/15/92	120	30	0.775	7.2	0.7
	10	rwp A, west-central Pond 10 fill	|||		2/15/92	200	30	0.095	7.0	0.9
	10	rwp C, west-central Pond 10 fill	|||		2/15/92	100	50	0.074	7.0	0.7
	10	rwp P, west-central Pond 10 fill	|||	ag, Ml, Ec, algae, mushrooms	2/15/92			0.166	6.9	0.3
	10	rwp Q, west-central Pond 10 fill	|||	ag, Ds, Ec, Ml	2/15/92	60	50	0.06	7.0	0.6
	10	S side, ≈0.15 km to Mud Slough	KR?		2/15/92	150	100	0.12	7.0	1.3
	10	S side, ≈0.6 km to Mud Sl., ≈0.3 km to Pond 9	|||	Bh, ag	2/16/92	270	80	0.138	7.0	0.0
	10	SE corner near Ponds 8 and 9	KR	Bh, Ds, ag	2/16/92	70		0.455	6.6	3.9
	11	LBL 0.5 ft excavation monitoring site P11S6	KR, excavated	Ct	2/11/92	7	20	0.100	1.6	1.4
	11	LBL 1.0 ft excavation monitoring site P11S12	KR, excavated	Ct, Bh,	2/11/92	50	25	0.401	7.4	8.4
	11	former UCR volatilization test area	KR	Ct	2/15/92	30000	100	0.725	6.8	5.5
	11	rwp 11D, E-NE area	|||		2/15/92	800	70	0.197	7.1	1.7
	11	≈50 m N of LBL site P11S12,	KR	Ds, Ct, Ec	2/15/92	150	100	0.505	6.7	5.8
	11	≈ 50 m E of LBL site P11S12	KR	Ds, Ct, Ec	2/15/92	90	90	1.346	6.6	30.8
	11	N-NW corner pool, labled "P11A"	|||		2/16/92	70	80	0.230	7.0	1.8
	12	E-SE area			2/16/92	230	100	0.144	6.8	3.2
	12	E-SE area			2/16/92	400	90	0.227	6.8	1.7
	12	E-SE area			2/16/92	800	80	0.194	7.0	2.1
	12	N-NW pool	KR		2/16/92	50	50	0.187	7.0	1.4
	12	S-central (near P11)	|||		2/16/92	500	50	0.669	6.9	3.3

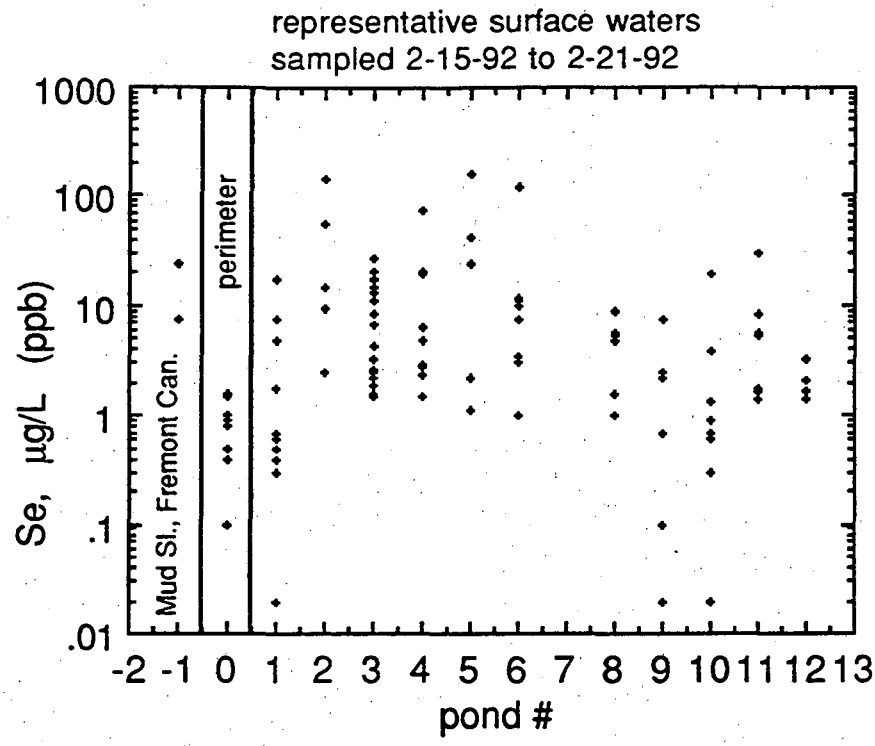

Figure 7.2. Selenium concentrations in various surface waters sampled within the first 10 days after the 2-12-92 rain storm. The data are ordered according to general locations within Kesterson Reservoir.

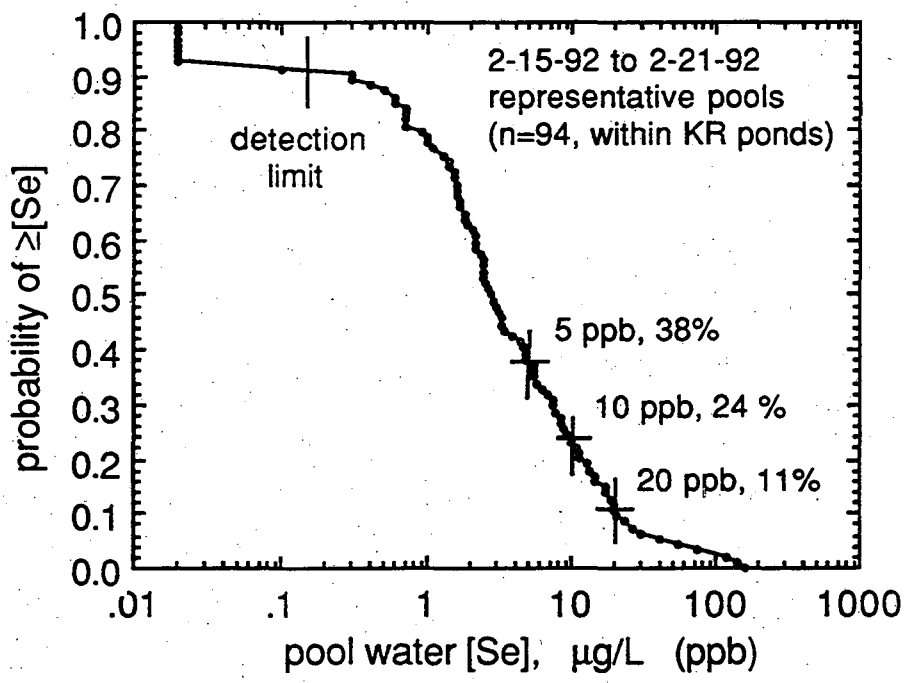

Figure 7.3. Estimated probability of exceeding particular selenium concentrations in the initially sampled February 1992 surface waters.

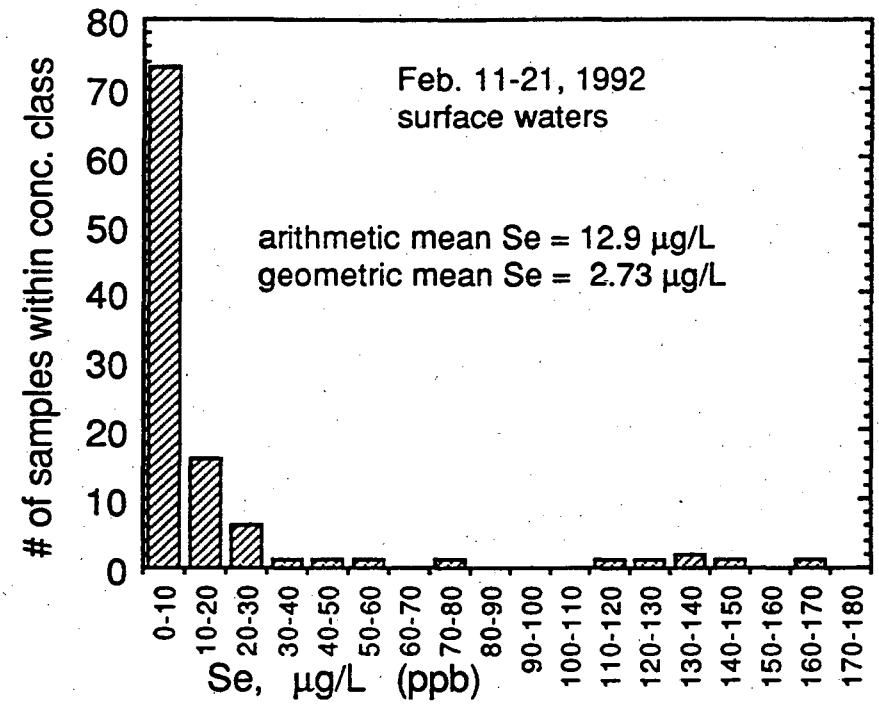

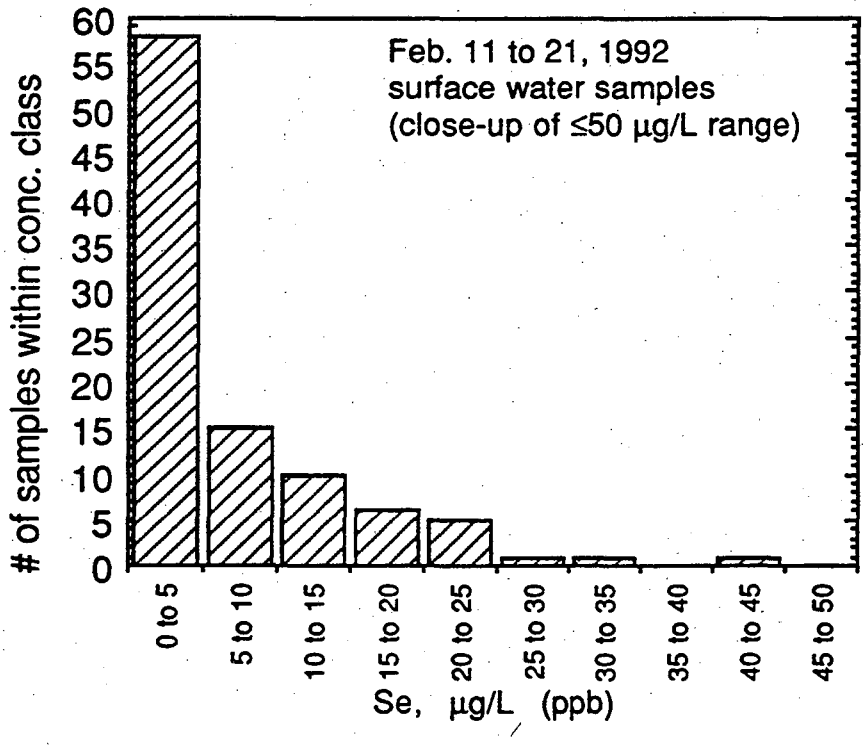

Figure 7.4. (a) Histogram of selenium concentrations in February 1992 surface water samples. (b) Close-up of data from (a) with [Se] ≤ 50 µg L^{-1}.

are roughly correlated with soil and vegetation type. Native Kesterson soil, especially when in formerly vegetated with cattails (Typha), generally provided more selenium in pool waters.

Comparison of these data with ephemeral pool water quality information from pre-fill years shows that pool water selenium concentrations were generally lower during 1992. The arithmetic mean and geometric mean selenium concentrations associated with samples collected within the first 10 days following the 2-12-92 storm were 12.9 and 2.7 $\mu g\ L^{-1}$ respectively. The most extensive pre-fill ephemeral pool water sampling following a single storm took place during March 1987. The arithmetic mean and geometric mean pool water selenium concentrations from that period were 373 and 197 $\mu g\ L^{-1}$ respectively. Another distinctly different ephemeral pool data set from past monitoring activities is that of the 1987-1988 wet season monitoring in the P6S12 excavated surface monitoring site. These previously reported data (LBL, 1989; LBL, 1990a; and Tokunaga and Benson, 1992) are from an ephemeral pool generated by shallow water table rise intercepting the soil surface. Surface water selenium concentrations under these conditions persistently exceeded 1,000 $\mu g\ L^{-1}$.

Note that most of the data in the pool water selenium:EC correlation diagram (Figure 7.5) plot well below the pre-closure line. Factors which contribute to this pattern include (1) persistence of most of the soil selenium inventory in various immobile forms; (2) more recent (1987 though mid-1988) flooding with nonseleniferous but saline waters in some ponds (especially in Ponds 1, 2, 5, and portions of 3, and 7); and (3) the much lower selenium:EC ratio found in the imported fill soil. If only rainfall and evaporation influenced the composition of waters in the soils and pools, the data in Figure 7.5 would have clustered about the diagonal line.

7.2. Time Trends in Ephemeral Pool Water Quality

Our time-trend sampling was limited to a small number of sites distributed throughout Kesterson Reservoir. Among the larger set of persistent pools, sampled sites were selected because of a previous history of ephemeral pool water sampling, because of areal extensiveness, or because of the long duration of ponding. The selected sites are listed in Table 7.2. Locations of these sites are shown in Figure 7.6.

7.2.1. Data

Time trends of selenium concentrations and electrical conductivities in the pools are plotted in Figures 7.7 through 7.16. Elapsed times are relative to the major storm event on Feb. 12, 1992.

7.2.2. Discussion

The time trends in salinities (ECs) in the pool waters all indicate net evaporative concentration of salts. The EC data ranged from 0.1 up to 7.7 dS m^{-1} during this period. The highest salinities occurred in the P10GC, P10GS, and P11-UCR sites. While all other ephemeral

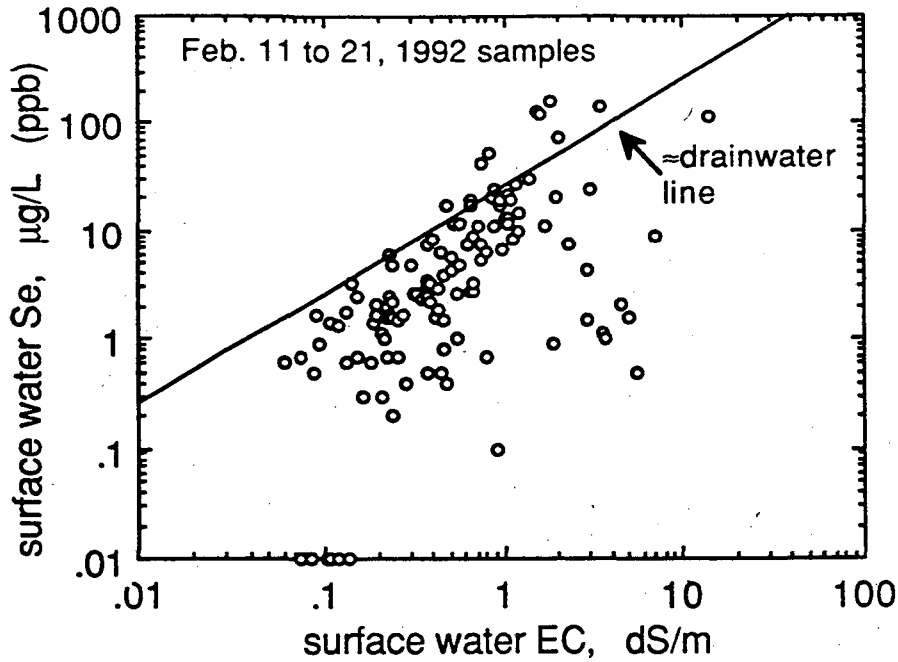

Figure 7.5. Correlations between selenium and EC in Kesterson Reservoir, February 1992 surface waters. The diagonal line represents the case where the original (pre-closure) seleniferous drainwaters are diluted with rain water or evaporatively concentrated.

pool ECs remained ≤ 4.3 dS m^{-1}, these three sites attained maximum values of 6.0, 5.9, and 7.7 dS m^{-1} respectively. The relative differences among the sites were consistent with expectations based on the various soil environments. The P10GC and P10GS sites are part of a small, very saline trough which formerly drained into Mud Slough. The P11UCR plot is an extensive region of high soil salinity. For comparison, the ECs in the original Kesterson Reservoir pond waters were typically in the range of 14 to 16 dS m^{-1}.

Lowest salinities were found in the filled sites, again reflecting surface soil characteristics.

Selenium concentrations in the periodically sampled pools were in ranges expected based upon the associated soil environments. As in the pools sampled immediately after the major rainfall event, selenium concentrations were highest in unfilled areas previously vegetated with cattails (Typha). Many of the pools formed over open cattail sites consisted of suspensions of dead cattail tissue and decomposing surface soil organic matter. Mixing of ponding rain waters with such selenium-rich litter resulted in the relatively higher selenium concentrations in pools formed in these settings. The pool waters sampled in the formerly cattail-vegetated P6S12 excavation test plot were also moderately high, despite the fact that the vegetation as well as the surface 0.3 m (1 ft) were removed in 1987. This observation may be due to both a moderately high surface soil soluble selenium inventory and some lateral mixing with cattail litter at the edges of the excavated plot.

Table 7.2. Summary of the soil type (habitat and dominant vegetation at the surface water sampling sites illustrated in Figure 7.6.

Pond No.	Pool site	Soil	Dominant Vegetation
1	UZ3	Kesterson, open	Typha, Bassia
1	UZ5	Kesterson, playa	Bassia
1	fp5	fill	Bassia
1	fp H	fill	annual grasses
3	SW	Kesterson	Cressa (sparse)
3	NNW	Kesterson	
3	WC	fill	
3	RWP 3F	Kesterson + fill	Bassia (sparse)
4	W	fill	
4	N	Kesterson, open	Typha
5	S	Kesterson, open	Typha, Bassia
5	W	Kesterson	Typha
6	S12	Kesterson, excavated	bare
6	PB	fill	
6	PC	Kesterson	Bassia, annual grasses
9	BE	Kesterson, playa	Bassia
9	H	fill	Bassia,
9	S	disked fill?	Bassia
9	E	fill	Bassia
10	GC	Kesterson, playa	Cressa
10	GS	Kesterson, excavated	Cressa
11	S6	Kesterson, excavated	Cressa
11	S12	Kesterson, excavated	
11	UCR	Kesterson	Cressa

Pools formed over thick deposits of initially clean fill soil were commonly low in selenium concentrations. The Pond 10 fill pools (Figure 7.13 a,b) represent such cases. However, in many fill areas either a mix of Kesterson and off-site soils were used, or only a thin layer of initially clean fill soil was emplaced. In such cases, higher selenium concentrations were often found. The pools in Pond 3 (Figure 7.8 a,b) represent these cases.

Time trends for selenium concentrations in the 1992 ephemeral pools were much less systematically varying than the EC data. Increases and decreases in selenium concentrations were observed during the monitoring period, often within the same pool. The more complex behavior of selenium concentrations is expected because selenium may be removed from solution under reducing conditions and through biological uptake. Factors which are likely to govern the rates of these processes such as concentrations of organic matter, nutrients, and dissolved oxygen probably varied substantially among the different pools.

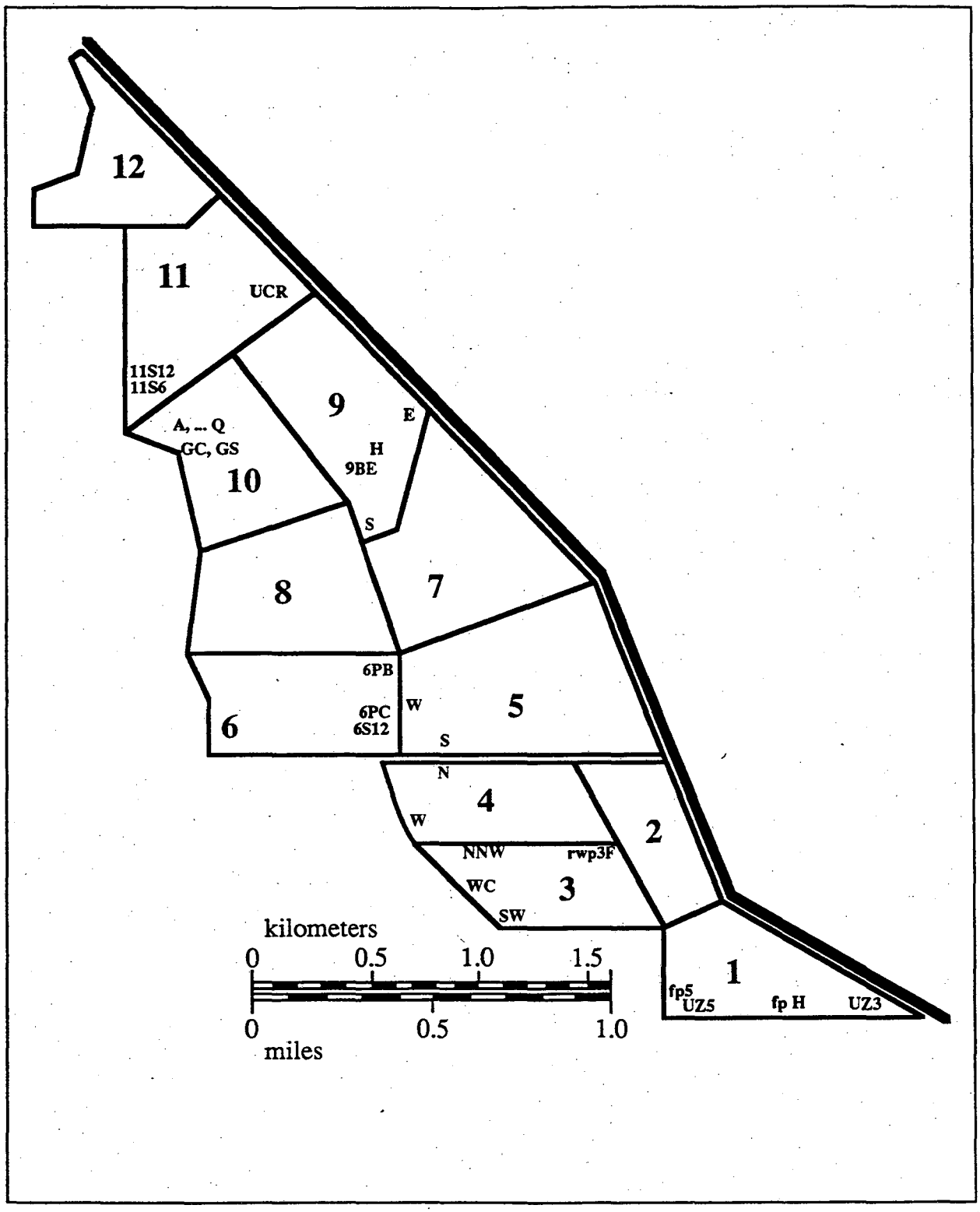

Figure 7.6. Locations of pools sampled for water quality time trends.

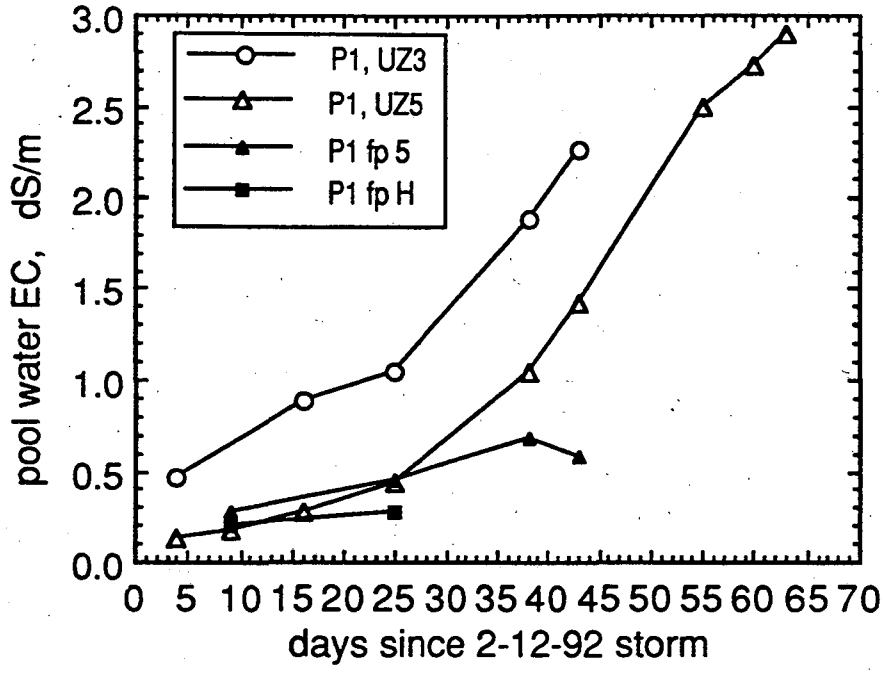

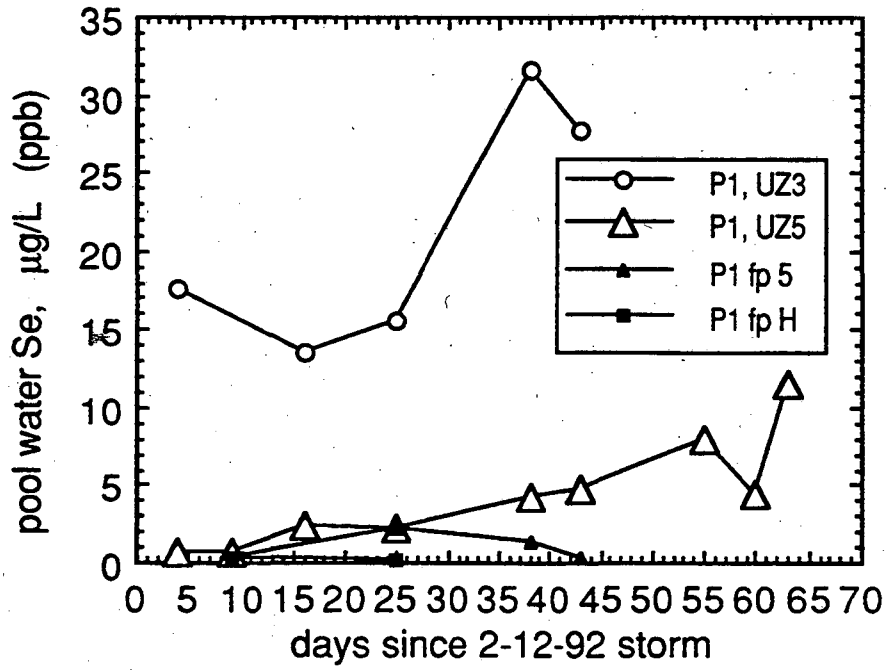

Figure 7.7. Pond 1 ephemeral pool time trends in (a) salinity (as indicated by EC), and (b) total selenium. Pools at P 1 UZ3 and P1 UZ5 formed over the original Kesterson Reservoir soils. Pools P1 fp 5 and P1 fp H formed over fill soil.

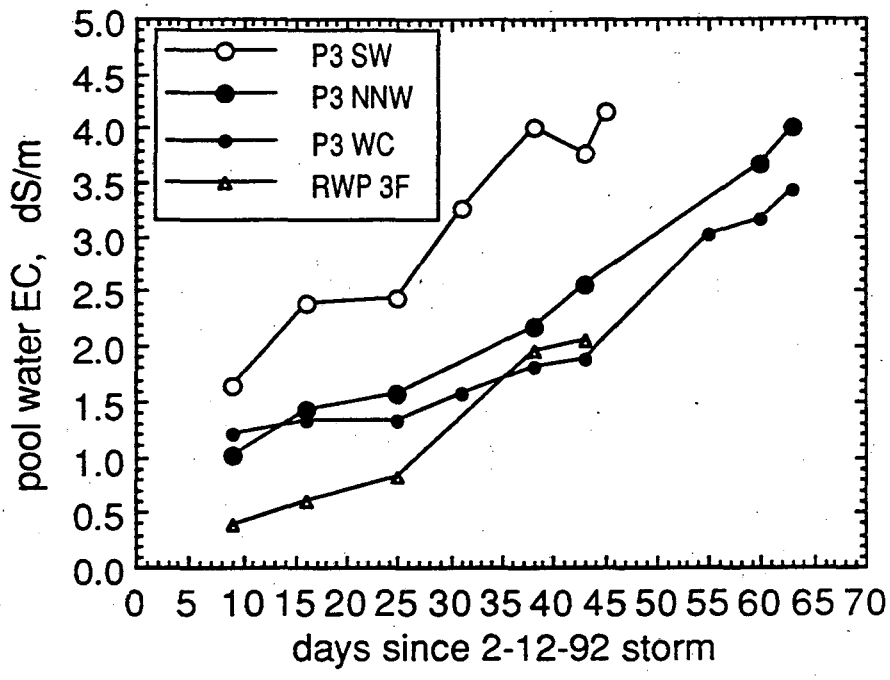

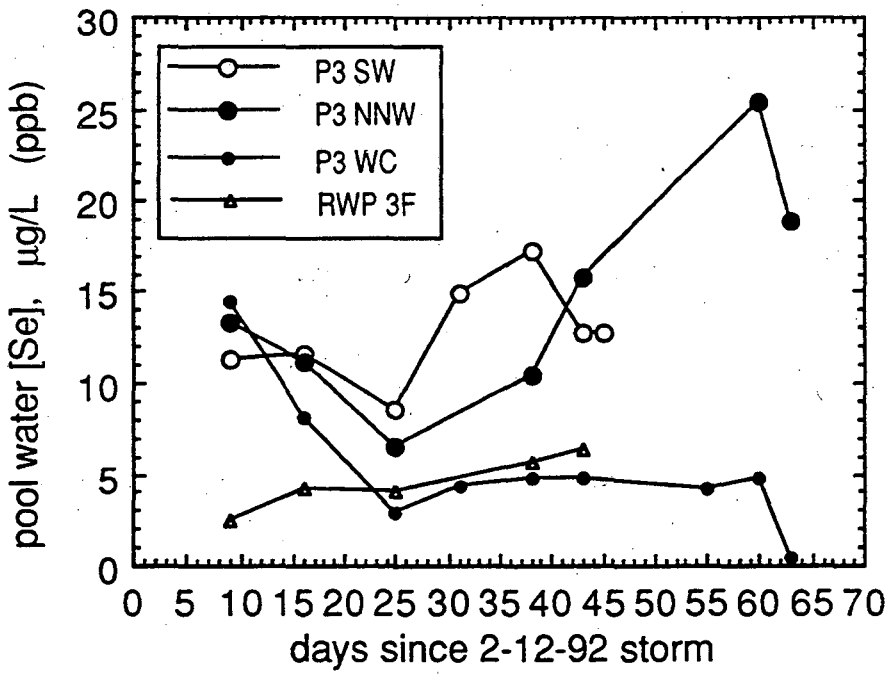

Figure 7.8. Pond 3 ephemeral pool time trends in (a) salinity (as indicated by EC), and (b) total selenium. With the possible exception of site P3 NNW, these pools formed over fill soil.

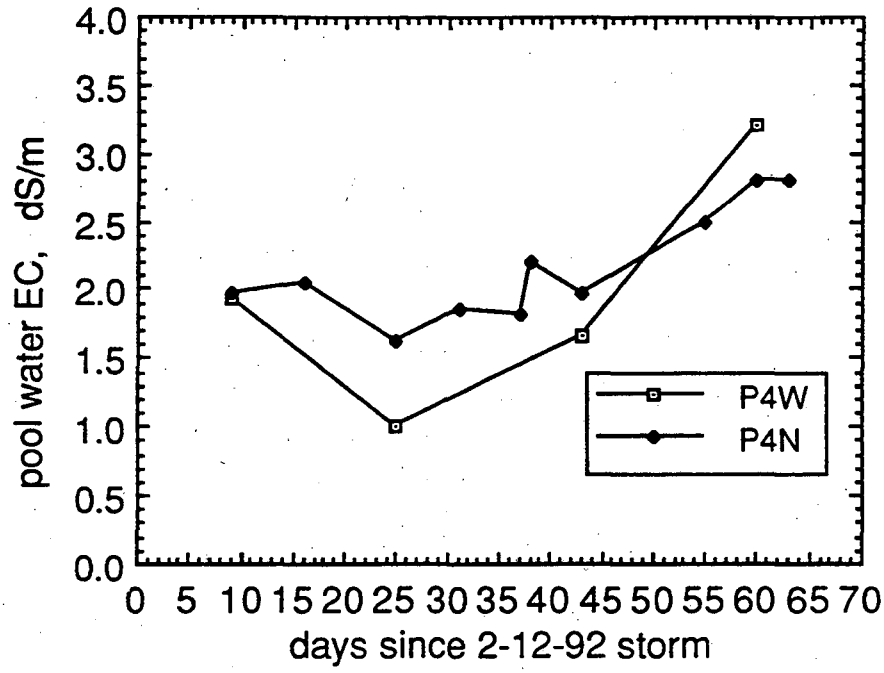

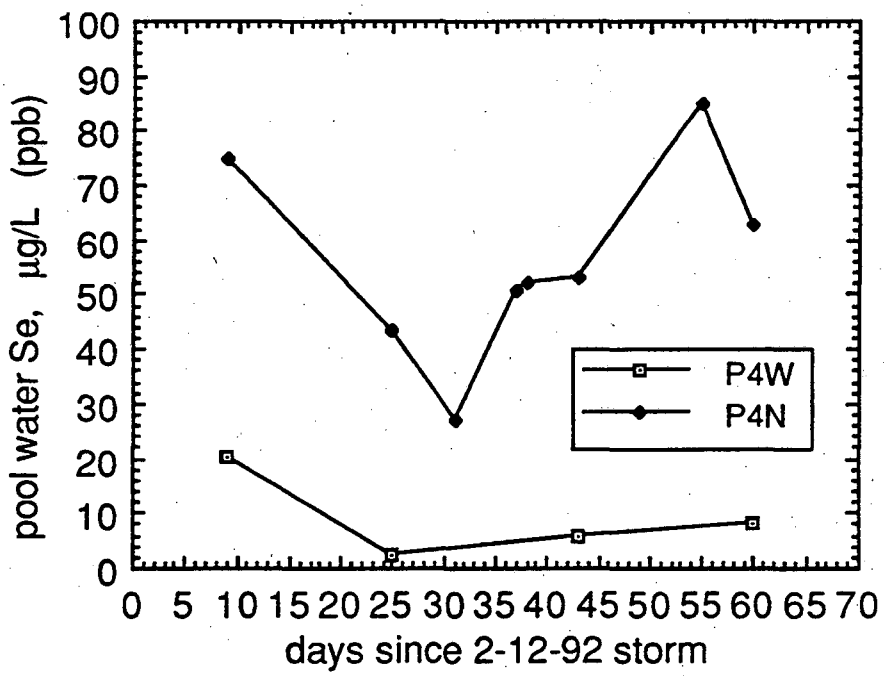

Figure 7.9. Pond 4 ephemeral pool time trends in (a) salinity (as indicated by EC), and (b) total selenium. The P4 N pool formed over original Kesterson Reservoir soils in cattail litter. The P4 W pool formed over fill soil.

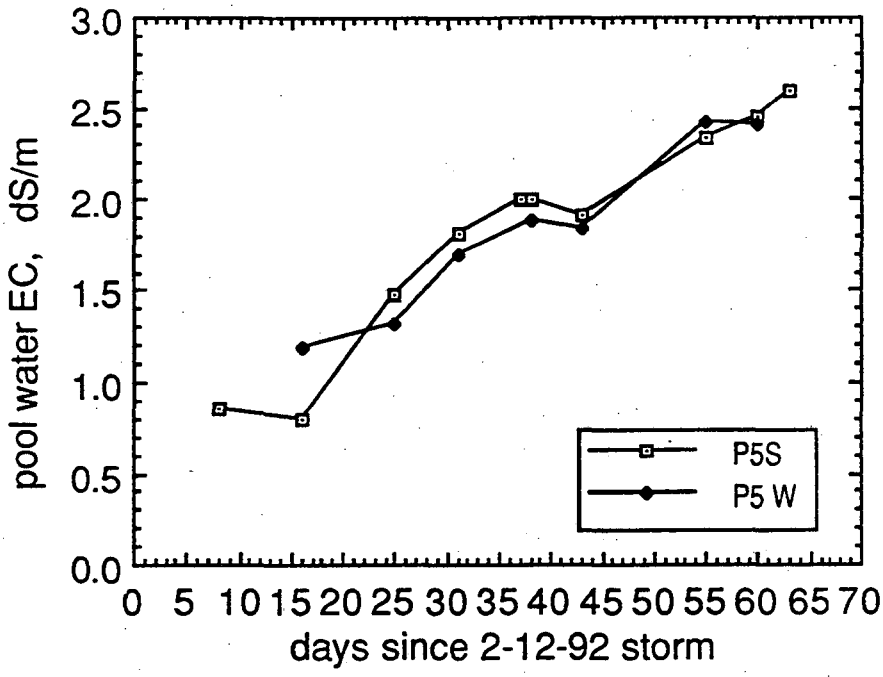

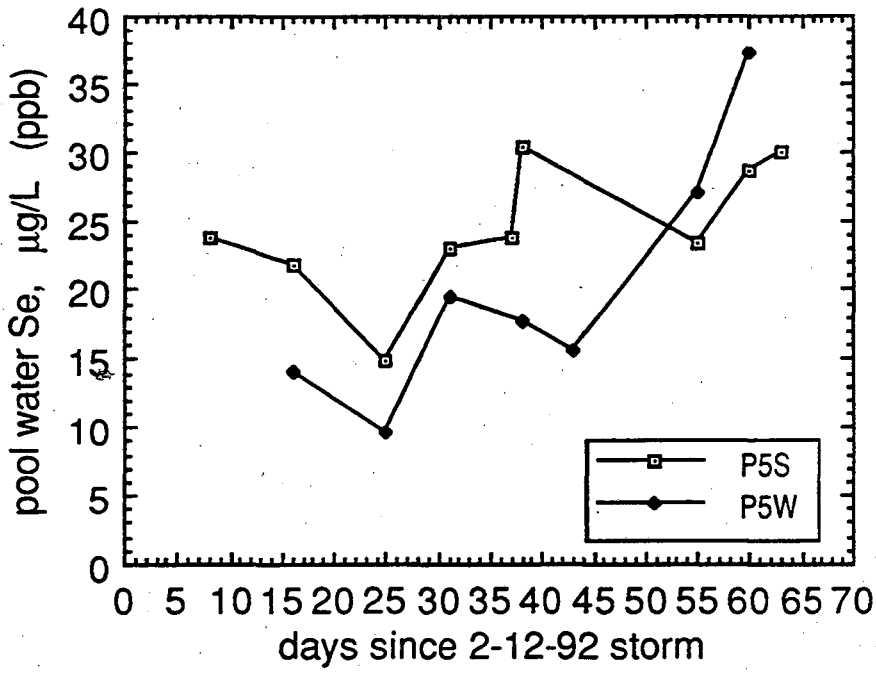

Figure 7.10. Pond 5 ephemeral pool time trends in (a) salinity (as indicated by EC), and (b) total selenium. Both the P5 S and P5 W pools formed over original Kesterson Reservoir soils in a mix of cattail litter and Bassia.

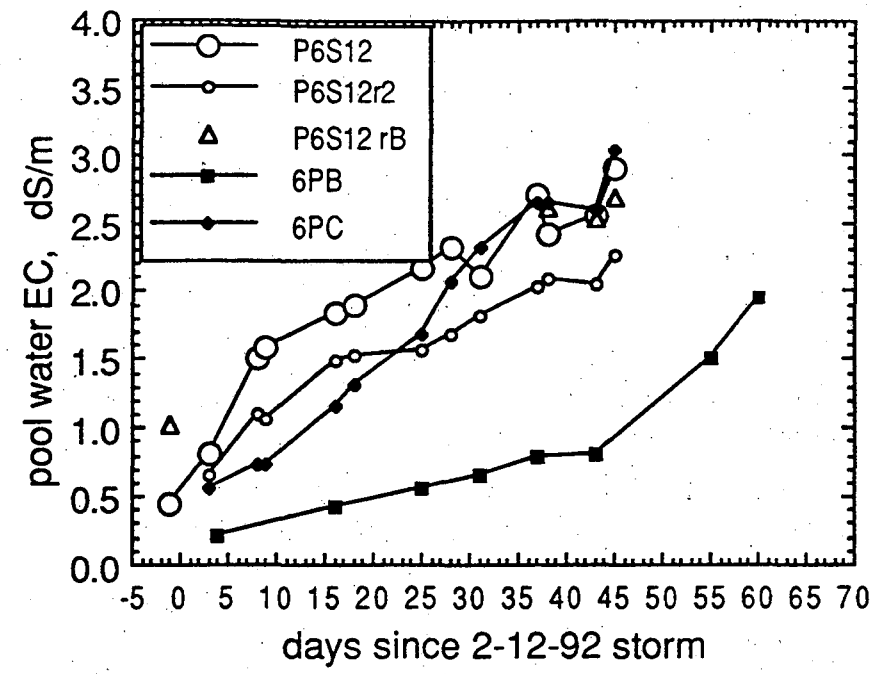

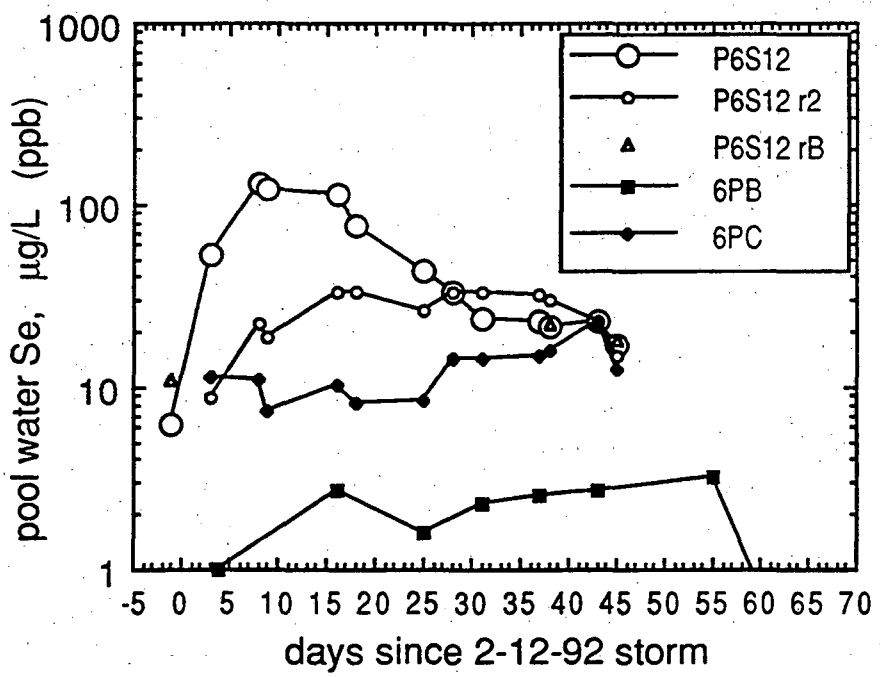

Figure 7.11. Pond 6 ephemeral pool time trends in (a) salinity (as indicated by EC), and (b) total selenium. All P6S12 data are from the 1 ft excavation test plot. This site was previously vegetated with cattails, but has been maintained as a bare soil since 1987. The 6 PB site is filled. The 6 PC site is on original Kesterson Reservoir soil, sparsely vegetated with annual grasses and Bassia.

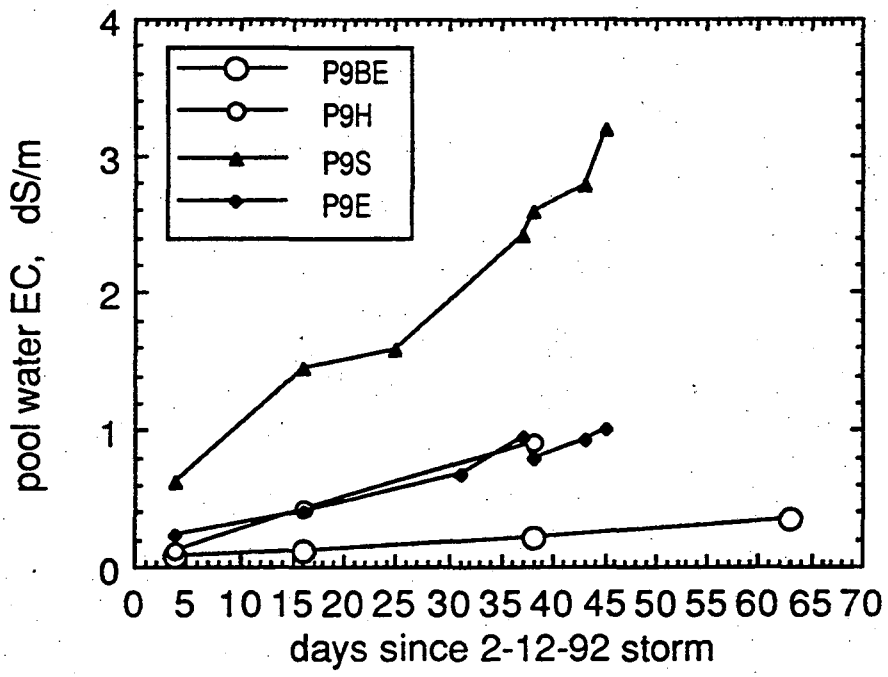

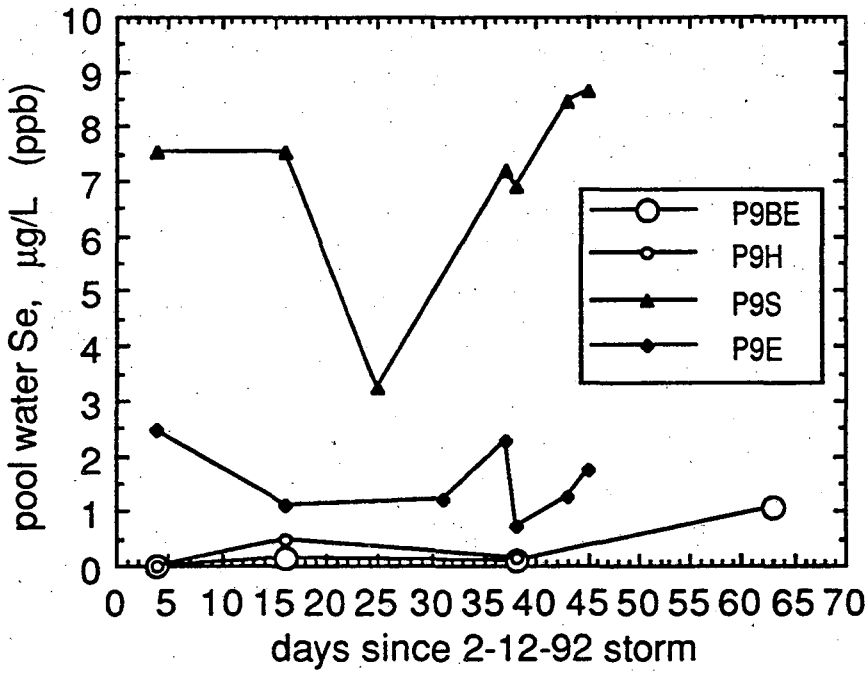

Figure 7.12. Pond 9 ephemeral pool time trends in (a) salinity (as indicated by EC), and (b) total selenium. Site P9BE is on original Kesterson Reservoir soil. Sites P9 H, P9 E, and P9 S are on fill soil.

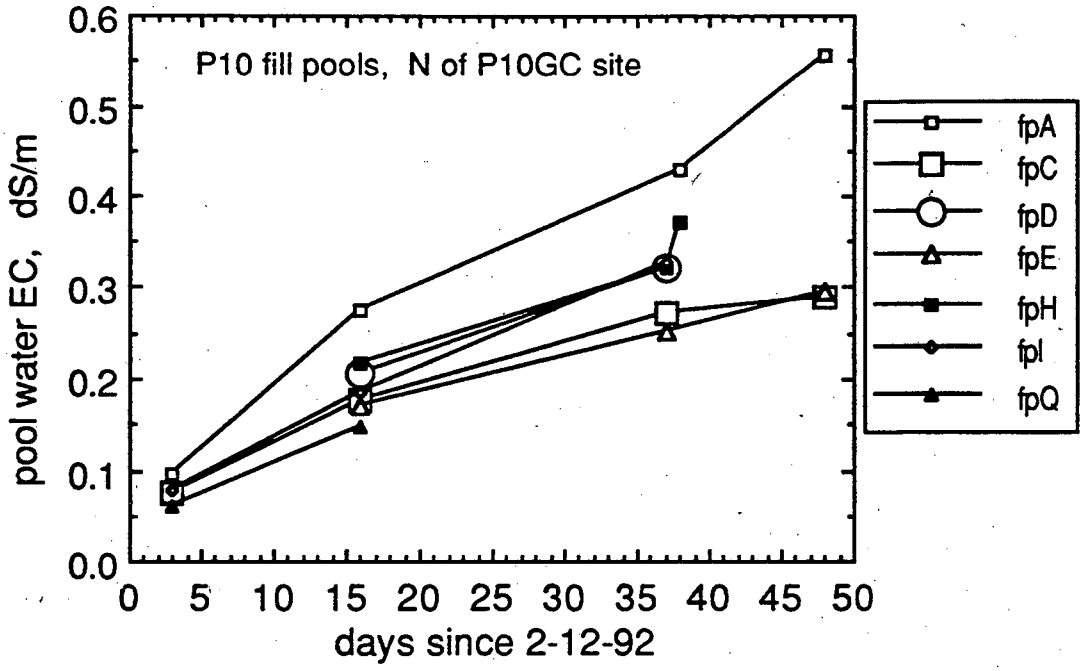

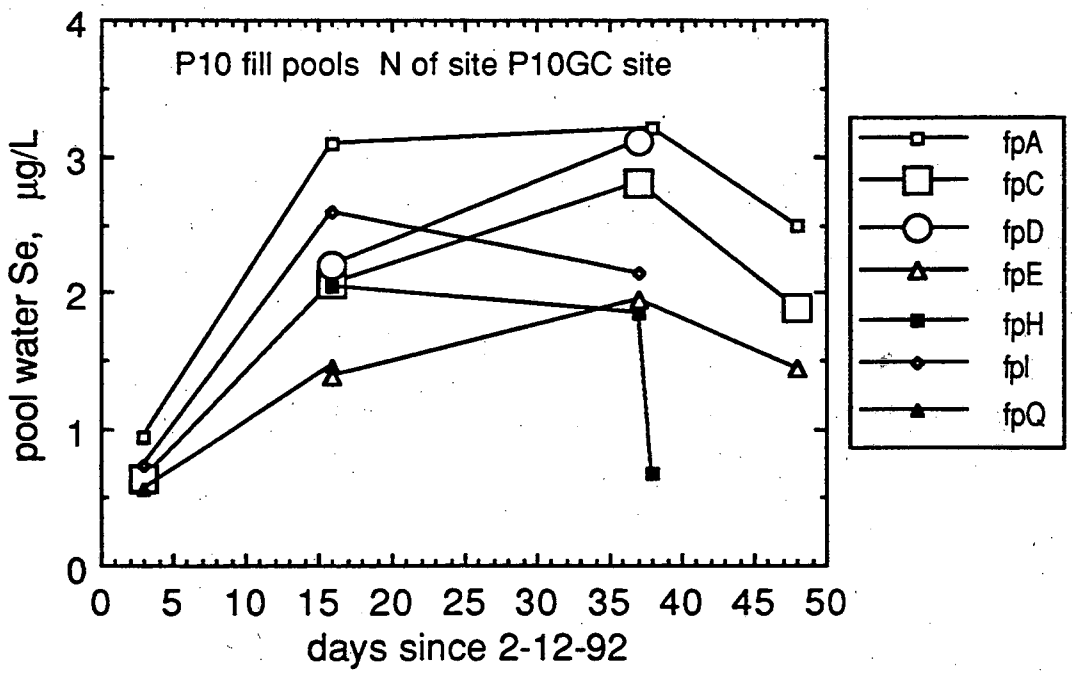

Figure 7.13. Pond 10 ephemeral pool time trends in (a) salinity (as indicated by EC), and (b) total selenium. The data shown here are all from filled areas.

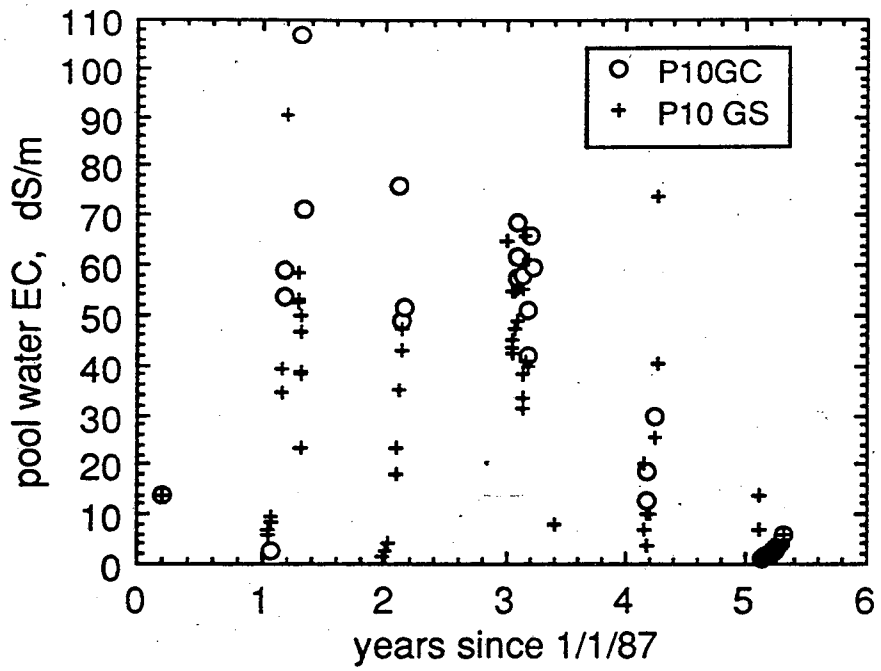

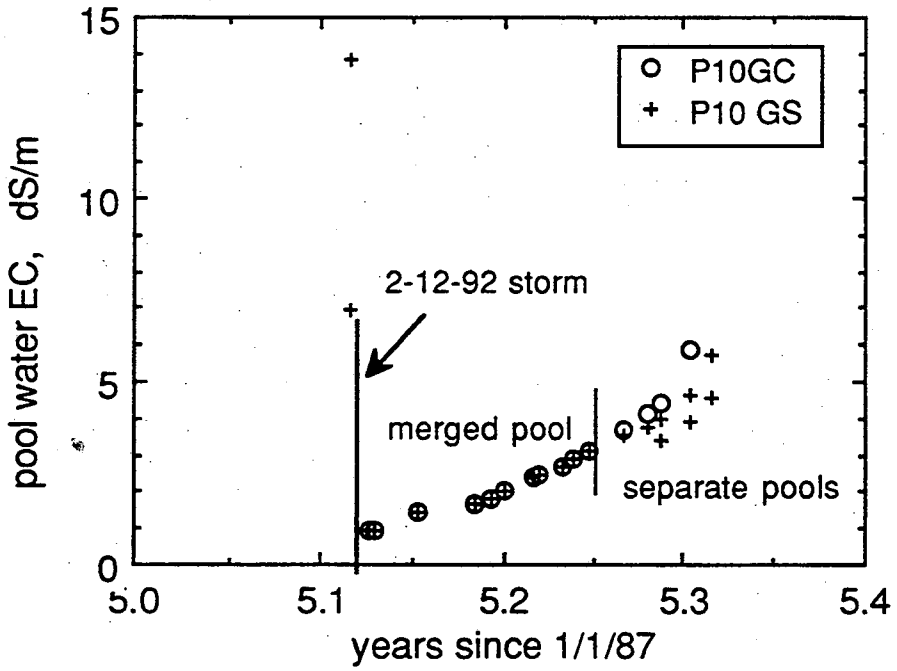

Figure 7.14. Pond 10 GC and GS ephemeral pool time trends in salinity (as indicated by EC). (a) Salinity data in ephemeral pools sampled since 1987. (b) Salinity in the sites during 1992. The time interval during which surface waters connected the two sites are indicated in (b).

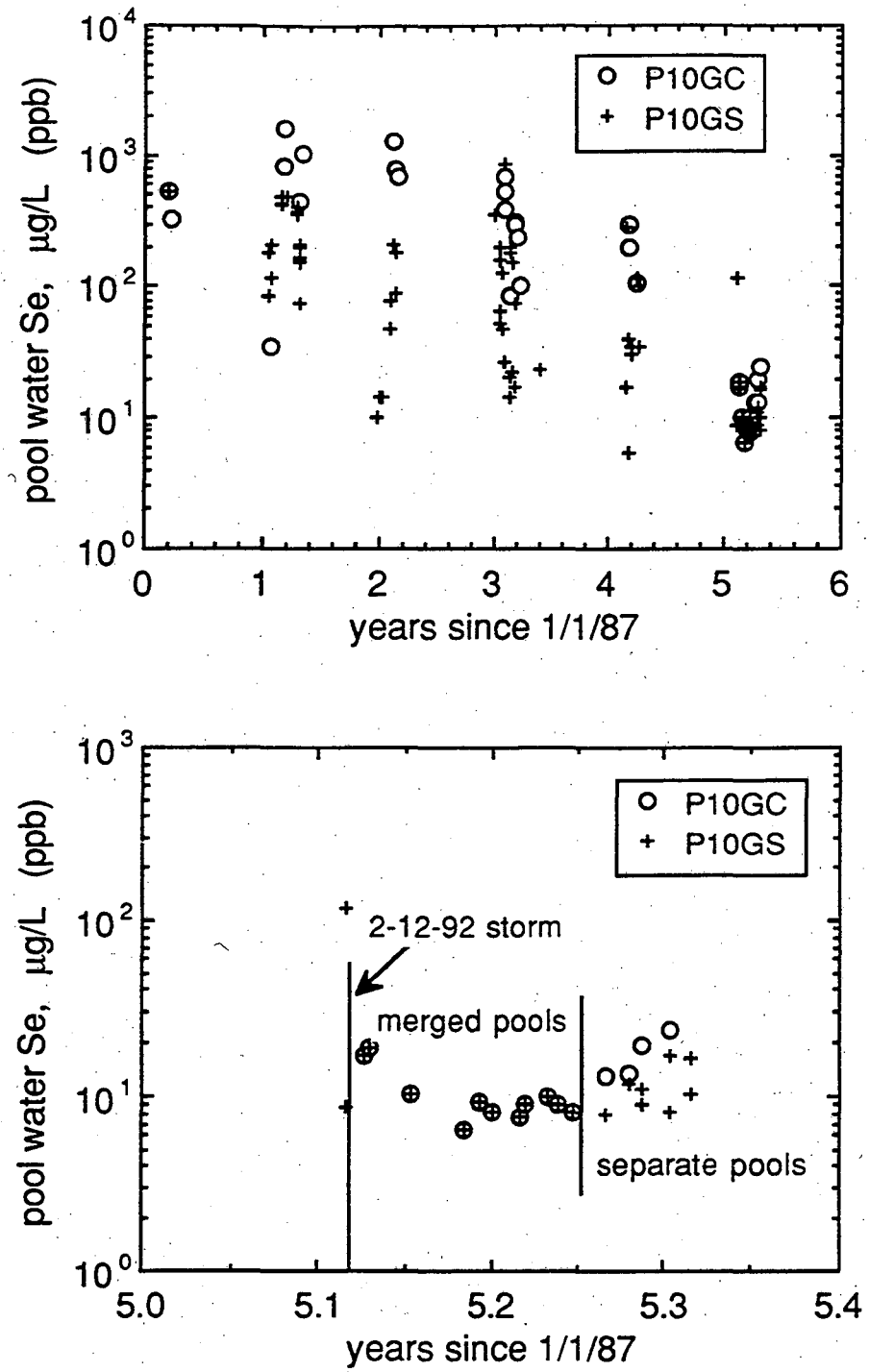

Figure 7.15. Pond 10 GC and GS ephemeral pool time trends in selenium (a) Selenium data in ephemeral pools sampled since 1987. (b) Selenium concentrations in the site surface waters during 1992. The time interval during which surface waters connected the two sites are indicated in (b).

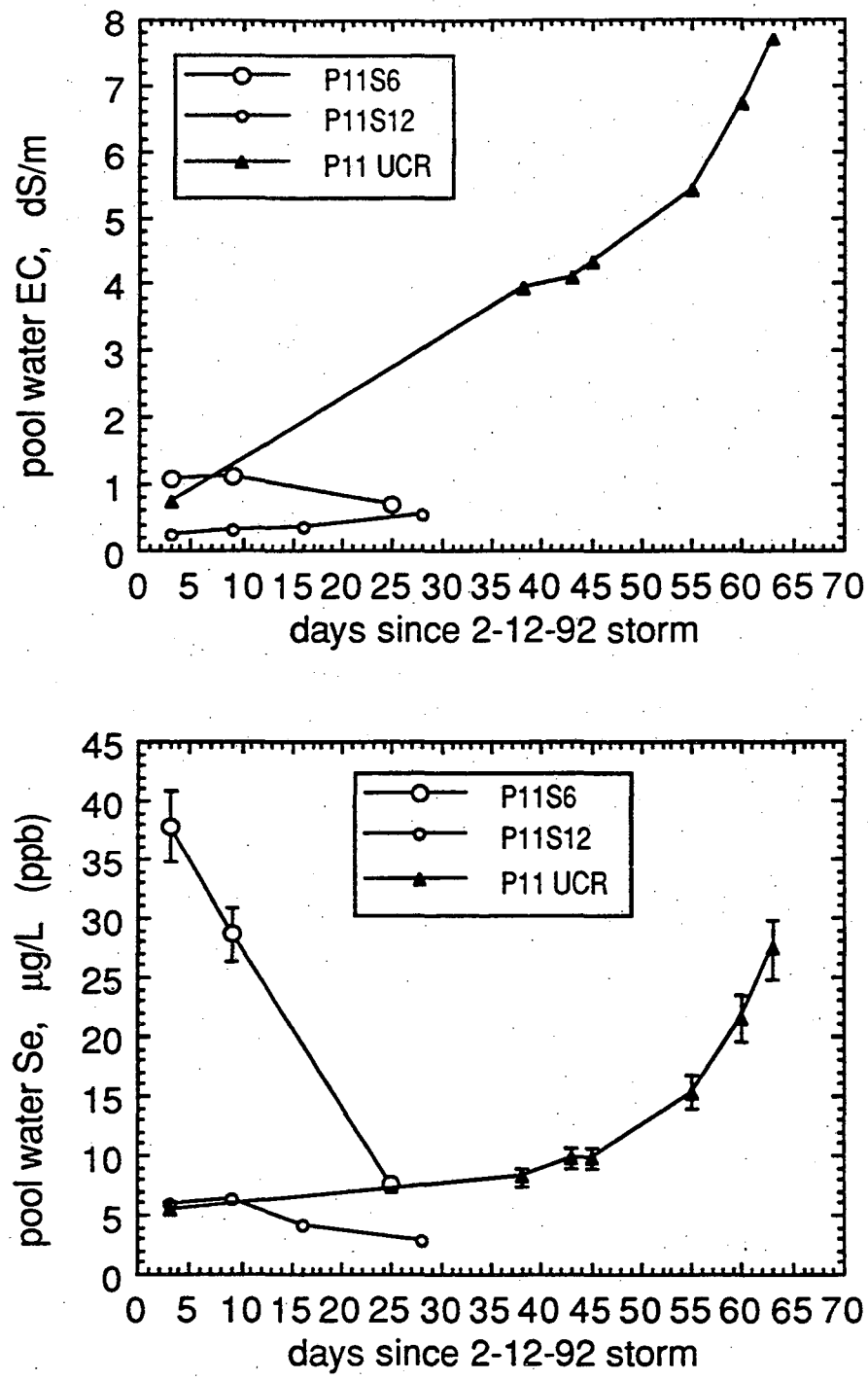

Figure 7.16. Pond 11 ephemeral pool time trends in (a) salinity (as indicated by EC), and (b) total selenium. Sites P11S6 and P11S12 are on excavated Kesterson Reservoir soils. The P11 UCR site is the former Pond 11 selenium volatilization test area operated by Dr. Frankenberger of U.C. Riverside.

8.0. Analytical Quality Control - June 1992

Leon Tsao
Earth Sciences Division
Lawrence Berkeley Laboratory

8.1. Introduction

The Kesterson Program at LBL has had a quality assurance program in operation for over five years, covering chemical analysis for selenium in samples collected from Kesterson Reservoir. In 1991 we experienced a change in analyst due to retirement. A part-time replacement analyst from another LBL-group was utilized for a month until an indefinite, full-time replacement could be hired. This resulted in a degradation of analytical quality with two changes in personnel, followed by slow improvement to previous performance levels as the new, full-time analyst gained experience. This report covers work done from October 1992 to June of 1992.

8.2. Measurement Statistics

Analytical chemistry has a number of means to judge the quality of the measurements made. Here we are considering the entire measurement process which includes the performance of the analyst and preparation of samples prior to measurement. This means that blind quality control samples must be placed in the sample preparation process. We use standard solutions to gauge accuracy and precision, duplicates to gauge precision with the natural matrix, blanks to gauge contamination and spiked samples or known addition to gauge interference.

8.3. Operations

Selenium analysis in water samples is performed by hydride generator AAS. Water samples are fed untreated into the instrument to read selenite (SeO_3^{-2}) concentration. Total selenium is analyzed by treating a 5.0 ml sample with 0.2 ml of a 2% w/v solution of ammonium persulfate and 5.0 ml of concentrated HCl. Our studies indicate that the concentration of organic forms of selenium in water samples is usually not significant and consequently, total selenium is believed to be the sum of the selenite and selenate species. For selenium analyses it is often necessary, after an initial reading, to dilute samples to bring them into the linear range of the instrument.

The analyst prepares and runs operational control samples consisting of a standard, a blank and a spiked sample for each 10 analytical samples. There is one operational duplicate for each 20 analytical samples. In addition, 15% of the sample load consists of blind quality control samples prepared by the

Quality Assurance Manager in containers intended to be indistinguishable from the others. These consist of standards, spiked samples, duplicates and blanks.

Calibration standard solutions with 10 and 20 ppb selenium are prepared fresh daily from a 1000 ppm (as selenite) selenium reference standard obtained from the Ricca Chemical Company. Blind standards containing both selenite and selenate are prepared from a stock solution which is itself prepared from a high concentration or "super" stock solution, which in turn is prepared from dry sodium selenite and sodium selenate. The standard solutions used for blind standards are also used for spiking samples.

8.4. Blanks

We distinguish between the instrument limit of detection (ILD) and the method limit of detection (MLD). The ILD is determined by analyzing a series of standards prepared to contain known amounts of the analyte. This has been determined to be 0.2 ppb for selenium. The MLD is determined by analyzing blanks prepared blind in the same manner as any research sample. The MLDs for the new analyst, for selenite and total selenium are 0.52 ppb and 0.77 ppb respectively. The method limits of quantification (MLQ) for selenite and total selenium are 1.73 ppb and 2.55 ppb respectively . Since we are now using log normal statistics for blanks these values are not comparable to those reported in previous years. Recalculating limits of detection and quantification for previously reported blank statistics gives values very close to current ones.

8.5. Selenium Standards

We have established standards with both selenite and selenate because speciation of selenium has been important in many of the studies we have performed. Because selenite solutions with concentrations in the range of 40 ppb or less oxidize rapidly we make up each standard from a concentrated stock. We report statistics on total selenium rather than selenate because total selenium is a direct analytical measurement and not a calculated quantity. Selenate concentrations may be calculated from the difference between total selenium and selenite concentrations.

Table 8.1 gives the relative deviations of series of repeat measurements of sets of standard solutions run during the last quarter of fiscal 1990 and all of 1991. They were run blind to the analyst and subject to all sample preparation procedures. They indicate that our precision varies with the concentration of selenium. Table 8.2 contains statistics for a similar set of standards run from 1991 to the present.

The smaller number of analyses of selenite is the result of researchers request for analyses of total selenium only and not due to rejection of more points. The greater relative deviations of total selenium measurements in all standards, in spite of more analyses being performed, is most likely due to divergence generated by sample preparation. The preparation for total selenium analysis involves the transfer of sample solution and addition of reagents which can all introduce volume error. There is also the possibility that the reactions converting selenium to a readable form are incomplete.

Table 8.1. Selenium standard statistics 6/6/90 - 10/30/91

	Se^{+4}			Σ Se		
Label	Conc.	r.d%	No. of analyses	Conc.	r.d%	No. of analyses
Se XV A	2.07	12.2	44	4.61	13.9	58
Se XV B	4.49	8.0	44	9.35	16.0	58
Se XV C	8.91	9.0	46	19.13	12.8	59
Se XV D	17.39	8.2	49	37.38	13.6	60
Se XVI A	54.80	7.1	50	110.1	7.1	58
Se XVI B	110.74	5.6	47	216.86	5.6	57

Table 8.2. Selenium standard statistics 3/12/91 - 6/10/92

	Se^{+4}			Σ Se		
Label	Conc.	r.d.%	No. of analyses	Conc.	r.d.%	No. of analyses
Se XVII A	2.03	5.9	59	4.39	6.8	66
Se XVII B	4.24	9.2	66	8.96	10.1	69
Se XVII C	8.71	9.8	62	17.82	9.7	69
Se XVII D	17.39	7.7	57	34.66	9.8	69
Se XVIII A	54.70	9.2	58	110.7	7.8	69
Se XVIII B	111.25	7.8	64	217.7	9.6	72

Comparison of relative deviations of the first series of standards with those of the second series shows the modest degradation in analytical quality for selenite. For total selenium there was improvement in the middle range and decline at both high and low concentrations. The average values are not statistically different. The greater relative deviations for the more recent standards are attributable to the inexperience of the new analyst. The control charts shown below indicate that there has been improvement over the tenure of the new analyst.

8.6. Spike Recoveries

A continuing drawback in our spike recovery measurements has been the difficulty in knowing *a priori* what the selenium concentrations of many samples are. Ideally the spike of analyte added is equal to the amount of the original analyte. Spikes less than one quarter or more than 4 of the original analyses are not statistically meaningful. Spiked sample analyses which prove to be out of this range are rejected. In the 21 month period under consideration, 321 selenite analyses and 320 total selenium analyses were in a statistically meaningful range. Our average recovery for a selenite spike was 93.7% and for a total

selenium spike it was 97.8%. This represents a slight improvement over previously reported spike recoveries.

Analysis of variance of spiked sample recoveries in earlier time periods has revealed that there are no statisitically significant differences in spike recoveries for samples from different sources. Although analysis of variance was not performed on spike sample recoveries for the period reported here, we believe this continues to be the case.

8.7. Duplicates

Duplicates provide a measure of our analytical precision which includes factors such as foaming, which repeated measurements of standards do not reflect. Duplicates with at least one of the values less than the MLQ were discarded, giving 123 selenite and 207 total selenium duplicates used to calculate the averages given below. The average relative difference for duplicate selenite analyses in the period covered by this report was 6.3% and for duplicate total selenium analyses was 8.8%. This represents a degradation of quality from previous reports. The most recent results indicate that quality, as reflected by relative differences, is recovering.

8.8. Personnel Change

The change of personnel can be a disruptive event for any organization and in an analytical laboratory this is manifested in the degradation of analytical quality. The retirement of an experienced analyst represents the loss of accumulated skill which is often not transferable. Unless the new analyst has been performing the same type of analyses, on the same matrices, there will be a period in which even the brightest analyst gains experience in the particular instrument used, the typical matrices of samples and in the dozens of minor skills which contribute to accurate, precise and rapid analysis.

Like all complex repeated human activities, chemical analysis displays a learning curve. In this particular situation the control charts maintained for the analyst serve that function and demonstrate the growing competence of the analyst. Figures 8.1 and 8.2 are control charts for selenite and total selenium for analytic standard Se XVII D. When these values which go into determination of the relative differences are plotted, they demonstrate improvement over time. This gives us the reasonable expectation that our analytical quality will return at least to its previous level.

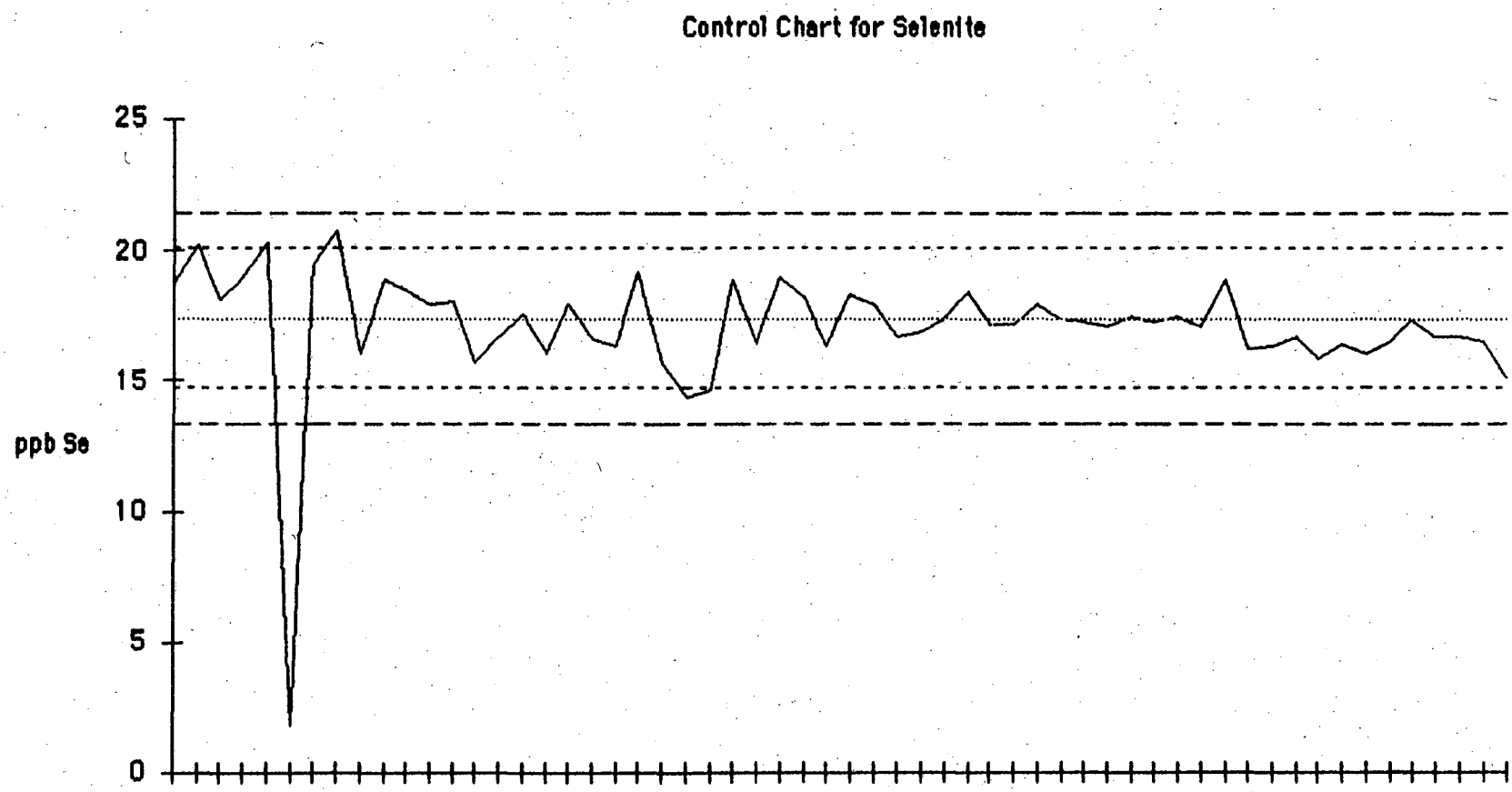

Figure 8.1. Control chart for selenite.

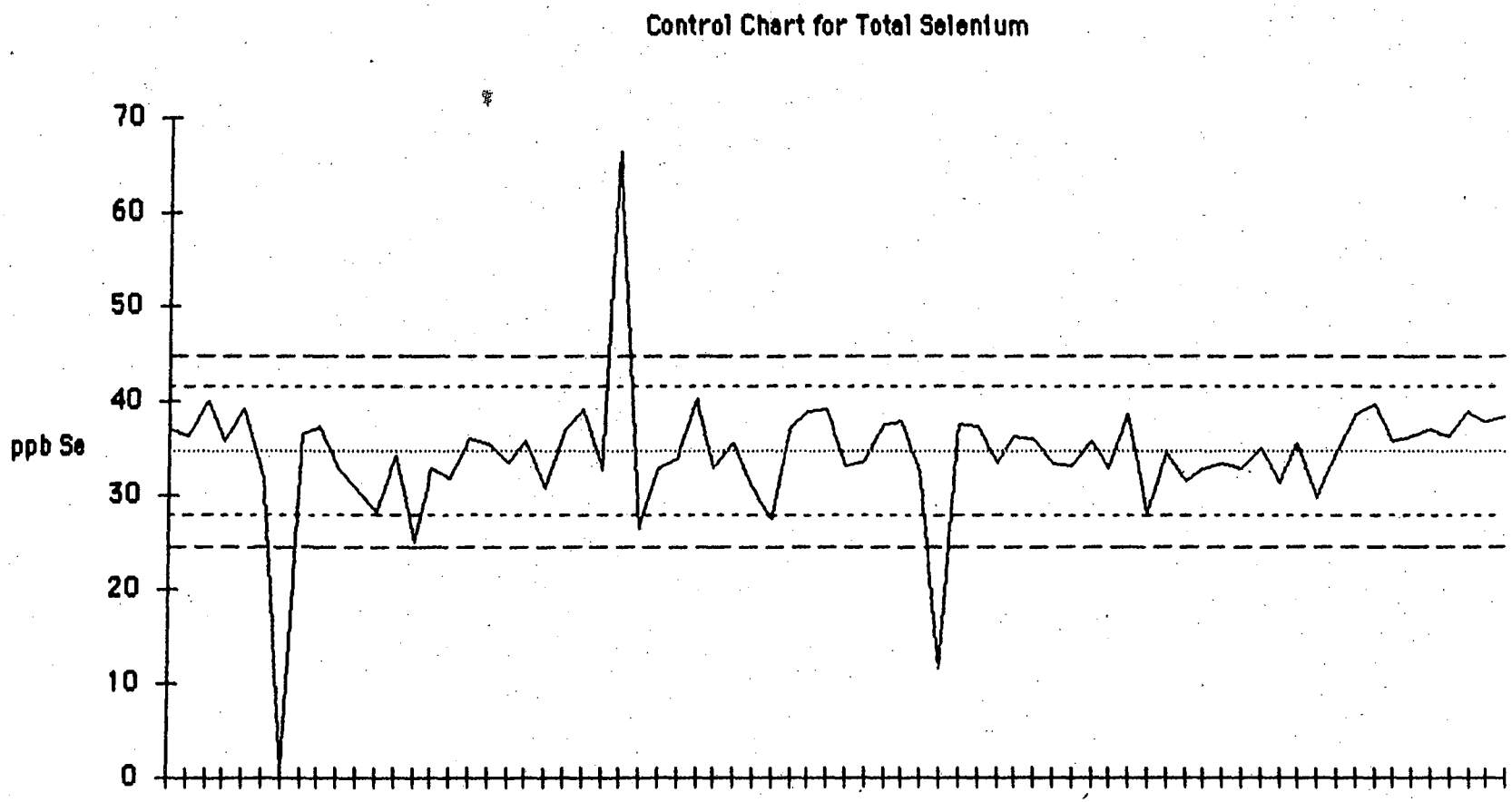

Figure 8.2. Control chart for total selenium.

9.0. References

ANR (Agriculture and Natural Resources Division, University of California), 1992. Soil-Water-Vegetation Management Studies of Selenium in Kesterson Reservoir and Containment Project, Draft Report.

Benson, S. M., A. F. White, S. F. Halfman, S. Flexser, and M. Alavi, 1991. Groundwater contamination at Kesterson Reservoir, California, Part 1. Hydrogeologic setting and conservative solute transport, *Water Resources Research, 27,* (6) 1071-1084.

Benson, S. M., M. Delamore, and S. Hoffman, 1990. Kesterson Crisis: Sorting out the facts. In S. C. Harris (ed.) Irrigation and Drainage Proceedings of the 1990 National Conference. American Society of Civil Engineers, New York.

Benson, S. M., T. K. Tokunaga, and P. T. Zawislanski. 1992. REFERENCE

Biggar, J. W., G. R. Jayaweera, and D. E. Rolston, 1990. Soil, plant and volatilization studies, in Hydrological, Geochemical, and Ecological Characterization of Kesterson Reservoir, Annual Report, October 1, 1988 - September 30, 1989, Lawrence Berkeley Laboratory Report, LBL-27993, Berkeley, CA.

Brock, T. D., 1974. *Biology of Microorganisms,* Prentice-Hall, Inc., Englewood Cliffs, New Jersey.

CH2M Hill, 1991. Kesterson Reservoir Biological Report (Draft). U.S. Bureau of Reclamation Mid Pacific Region.

CH2M Hill, 1992. Ecological Risk Assessment for Kesterson Reservoir, report prepared for the U. S. Bureau of Reclamation, Sacramento, CA.

Doran, J. W. and M. Alexander, 1977. Microbial transformations of selenium, *Applied and Environmental Microbiology, 33,* 31-37.

Doran, J. W., 1982, Microorganisms and the biological cycling of selenium, *Adv. Microbiol. Ecol., 6,* 1-32.

Elrashidi, M. A., D. C. Adriano, S. M. Workman, and W. L. Lindsay. 1987. Chemical equilibria of selenium in soils: A theoretical development, *Soil Science, 144*, (2) 141-152.

Flaschla. H. A. A. J. Barnard. Jr., and P. E. Sturrock, 1969. *Quantitative Analytical Chemistry,* Vol. I, Barnes and Noble.

Frankenberger, W. T., 1990. Dissipation of Soil Selenium by Microbiol Volatilization at Kesterson Reservoir, Final Report to the U.S. Bureau of Reclamation.

Frankenberger, W. T., and U. Karlson, 1988. Dissipation of Soil Selenium by Microbial Volatilization at Kesterson Reservoir, Final Report to the U.S. Bureau of Reclamation.

Geering, H. R., E. E. Cary, L. H Jones, and W. H. Allaway, 1968. Solubility and redox criteria for the possible forms of selenium in soils, *Soil Science of America Proceedings, 32,* 35-40.

Giauque, R. D., R. B. Garrett, and L. Y. Goda. 1976. Energy-dispersive x-ray fluorescence spectrometry for determination of twenty-six trace and two major elements in geochemical specimens, *Anal. Chem. 49*:, 62-67.

Goldhammer, D. A., and M. H. Alemi, 1990. The effect of irrigation strategy on dissipation of selenium, in Hydrological, Geochemical, and Ecological Characterization of Kesterson Reservoir, Annual Report, October 1, 1988 - September 30, 1989, Lawrence Berkeley Laboratory Report, LBL-27993, Berkeley, CA.

Goldstein, N. E., S. L. Pillsbury, J. S. Daggett, and S. M. Benson, 1989. Contaminant Plume Monitoring Adjacent to Kesterson Reservoir, CA., Lawrence Berkeley Laboratory Report, LBL-26557, Berkeley, CA.

Ita, S. P., and S. M. Benson, 1992. Field investigation of the effect of rainfall infiltration on soil selenium and salinity at Kesterson Reservoir, in Earth Sciences Division Annual Report, Lawrence Berkeley Laboratory Report, LBL -31500, Berkeley, CA.

Lawrence Berkeley Laboratory Annual Report, 1987. LBL-24250, Berkeley, CA.

Lawrence Berkeley Laboratory, 1988. Hydrological, Geochemical, and Ecological Characterization of Kesterson Reservoir, Annual Report, Lawrence Berkeley Laboratory Report, LBL-26438, Berkeley, CA.

Lawrence Berkeley Laboratory, 1990a. Hydrological, Geochemical, and Ecological Characterization of Kesterson Reservoir, Annual Report, October 1, 1988 - September 30, 1989, Lawrence Berkeley Laboratory Report, LBL-27993, Berkeley, CA.

Lawrence Berkeley Laboratory, 1990b. Hydrological and Geochemical Investigations of Selenium Behavior at Kesterson Reservoir, Lawrence Berkeley Laboratory Report, LBL-29689, Berkeley, CA.

Long, R. H., S. M. Benson, T. K. Tokunaga, and T. N. Narasimhan, 1990. Selenium immobilization in a pond bottom sediment at Kesterson Reservoir, *Journal of Environmental Quality, 19,* (2) 302-311.

Long, R. H., 1988. Analysis of Selenium and Chloride Movement through a Shallow Pond Sediment at Kesterson Reservoir, M.S. Thesis, University of California, Berkeley, CA.

Masscheleyn, P. H., R. D. Delaune, and W. H. Patrick, Jr., , 1990. Transformations of selenium as affected by sediment oxidation-reduction potential and pH, *Environ. Sci. Technol., 24,* 91–96.

Mead, R, 1988. *Design of Experiments: Statistical Principles for Practical Applications,* Cambridge University Press, Cambridge, England.

Oremland, R. S., J. T. Hollibaugh, A. S. Maest, T. S. Presser, L. G. Miller, and C. W. Culbertson, 1989, Selenate reduction to elemental selenium by anaerobic bacteria in sediments and culture: Biogeochemical significance of a novel, sulfate-independent respiration, *Applied and Environmental Microbiology, 55,* (9), 2333-2343.

Saratchandra, S. U., and J. H. Watkinson, 1981. Oxidation of elemental selenium to selenite by *Bacillus megaterium, Science, 211*, 600-601.

Terry, N., M. Rao, and C. Carlson, 1990. Volatilization of selenium from different types for plants for the removal of selenium from Kesterson soils, in Hydrological, Geochemical, and Ecological Characterization of Kesterson Reservoir, Annual Report, October 1, 1988 - September 30, 1989, Lawrence Berkeley Laboratory Report, LBL-27993, Berkeley, CA.

Tokunaga, T. K., 1990. Diffusive and convective transport of volatile selenium through Kesterson Reservoir soils, in Hydrological, Geochemical, and Ecological Characterization of Kesterson Reservoir, Annual Report, October 1, 1988 - September 30, 1989, Lawrence Berkeley Laboratory Report, LBL-27993, Berkeley, CA.

Tokunaga, T. K., and S. M. Benson, 1992. Selenium in ephemeral pools formed by groundwater rise at Kesterson Reservoir: I. Field study, *Journal of Environmental Quality, 21,* 246-251.

Tokunaga, T. K., D. S. Lipton, S. M. Benson, A. W. Yee, J. M. Oldfather, E. C. Duckart, P. W. Johannis, and K. Halvorsen, 1991. Soil selenium fractionation , depth profiles and time trends in a vegetated site at Kesterson Reservoir, *Water, Air and Soil Pollution, 57-58*, 31-41.

USBR (United States Bureau of Reclamation), 1984. San Luis Unit, Central Valley Project, Ca. Information Bulletin 1, 2, 3, and 4, USBR, Mid-Pacific Region, Sacramento, CA.

USBR (United States Bureau of Reclamation), 1986. Final Environmental Impact Statement, Volume 2, Kesterson Program, Sacramento, CA.

USBR.(United States Bureau of Reclamation), 1992. Revised Monitoring and Reporting Program #87-149, Kesterson Reservoir Merced County, Annual Report, October 15..

Wahl, C., 1992. Analysis of Temporal and Spatial Trends in Soil Selenium Concentrations at Kesterson Reservoir, Merced County, California, M. S. Thesis, State University of New York, Syracuse, New York.

Warrick, A. W., and D. R. Nielson, 1980. Spatial variability of soil physical properties in the field, in D. Hillel (Ed.) *Application of Soil Physics,* Academic Press, NY.

Weres, O., A. F. White, H. A. Wollenberg, and A. Yee, 1985. Progress Report: Geochemistry of Selenium in the Kesterson Reservoir and Possible Remedial Measures, Lawrence Berkeley Laboratory Report, LBID-1014, Berkeley, CA.

Weres, O. A., A.-R. Jaouni, and L. Tsao, 1989. The distribution, speciation and geochemical cycling of selenium in a sedimentary environment, Kesterson Reservoir, CA, U.S.A., *Applied Geochemistry, 4*, 543-563.

Weres, O. A., A. F. White, H. A. Wollenberg, and A. Yee. 1985. Geochemistry of selenium at Kesterson Reservoir: Possible remediation measures, Earth Sciences (Lawrence Berkeley Laboratory Publication-431) 8 (3) 1-8.

White, A. F., S. M. Benson, A. W. Yee, H. A. Wollenberg, and S. Flexser, 1991. Groundwater contamination at Kesterson Reservoir, California, Part 2. Geochemical parameters influencing selenium mobility, *Water Resources Research, 27,* (6) 1085-1098.

Wu, L., J. W. Biggar, Z. Z. Huang, 1990. Biomass, species diversity and selenium concentrations in Kesterson plants, in Hydrological and Geochemical Investigations of Selenium Behavior at Kesterson Reservoir, Lawrence Berkeley Laboratory Report, LBL-29689, Berkeley, CA.

Yee, A., 1990. Selenium volatilization from fractionated soil, in Hydrological and Geochemical Investigations of Selenium Behavior at Kesterson Reservoir, Lawrence Berkeley Laboratory Report, LBL-29689, Berkeley, CA.

Zawislanski, P, 1990. Multiple extractions of surface salt crust and soil for the determination of selenium association, in Hydrological and Geochemical Investigations of Selenium Behavior at Kesterson Reservoir, Lawrence Berkeley Laboratory Report, LBL-29689, Berkeley, CA.

Zawislanski, P. T., 1989. Bare Soil Evaporation at Kesterson Reservoir, Merced, County, California: Estimation by Physical and Chemical Methods, M. S. Thesis, University of California, Berkeley, CA.

Zawislanski, P., T. Tokunaga, S Benson, J. Oldfather and T. N. Narasimhan, 1992. Bare soil evaporation and solute movement of selenium in contaminated soils at Kesterson Reservoir, California, *Journal of Environmental Quality, 21,* 447-457.

Zawislanski, P. T., and M. Zavarin, 1992. Laboratory accelerations of selenium transformations, in Hydrological, Geochemical, and Ecological Characterization of Kesterson Reservoir, Annual Report, October 1990 - March 1992, Lawrence Berkeley Laboratory Report (in preparation), Berkeley, CA.

LAWRENCE BERKELEY LABORATORY
UNIVERSITY OF CALIFORNIA
TECHNICAL INFORMATION DEPARTMENT
BERKELEY, CALIFORNIA 94720